# COVERAGE PREDICTIONS FOR THE NAVY'S FIXED VLF TRANSMITTERS

James P. Hauser, et al

Naval Research Laboratory
Washington, D. C.

September 1974

NRL Memorandum Report 2884

# Coverage Predictions for the Navy's Fixed VLF Transmitters



JAMES P. HAUSER AND FRANKLIN J. RHOADS

*Electromagnetic Propagation Branch*
*Communications Sciences Division*

September 1974



NAVAL RESEARCH LABORATORY
Washington, D.C.

UNCLASSIFIED

SECURITY CLASSIFICATION OF THIS PAGE *(When Data Entered)*

AD/A-001701

| REPORT DOCUMENTATION PAGE | | READ INSTRUCTIONS BEFORE COMPLETING FORM |
|---|---|---|
| 1 REPORT NUMBER<br>NRL Memorandum Report 2884 | 2 GOVT ACCESSION NO. | 3. RECIPIENT'S CATALOG NUMBER |
| 4 TITLE *(and Subtitle)*<br>COVERAGE PREDICTIONS FOR THE NAVY'S FIXED VLF TRANSMITTERS | | 5 TYPE OF REPORT & PERIOD COVERED<br>Final Report<br>6. PERFORMING ORG. REPORT NUMBER |
| 7. AUTHOR(s)<br>James P. Hauser and F. J. Rhoads | | 8. CONTRACT OR GRANT NUMBER(s) |
| 9. PERFORMING ORGANIZATION NAME AND ADDRESS<br>Naval Research Laboratory<br>Washington, D.C. 20375 | | 10 PROGRAM ELEMENT, PROJECT, TASK AREA & WORK UNIT NUMBERS<br>NRL Prob. 54R07-22<br>Project X1508 Task G<br>Project X3297 Task G |
| 11 CONTROLLING OFFICE NAME AND ADDRESS<br>Naval Electronic Systems Command<br>Washington, D.C.<br>Defense Communications Agency, Washington, D.C. | | 12 REPORT DATE<br>September 1974<br>13. NUMBER OF PAGES<br>153 |
| 14 MONITORING AGENCY NAME & ADDRESS*(if different from Controlling Office)* | | 15 SECURITY CLASS. *(of this report)*<br>UNCLASSIFIED<br>15a. DECLASSIFICATION/DOWNGRADING SCHEDULE |

16 DISTRIBUTION STATEMENT *(of this Report)*

Approved for public release; distribution unlimited.

17. DISTRIBUTION STATEMENT *(of the abstract entered in Block 20, if different from Report)*

18 SUPPLEMENTARY NOTES

19. KEY WORDS *(Continue on reverse side if necessary and identify by block number)*

VLF
Communications Coverage Predictions
Fixed VLF Transmitters



20 ABSTRACT *(Continue on reverse side if necessary and identify by block number)*

(U) This report is the eighth in a series which presents signal strength and signal-to-noise ratio predictions for the Navy's fixed very-low-frequency transmitters. Predictions given here are for all four seasons of the year. A new atmospheric noise prediction model used for these predictions is briefly discussed and the meaning of the predictions explained. This report supercedes all previous reports in this series.

DD FORM 1 JAN 73 1473 EDITION OF 1 NOV 65 IS OBSOLETE
S/N 0102-014-6601



UNCLASSIFIED
SECURITY CLASSIFICATION OF THIS PAGE *(When Data Entered)*

CONTENTS

# COVERAGE PREDICTIONS FOR THE NAVY'S FIXED VLF TRANSMITTERS

## INTRODUCTION

The Navy, because of its need for accurate predictions of the reliability of its very-low-frequency (VLF) communications circuits, has tasked the Naval Research Laboratory (NRL) with the responsibility of maintaining a Long Wave Propagation Center and providing communications coverage predictions. NRL has published a series of reports, references (1-7), which provide communications coverage predictions for the Navy's fixed VLF transmitters. This report is a continuation of that series, being the eighth such report to be published.

This report differs from the previous reports in the series in three respects: (1) it contains predictions for all four seasons rather than a separate report for each season, (2) it is unclassified because it does not present coverage for specific systems, and (3) it makes use of a new atmospheric noise prediction model developed by Westinghouse Corporation, reference (8), and refined by NRL, reference (9). The new noise model replaces the CCIR noise model, reference (10), which was used in the previous reports. A classified appendix will be published giving coverage areas of the most strategic Navy systems, both operational and proposed.

The purpose of publishing a new prediction manual at this time is to show the effects of the new and improved atmospheric noise model in predicting communications coverage for the Navy's fixed VLF transmitters.

## ATMOSPHERIC NOISE MODEL

Several inadequacies exist in the CCIR noise model. Three of these inadequacies are particularly relevant to the communications coverage predictions presented in this series of reports. (1) Using the CCIR model to generate worldwide contours of atmospheric noise in universal time leads to discontinuities between time zones and across the equator (Figure 1). (2) The CCIR model predicts the standard deviation and the voltage deviation, i.e., the difference in dB between the noise power and the voltage of the noise, as functions of time and frequency only, when it is known that these parameters are functions of location as well. (3) The validity of the CCIR model is especially questionable in areas far removed from atmospheric noise recording

Manuscript submitted August 23, 1974.

sites. During preparation of the CCIR model, thunderstorm day contour maps prepared by the World Meteorological Organization (WMO) were used as guidelines in extrapolating noise parameters into areas for which no atmospheric noise data existed; however, the extrapolation technique was not based on exact mathematical expressions relating thunderstorm activity to atmospheric noise and the WMO maps themselves were based on few data.

In order to eliminate these as well as other shortcomings, NRL initiated the development of a new atmospheric noise prediction model at Westinghouse Georesearch Laboratory (WGL) under the direction of E. L. Maxwell, reference (8). A major portion of this effort was concentrated on producing an improved set of thunderstorm day contour maps. The improved WGL maps (Figure 2) include data from many locations for which the WMO maps (Figure 3) have no data. The WGL noise model then uses mathematical expressions based on the physics of lightning discharges to convert the improved thunderstorm day data into electromagnetic energy radiated from each area of the earth's surface. Each area is treated as an effective transmitter of noise energy propagated to the receiver location. The propagation model used is taken from Watt, reference (11), and is based on the work of Wait and Spies. The combined energies of all transmitters at the receiver location constitutes the WGL prediction of mean atmospheric noise. The other noise parameters, standard deviation and voltage deviation, are calculated from the thunderstorm day data using empirically derived mathematical relationships.

The WGL model eliminates the discontinuities inherent in the CCIR model and also predicts the standard deviation and voltage deviation as functions of location as well as of time and frequency. Most important, however, is the fact that it predicts atmospheric noise parameters more accurately than does the CCIR model, as can be seen by comparing Figures 4 and 5. The data used for the histograms in Figures 4 and 5 were recorded by a worldwide network of ARN-2 atmospheric radio noise recorders run by the Environmental Science Services Administration (ESSA). Further refinement of the WGL model by NRL, reference (9), produced even better agreement with the ESSA noise data (Figure 6). Figures 7 thru 30 present contours of atmospheric radio noise generated by NRL's empirically refined version of the WGL model. The figures are grouped by season and ordered by Universal Time (UT).

## PROPAGATION MODEL

The propagation model used for this report is identical to the model used in references (4-7). Although the propagation models are the same, the designation of the coverage prediction program, which includes both the noise and the propagation models, has been changed from NCPP 70 to NCPP 74 because of the new noise model. Additional references pertinent to the development of the propagation model are given in references (1-7).

## PREDICTIONS

Tables 1 and 2 list the figure numbers for the signal strength and signal-to-atmospheric noise ratio predictions respectively. The figure numbers of the prediction contour maps are arranged to correspond directly to the figure numbers appearing in the previous reports of the series. This allows for ease in comparing these predictions with previous ones. For convenience, the figures have been grouped by season - Summer (June, July, August), Fall (September, October, November), Winter (December, January, February), and Spring (March, April, May) - and the figure numbers have been prefixed by the first two letters of the season which they are for.

The signal strength predictions are based on the frequencies and nominal, effective radiated powers (ERP) given in Table 1. The ERP's used here have been deduced from the most recent radiation resistance measurements and antenna current logs available for each transmitter, and therefore reflect the nominal operating power of each transmitter as of June 1974. These ERP's differ little from those used in previous reports with the exception of NPG/NLK, which is now operating at roughly 130 kW rather than 250 kW due to a reduction in antenna current.

The signal strength contour levels are in decibels relative to one microvolt per meter (dB > 1μv/m) and represent the expected values that the signal strength will equal or exceed for the stated percentage of all hours of the season. For example, if one were to measure the signal strength of NAA continuously day and night for the entire summer season at 5°N, 30°W, 90 percent of the measurements should equal or exceed 60 dB > 1μv/m, the value determined from Figure SU 1. From Figure SU 2 at the same location, 99 percent of the measurements should equal or exceed 56 dB > 1μv/m.

The signal-to-atmospheric noise ratio predictions are listed in Table 2 and are based on a 1 kHz bandwidth and the same transmitter frequencies and ERP's as the signal strength predictions. The contour levels are given in dB and are interpreted in the same fashion as the signal strength contours.

## APPLICATION

Since the received signal strength and signal-to-noise ratio are both linearly proportional to the transmitter ERP in dB, the signal and signal-to-noise ratio contours directly show the effect of changing the transmitter ERP. The area between adjacent signal-to-noise ratio contours is the extended coverage area gained by increasing the transmitter ERP by increments of 3 dB. For example, the area within which the signal-to-noise ratio is -3 dB or better is extended out from the -3 dB contour to the -6 dB contour if the transmitter ERP is increased 3 dB, and so on.

Of prime importance to the communication engineer and the communicator are the signal-to-noise ratio contours. For a given communication system the reliability with which a true message may be deciphered from one containing errors is a function of the character error rate (CER). For a given receiving system, type of modulation, coding, and information rate, the CER is a function of the received signal-to-noise ratio. Thus, once a system is specified, a tolerable CER can be specified, and in turn, a required signal-to-noise ratio can be determined which will provide reliable communications. With the required signal-to-noise ratio established, the corresponding signal-to-noise contour bounds the area within which receiver terminals can be deployed for reliable communications. A classified appendix to this report will be published treating coverage of the most strategic Navy systems, both operational and proposed.

TABLE 1

SIGNAL STRENGTH PREDICTIONS

| Figure* Number | Time Availability | Transmitter | Frequency (kHz) | ERP (kW) |
|---|---|---|---|---|
| 1 | 90% | NAA, Cutler | 17.8 | 1000 |
| 2 | 99% | | | |
| 3 | 90% | NWC, North West Cape | 22.3 | 1000 |
| 4 | 99% | | | |
| 5 | 90% | NPG/NLK, Jim Creek | 18.6 | 130 |
| 6 | 99% | | | |
| 7 | 90% | NBA, Balboa | 24.0 | 110 |
| 8 | 99% | | | |
| 9 | 90% | NDT, Yosami | 17.4 | 40 |
| 10 | 99% | | | |
| 11 | 90% | NSS, Annapolis | 21.4 | 400 |
| 12 | 99% | | | |
| 13 | 90% | NPM, Lualualei | 23.4 | 630 |
| 14 | 99% | | | |

*Each figure number in the table represents four figures, one for each season, in the body of the report. In the body of the report, each figure number is prefixed by the first two letters of the season for which the prediction is given.

TABLE 2

SIGNAL-TO-ATMOSPHERIC NOISE RATIO PREDICTIONS

| Figure* Number | Time Availability | Transmitter | Frequency (kHz) | ERP (kW) |
|---|---|---|---|---|
| 15<br>16 | 90%<br>99% | NAA, Cutler | 17.8 | 1000 |
| 17<br>18 | 90%<br>99% | NWC, North West Cape | 22.3 | 1000 |
| 19<br>20 | 90%<br>99% | NPG/NLK, Jim Creek | 18.6 | 130 |
| 21<br>22 | 90%<br>99% | NBA, Balboa | 24.0 | 110 |
| 23<br>24 | 90%<br>99% | NDT, Yosami | 17.4 | 40 |
| 25<br>26 | 90%<br>99% | NSS, Annapolis | 21.4 | 400 |
| 27<br>28 | 90%<br>99% | NPM, Lualualei | 23.4 | 630 |

*Each figure number in the table represents four figures, one for each season, in the body of the report. In the body of the report, each figure number is prefixed by the first two letters of the season for which the prediction is given.

## REFERENCES


1. J. P. Hauser and F. J. Rhoads, "Coverage Predictions for the Navy, Fixed, VLF Transmitter Facilities for June, July, and August," (U), NRL Confidential Memorandum Report 2029

2. J. P. Hauser and F. J. Rhoads, "Coverage Predictions for the Navy, Fixed, VLF Transmitter Facilities for December, January, and February," (U), NRL Confidential Memorandum Report 2059

3. J. P. Hauser and F. J. Rhoads, "Coverage Predictions for the Navy, Fixed, VLF Transmitter Facilities for March, April, and May," (U), NRL Confidential Memorandum Report 2090

4. J. P. Hauser and M. C. Lawrence, "Coverage Predictions for the Navy, Fixed, VLF Transmitter Facilities for June, July, and August," (U), NRL Confidential Memorandum Report 2134

5. J. P. Hauser, "Coverage Predictions for the Navy, Fixed, VLF Transmitter Facilities for September, October, and November," (U), NRL Confidential Memorandum Report 2157

6. J. P. Hauser, "Coverage Predictions for the Navy, Fixed, VLF Transmitter Facilities for December, January, and February," (U), NRL Confidential Memorandum Report 2179

7. J. P. Hauser, "Coverage Predictions for the Navy, Fixed, VLF Transmitter Facilities for March, April, and May," (U), NRL Confidential Memorandum Report 2211

8. E. L. Maxwell, Westinghouse Georesearch Laboratory, "Development of a VLF Atmospheric Noise Prediction Model", 1970

9. J. P. Hauser and F. J. Rhoads, "Analysis of a VLF Atmospheric Noise Prediction Model", NRL Memorandum Report to be published November 1974

10. CCIR Report 322, "World Distribution and Characteristics of Atmospheric Radio Noise", 1964

11. A. D. Watt, "VLF Radio Engineering", International Series of Monographs in Electromagnetic Waves, Volume 14.

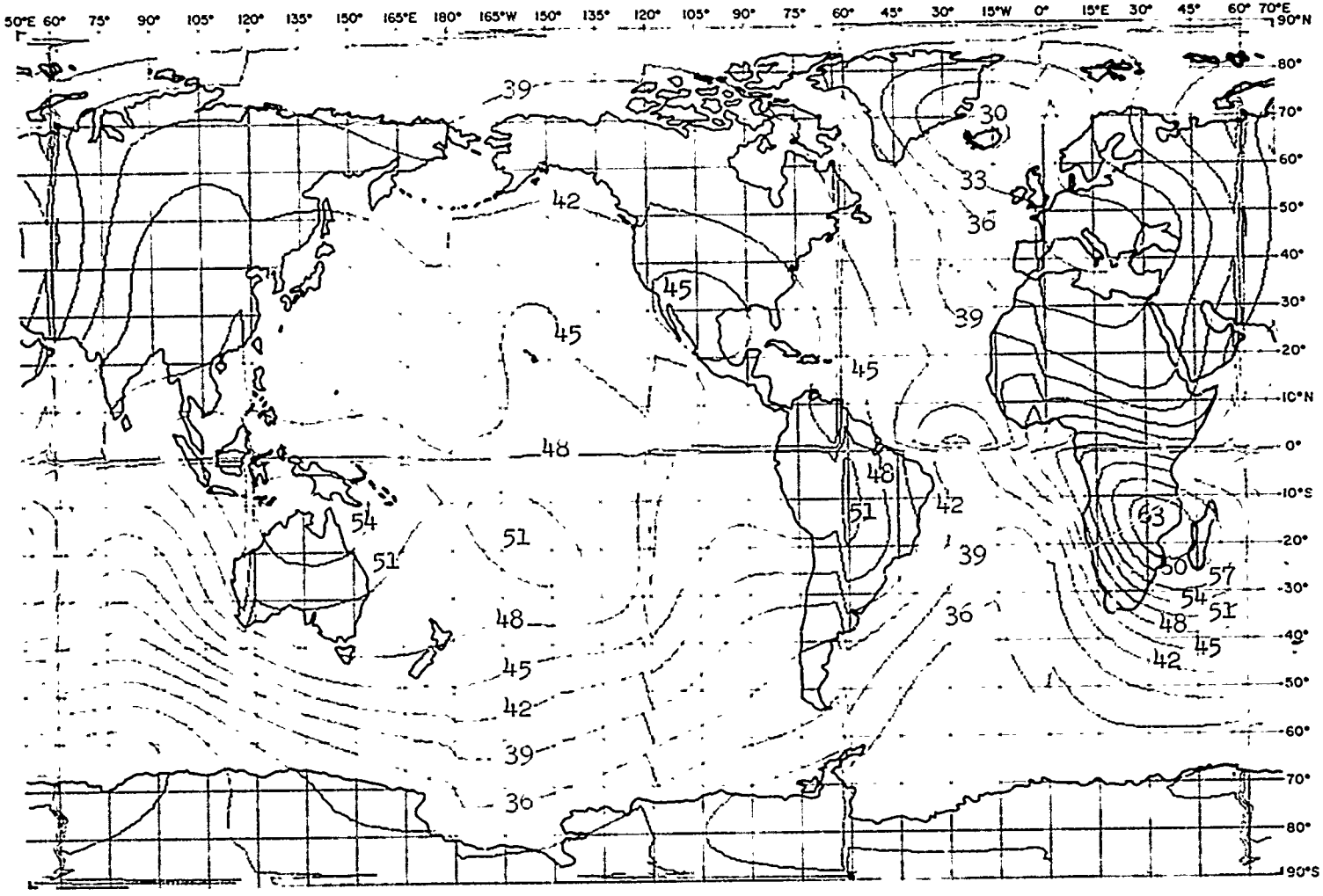


Fig. 1 - Atmospheric noise contours (dB>1μv/m - 1 kHz BW) for 20 kHz (January, 1200 UT) using the CCIR atmospheric noise model

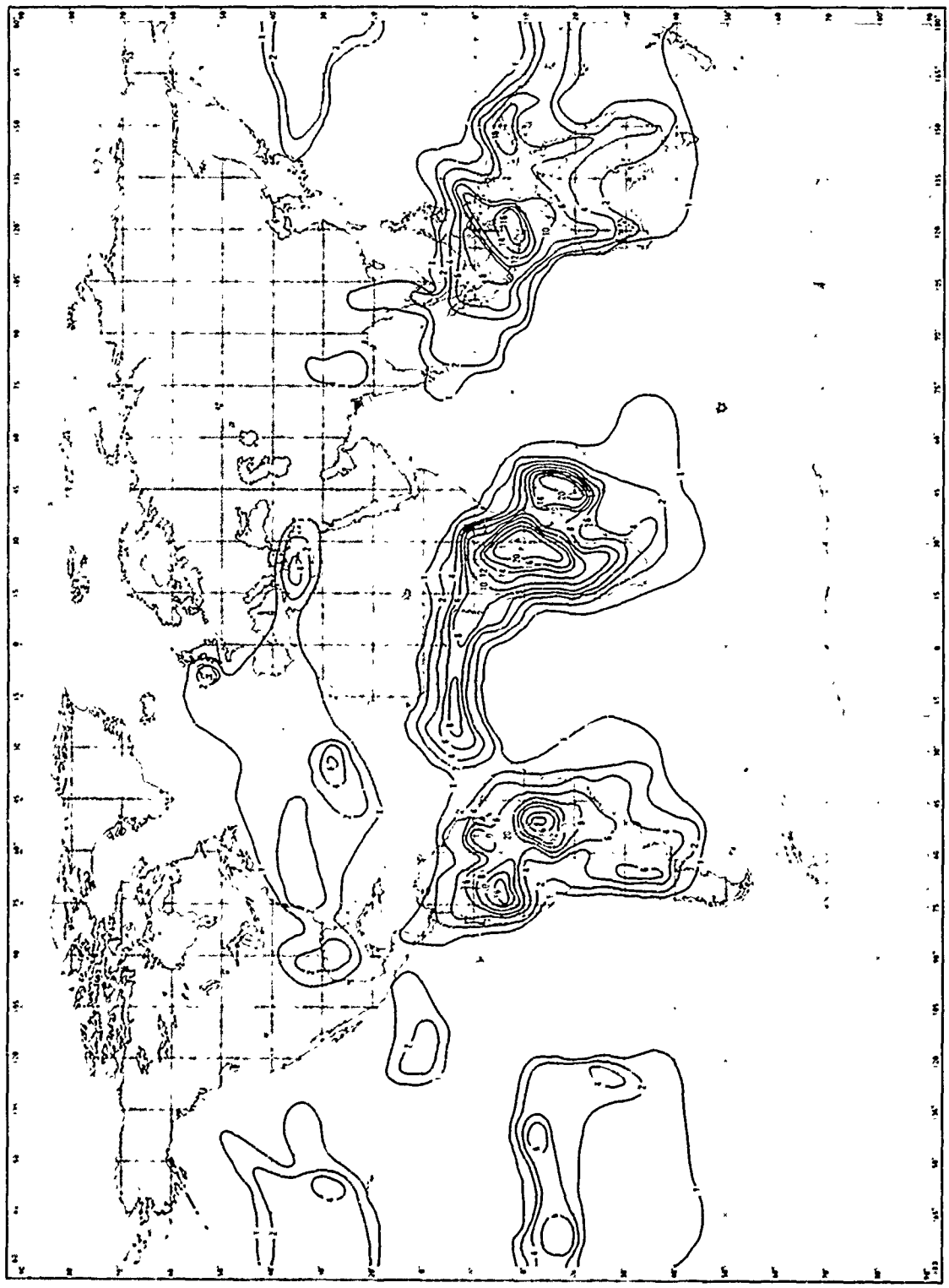

Fig. 2 - AGL thunderstorm ray contour map for January

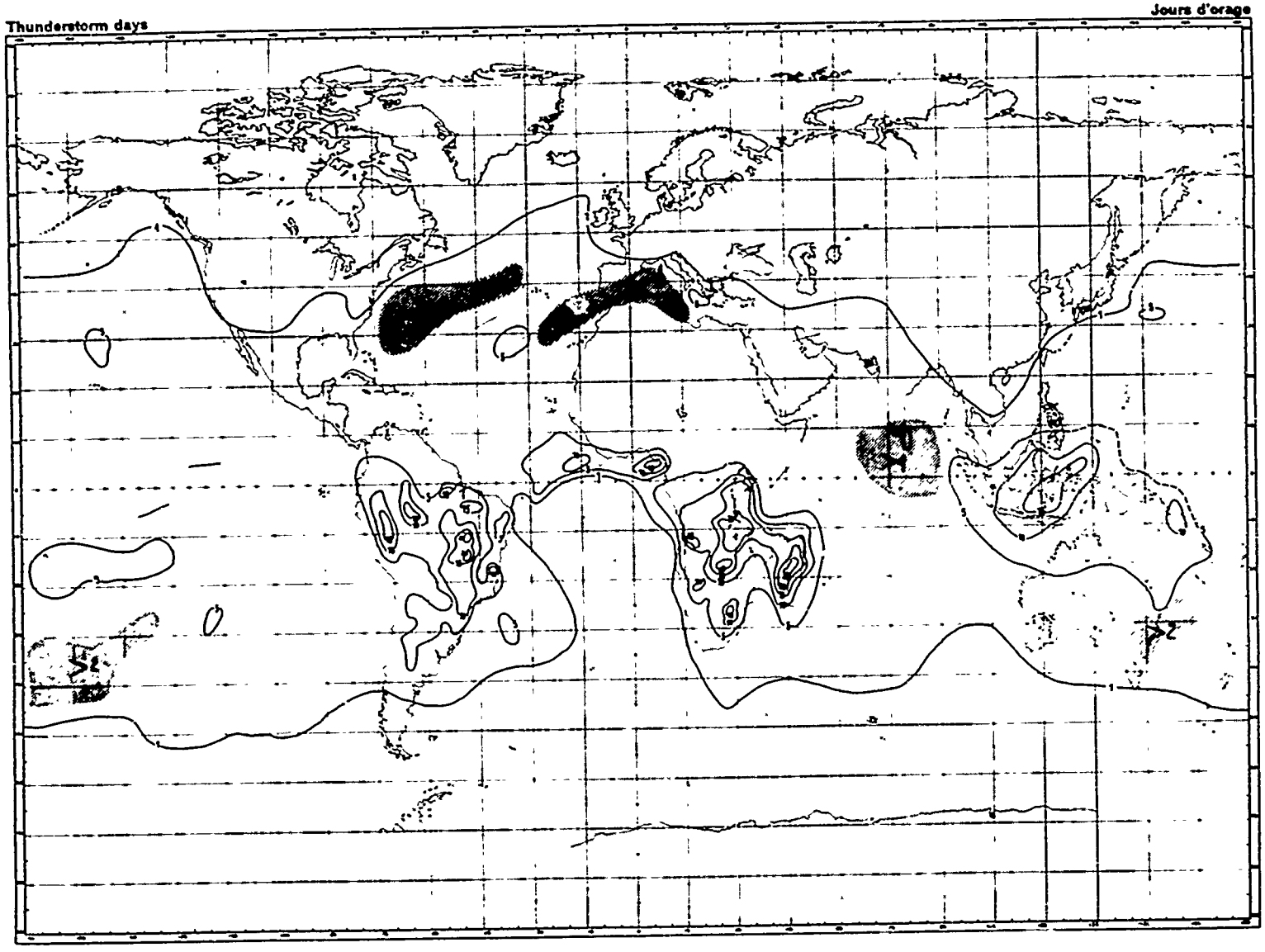


Fig. 3 - WMO thunderstorm day contour map for January

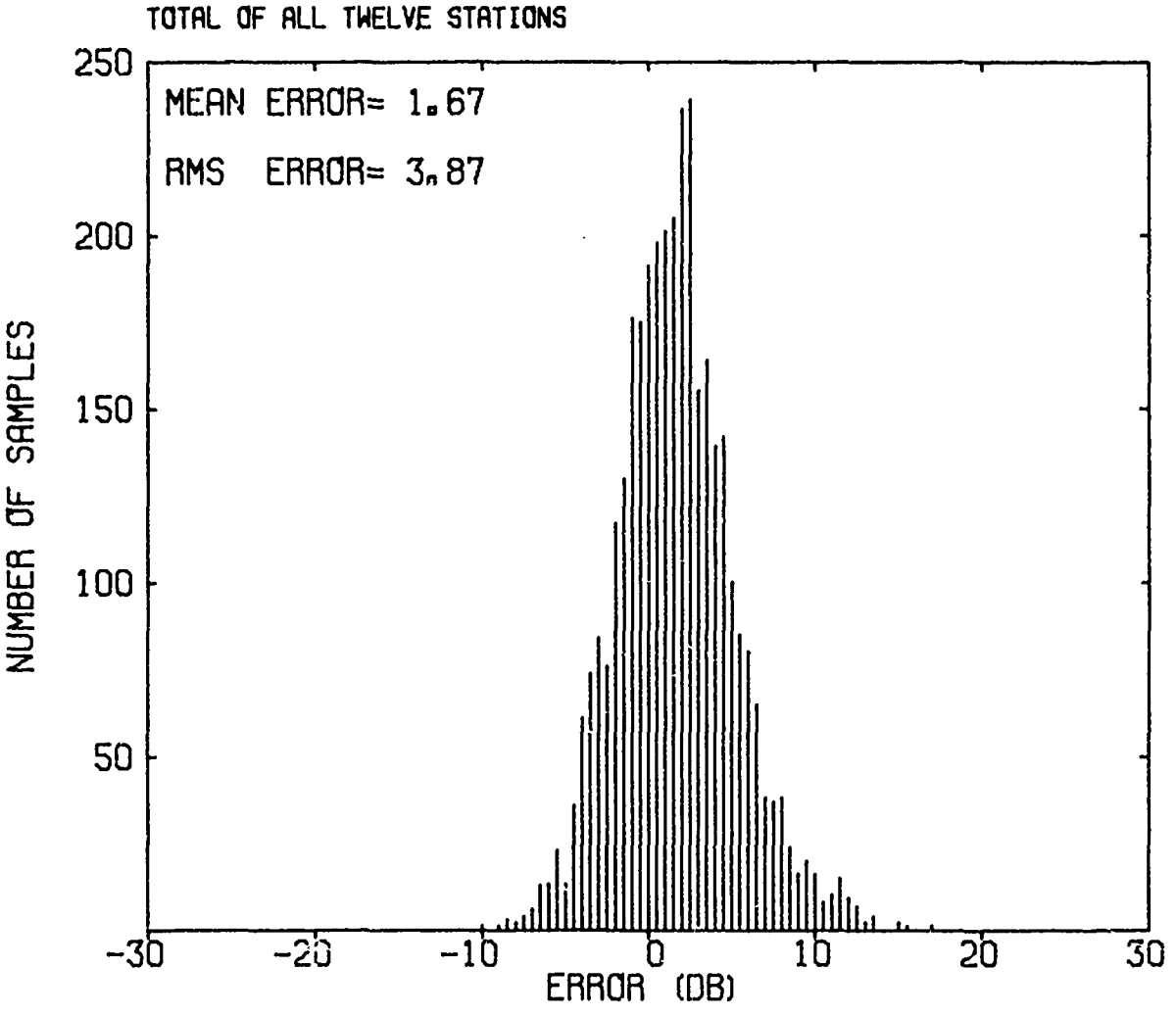


Fig. 1 - Histogram of errors in predicting mean atmospheric noise power using the CCIR model

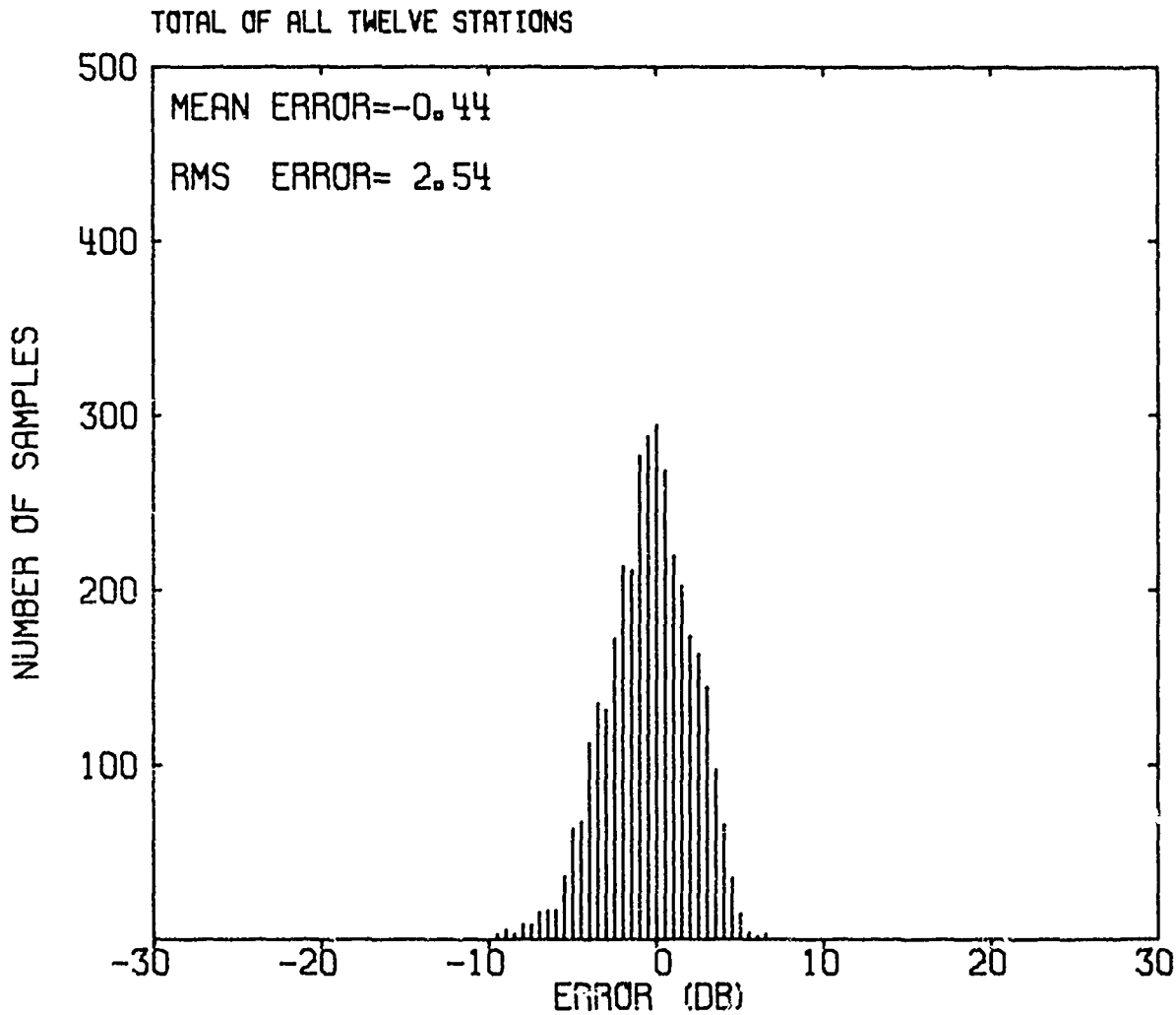


Fig. 5 - Histogram of errors in predicting median atmospheric noise power using the WGL model

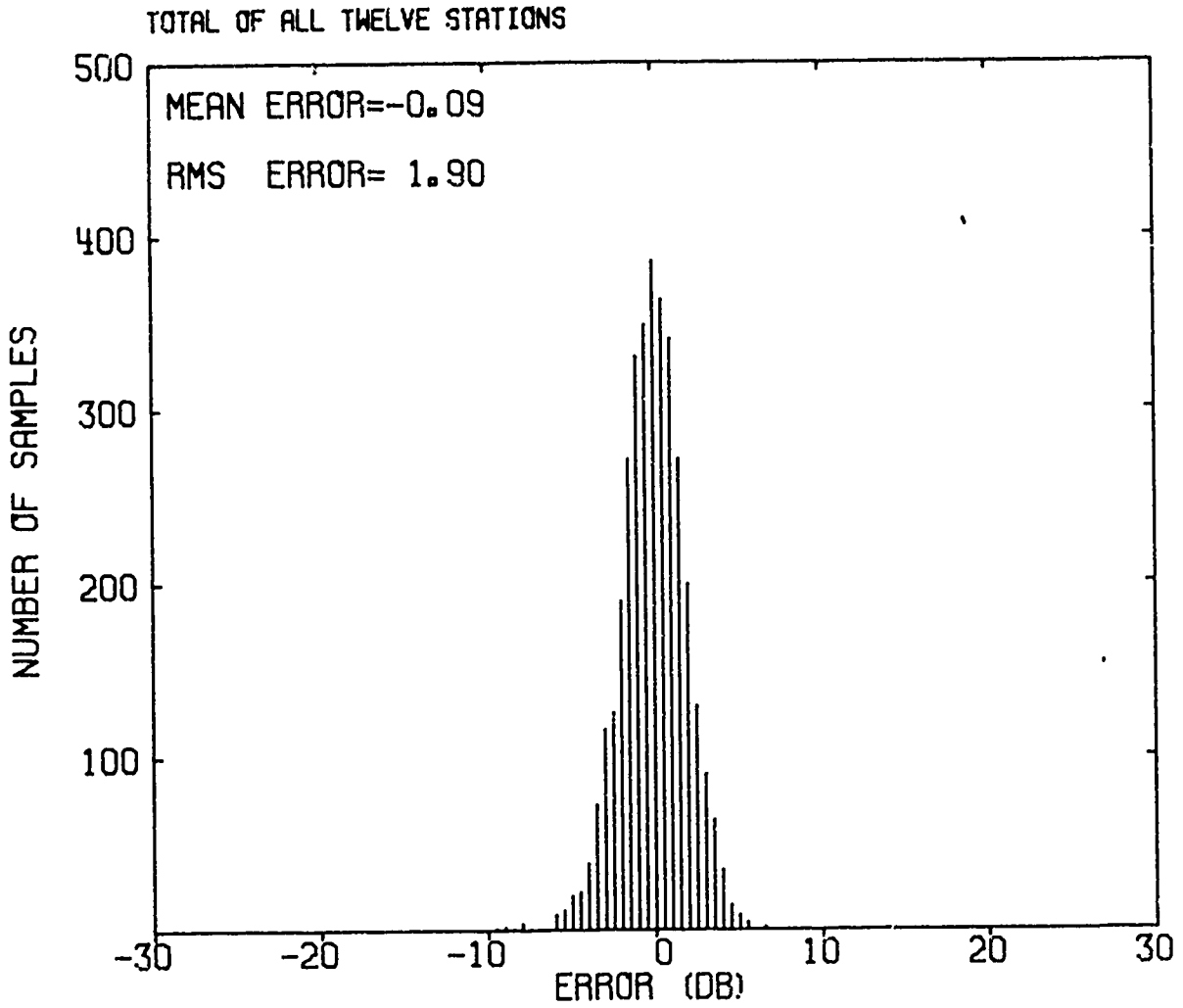


Fig. 6 - Histogram of errors in predicting mean atmospheric noise power using the NRL empirically refined version of the WGL model

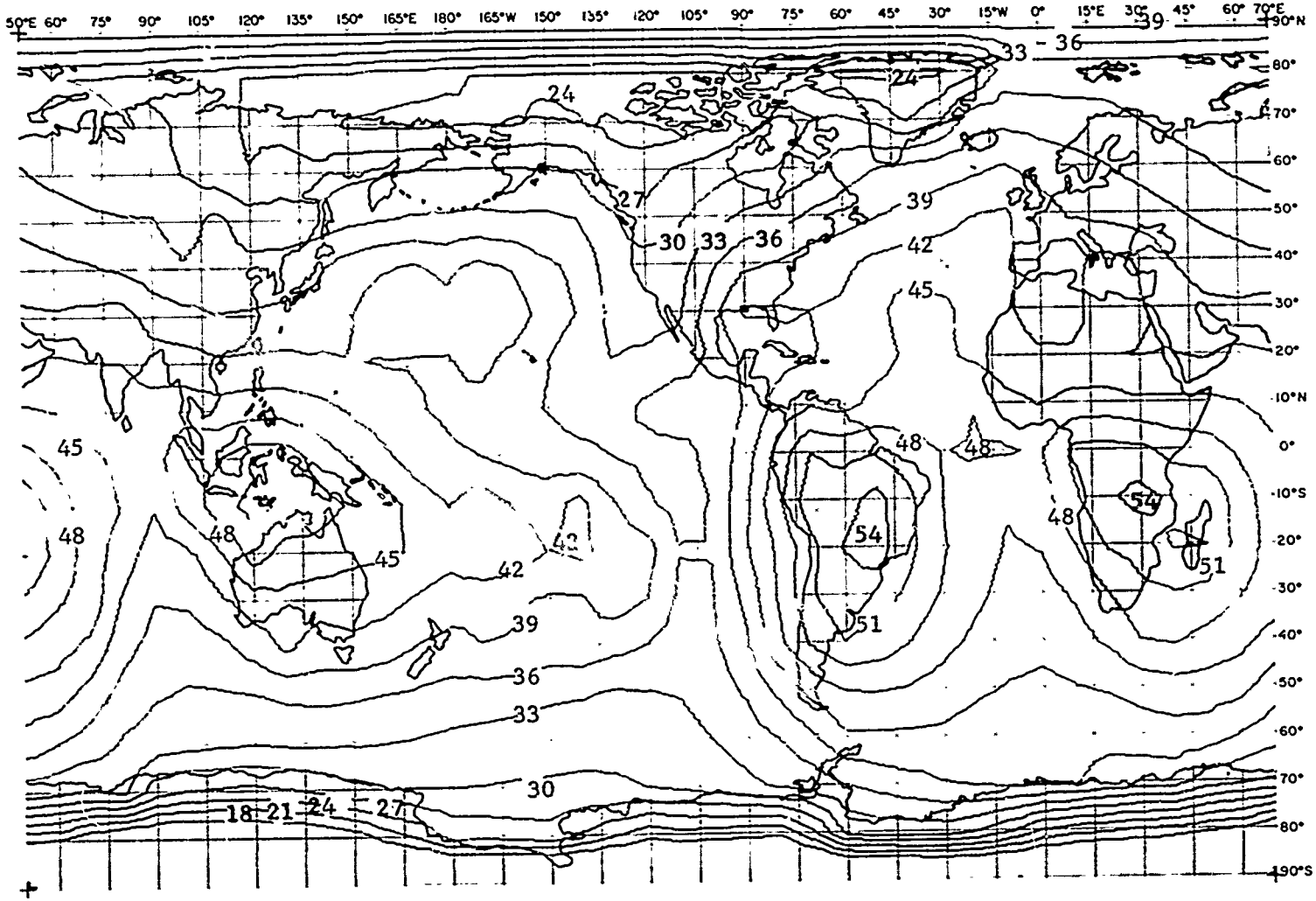


Fig. 7 - Atmospheric noise contours (dB>1μv/m - 1 kHz BW) for 20 kHz (January, 0000 UT) using the NRL empirically refined version of the WGL model

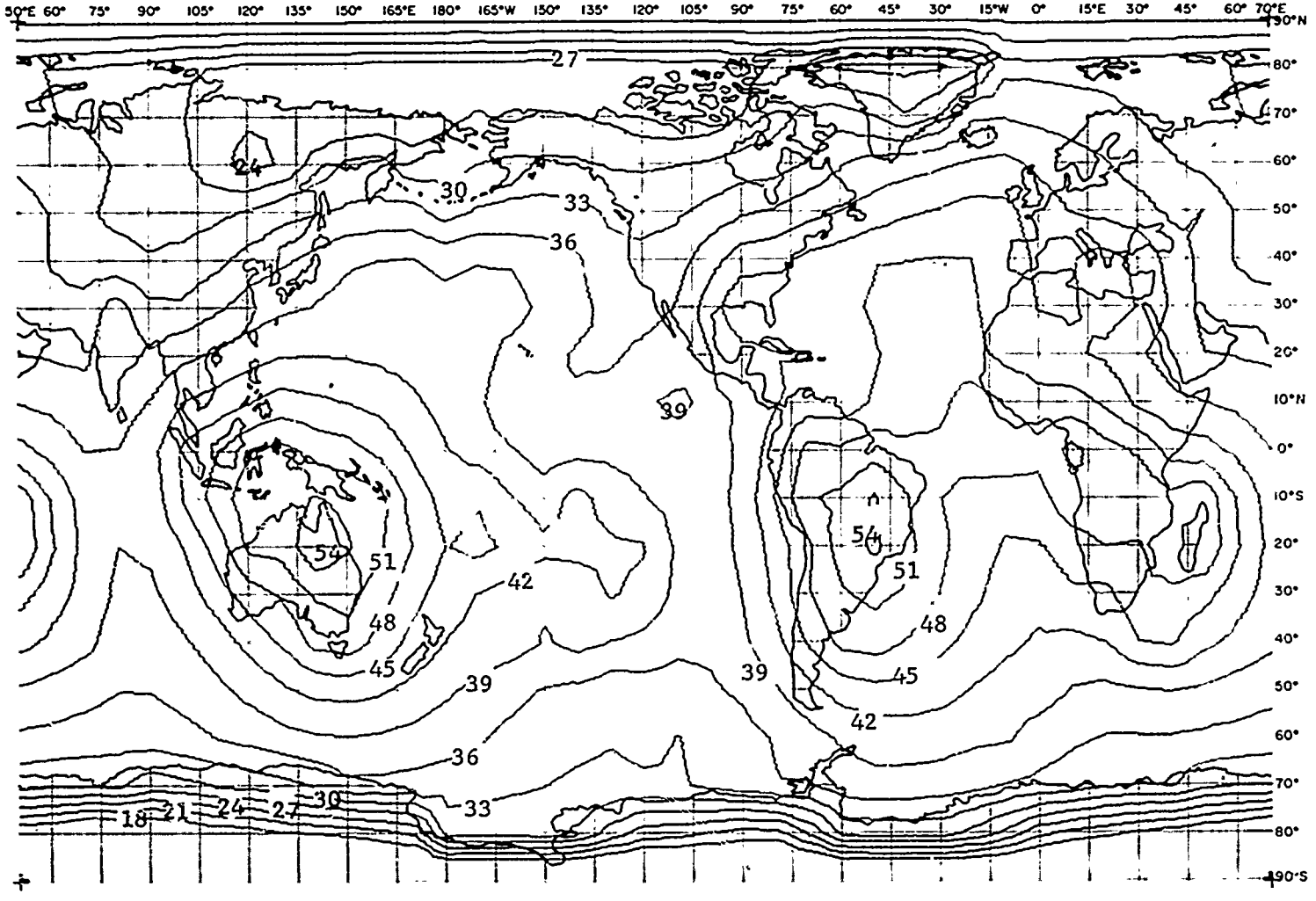


Fig. 8 - Atmospheric noise contours (dB>1μv/m - 1 kHz BW) for 20 kHz (January, 0400 UT) using the NRL empirically refined version of the WGL model

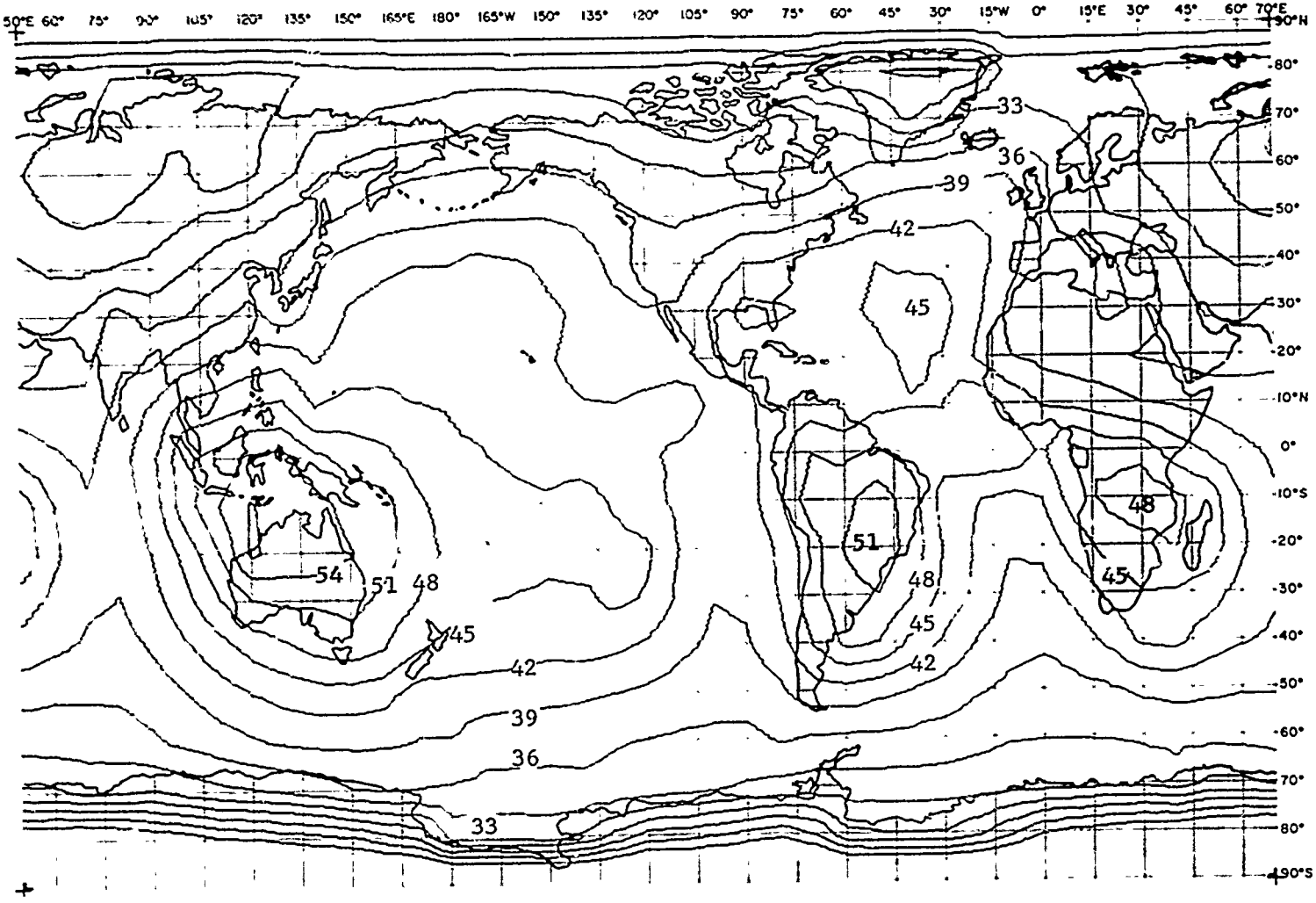


Fig. 9 - Atmospheric noise contours (dB>1μv/m - 1 kHz BW) for 20 kHz (January, 0800 UT) using the NRL empirically refined version of the WGL model

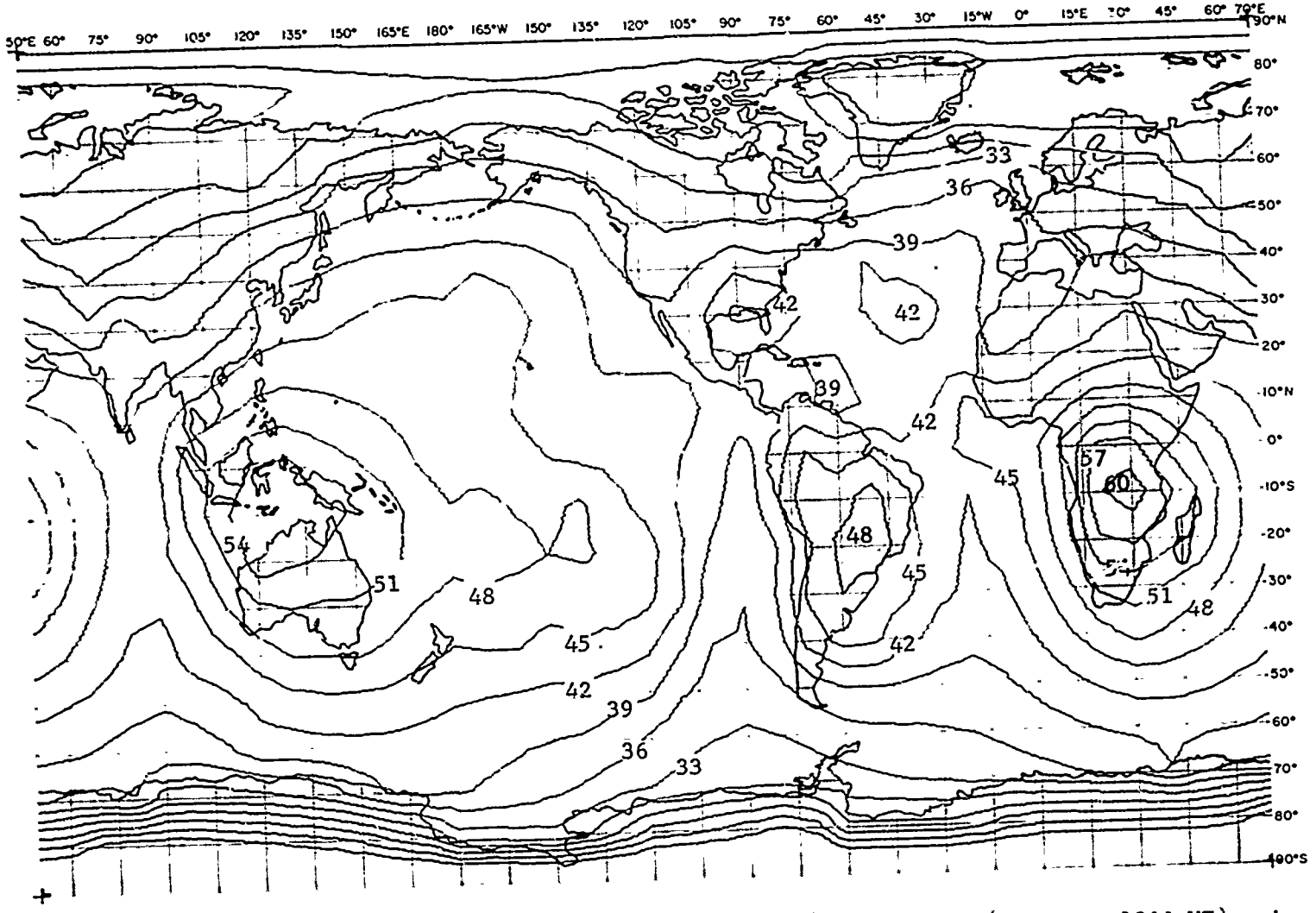


Fig. 10 - Atmospheric noise contours (dB>1μv/m - 1 kHz BW) for 20 kHz (January, 1200 UT) using the NRL empirically refined version of the WGL model

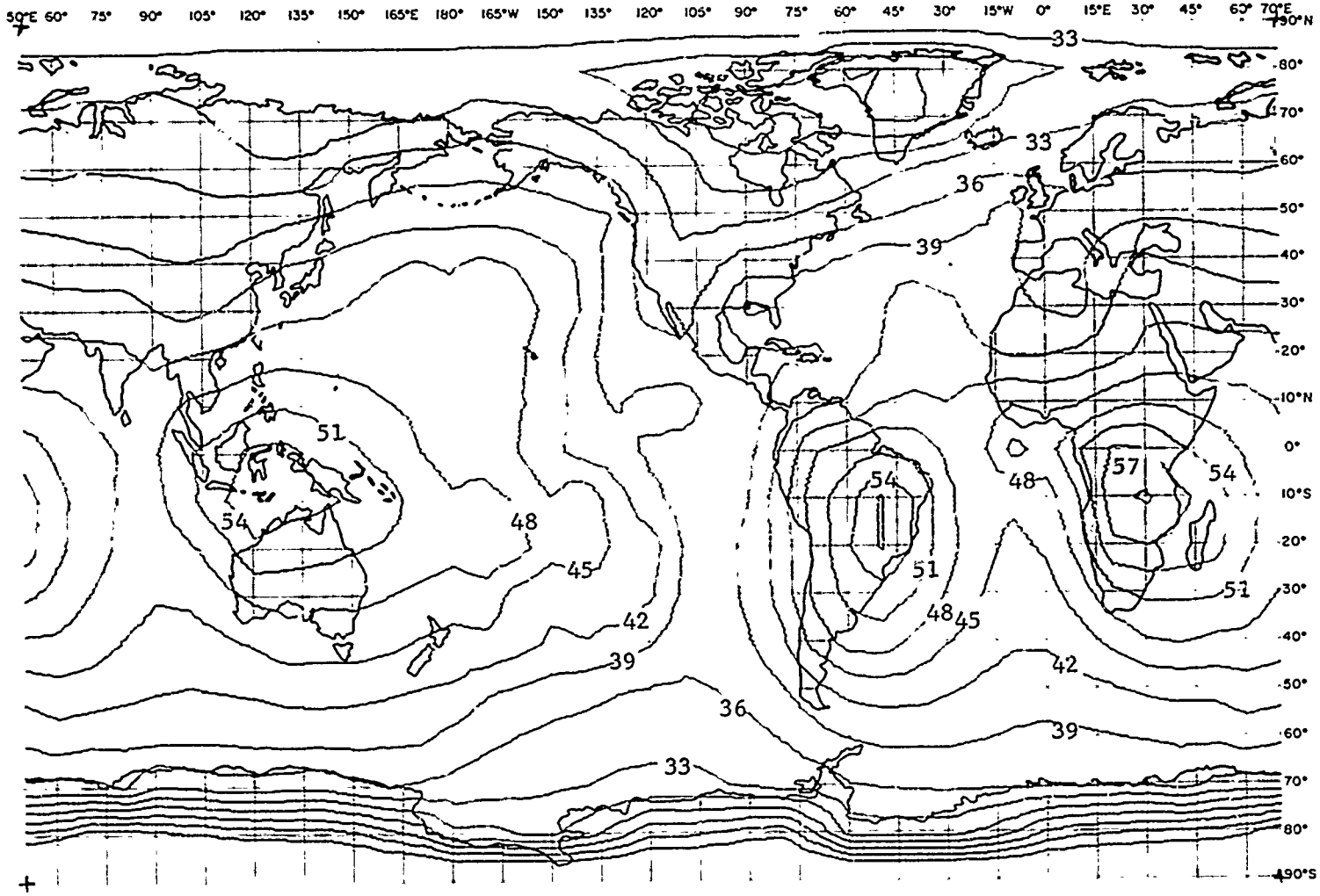


Fig. 11 - Atmospheric noise contours (dB>1μv/m - 1 kHz BW) for 20 kHz (January, 1600 UT) using the NRL empirically refined version of the WGL model

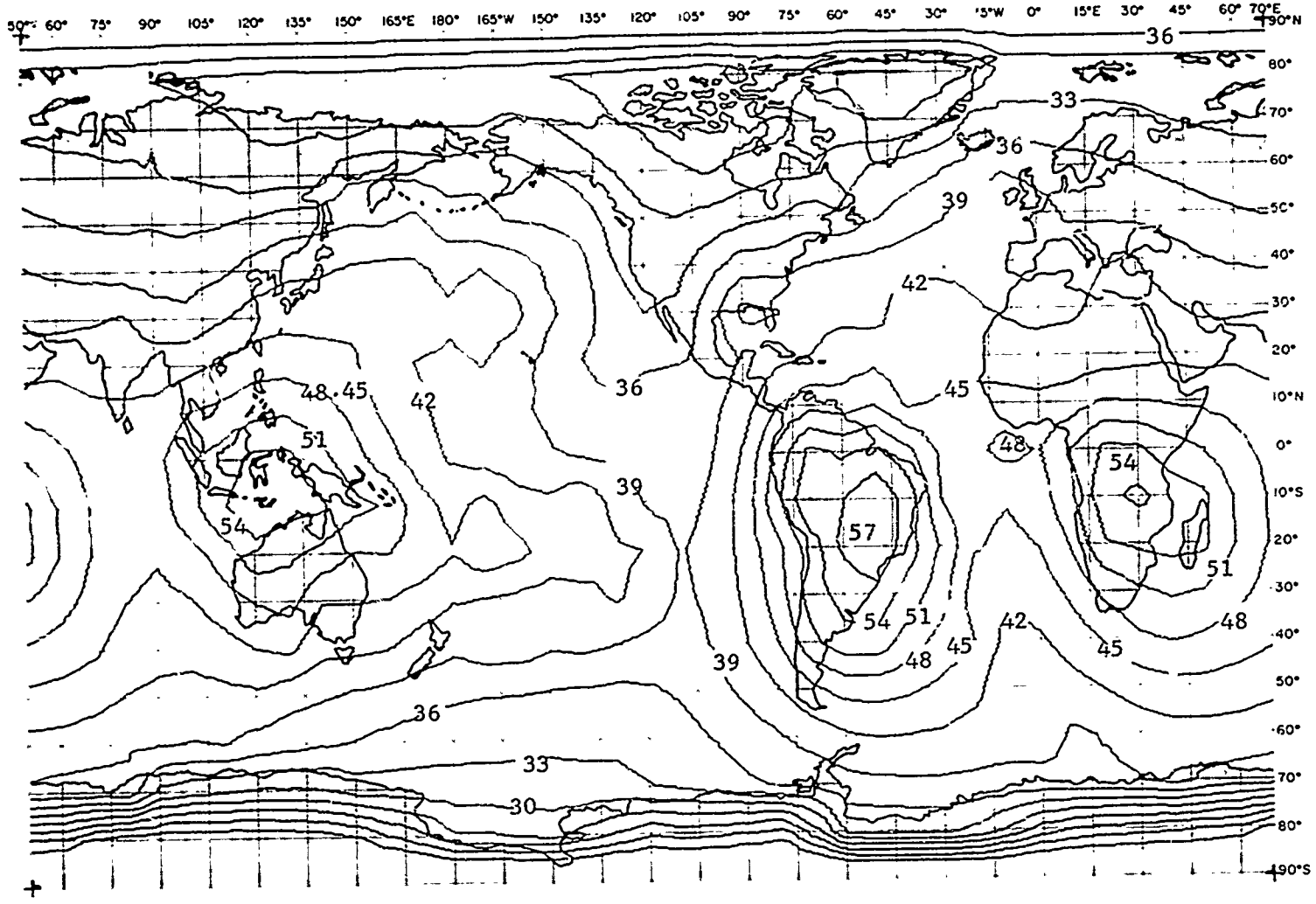


Fig. 12 - Atmospheric noise contours (dB>1μv/m - 1 kHz BW) for 20 kHz (January, 2000 UT) using the NRL empirically refined version of the WGL model

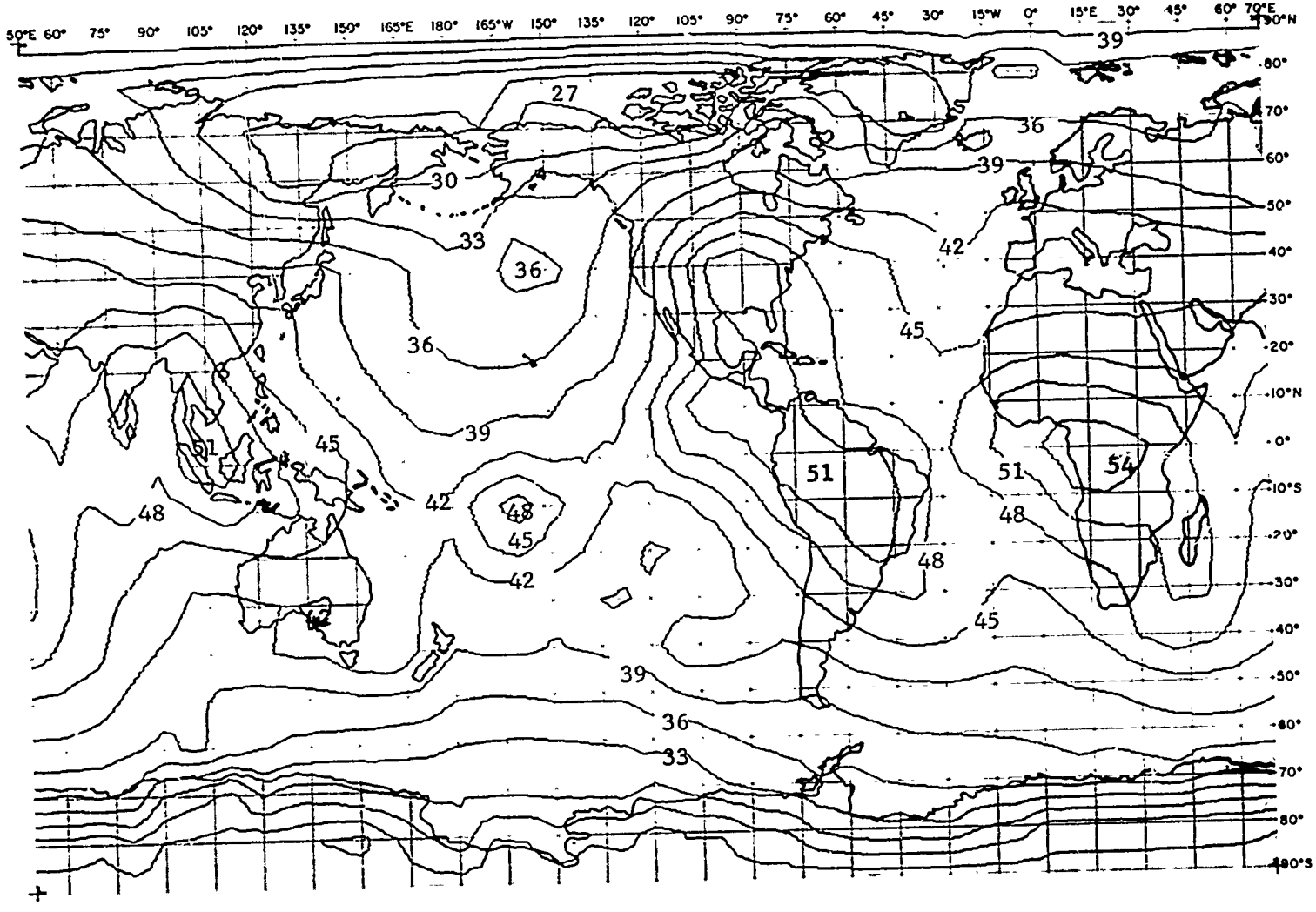


Fig. 13 - Atmospheric noise contours (dB>1μv/m - 1 kHz BW) for 20 kHz (April, 0000UT) using the NRL empirically refined version of the WGL model

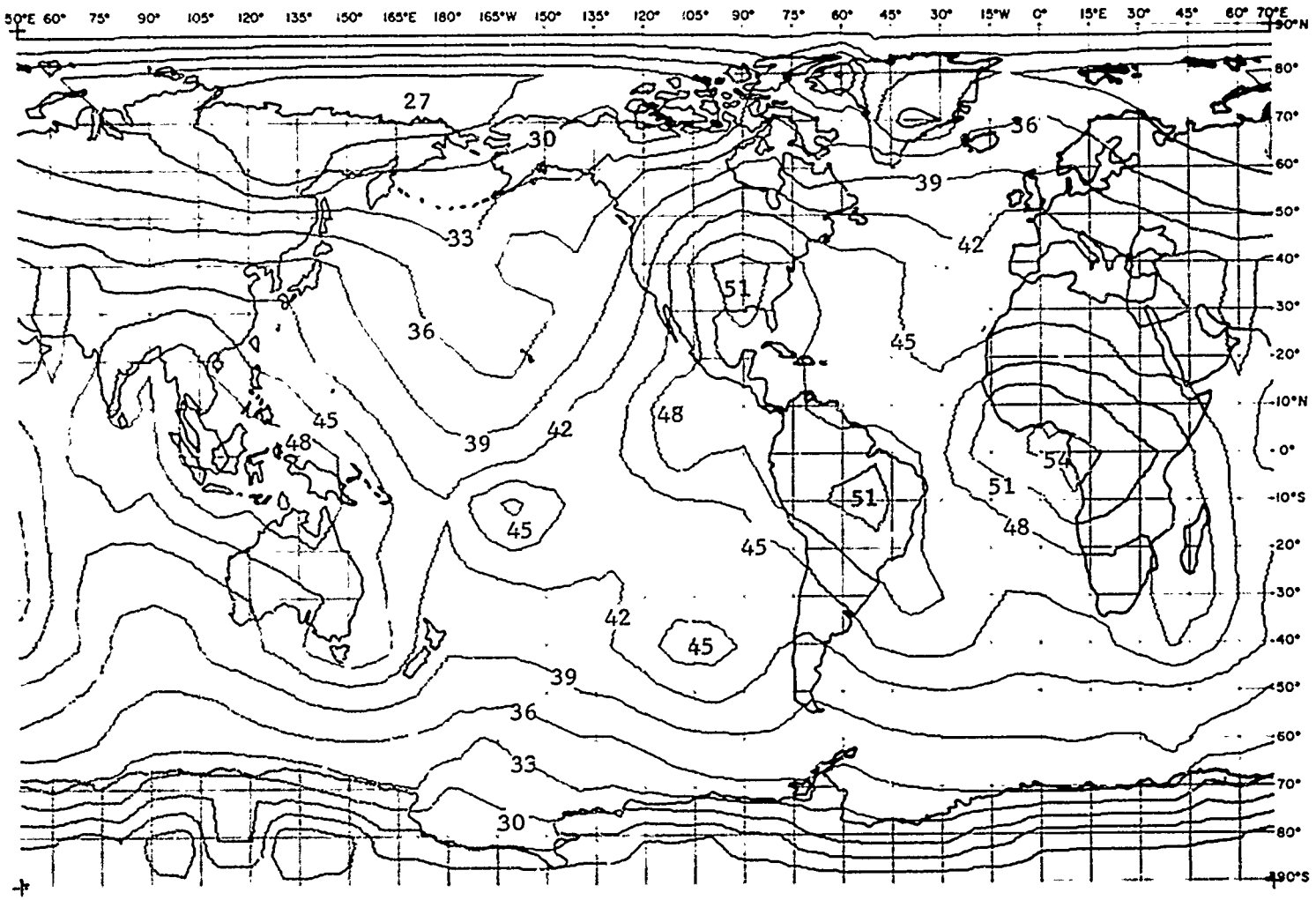


Fig. 14 - Atmospheric noise contours (dB>1μv/m - 1 kHz BW) for 20 kHz (April, 0400 UT) using the NRL empirically refined version of the WGL model

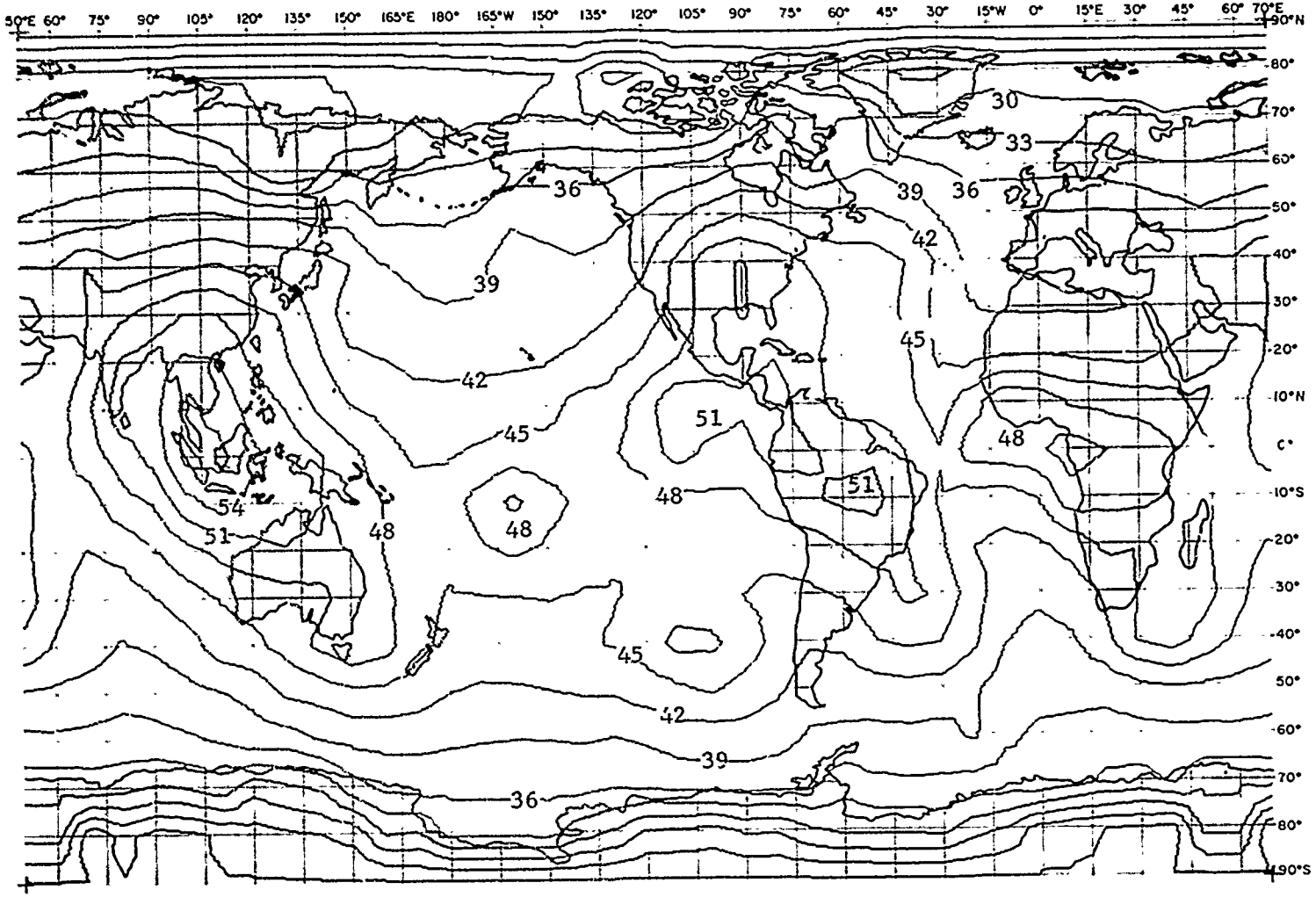


Fig. 15 - Atmospheric noise contours (dB>1μv/m - 1 kHz BW) for 20 kHz (April, 0800 UT) using the NRL empirically refined version of the WGL model

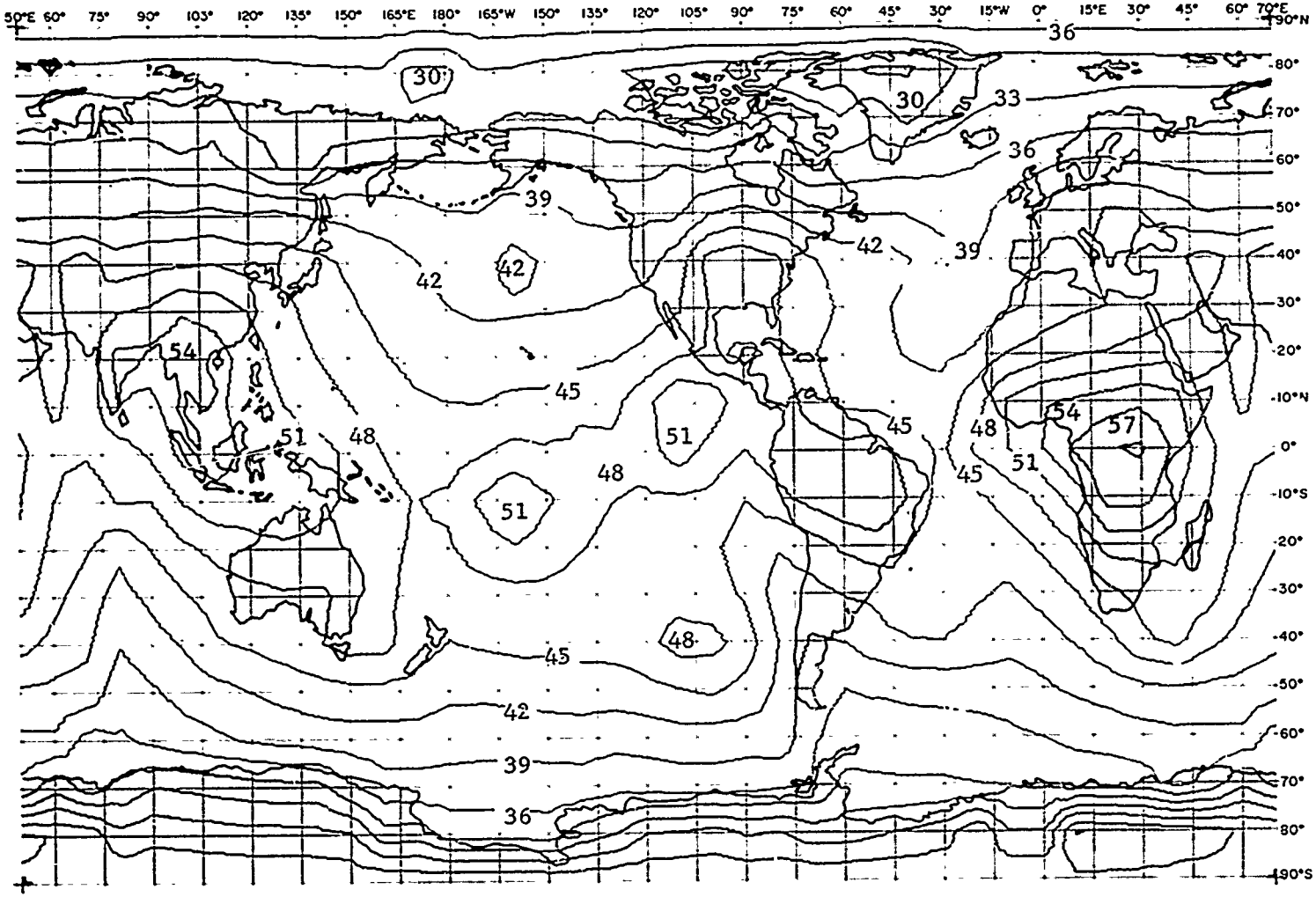


Fig. 16 - Atmospheric noise contours ($iB>1\mu v/m$ - 1 kHz BW) for 20 kHz (April, 1200 UT) using the NRL empirically refined version of the WGL model

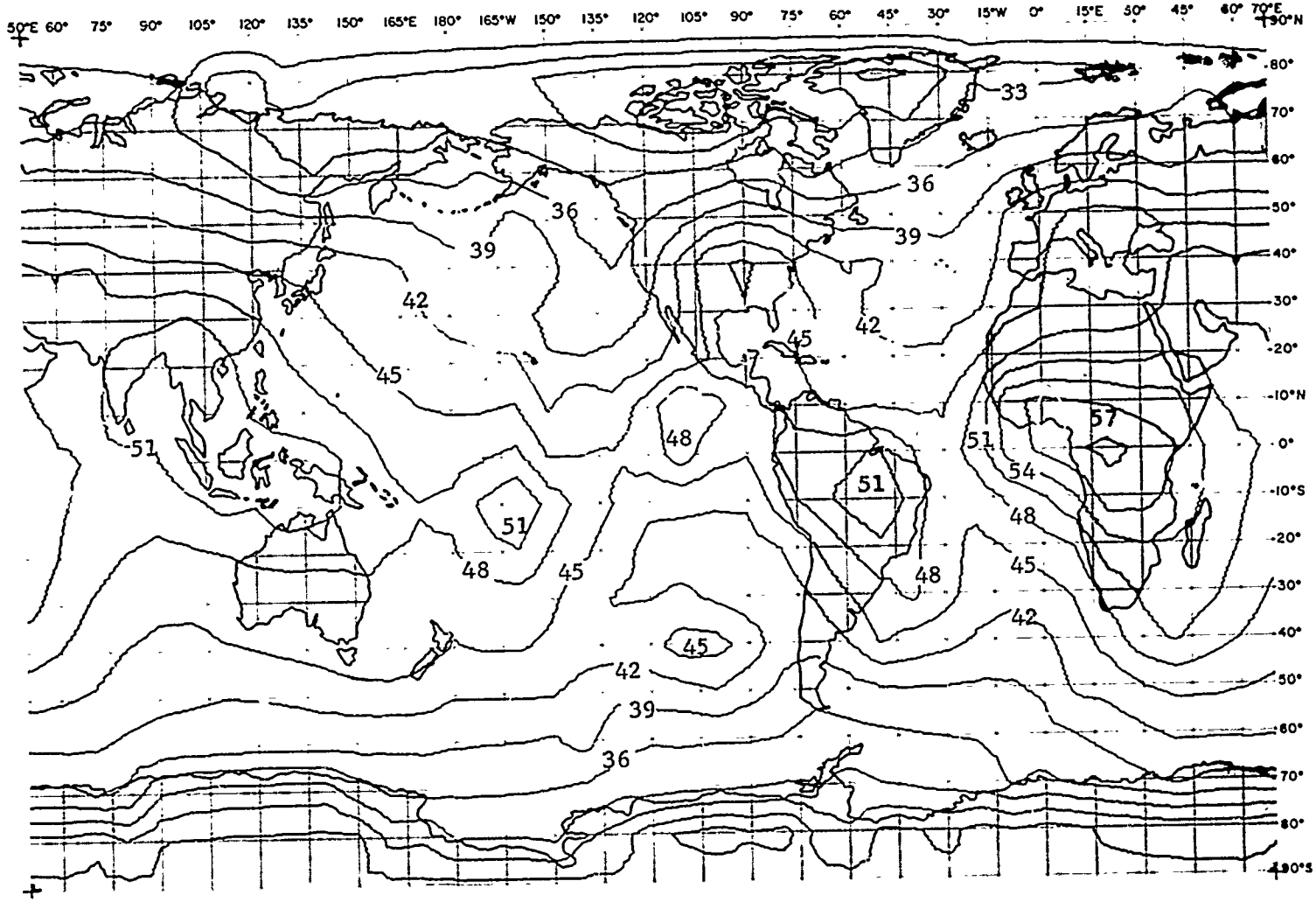


Fig. 17 - Atmospheric noise contours ($F_a$>1μv/m - 1 kHz BW) for 20 kHz (April, 1600 UT) using the NRL empirically refined version of the WGL model

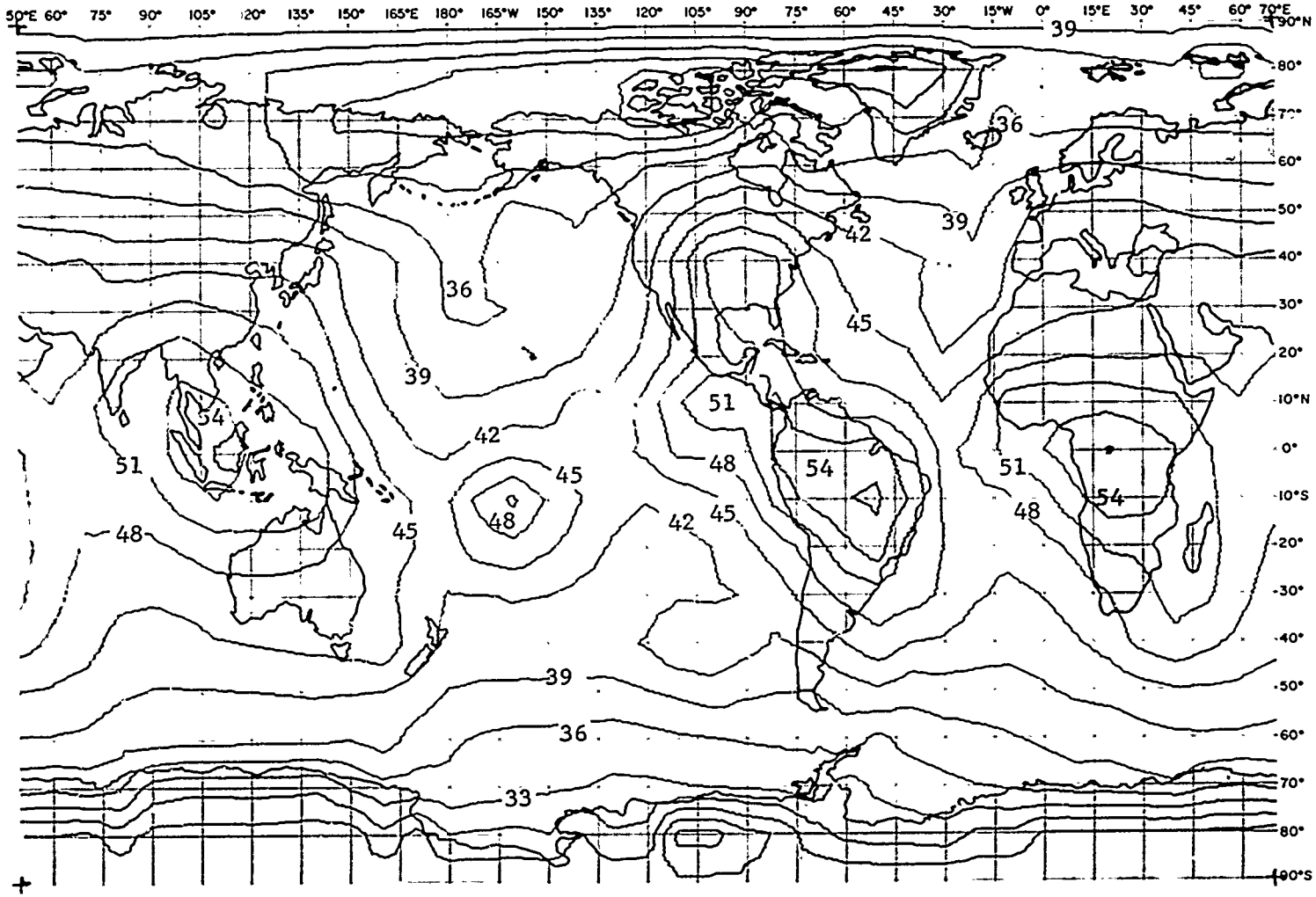


Fig. 18 - Atmospheric noise contours (dB>1μv/m - 1 kHz BW) for 20 kHz (April, 2000 UT) using the NRL empirically refined version of the WGL model

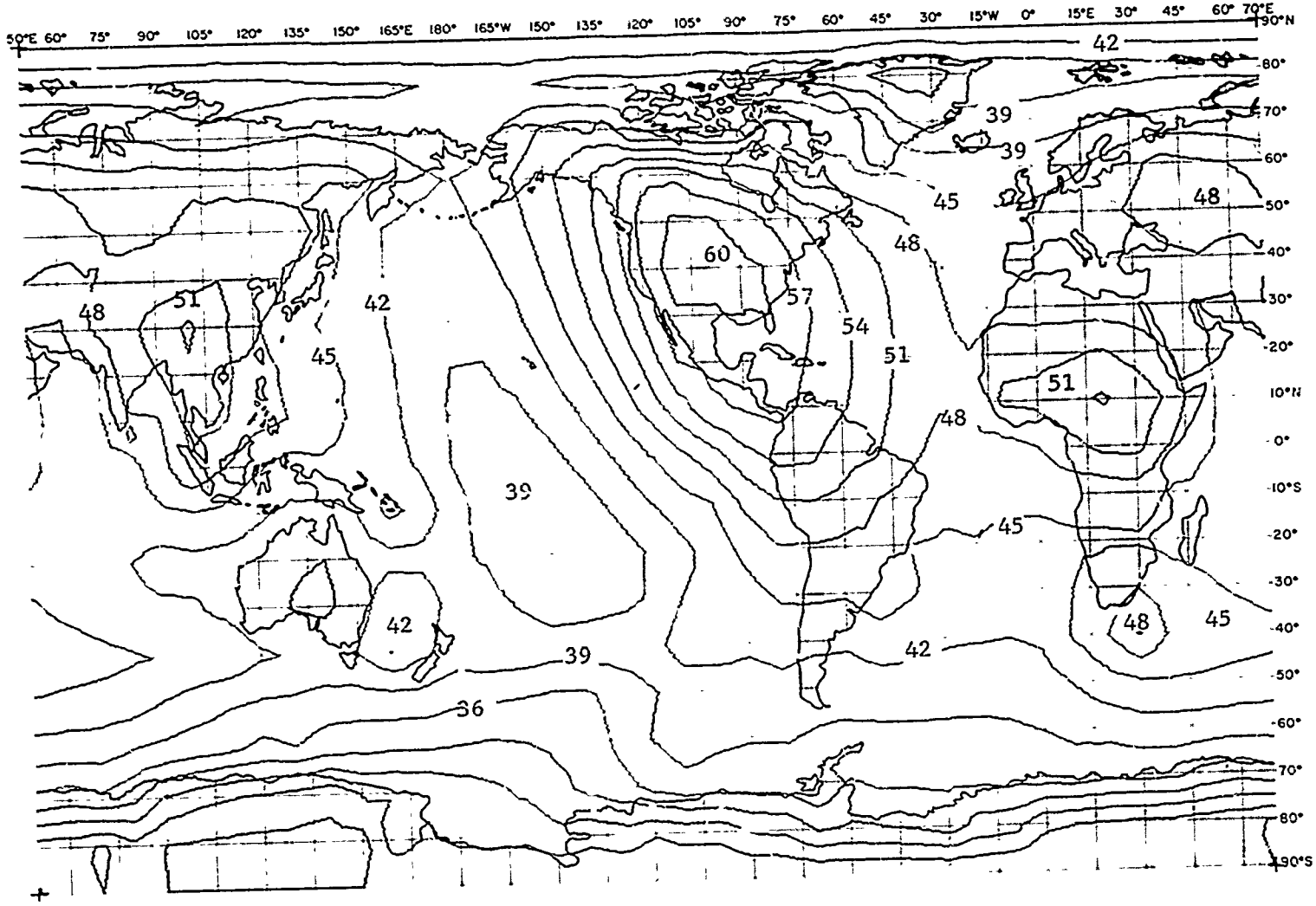


Fig. 19 - Atmospheric noise contours (dB>1μv/m - 1 kHz BW) for 20 kHz (July, 0000 UT) using the NRL empirically refined version of the WGL model

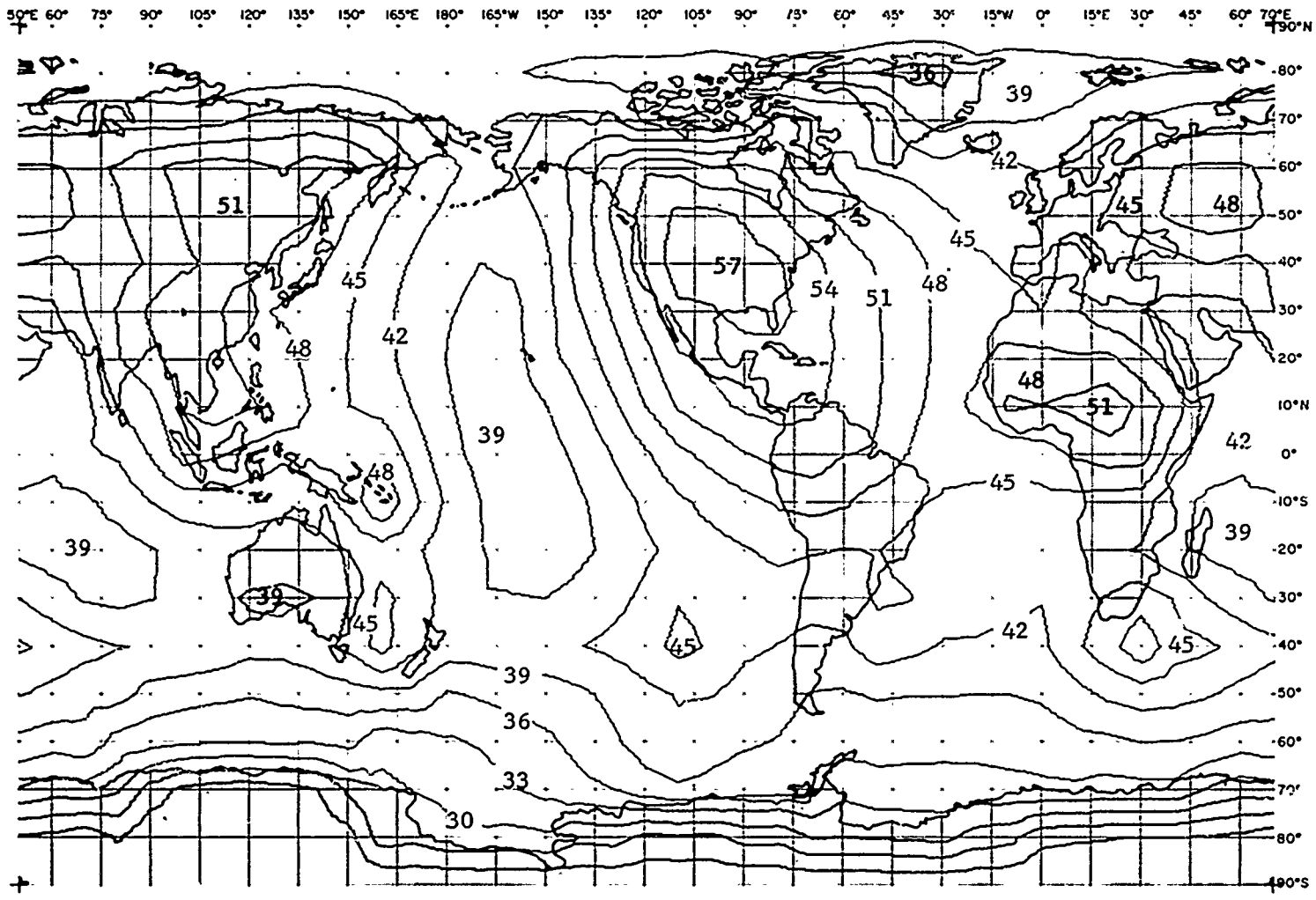


Fig. 20 - Atmospheric noise contours (iB>1μv/m - 1 kHz BW) for 20 kHz (July, 0400 UT) using the NRL empirically refined version of the WGL model

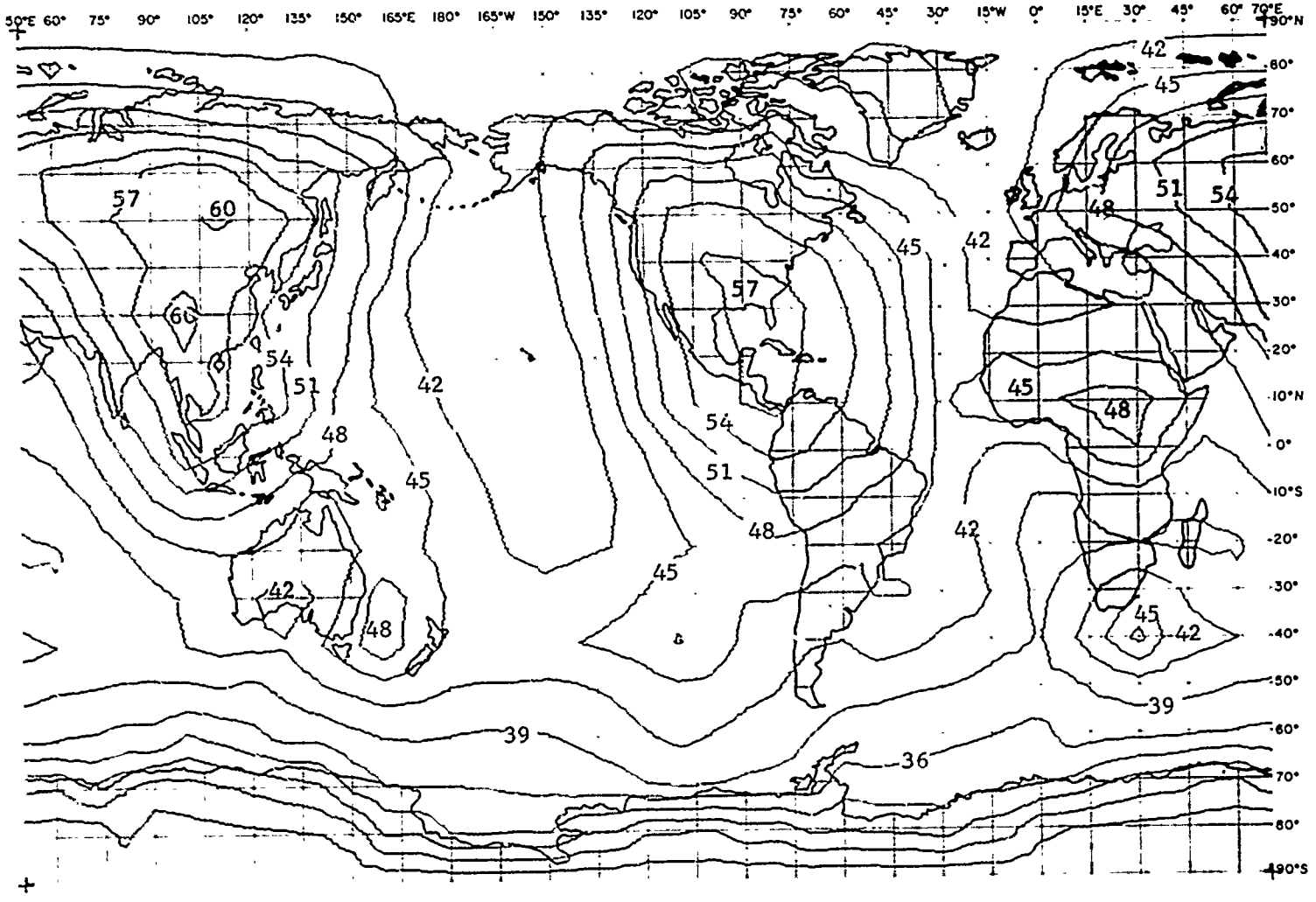


Fig. 21 - Atmospheric noise contours (dB>1uv/m - 1 kHz BW) for 20 kHz (July, 0300 UT) using the NRL empirically refined version of the NGL model

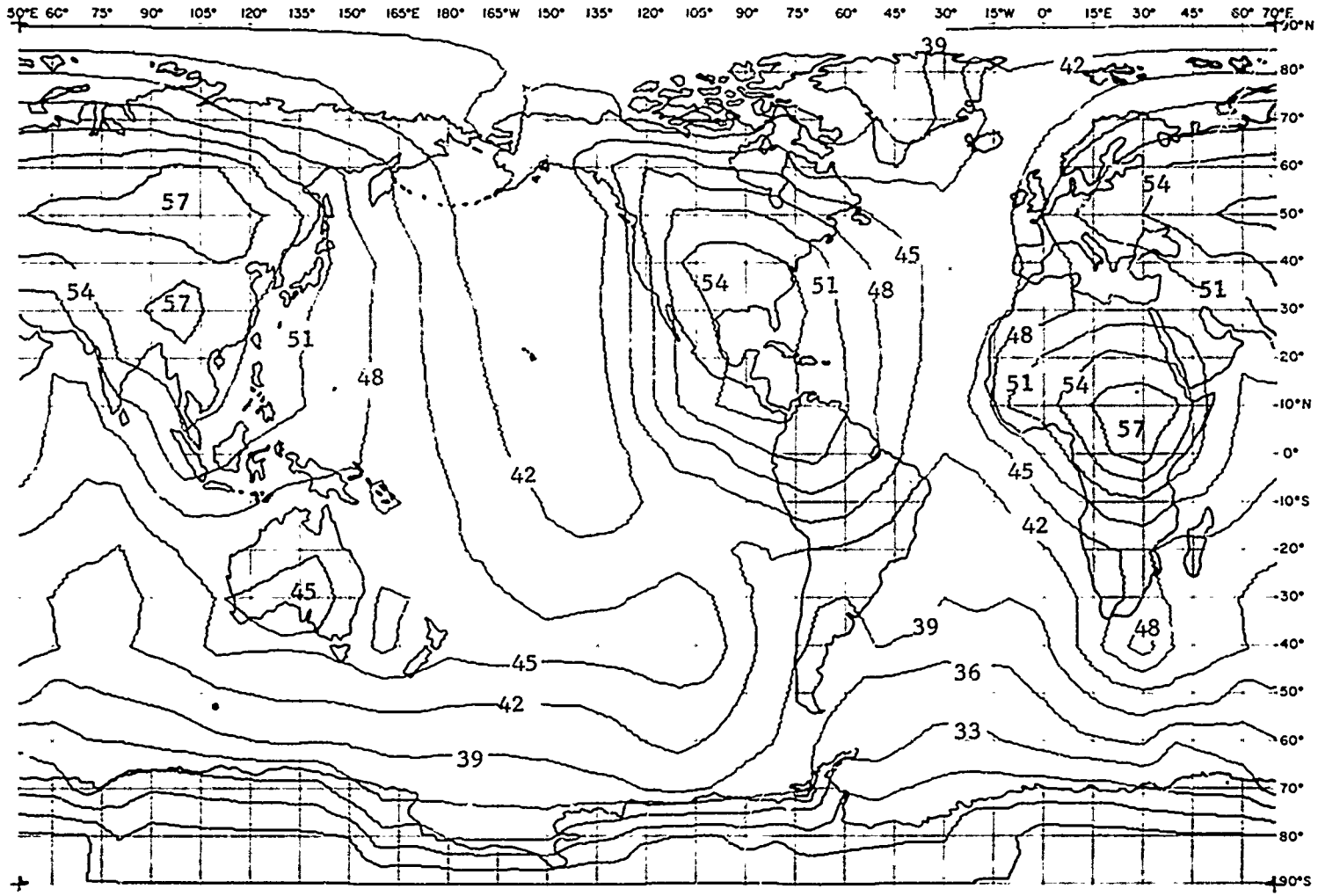


Fig. 22 - Atmospheric noise contours ($dB>1\mu v/m$ - 1 kHz BW) for 20 kHz (July, 1200 UT) using the NRL empirically refined version of the WGL model

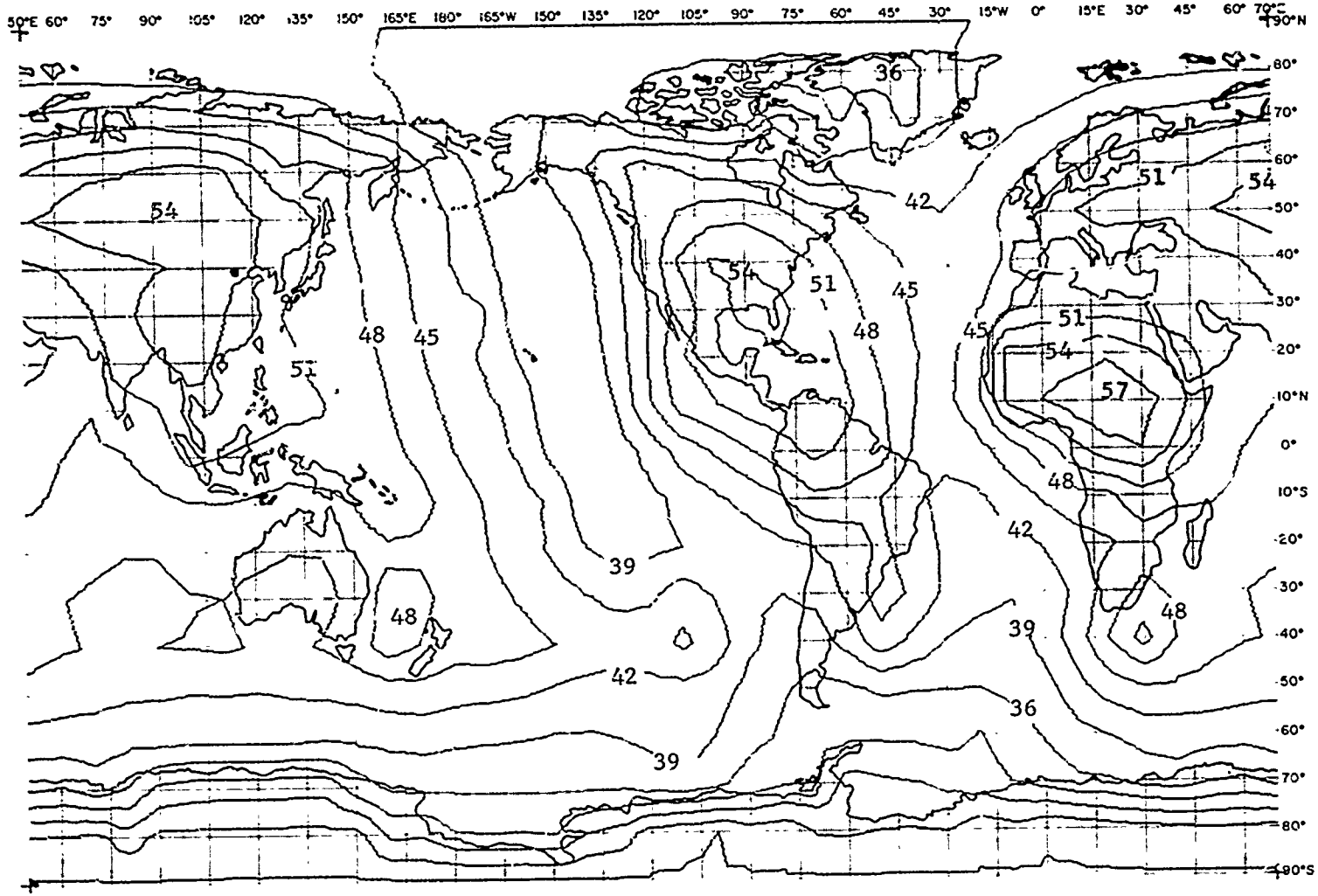


Fig. 23 - Atmospheric noise contours (dB>luv/m - 1 kHz BW) for 20 kHz (July, 1600 UT) using the NRL empirically refined version of the WGL model

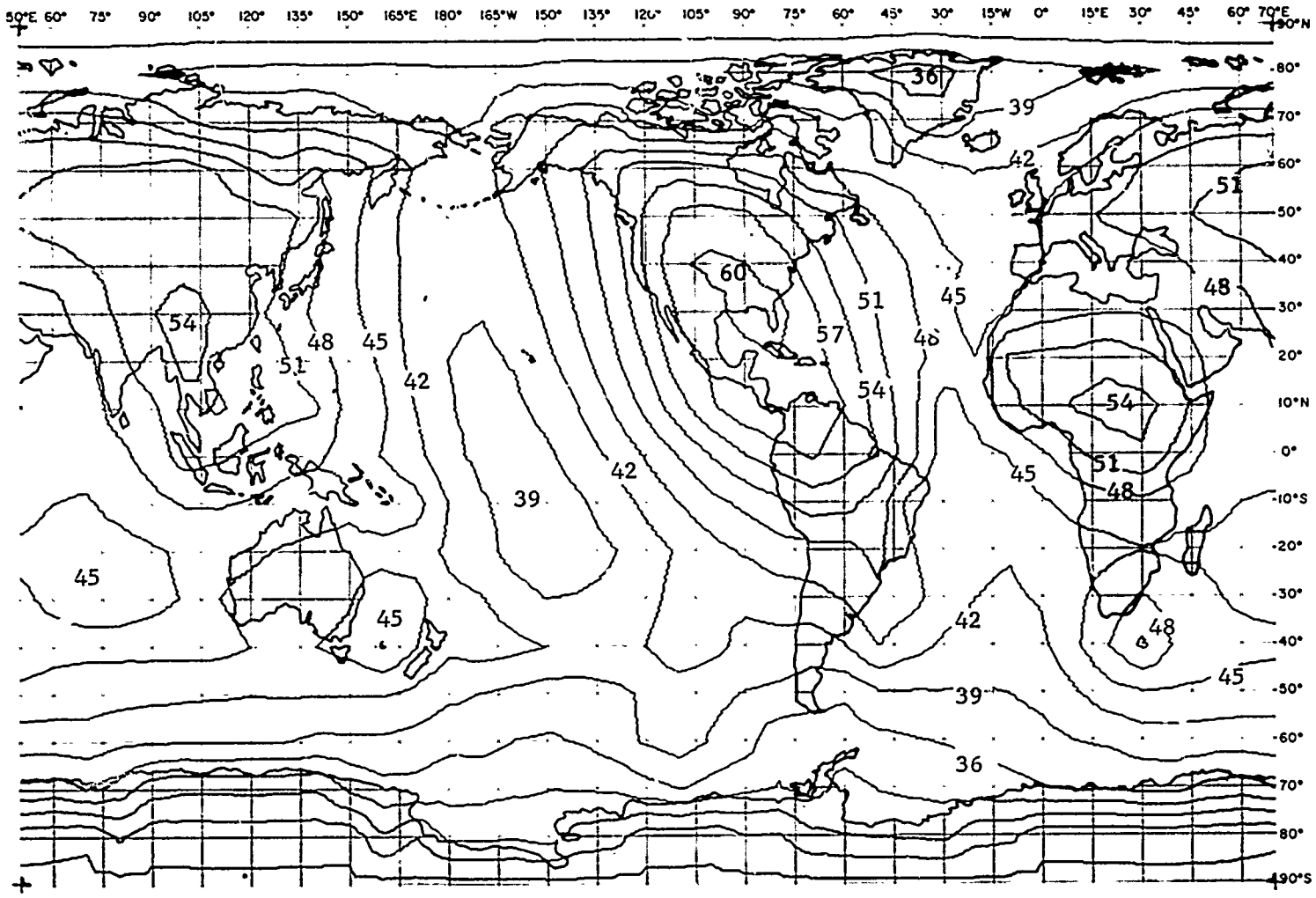


Fig. 24 - Atmospheric noise contours (iB>1μv/m - 1 kHz BW) for 20 kHz (July, 2000 UT) using the NRL empirically refined version of the WGL model

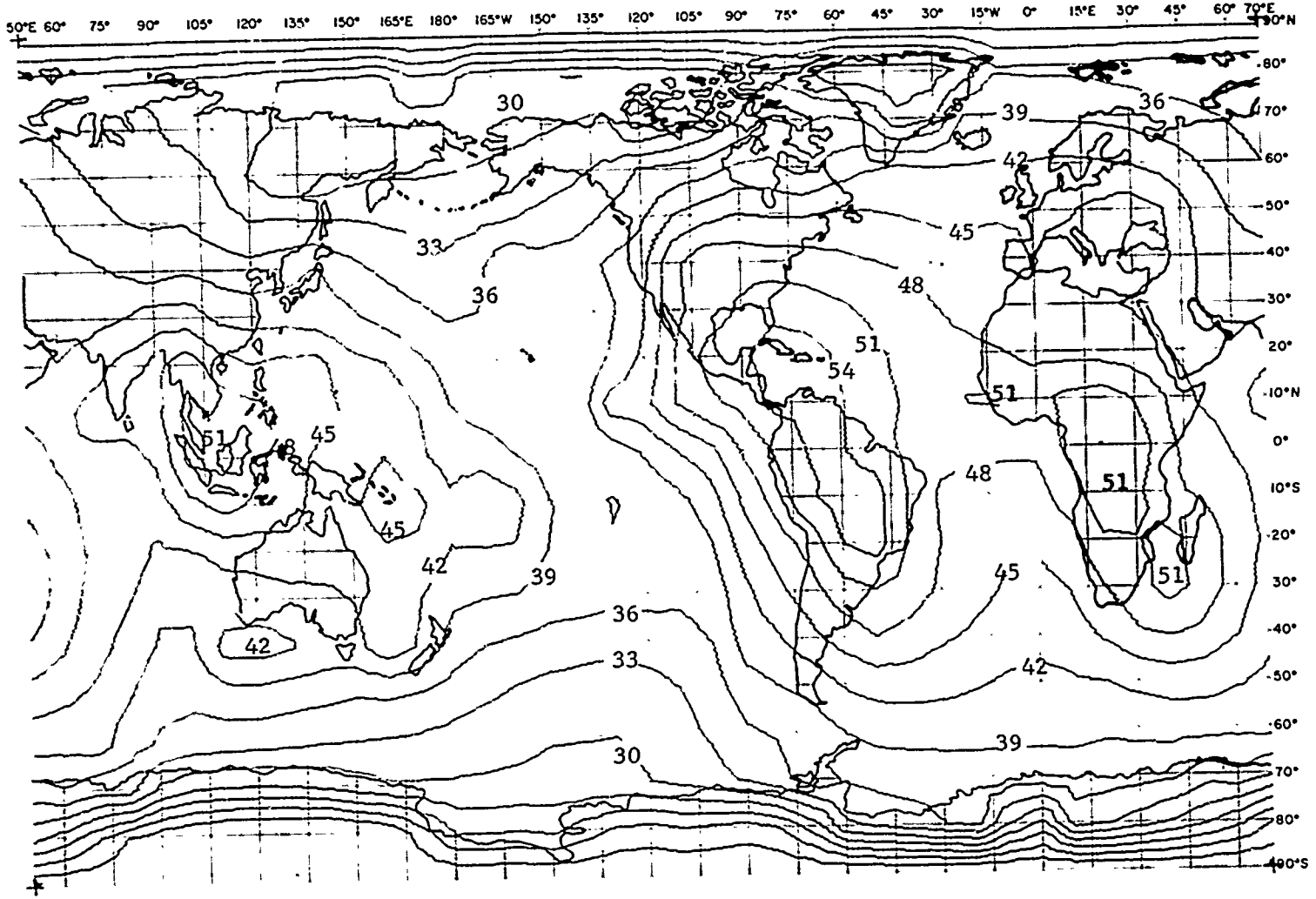


Fig. 25 - Atmospheric noise contours (dB>1μv/m - 1 kHz BW) for 20 kHz (October, 0000 UT) using the NRL empirically refined version of the WGL model

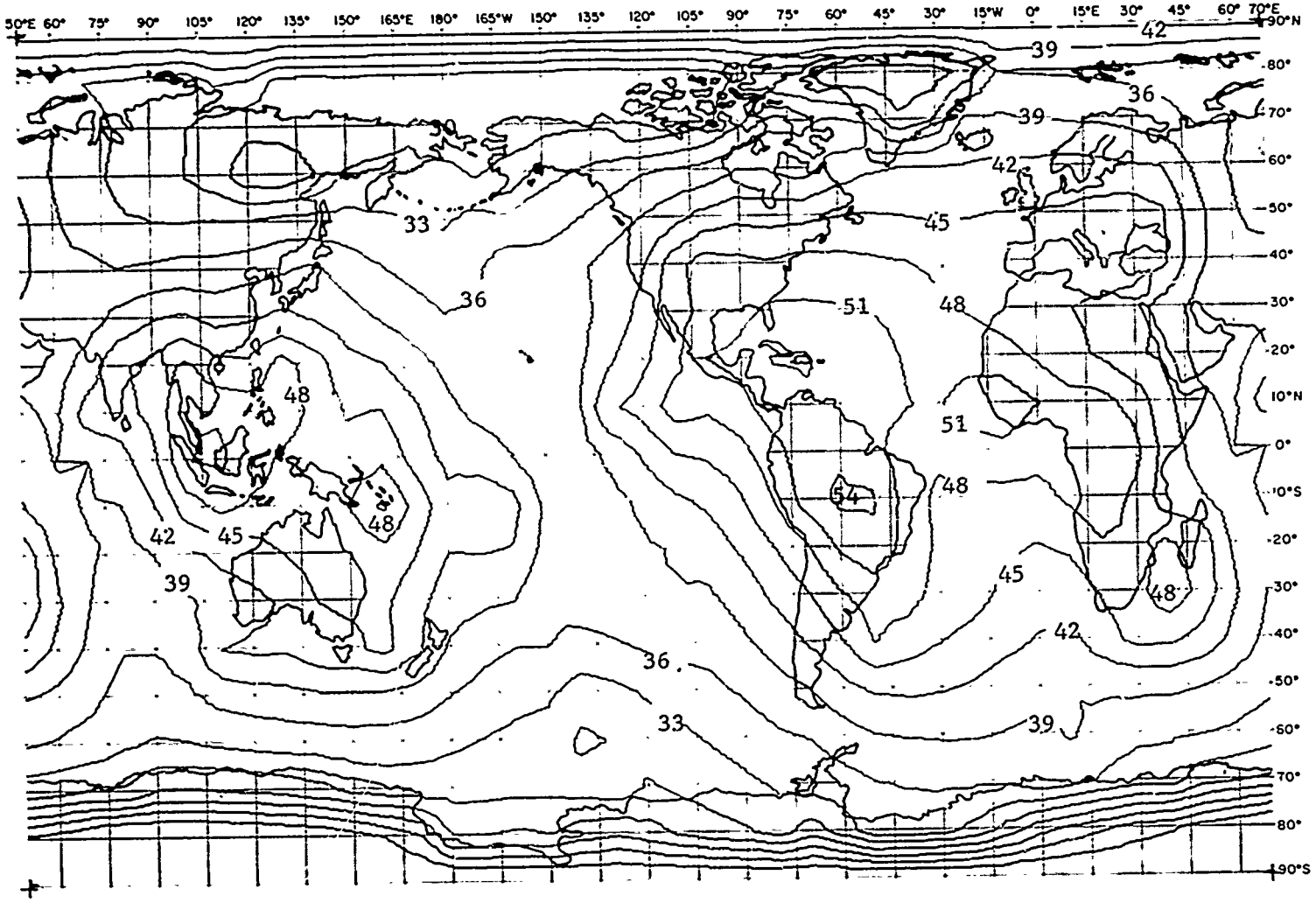


Fig. 26 - Atmospheric noise contours (dB>1μv/m - 1 kHz BW) for 20 kHz (October, 0400 UT) using the NRL empirically refined version of the WGL model

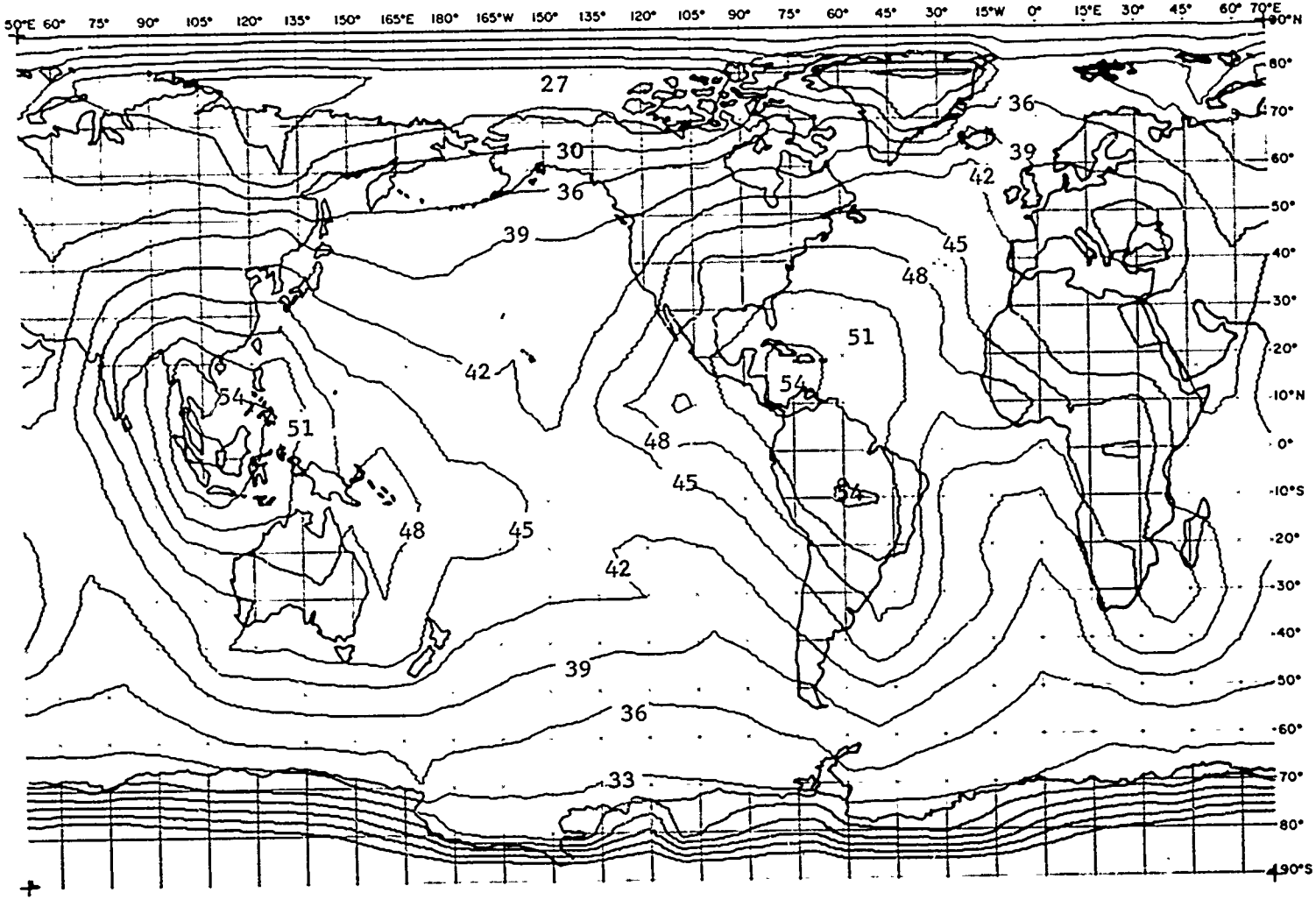


Fig. 27 - Atmospheric noise contours (dB>1μv/m - 1 kHz BW) for 20 kHz (October, 0800 UT) using the NRL empirically refined version of the WGL model

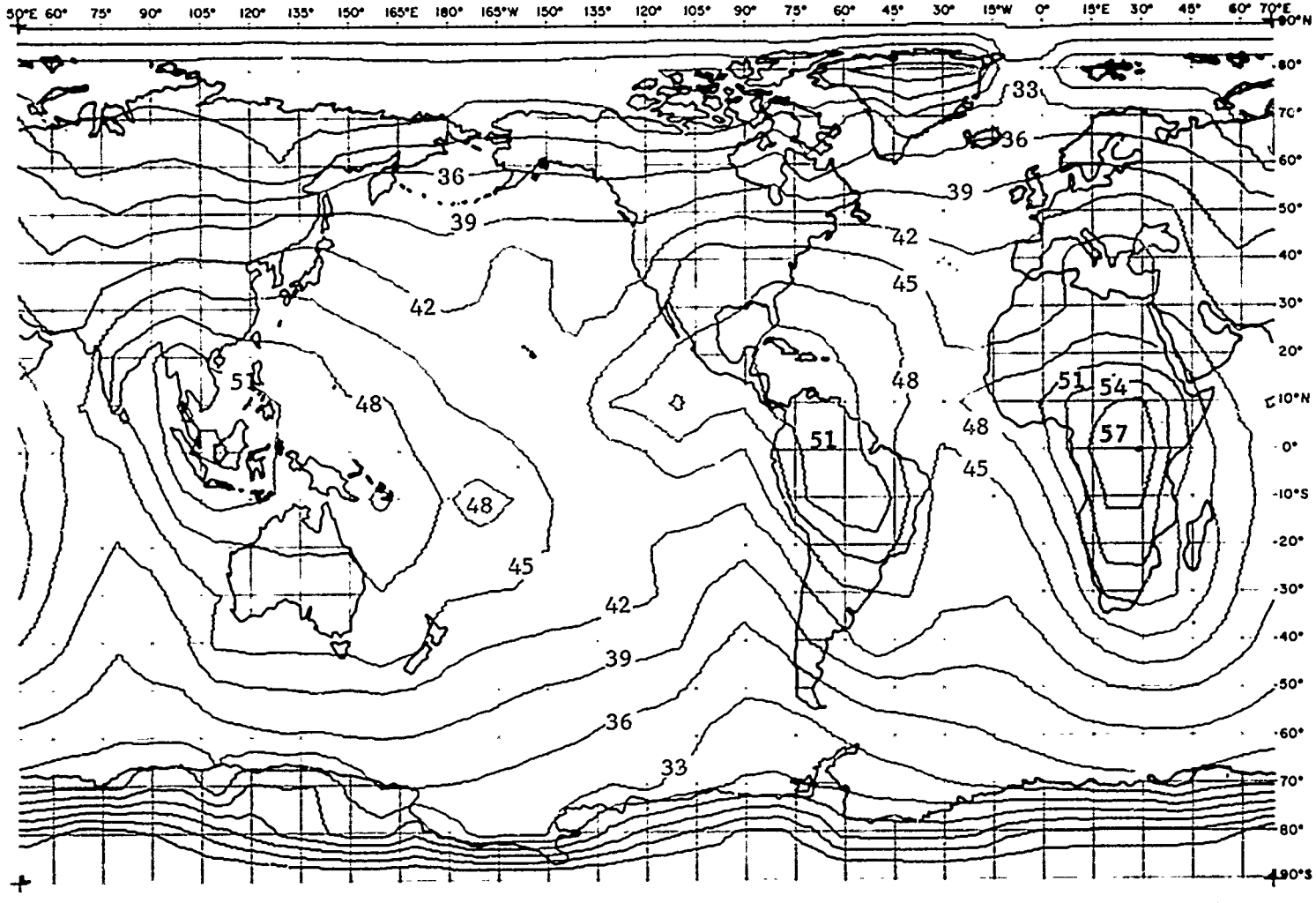


Fig. 28 - Atmospheric noise contours (dB>1μv/m - 1 kHz BW) for 20 kHz (October, 1200 UT) using the NRL empirically refined version of the WGL model

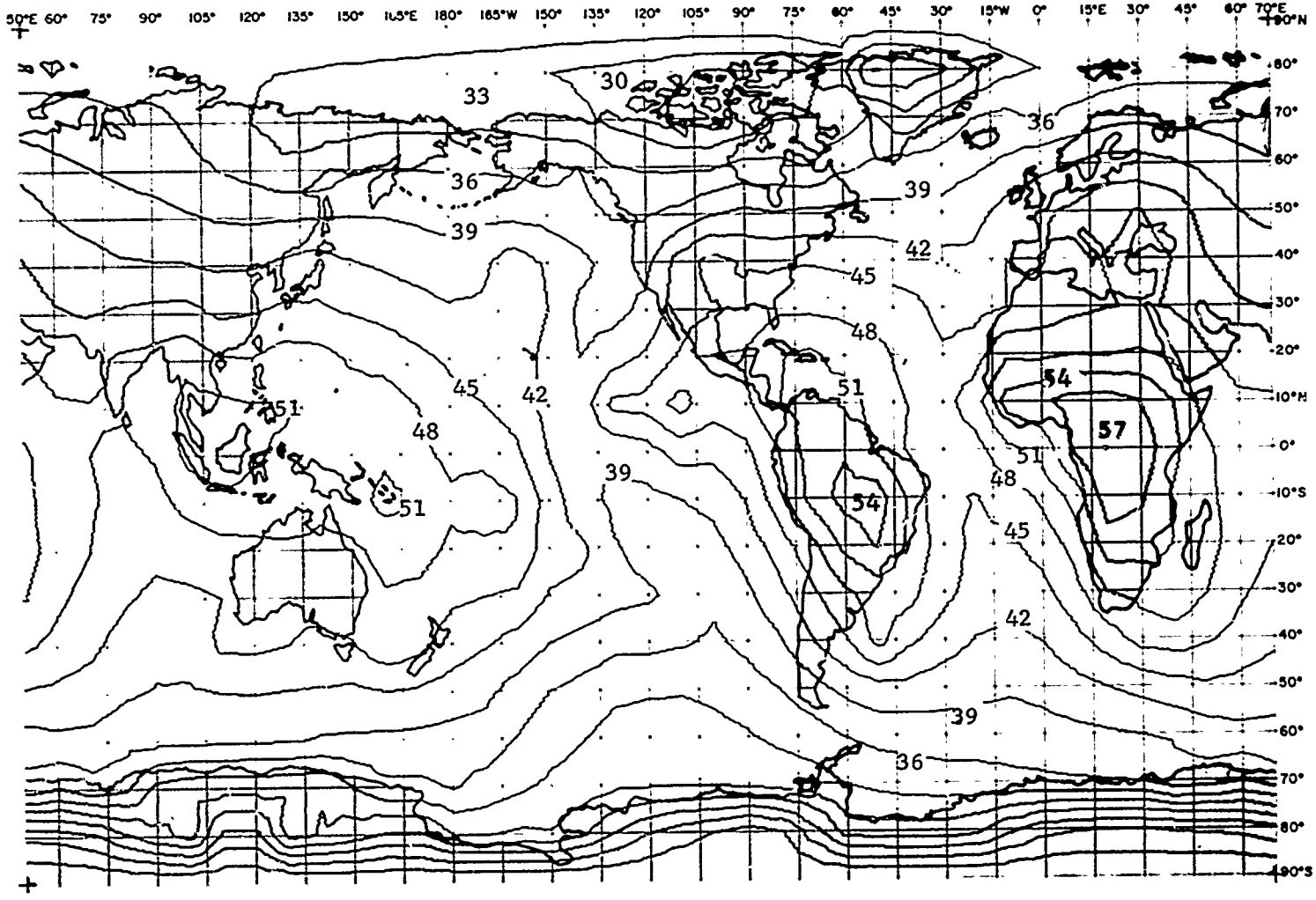


Fig. 29 - Atmospheric noise contours (dB>1μv/m - 1 kHz BW) for 20 kHz (October, 1600 UT) using the NRL empirically refined version of the WGL model

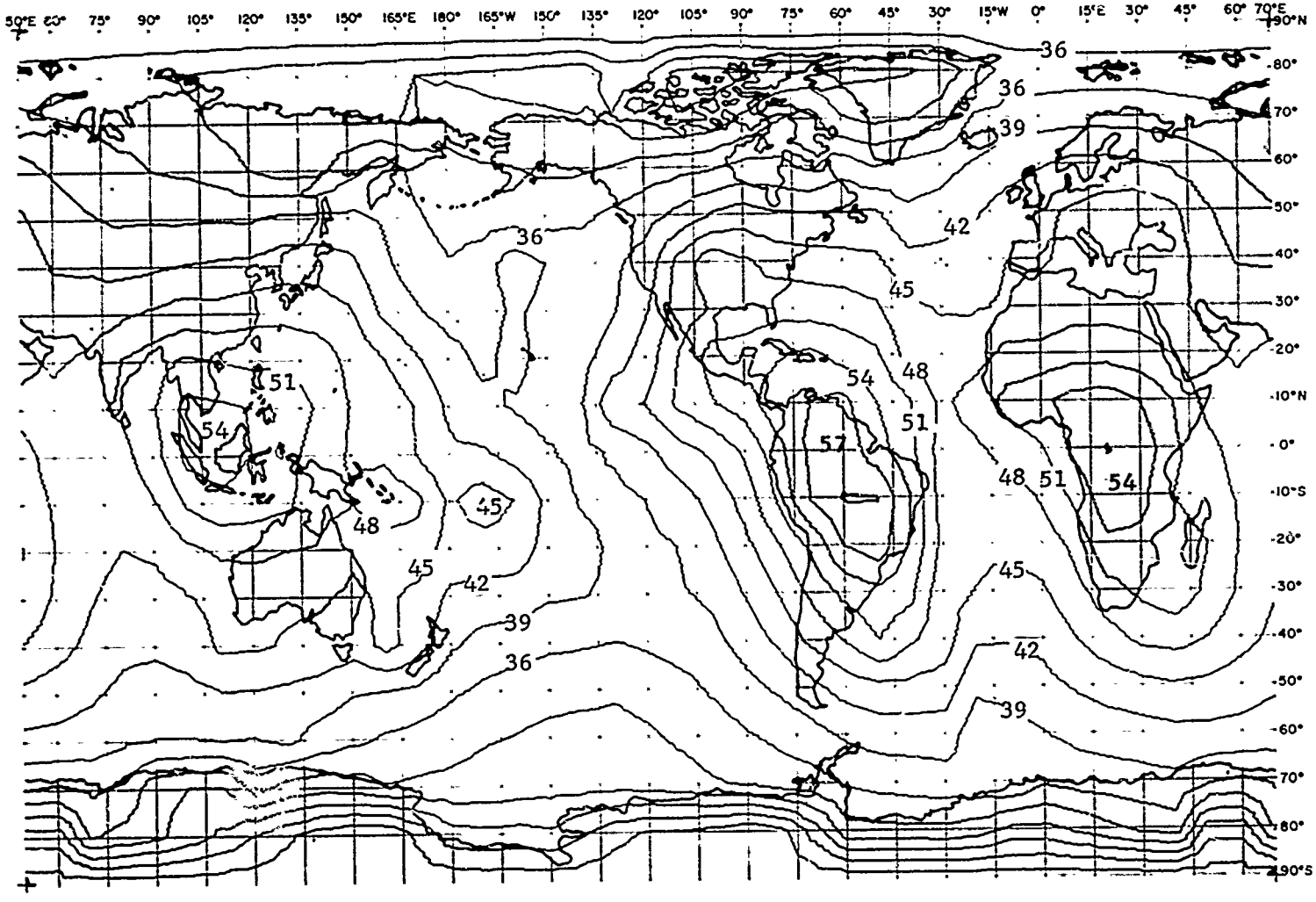


Fig. 30 - Atmospheric noise contours ($dB > 1\mu v/m$ - 1 kHz BW) for 20 kHz (October, 2000 UT) using the NRL empirically refined version of the WGL model

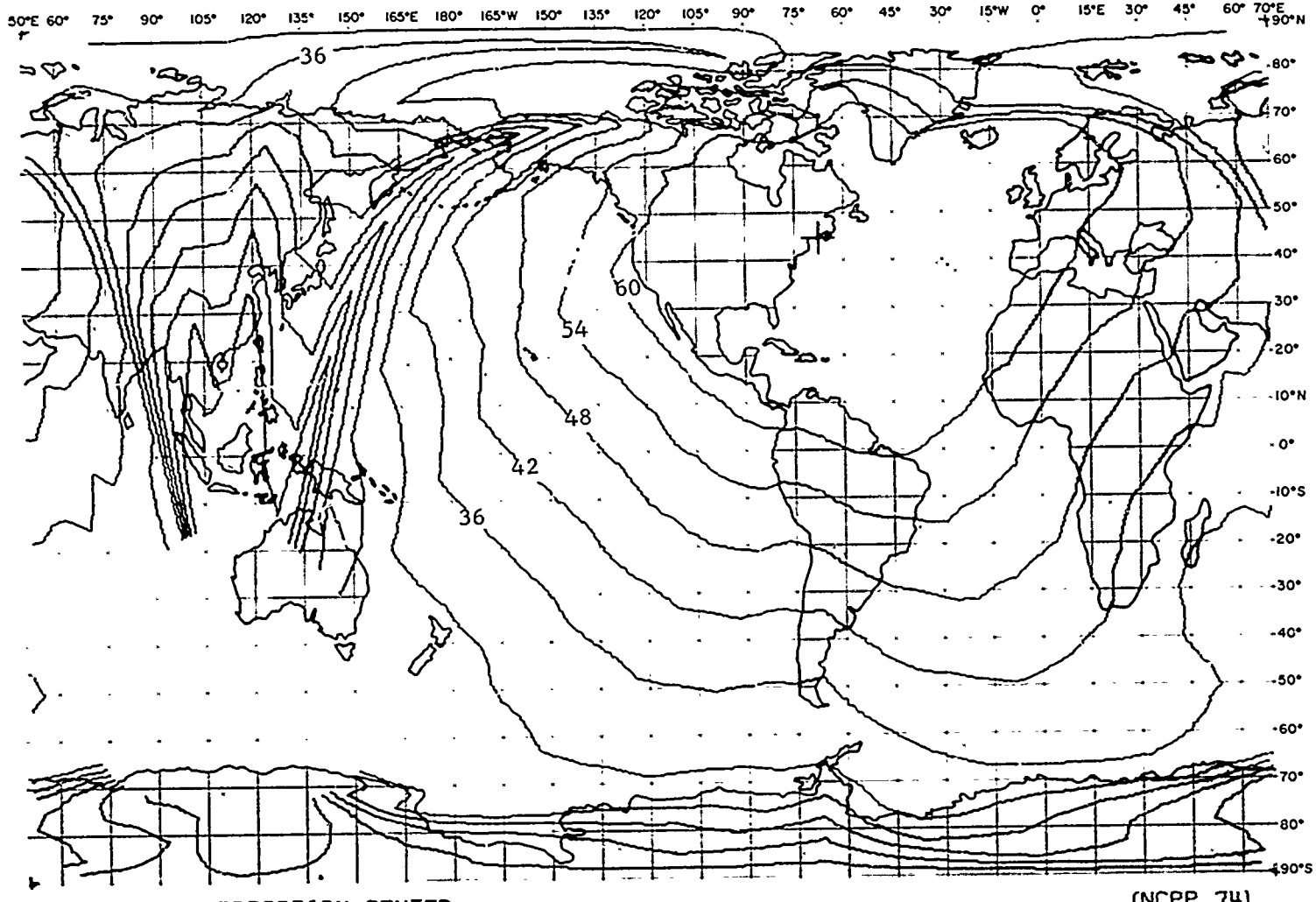


FIG. SU 1 - SIGNAL LEVEL CONTOURS IN dB>1UV/M
NAA (17.8KHZ, 1000KW) , CUTLER
SUMMER 90% TIME AVAILABILITY

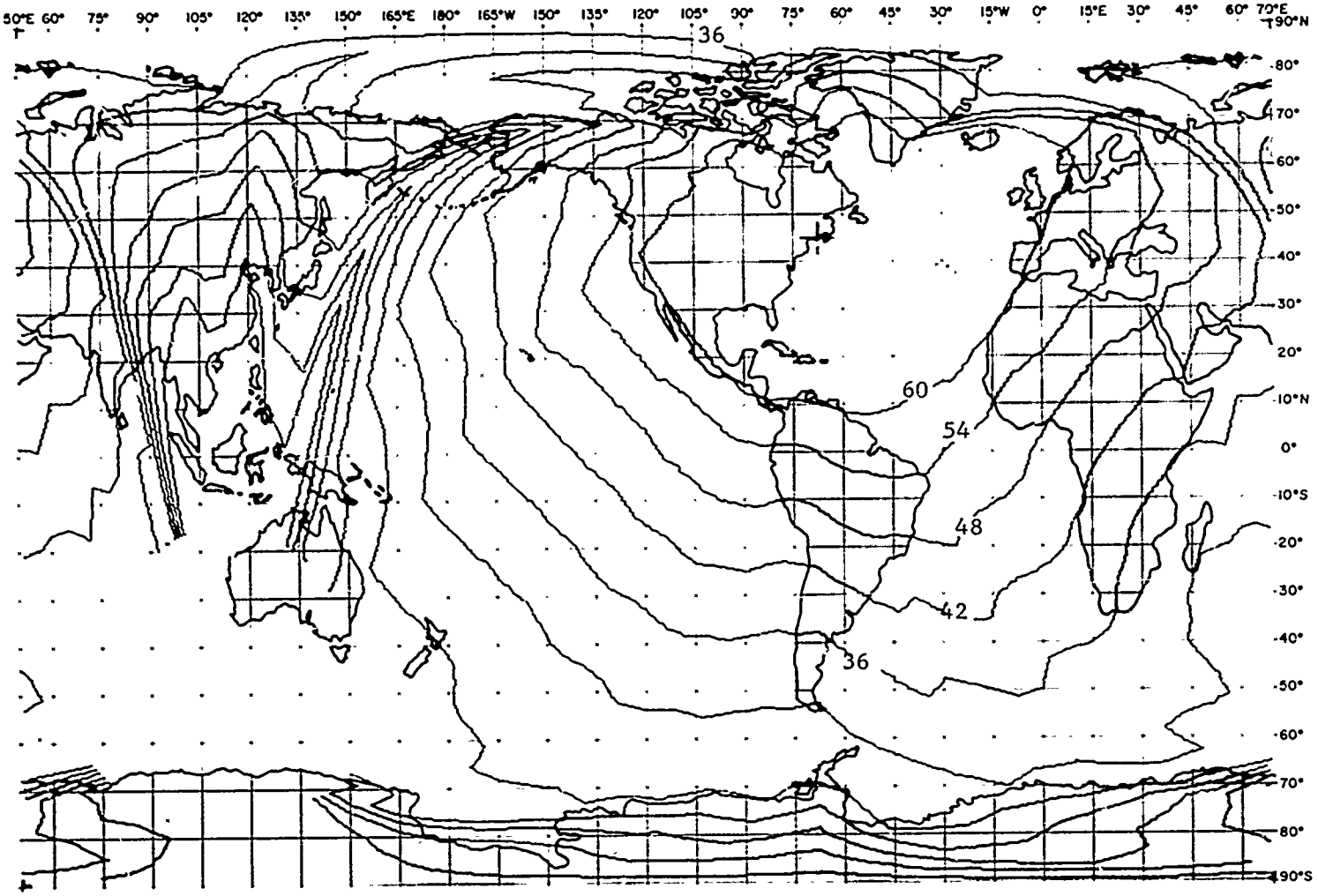


FIG. SU 2 - SIGNAL LEVEL CONTOURS IN dB>1μV/M
NAA (17.8KHZ, 1000KW) , CUTLER
SUMMER 99% TIME AVAILABILITY

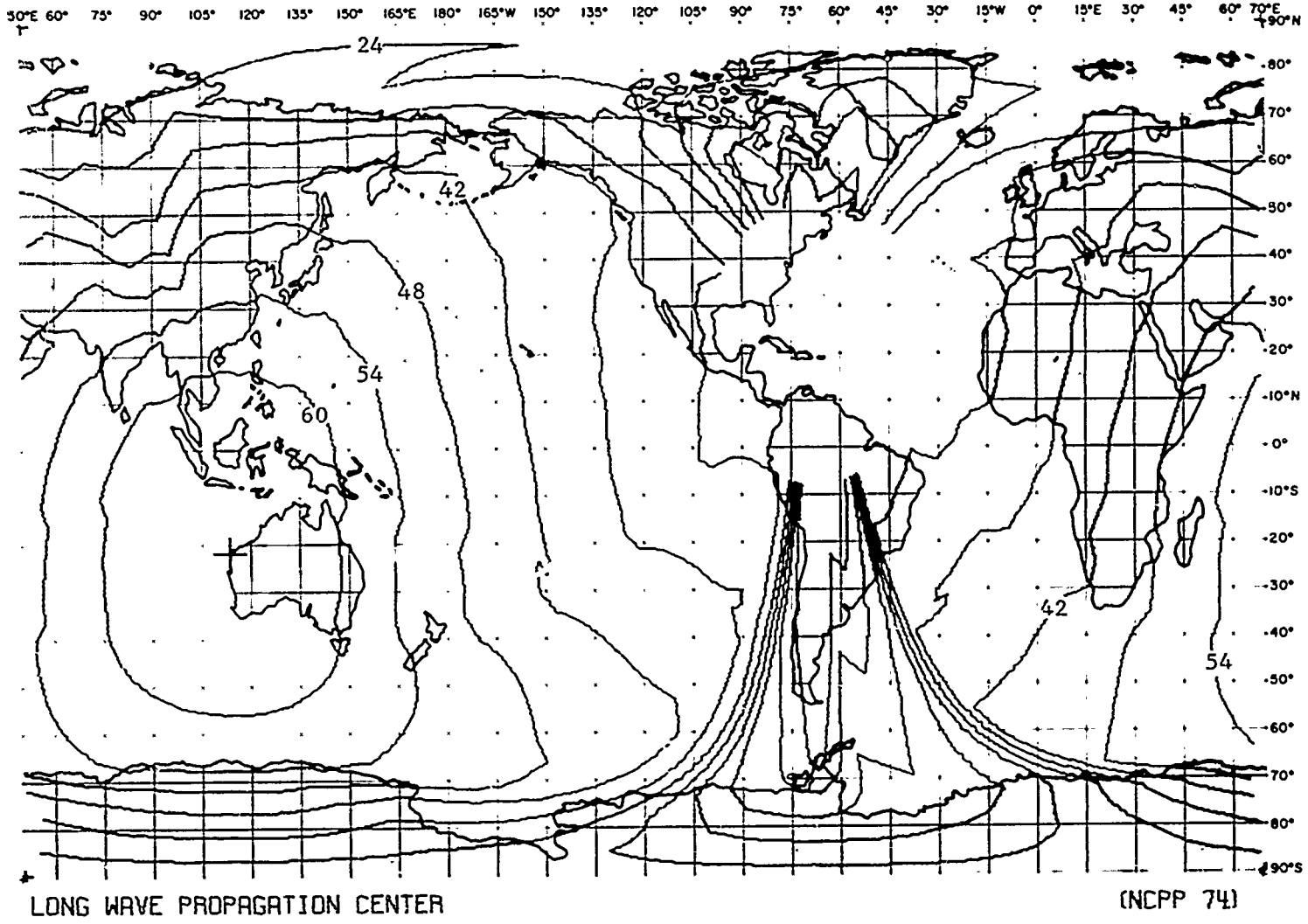


FIG. SU 3 - SIGNAL LEVEL CONTOURS IN dB>1μV/M
NWC (22.3KHZ, 1000KW) , NORTHWEST CAPE
SUMMER 90% TIME AVAILABILITY

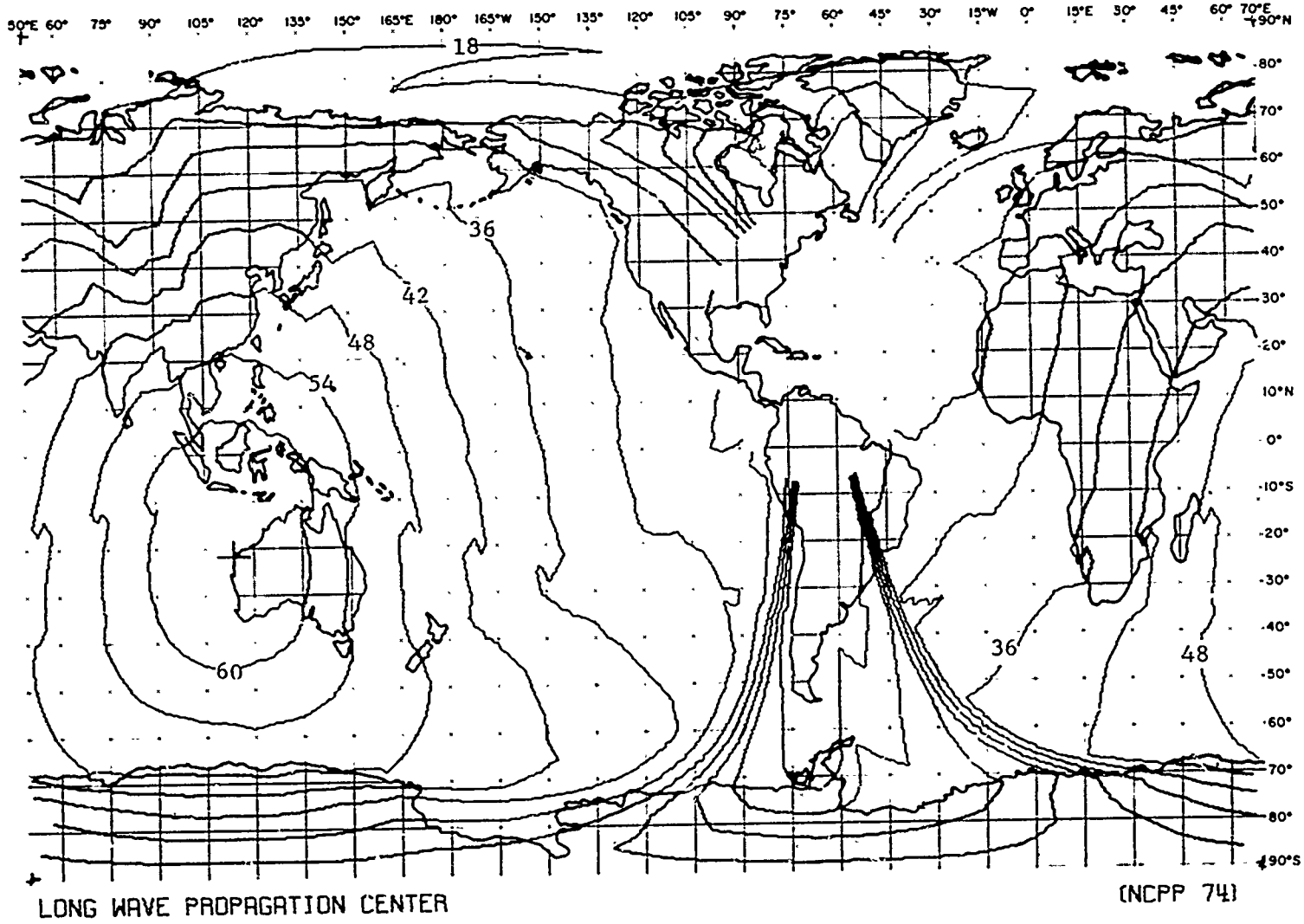


FIG. SU 4 - SIGNAL LEVEL CONTOURS IN dB>1μV/M
NWC (22.3KHZ, 1000KW) , NORTHWEST CAPE
SUMMER 99% TIME AVAILABILITY

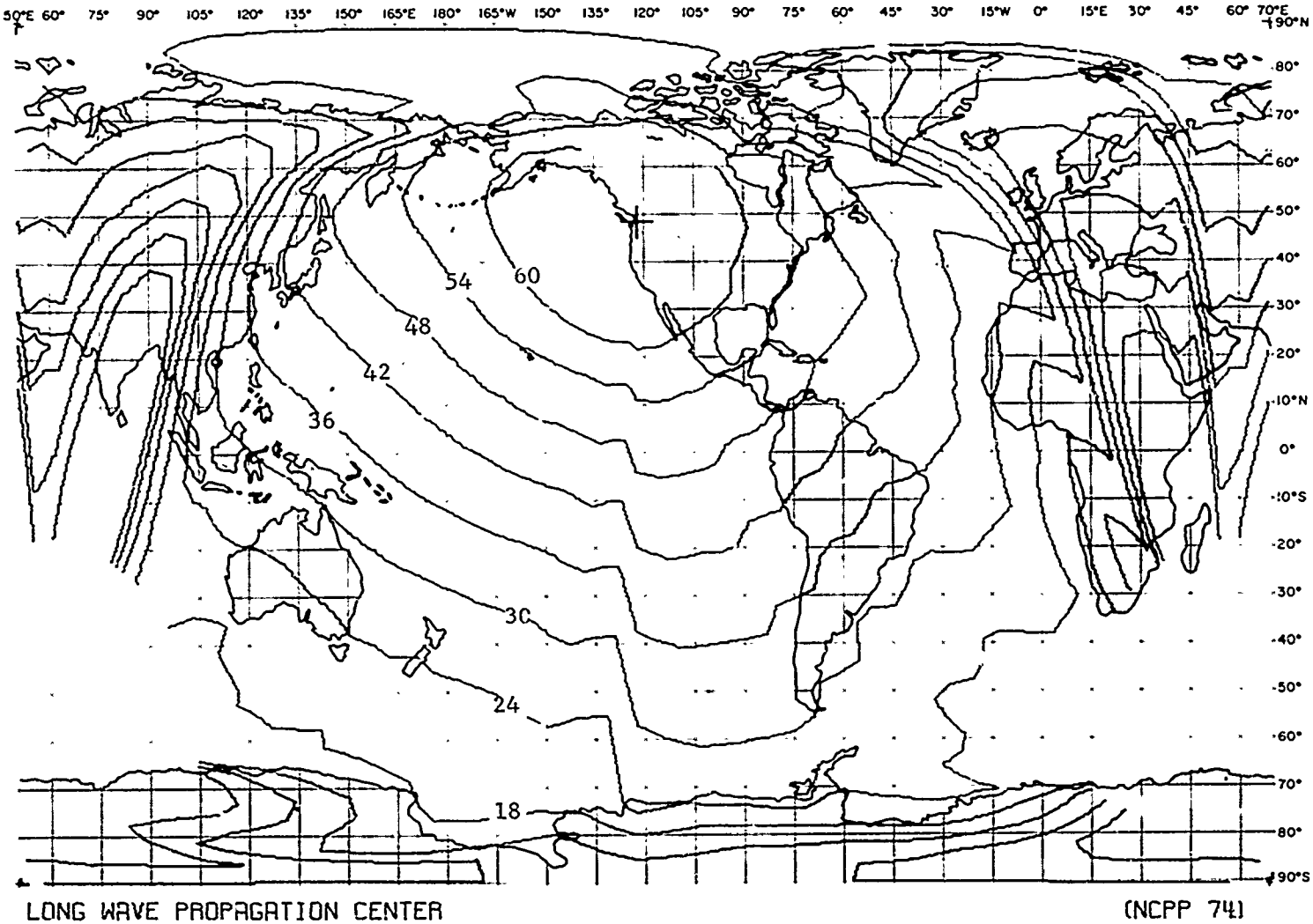


FIG. SU 5 - SIGNAL LEVEL CONTOURS IN dB>1μV/M
NPG (18.6KHZ, 130KW) , JIM CREEK
SUMMER 90% TIME AVAILABILITY

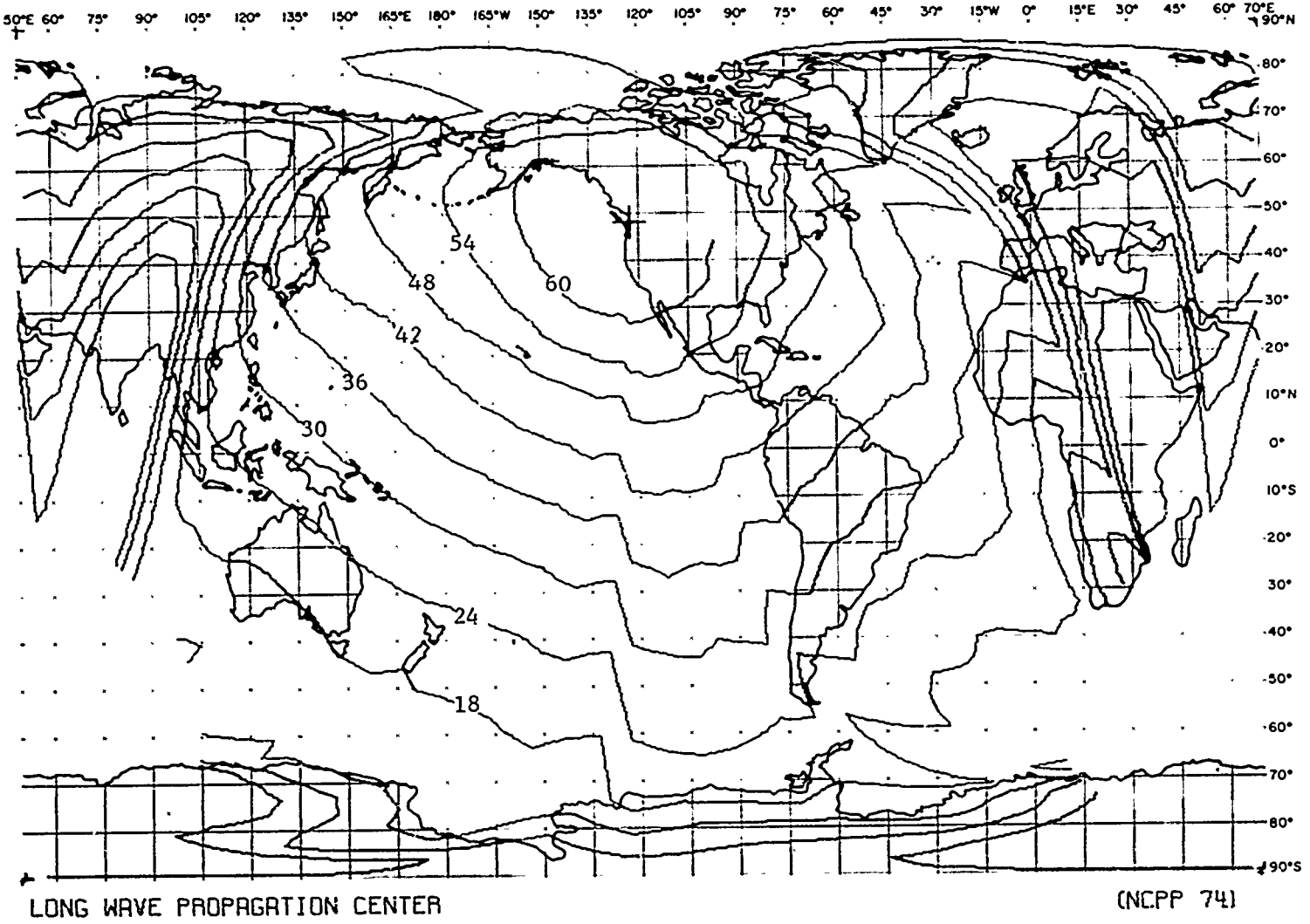


FIG. SU 6 - SIGNAL LEVEL CONTOURS IN dB>1μV/M
NPG (18.6KHZ, 130KW) , JIM CREEK
SUMMER 99% TIME AVAILABILITY

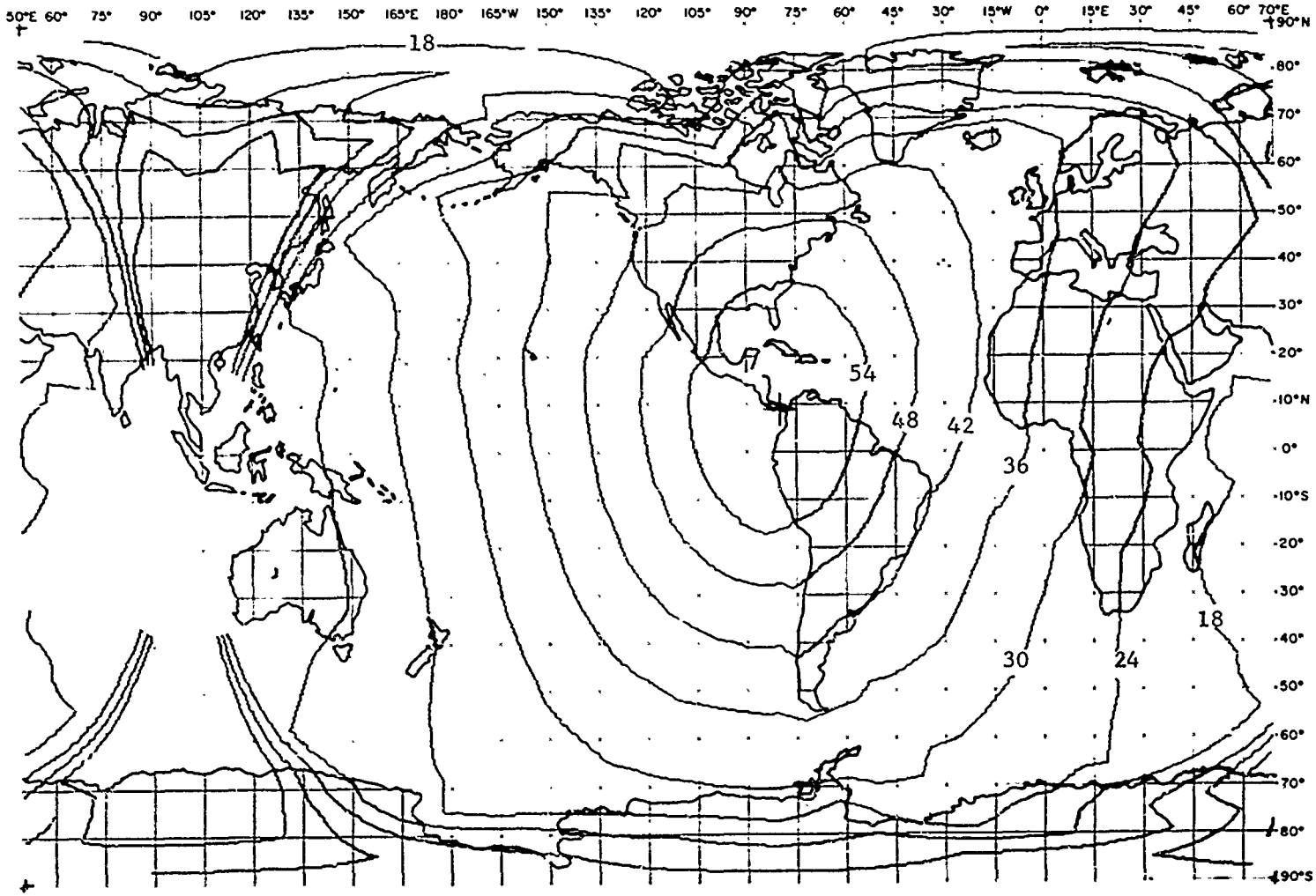


FIG. SU 7 - SIGNAL LEVEL CONTOURS IN dB>1μV/M
NBA (24.0KHZ, 110KW), BALBOA
SUMMER 90% TIME AVAILABILITY

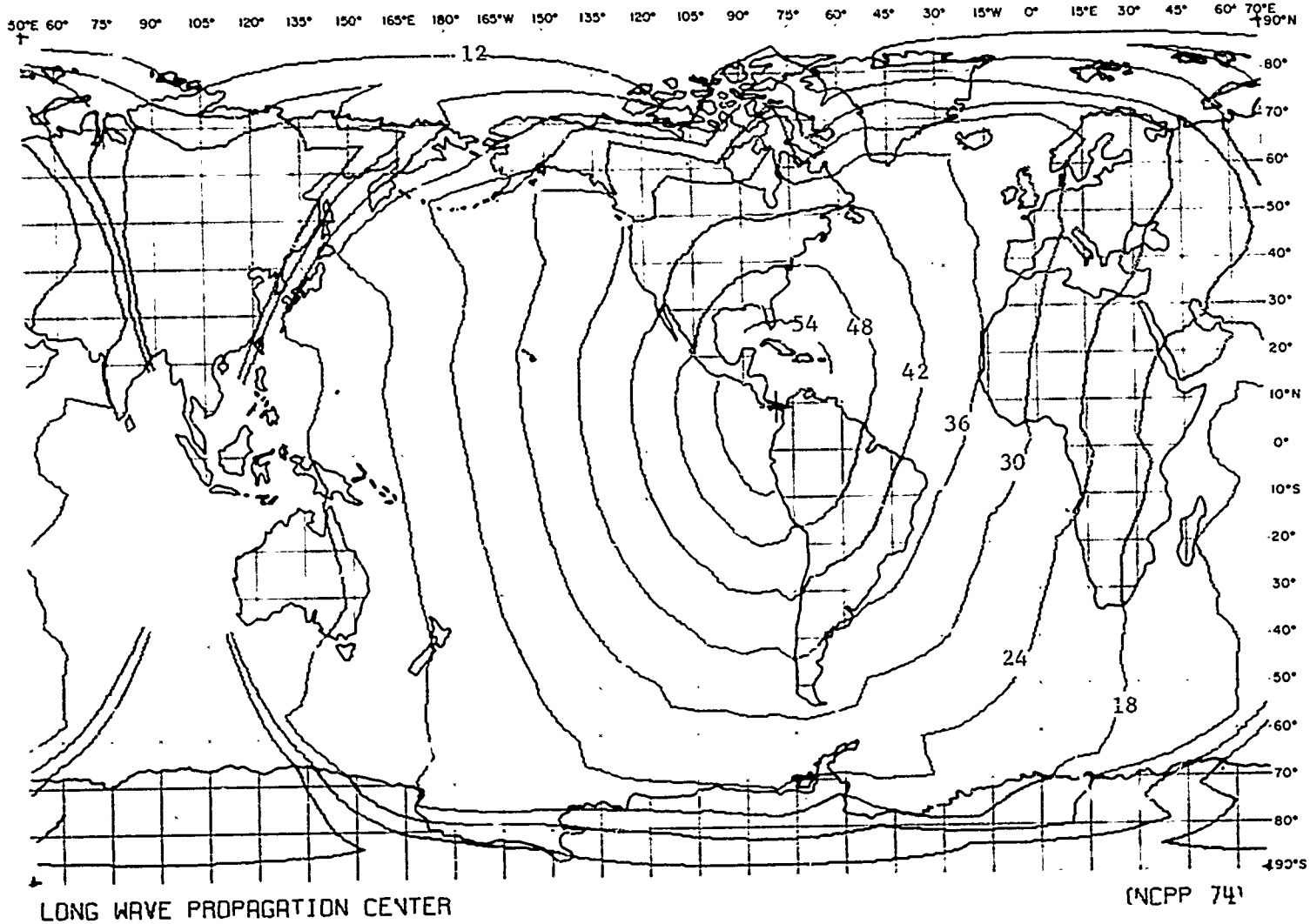


FIG. SU 8 - SIGNAL LEVEL CONTOURS IN dB>1μV/M
NBA (24.0KHZ. 110KW) , BALBOA
SUMMER 99% TIME AVAILABILITY

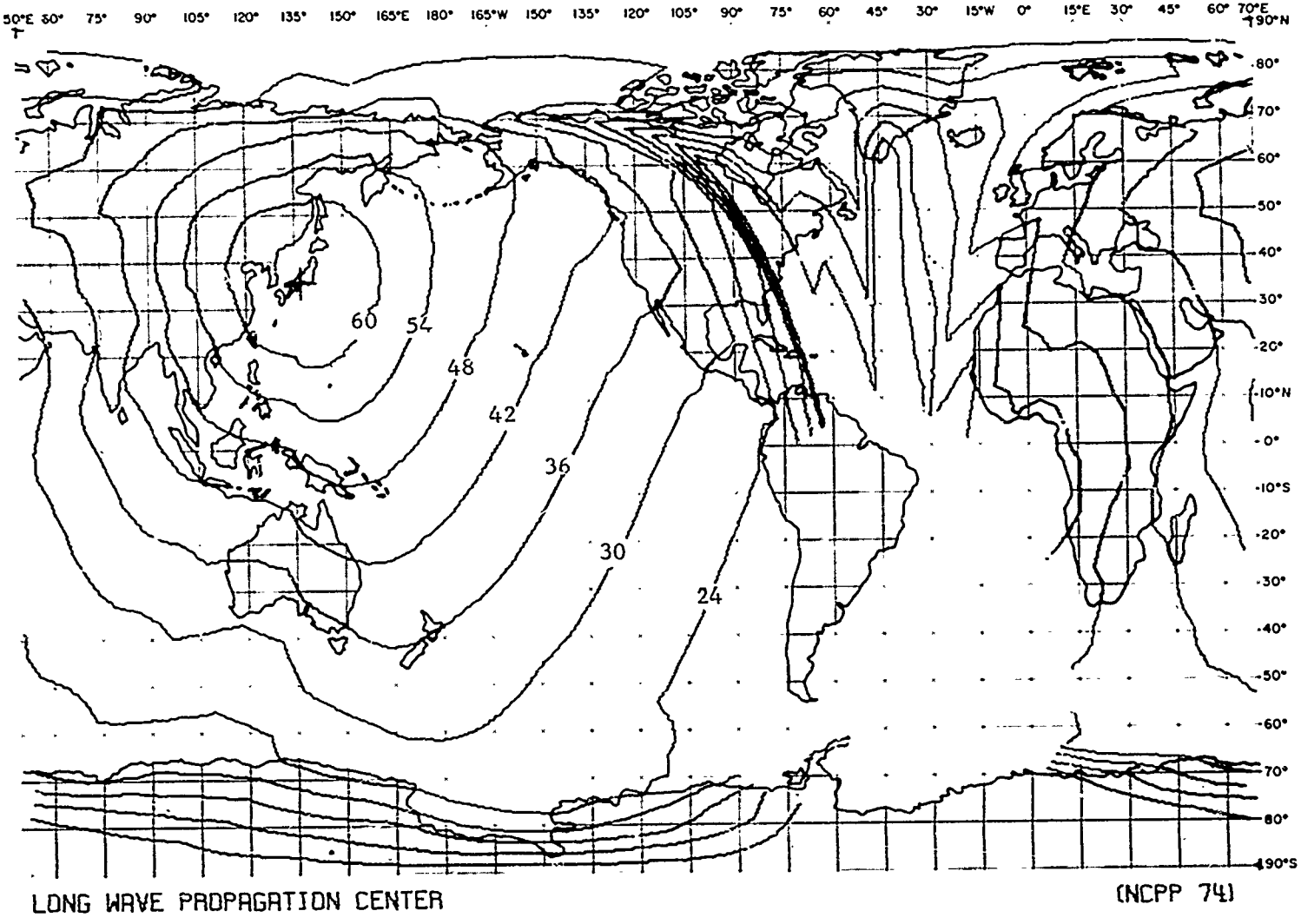


FIG. SU 9 - SIGNAL LEVEL CONTOURS IN dB>1μV/M
NDT (17.4KHZ, 40KW) , YOSAMI
SUMMER 90% TIME AVAILABILITY

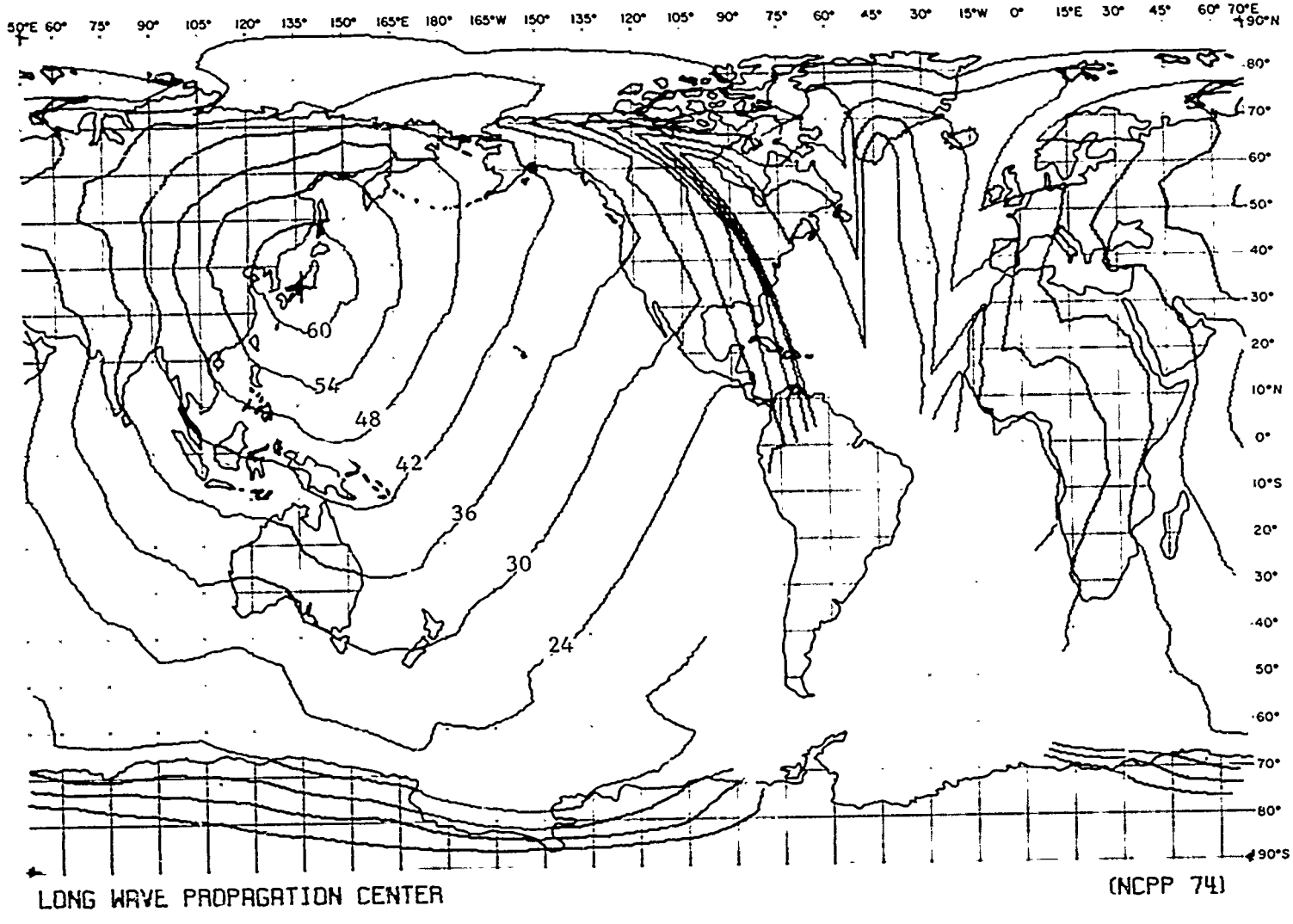


FIG. SU 10 - SIGNAL LEVEL CONTOURS IN dB>1μV/M
NDT (17.4KHZ, 40KW), YOSAMI
SUMMER 99% TIME AVAILABILITY

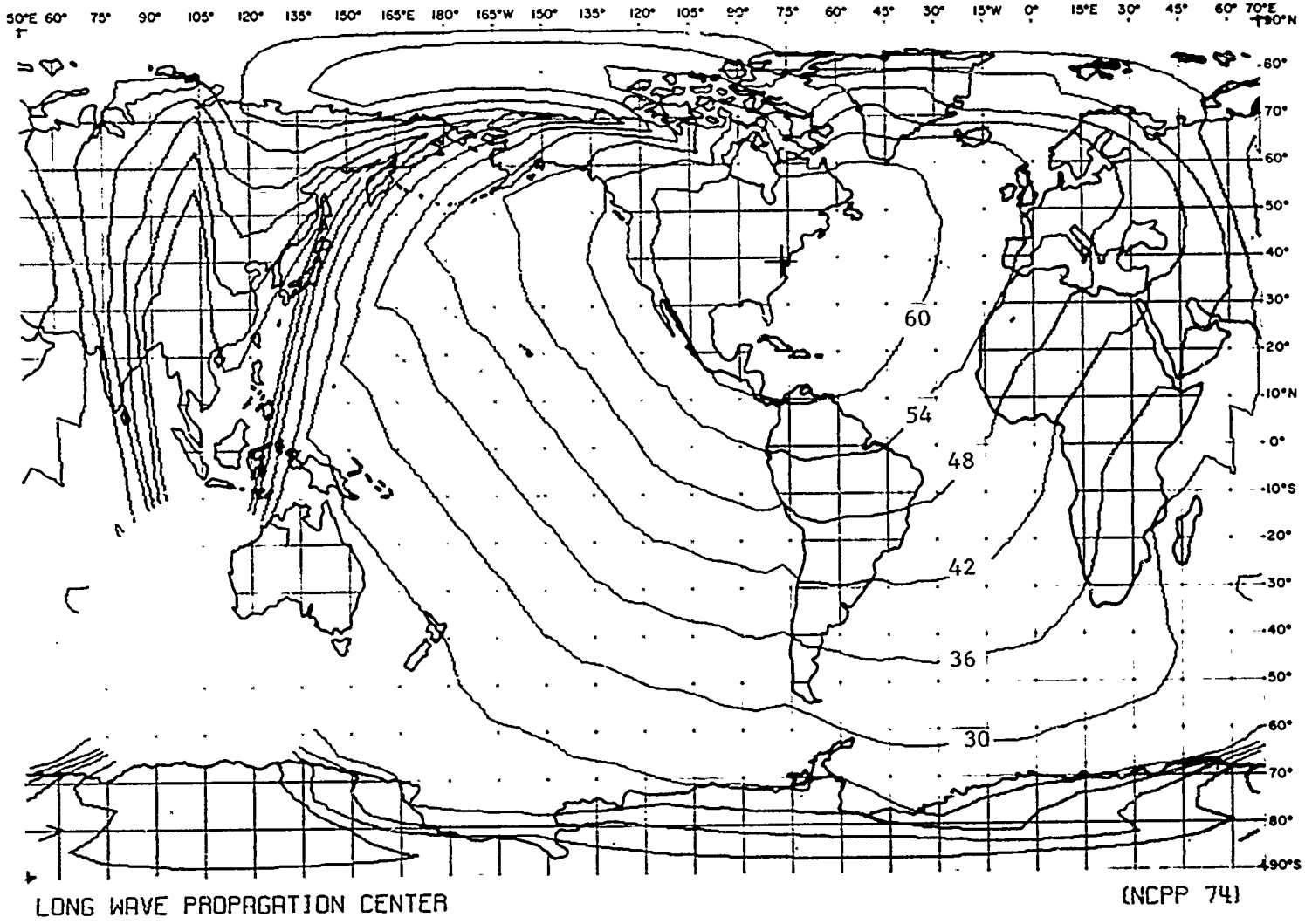


FIG. SU 11 - SIGNAL LEVEL CONTOURS IN dB>1μV/M
NSS (21.4KHZ, 400KW) , ANNAPOLIS
SUMMER 90% TIME AVAILABILITY

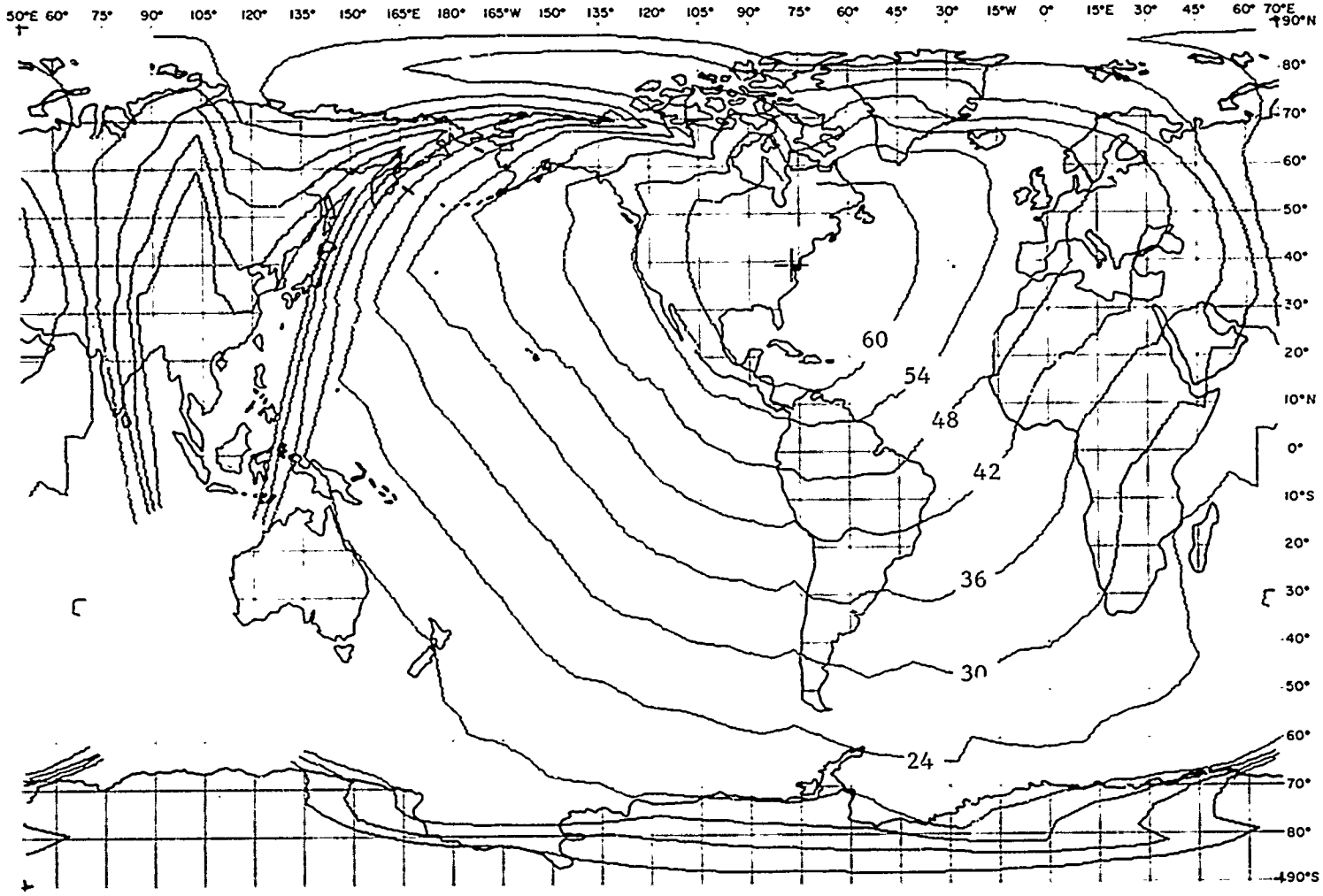


FIG. SU 12 - SIGNAL LEVEL CONTOURS IN dB>1μV/M
NSS (21.4KHZ, 400KW) , ANNAPOLIS
SUMMER 99% TIME AVAILABILITY

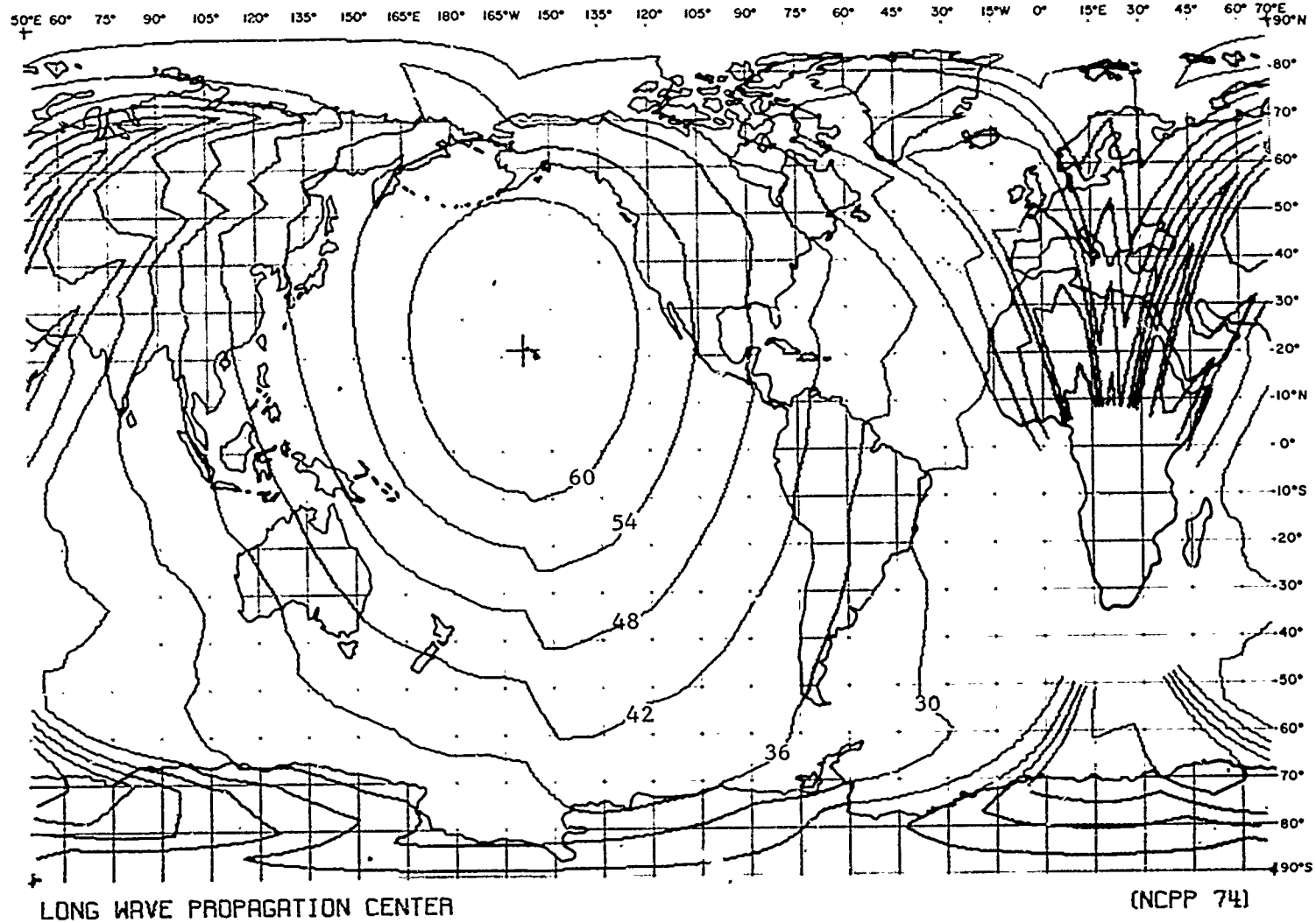


FIG. SU 13 - SIGNAL LEVEL CONTOURS IN dB>1μV/M
NPM (23.4KHZ, 630KW) , LURLURLEI
SUMMER 90% TIME AVAILABILITY

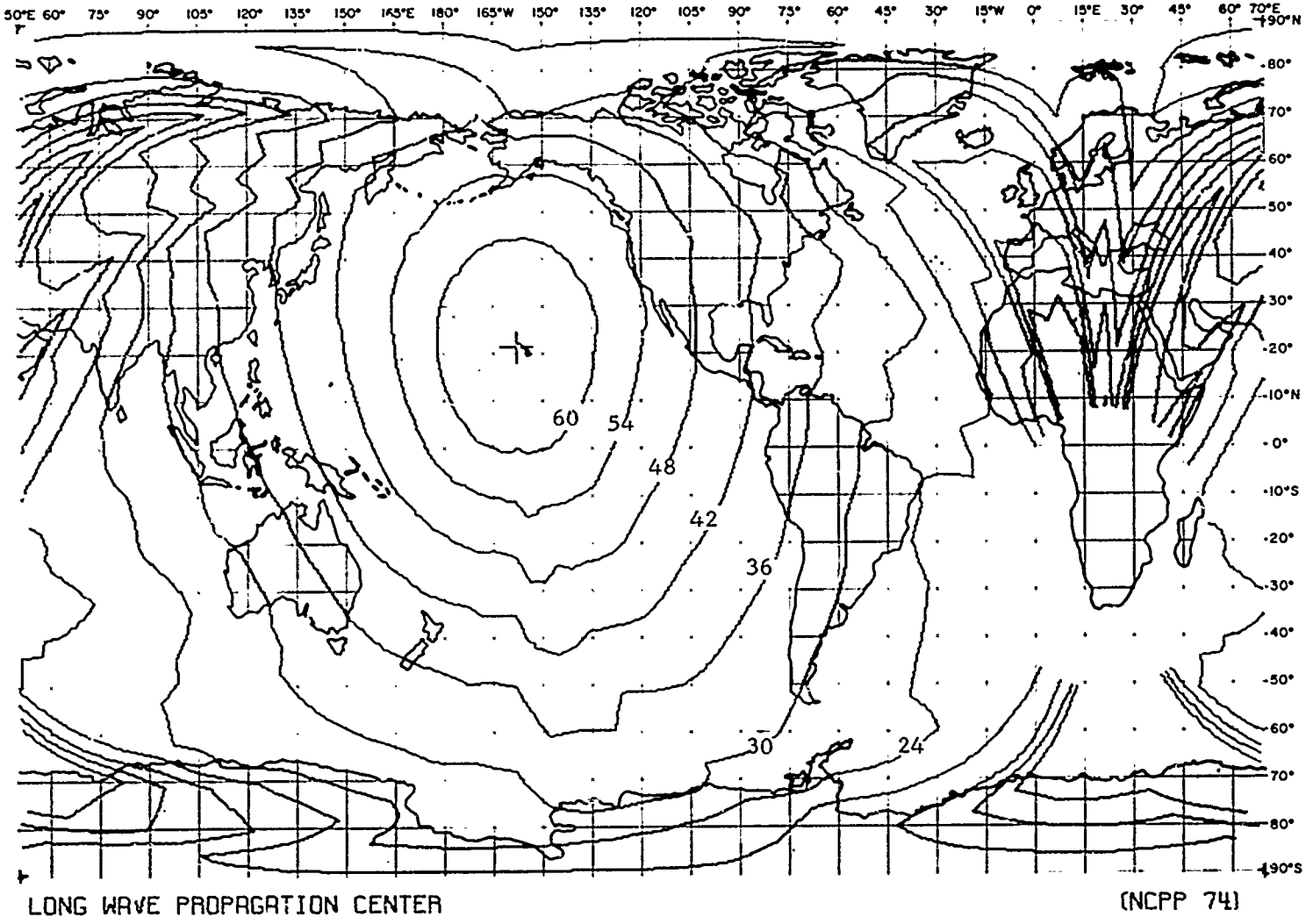


FIG. SU 14 - SIGNAL LEVEL CONTOURS IN dB>1μV/M
NPM (23.4KHZ, 630KW) , LURLURLEI
SUMMER 99% TIME AVAILABILITY

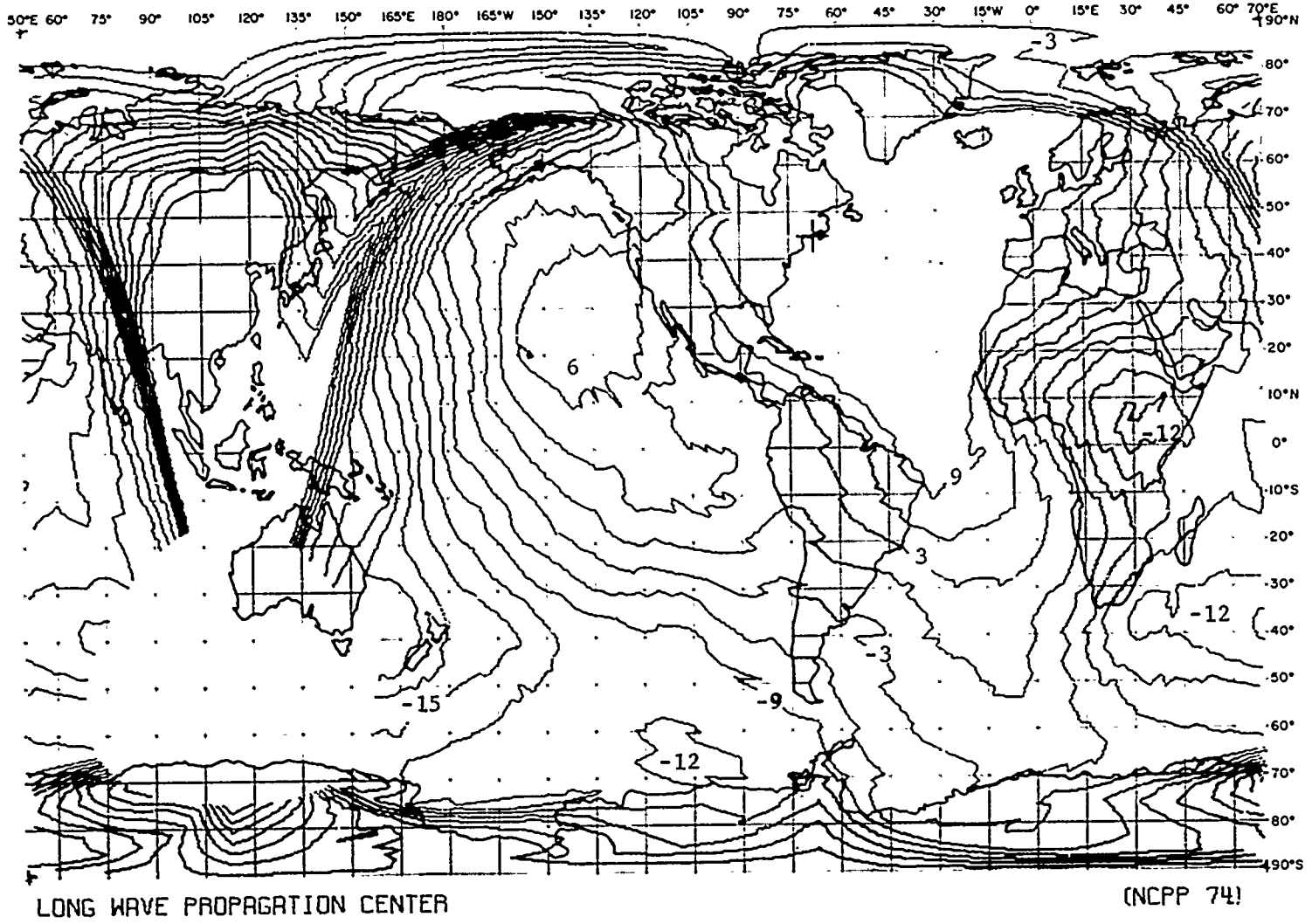


FIG. SU 15 - SIGNAL-TO-ATMOSPHERIC NOISE RATIO CONTOURS IN dB
NAR (17.8KHZ, 1000KW) , CUTLER
SUMMER 90% TIME AVAILABILITY 1KHZ BANDWIDTH

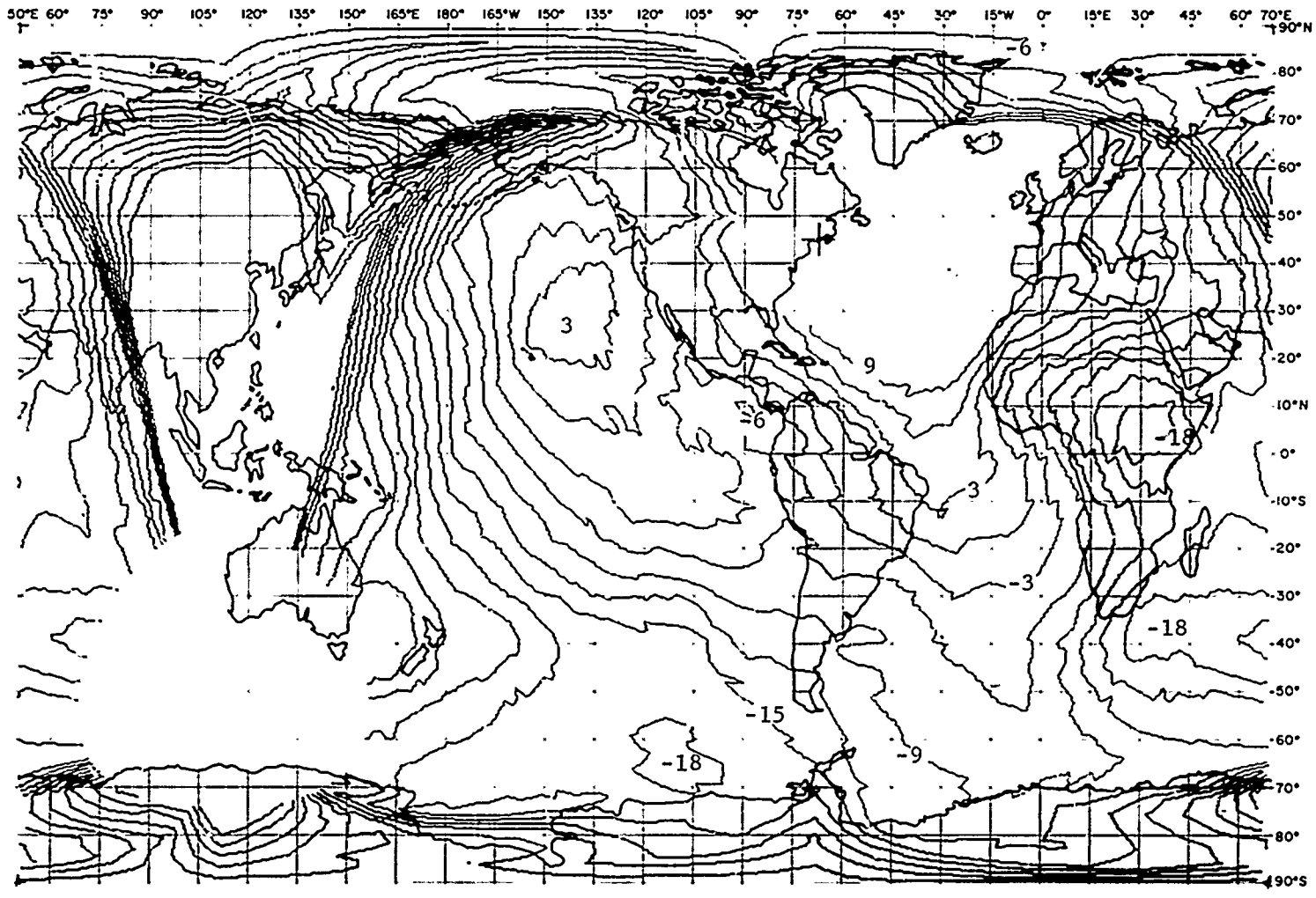


FIG. SU 16 - SIGNAL-TO-ATMOSPHERIC NOISE RATIO CONTOURS IN dB
NAR (17.8KHz, 1000KW) , CUTLER
SUMMER 99% TIME AVAILABILITY 1KHZ BANDWIDTH

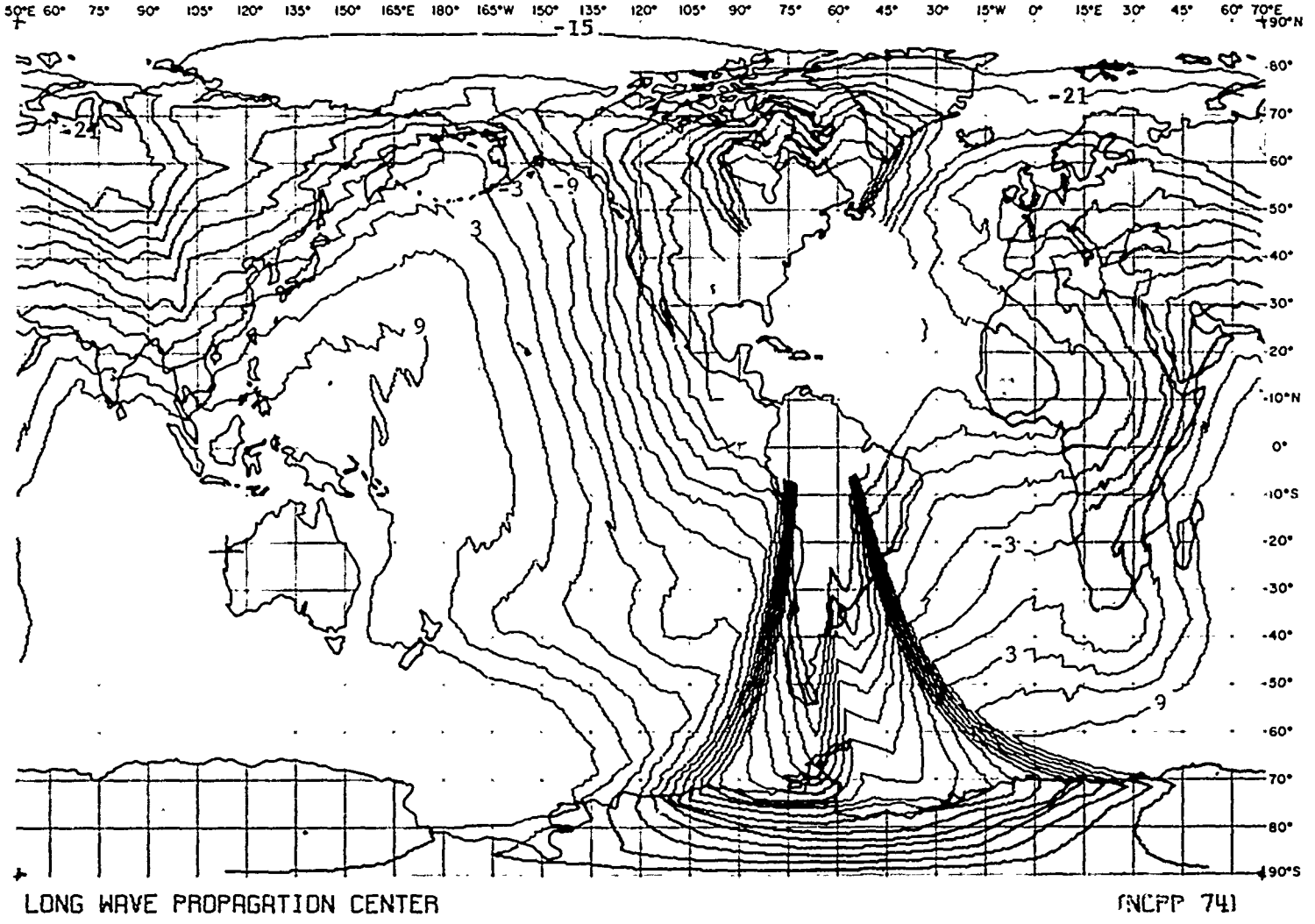


FIG. SU 17 - SIGNAL-TO-ATMOSPHERIC NOISE RATIO CONTOURS IN dB
NWC (22.3KHZ, 1000KW) , NORTHWEST CAPE
SUMMER 90% TIME AVAILABILITY 1KHZ BANDWIDTH

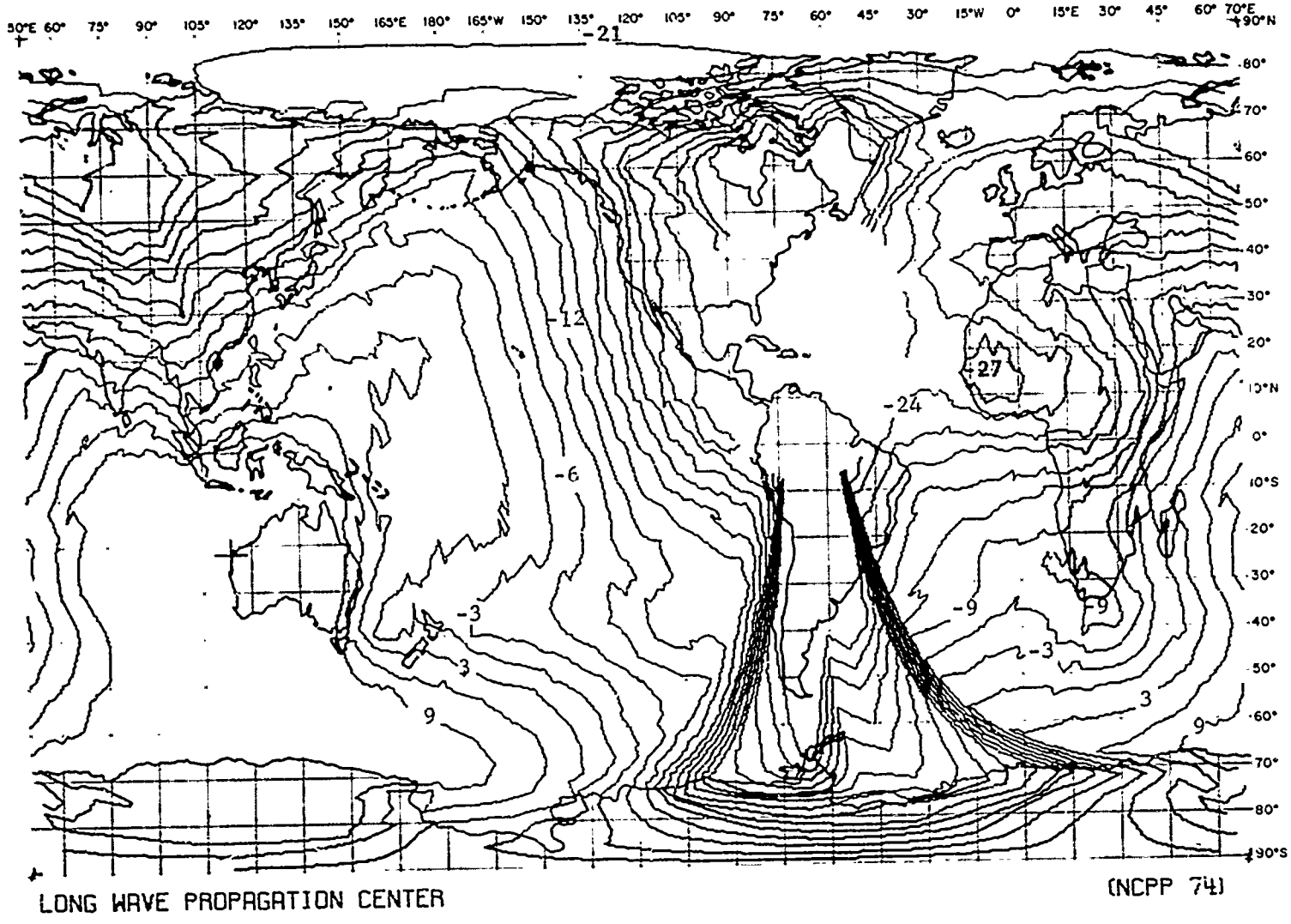


FIG. SU 18 - SIGNAL-TO-ATMOSPHERIC NOISE RATIO CONTOURS IN dB
NWC (22.3KHZ, 1000KW) , NORTHWEST CAPE
SUMMER 99% TIME AVAILABILITY 1KHZ BANDWIDTH

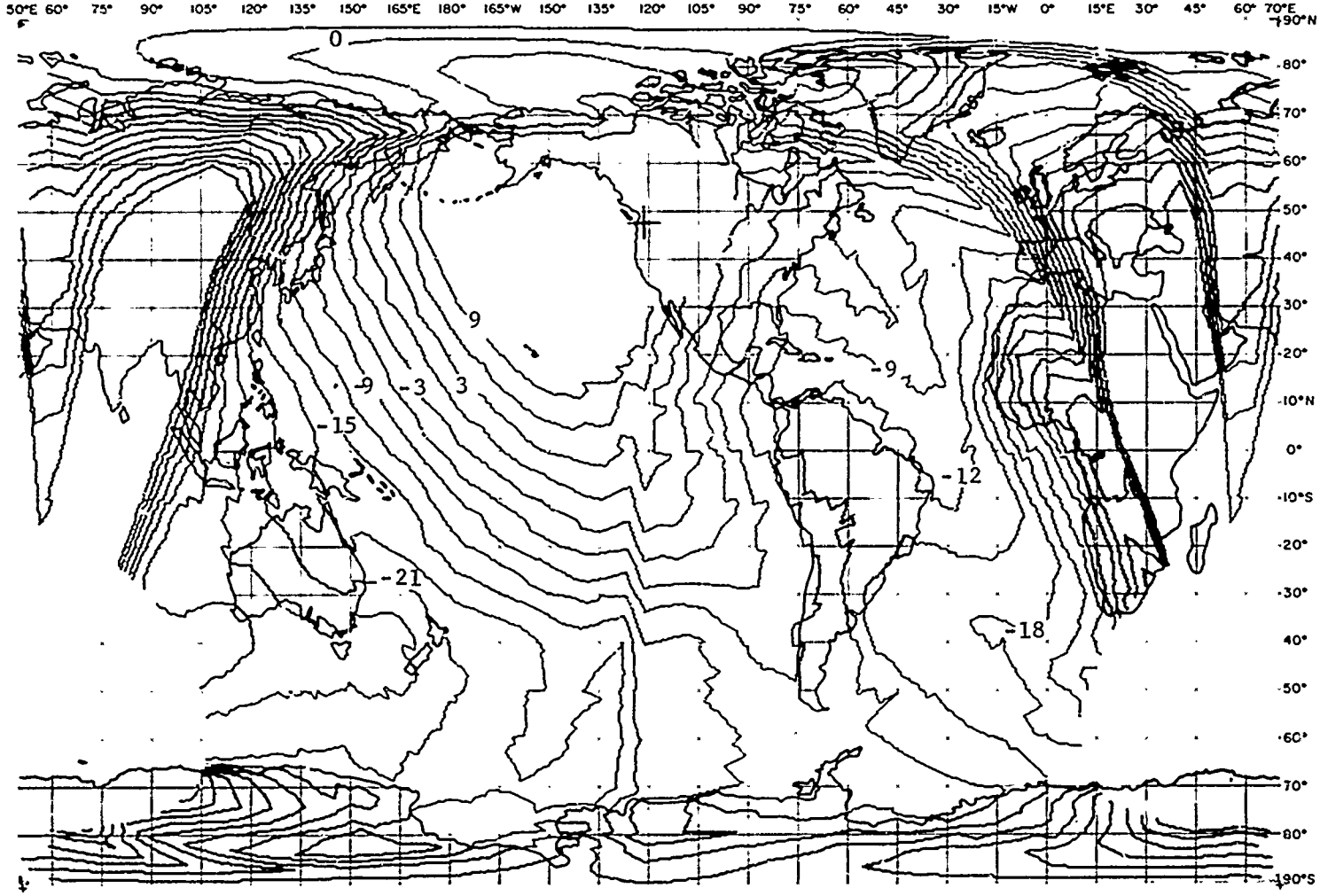


FIG. SU 19 - SIGNAL-TO-ATMOSPHERIC NOISE RATIO CONTOURS IN dB
NPG (18.6KHz, 130KW) , JIM CREEK
SUMMER 90% TIME AVAILABILITY 1KHZ BANDWIDTH

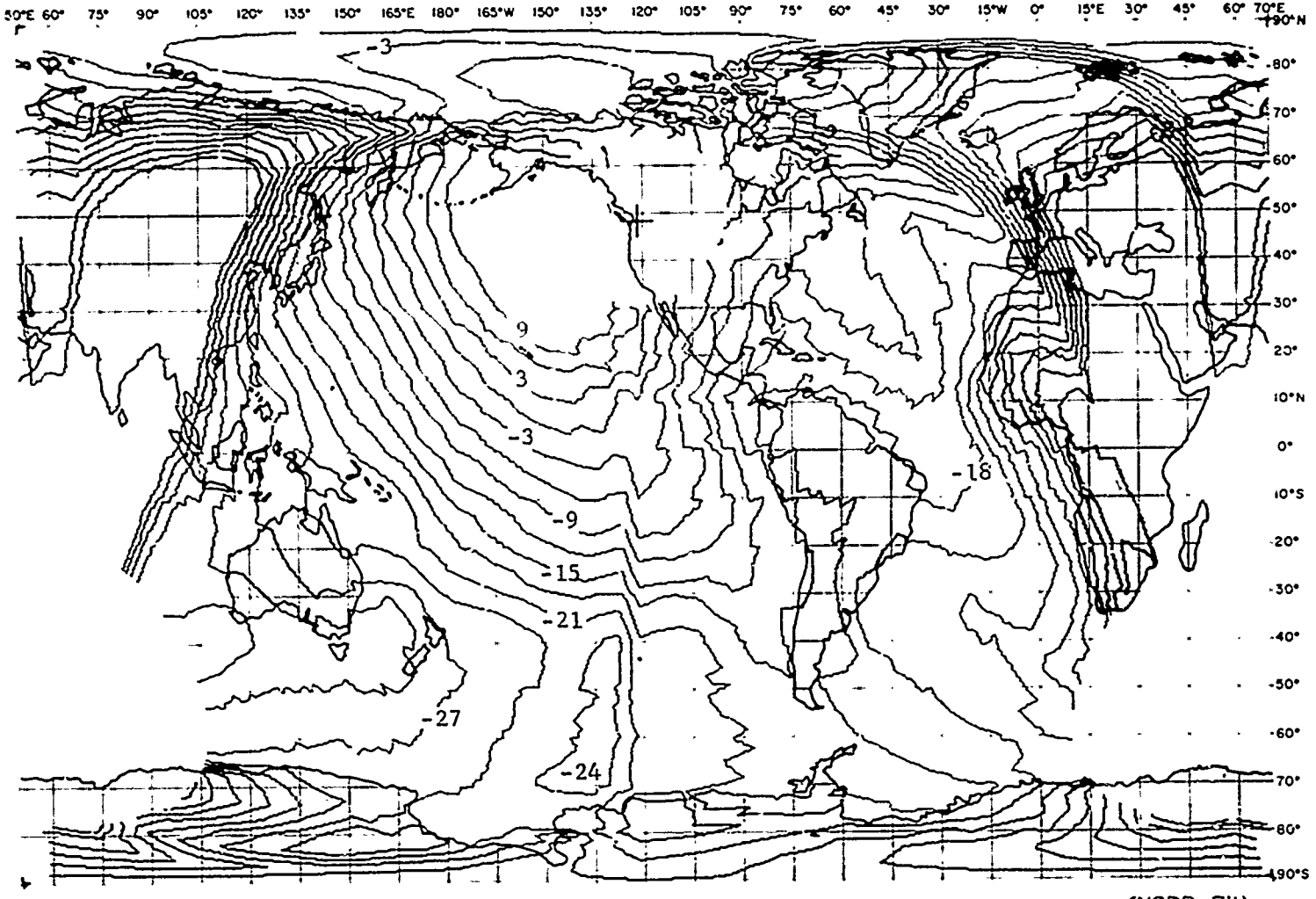


FIG. SU 20 - SIGNAL-TO-ATMOSPHERIC NOISE RATIO CONTOURS IN dB
NPG (18.6KHz, 130KW), JIM CREEK
SUMMER 99% TIME AVAILABILITY 1KHZ BANDWIDTH

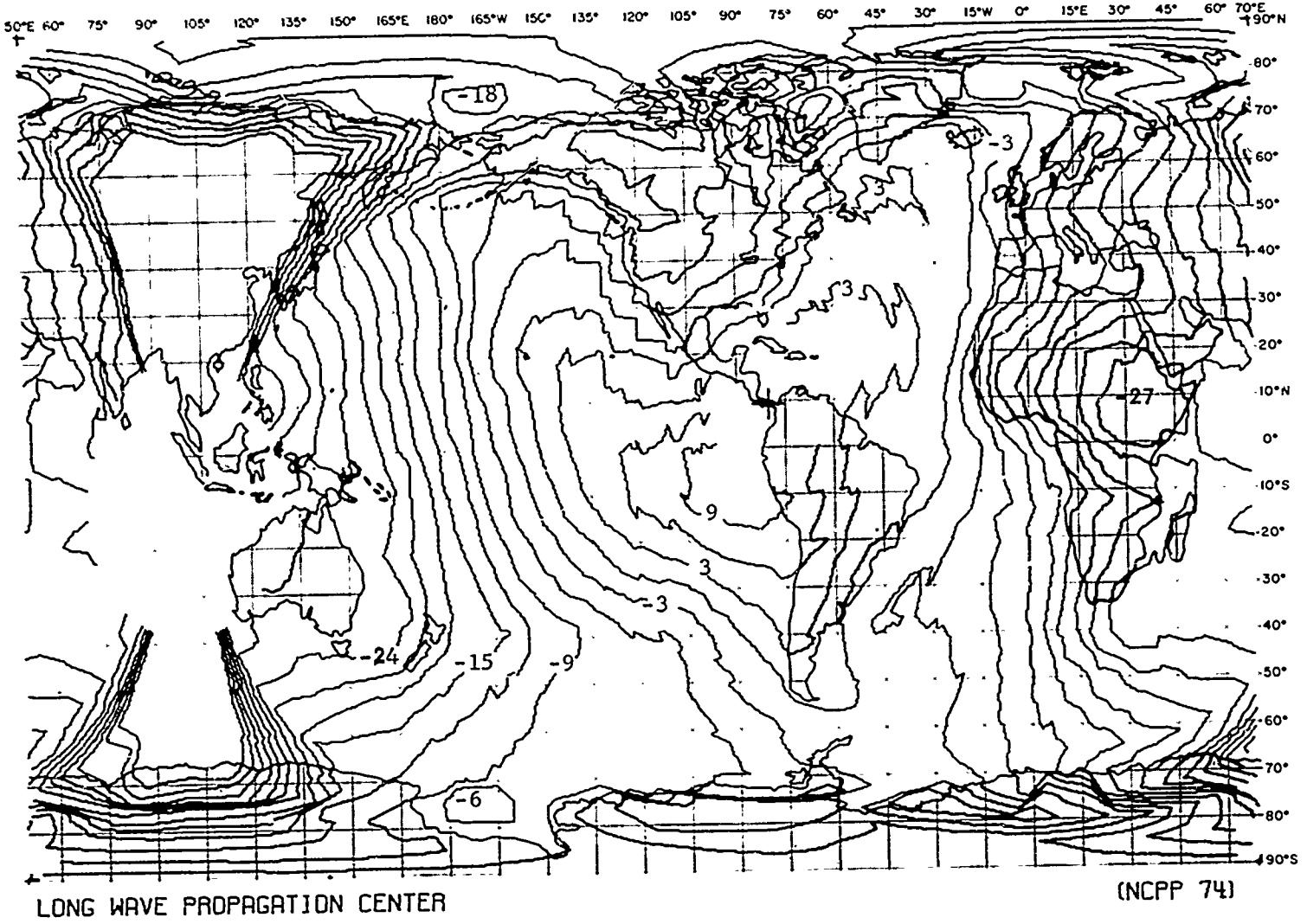


FIG. SU 21 - SIGNAL-TO-ATMOSPHERIC NOISE RATIO CONTOURS IN dB
NBA (24.0KHZ, 110KW) , BALBOA
SUMMER 90% TIME AVAILABILITY 1KHZ BANDWIDTH

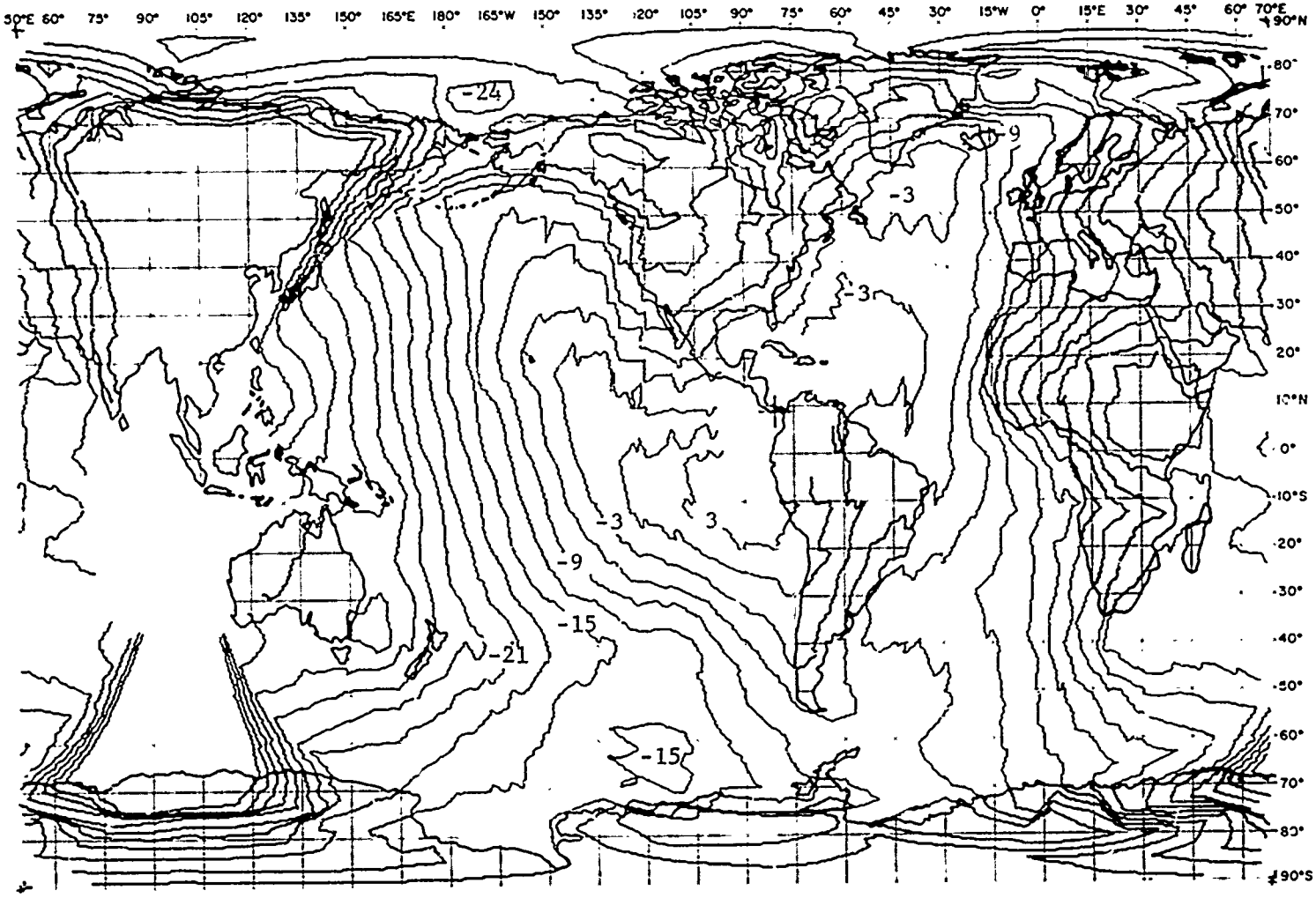


FIG. SJ 22 - SIGNAL-TO-ATMOSPHERIC NOISE RATIO CONTOURS IN dB
NBA (24.0KHZ, 110KW), BALBOA
SUMMER 99% TIME AVAILABILITY 1KHZ BANDWIDTH

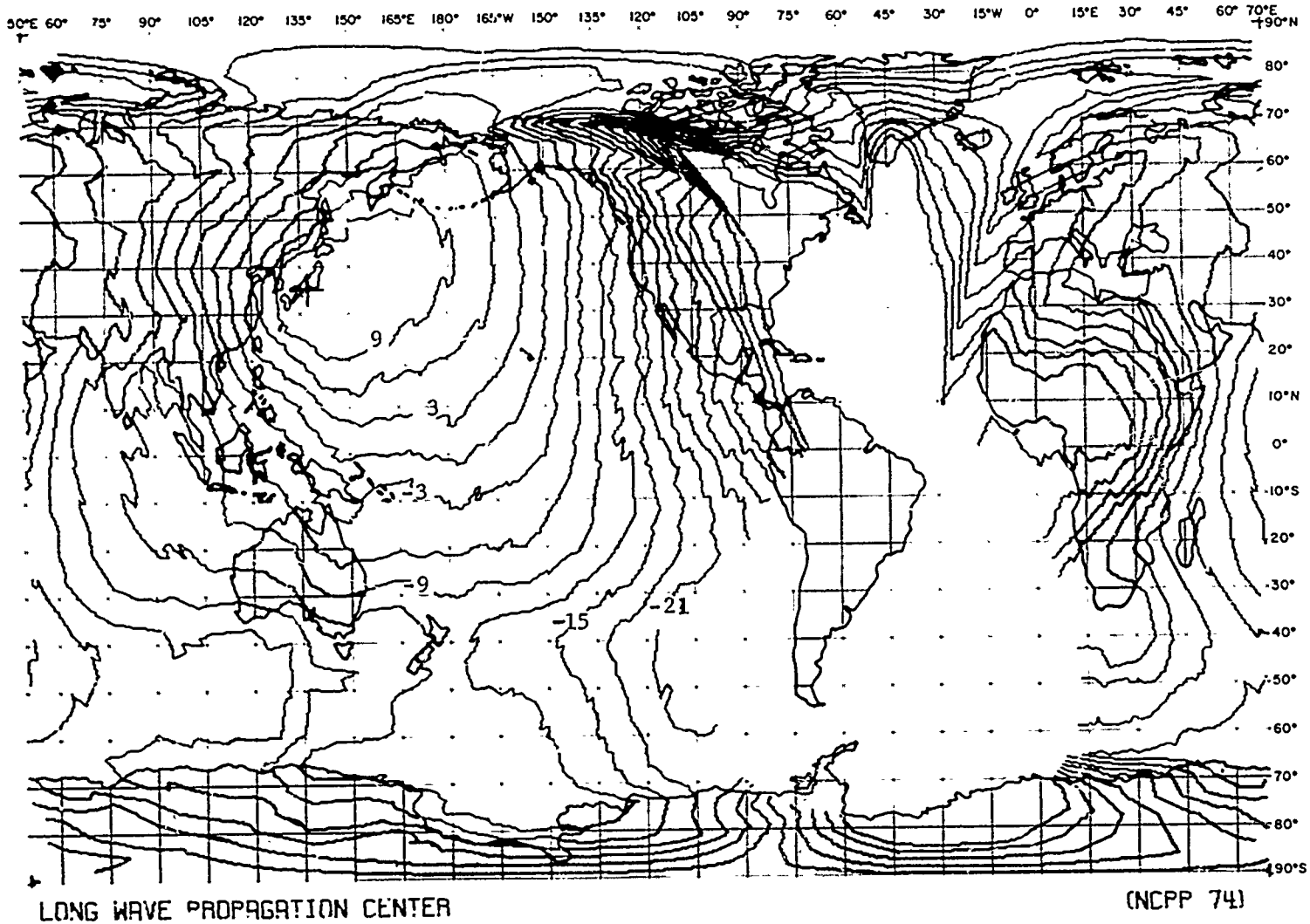


FIG. SU 23 -- SIGNAL-TO-ATMOSPHERIC NOISE RATIO CONTOURS IN dB
NDT (17.4KHZ, 40KW) , YOSAMI
SUMMER 90% TIME AVAILABILITY 1KHZ BANDWIDTH

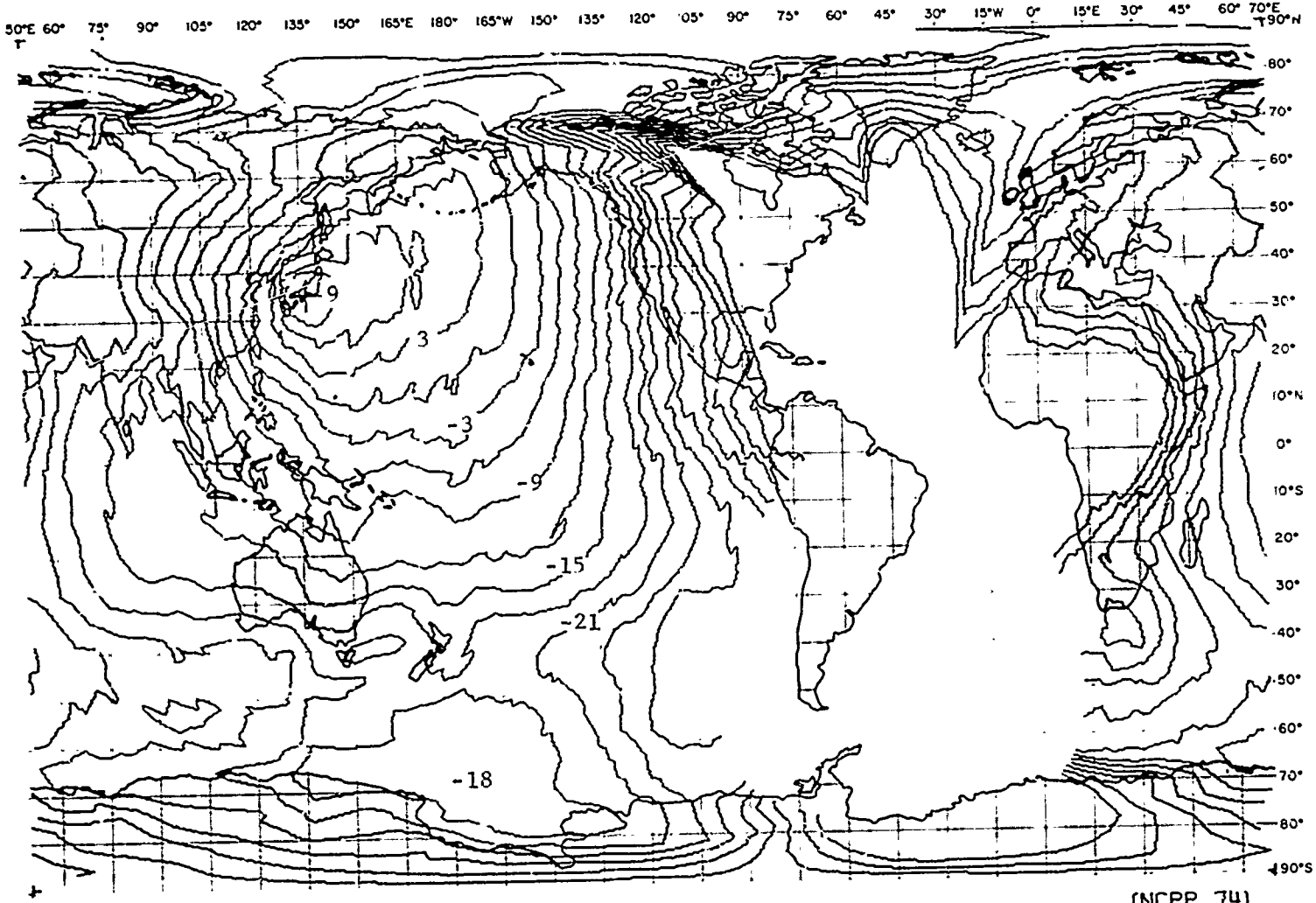


FIG. SU 24 - SIGNAL-TO-ATMOSPHERIC NOISE RATIO CONTOURS IN dB
NDT (17.4KHZ, 40KW) , YOSAMI
SUMMER 99% TIME AVAILABILITY 1KHZ BANDWIDTH

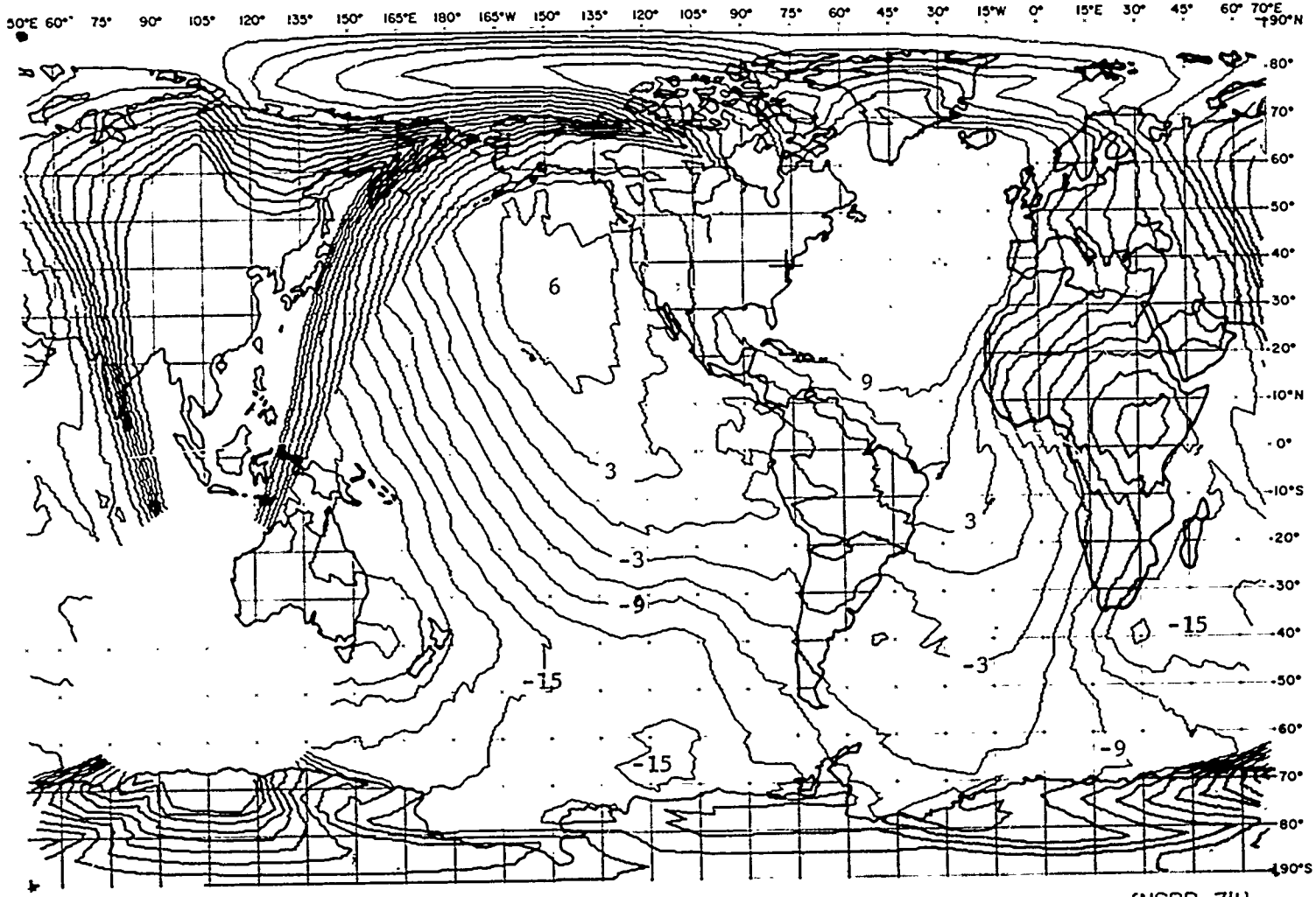


FIG. SU 25 - SIGNAL-TO-ATMOSPHERIC NOISE RATIO CONTOURS IN dB
NSS (21.4KHZ, 400KW) , ANNAPOLIS
SUMMER 90% TIME AVAILABILITY 1KHZ BANDWIDTH

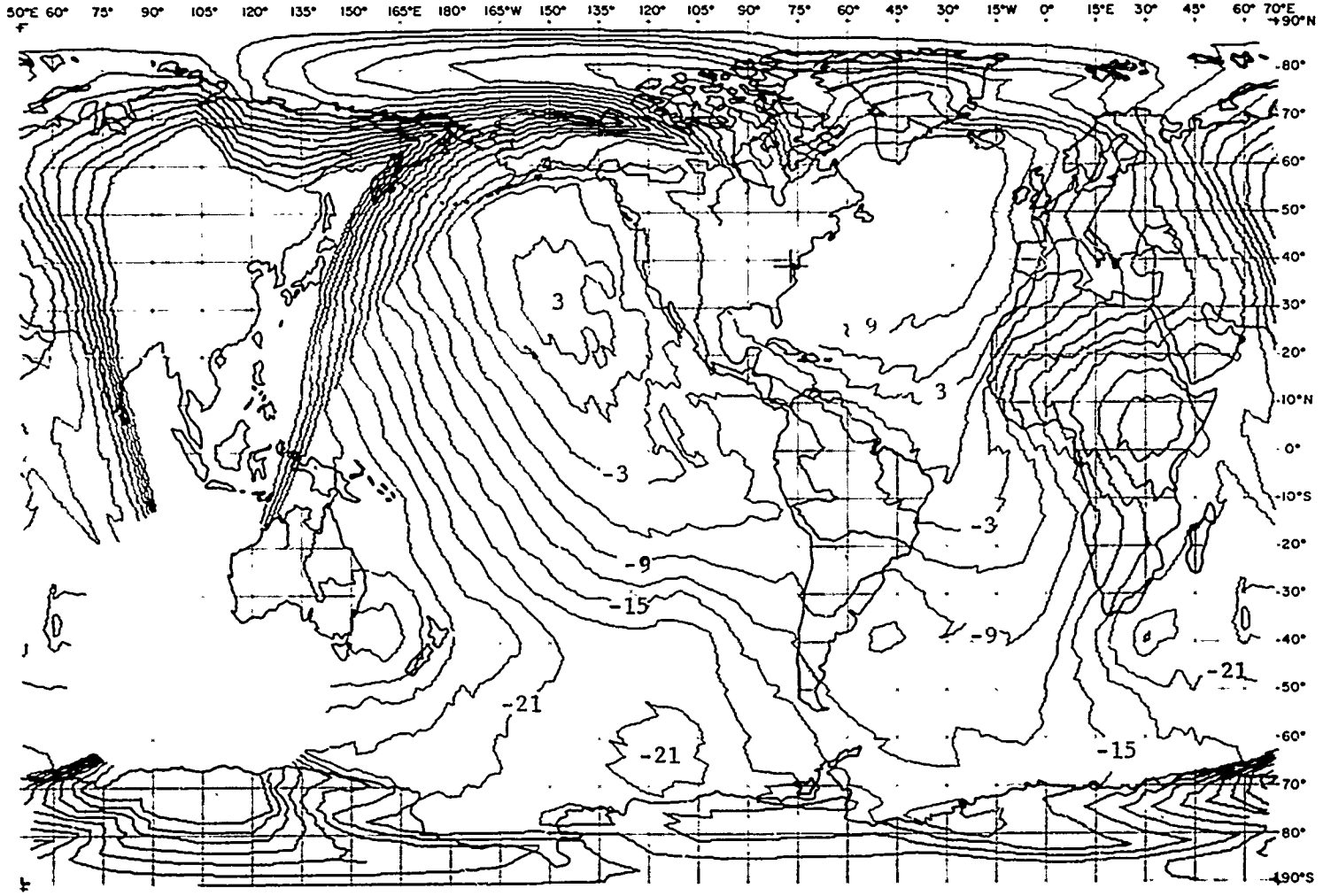


FIG. SU 26 - SIGNAL-TO-ATMOSPHERIC NOISE RATIO CONTOURS IN dB
NSS (21.4KHz, 400KW), ANNAPOLIS
SUMMER 99% TIME AVAILABILITY 1KHz BANDWIDTH

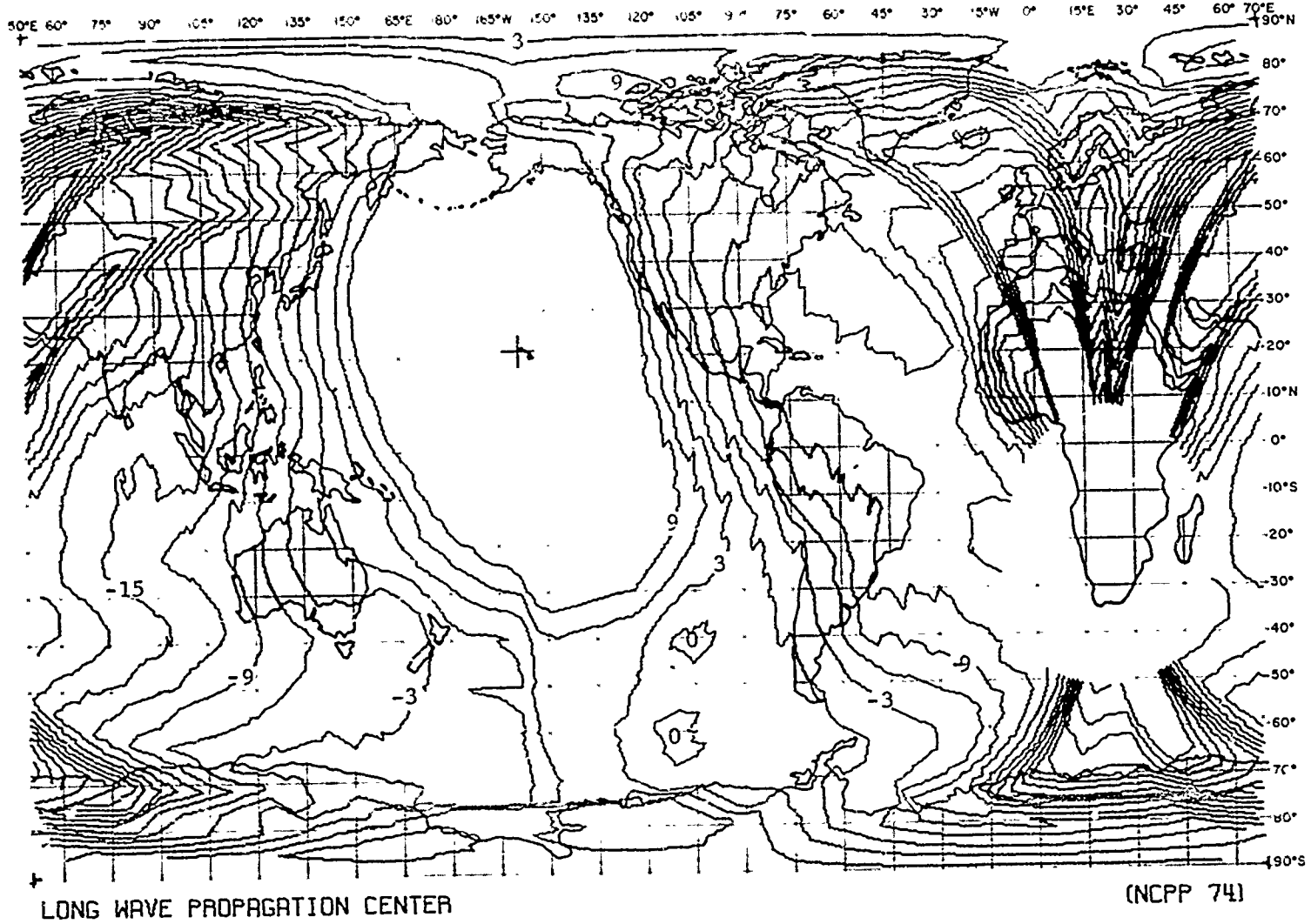


FIG. SU 27 - SIGNAL-TO-ATMOSPHERIC NOISE RATIO CONTOURS IN dB
NPM (23.4KHz, 630KW) , LURLURLEI
SUMMER 90% TIME AVAILABILITY 1KHZ BANDWIDTH

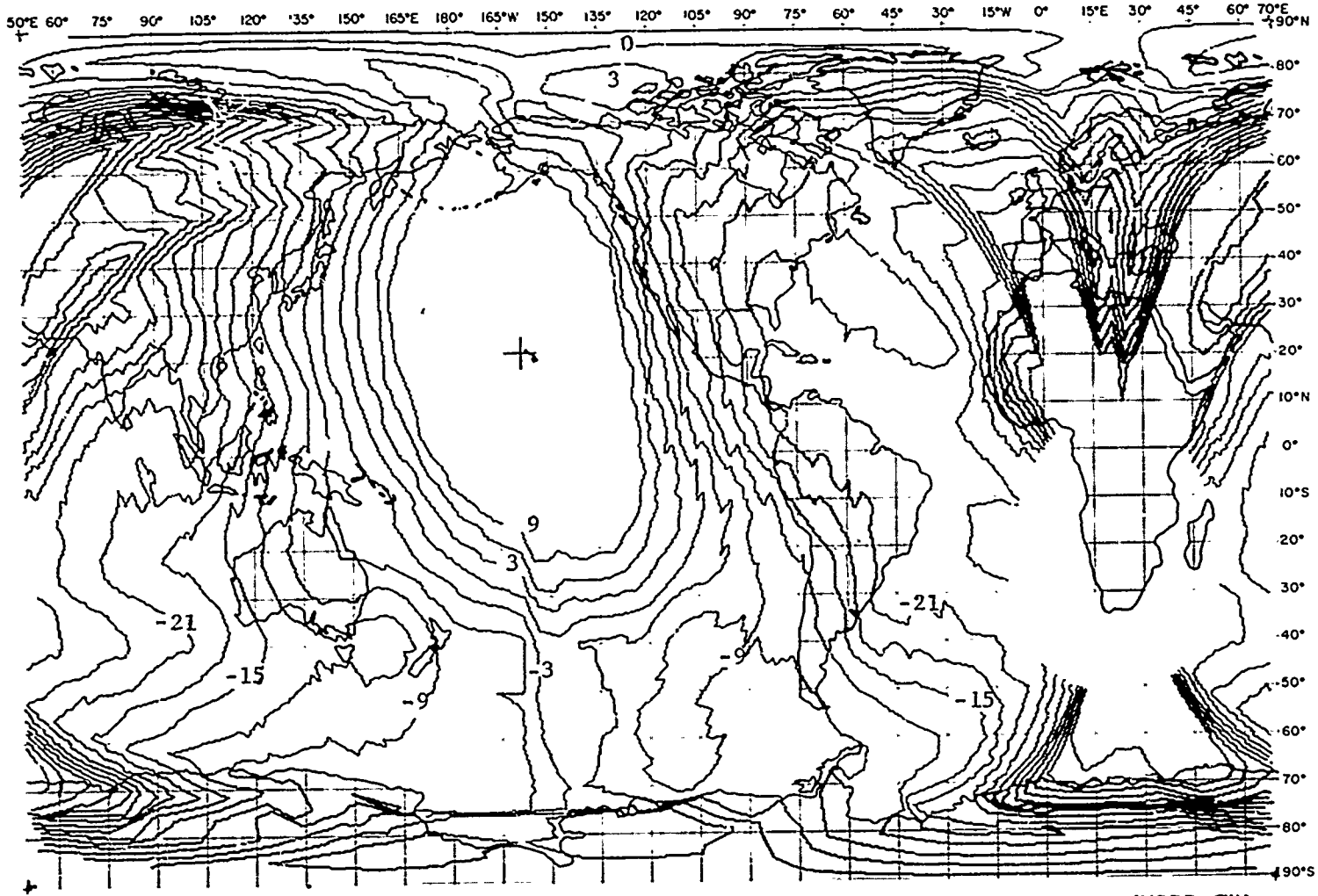


FIG. SU 28 - SIGNAL-TO-ATMOSPHERIC NOISE RATIO CONTOURS IN dB
NPM (23.4KHZ, 630KW) , LURLURLEI
SUMMER 99% TIME AVAILABILITY 1KHZ BANDWIDTH

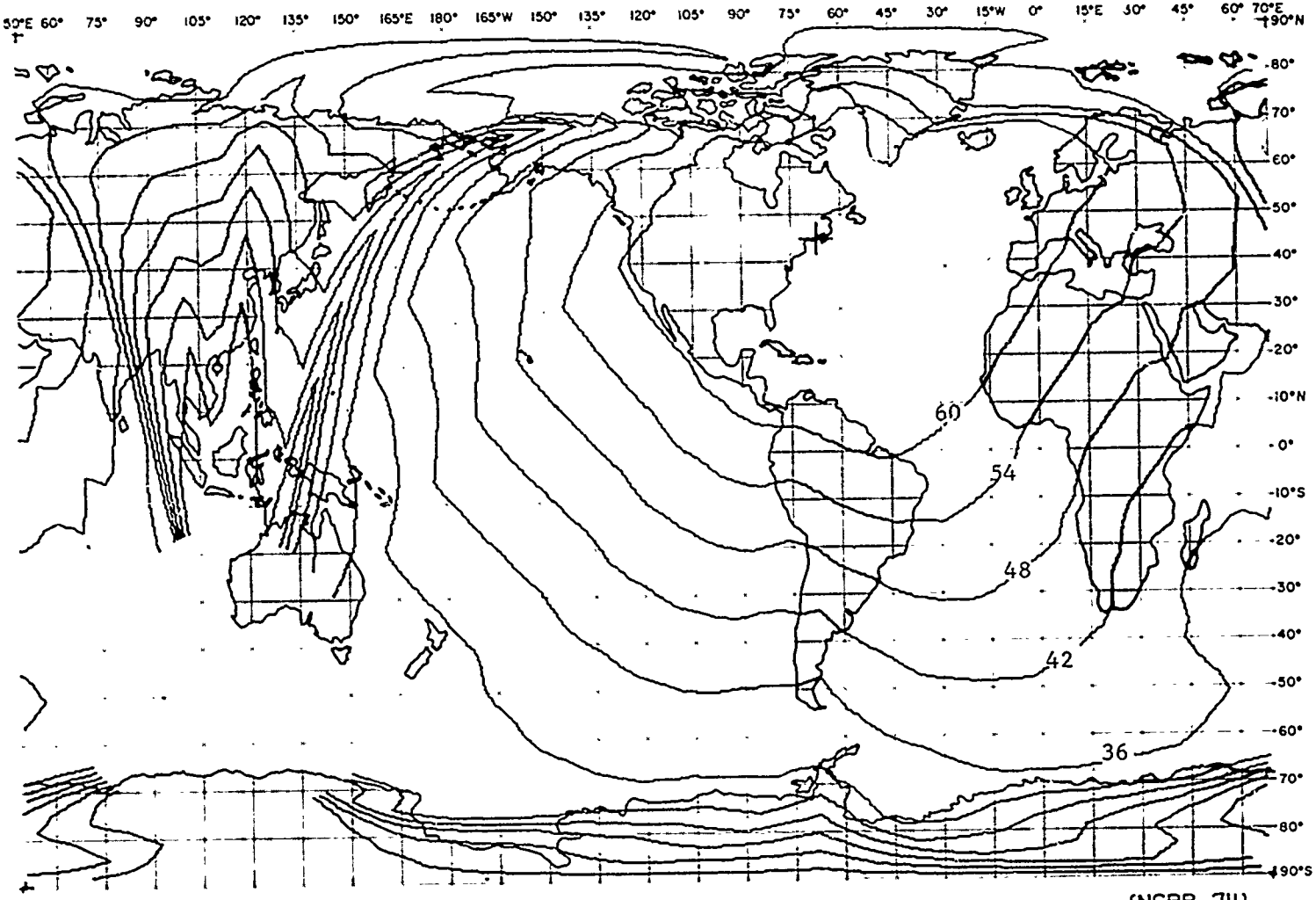


FIG. FR 1 - SIGNAL LEVEL CONTOURS IN dB>1μV/M
NAA (17.8KHZ, 1000KW) , CUTLER
FALL 90% TIME AVAILABILITY

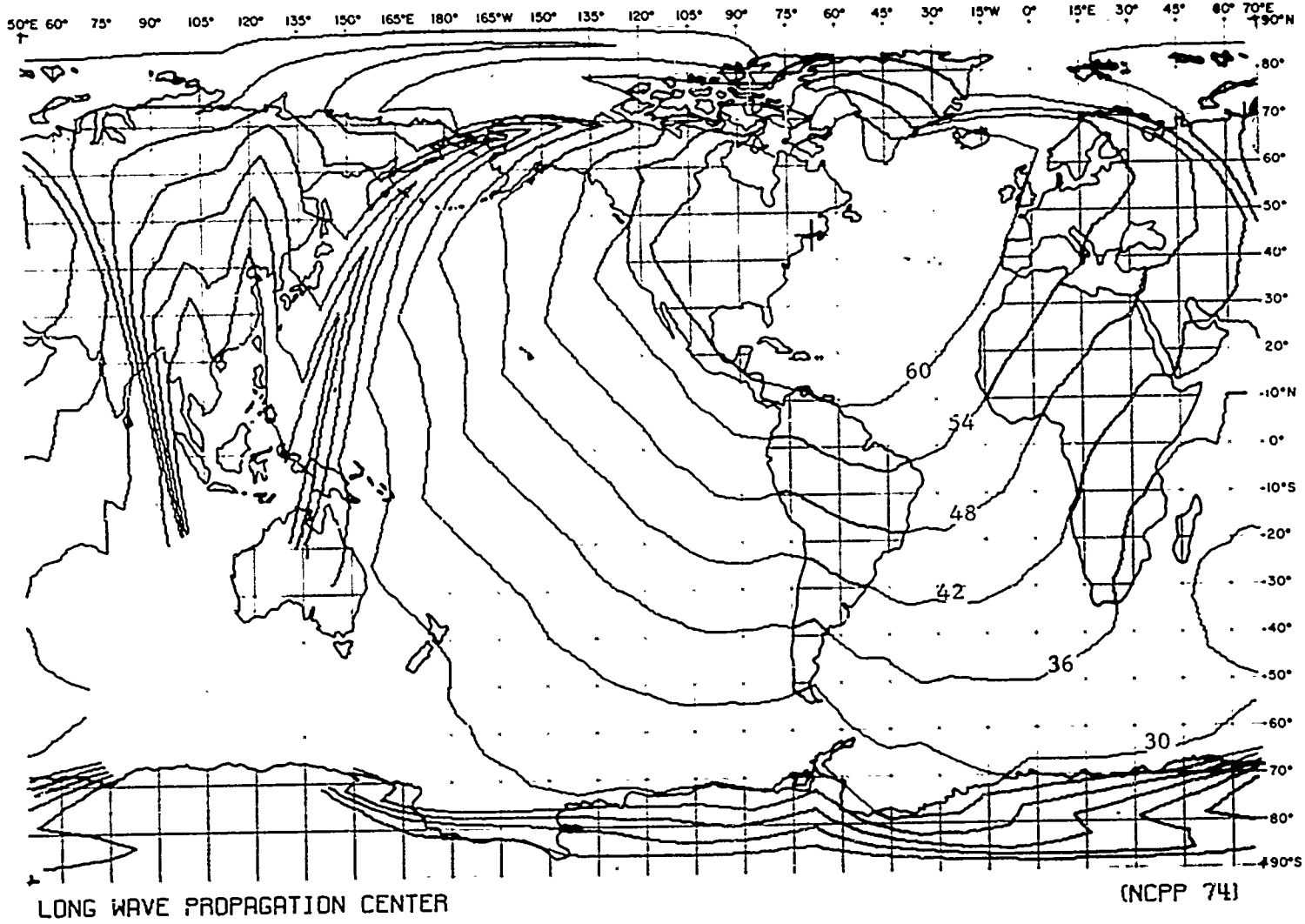


FIG. FA 2 - SIGNAL LEVEL CONTOURS IN dB>1μV/M
NAA (17.8KHZ, 1000KW) , CUTLER
FALL 99% TIME AVAILABILITY

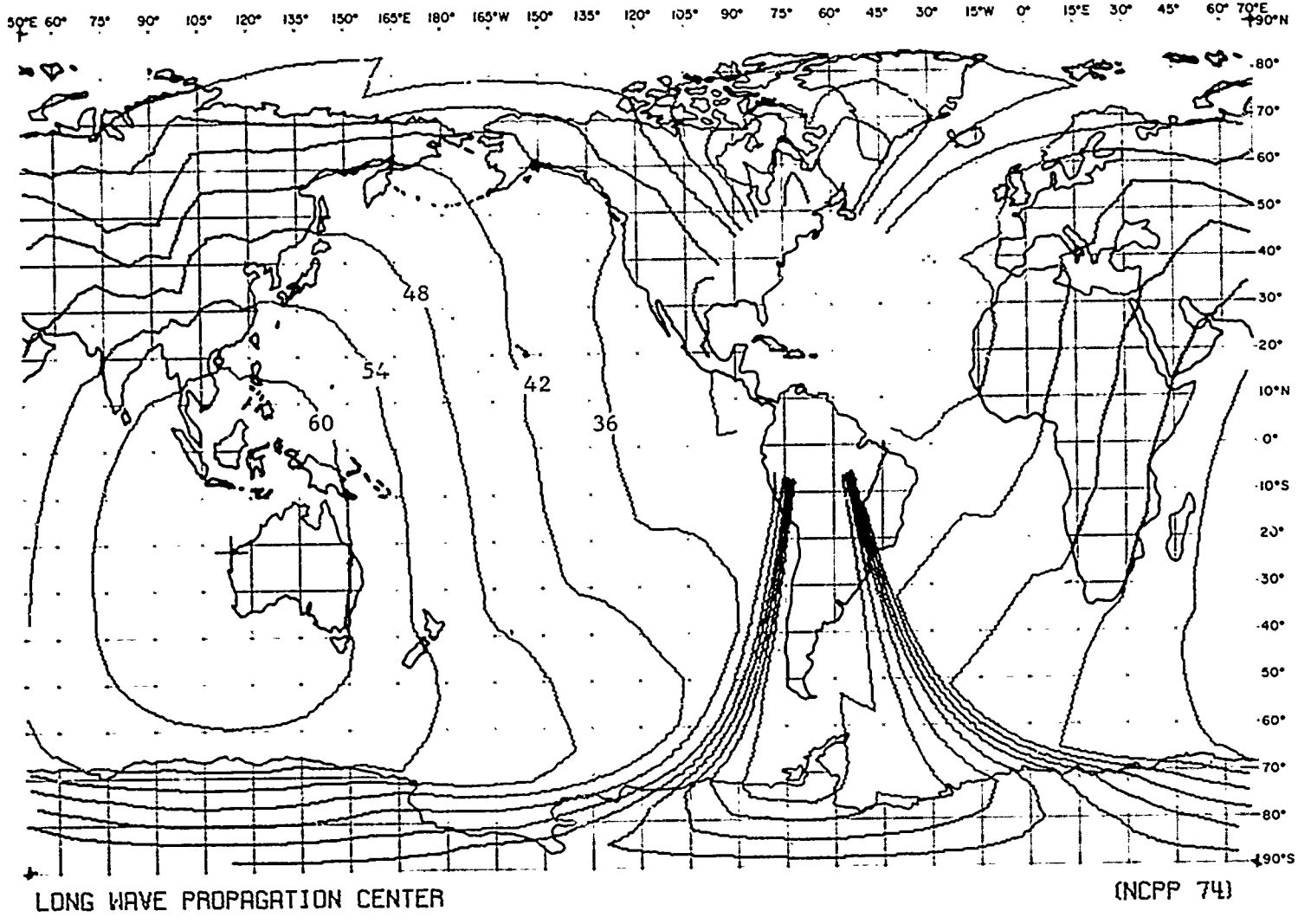


FIG. FA 3 – SIGNAL LEVEL CONTOURS IN dB>1μV/M
NWC (22.3KHZ, 1000KW) , NORTHWEST CAPE
FALL 90% TIME AVAILABILITY

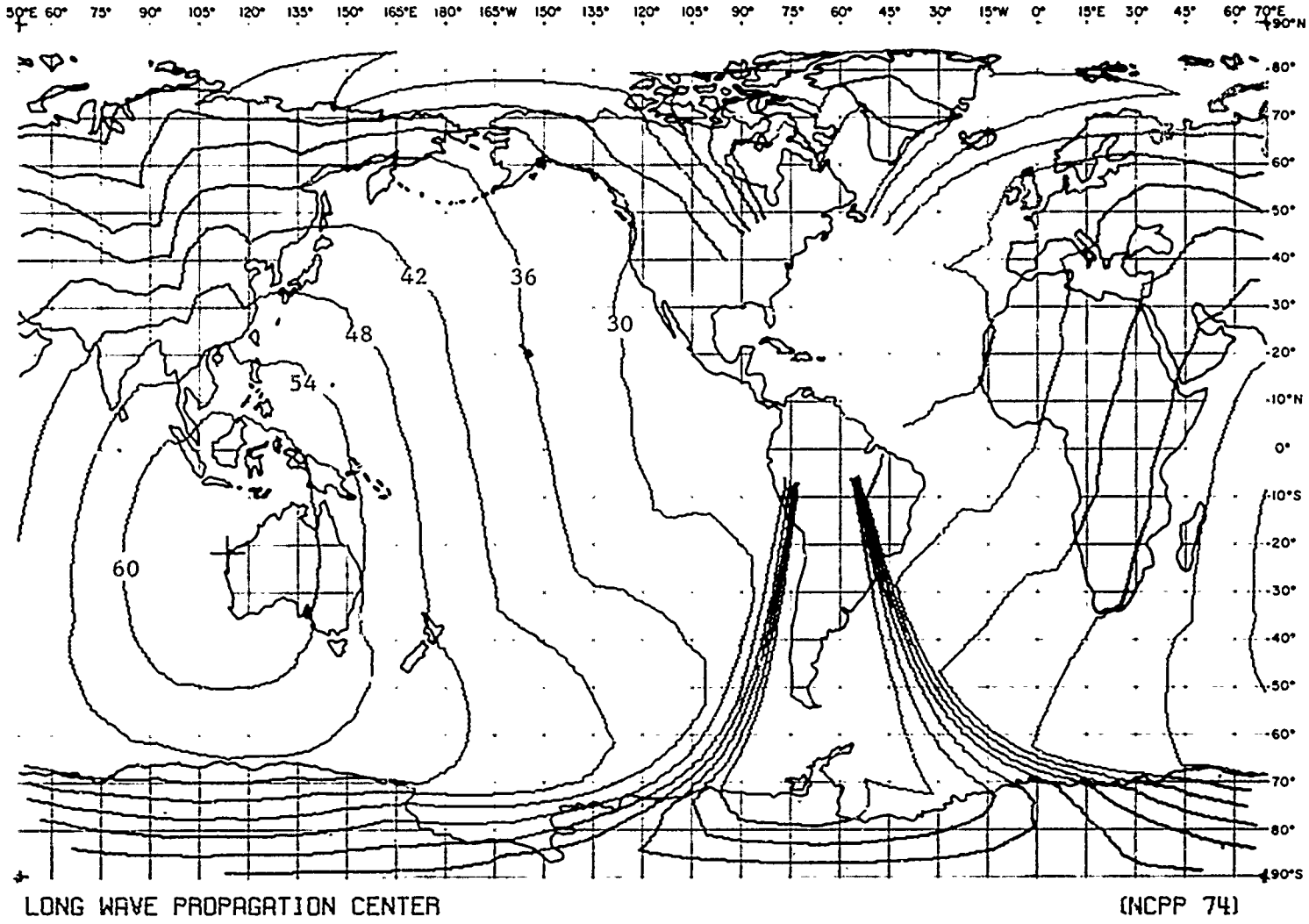


FIG. FA 4 - SIGNAL LEVEL CONTOURS IN dB>1μV/M
NWC (22.3KHZ, 1000KW) , NORTHWEST CAPE
FALL 99% TIME AVAILABILITY

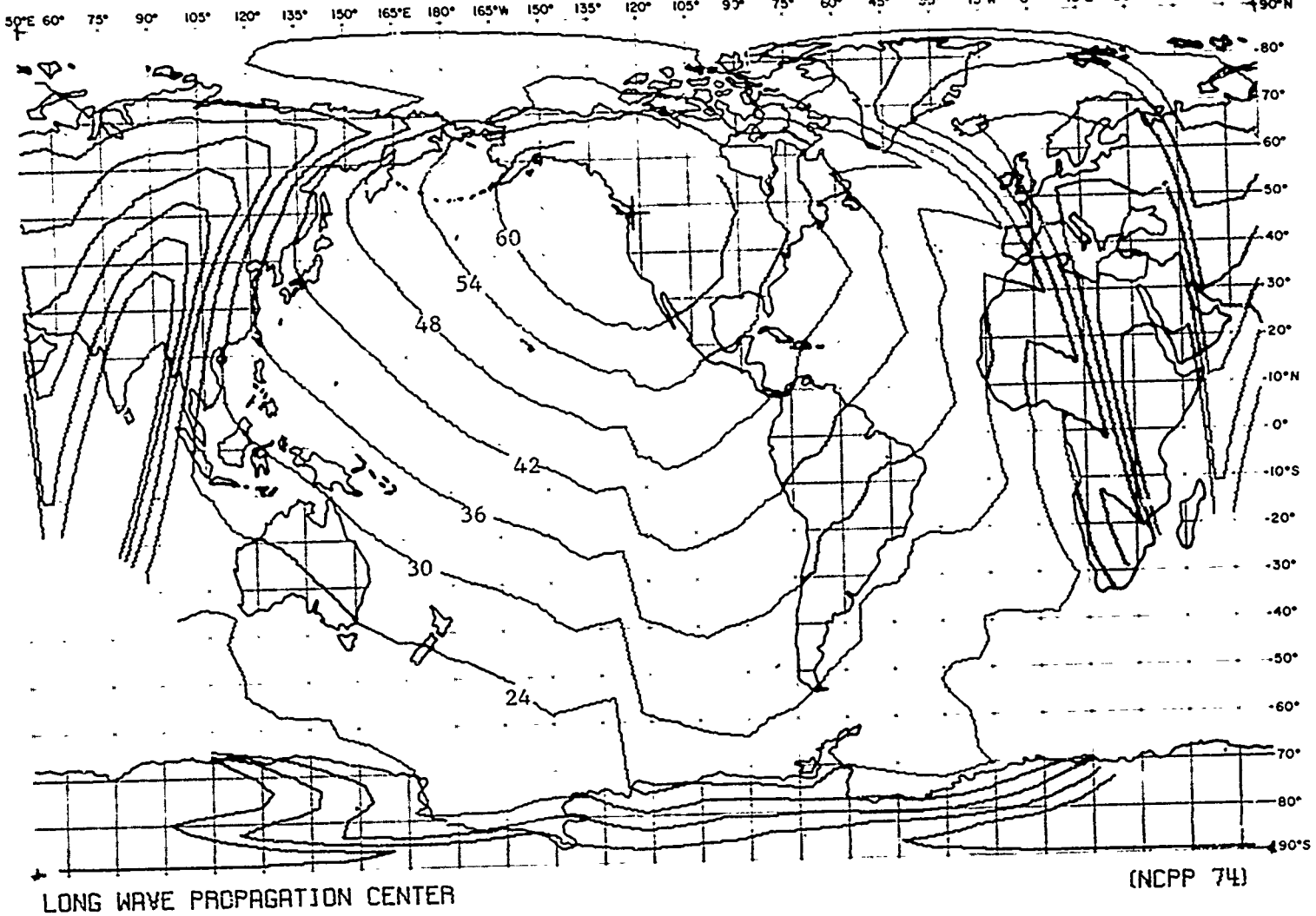


FIG. FA 5 - SIGNAL LEVEL CONTOURS IN dB>1μV/M
NPG (18.6KHZ, 130KW), JIM CREEK
FALL 90% TIME AVAILABILITY

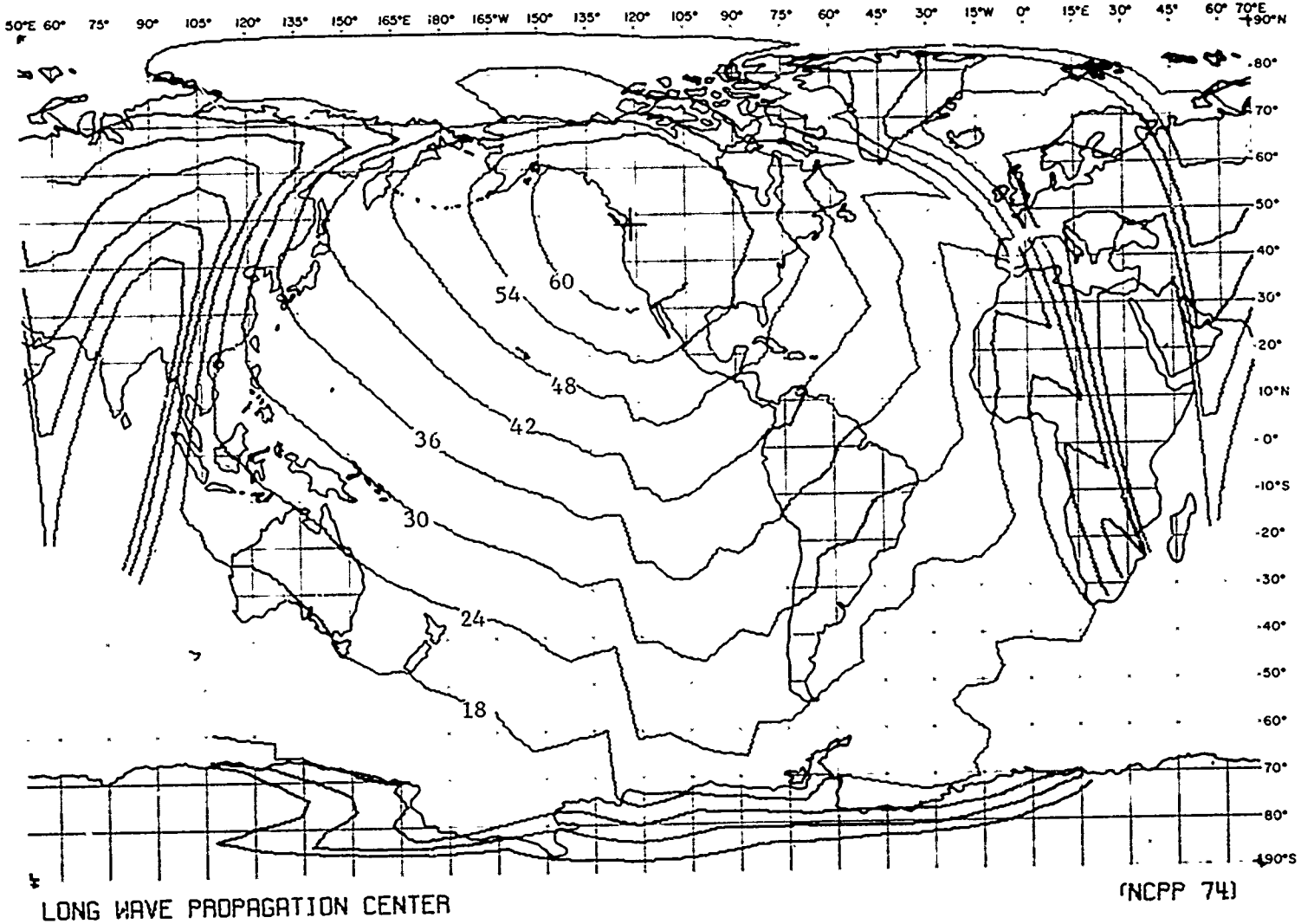


FIG. FA 6 - SIGNAL LEVEL CONTOURS IN dB>1μV/M
NPG (18.6KHZ, 130KW), JIM CREEK
FALL 99% TIME AVAILABILITY

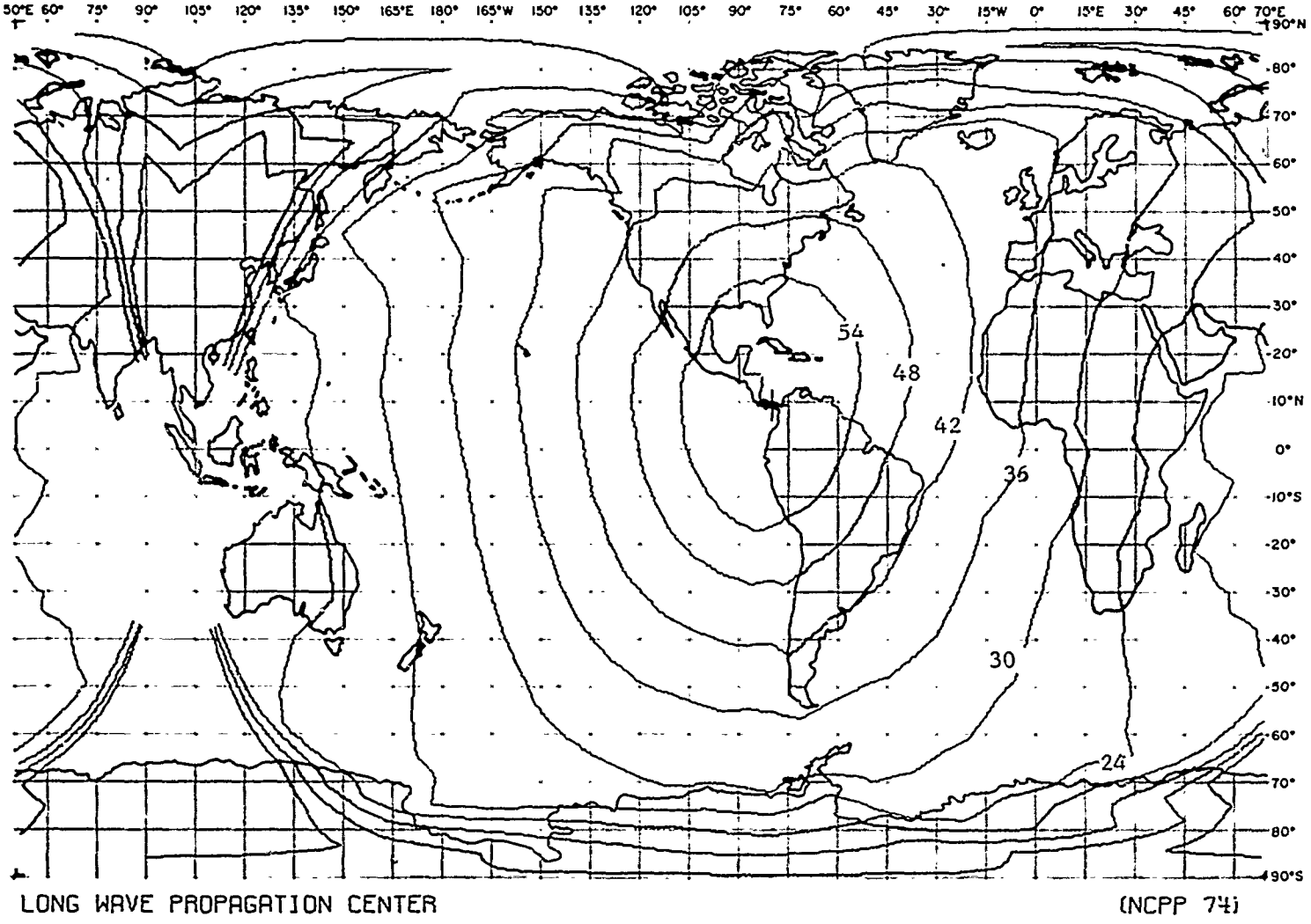


FIG. FR 7 - SIGNAL LEVEL CONTOURS IN dB>1μV/M
NBA (24.0KHZ, 110KW) , BALBOA
FALL 90% TIME AVAILABILITY

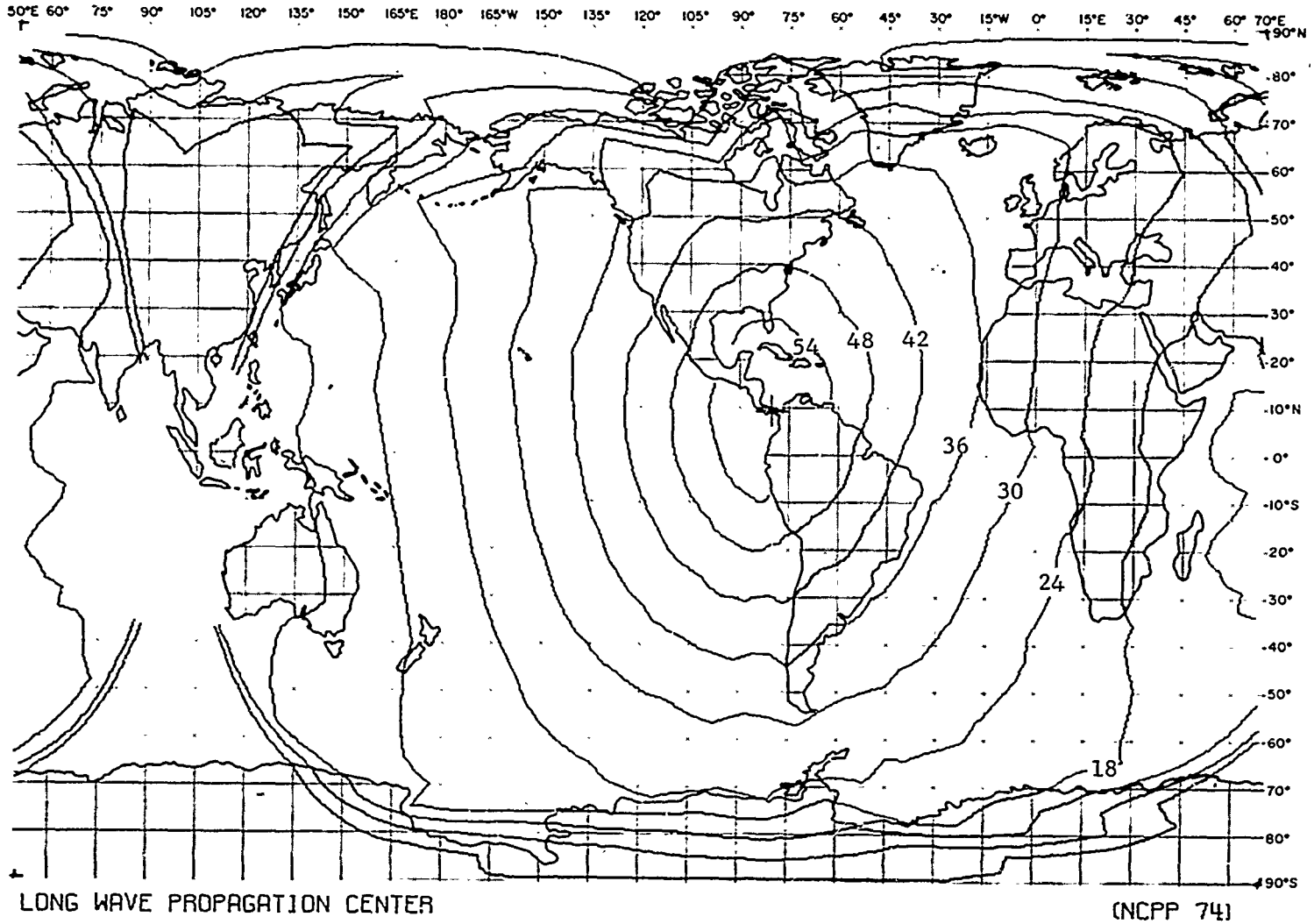


FIG. FR 8 - SIGNAL LEVEL CONTOURS IN dB>1μV/M
NBA (24.0KHZ, 110KW) , BALBOA
FALL 99% TIME AVAILABILITY

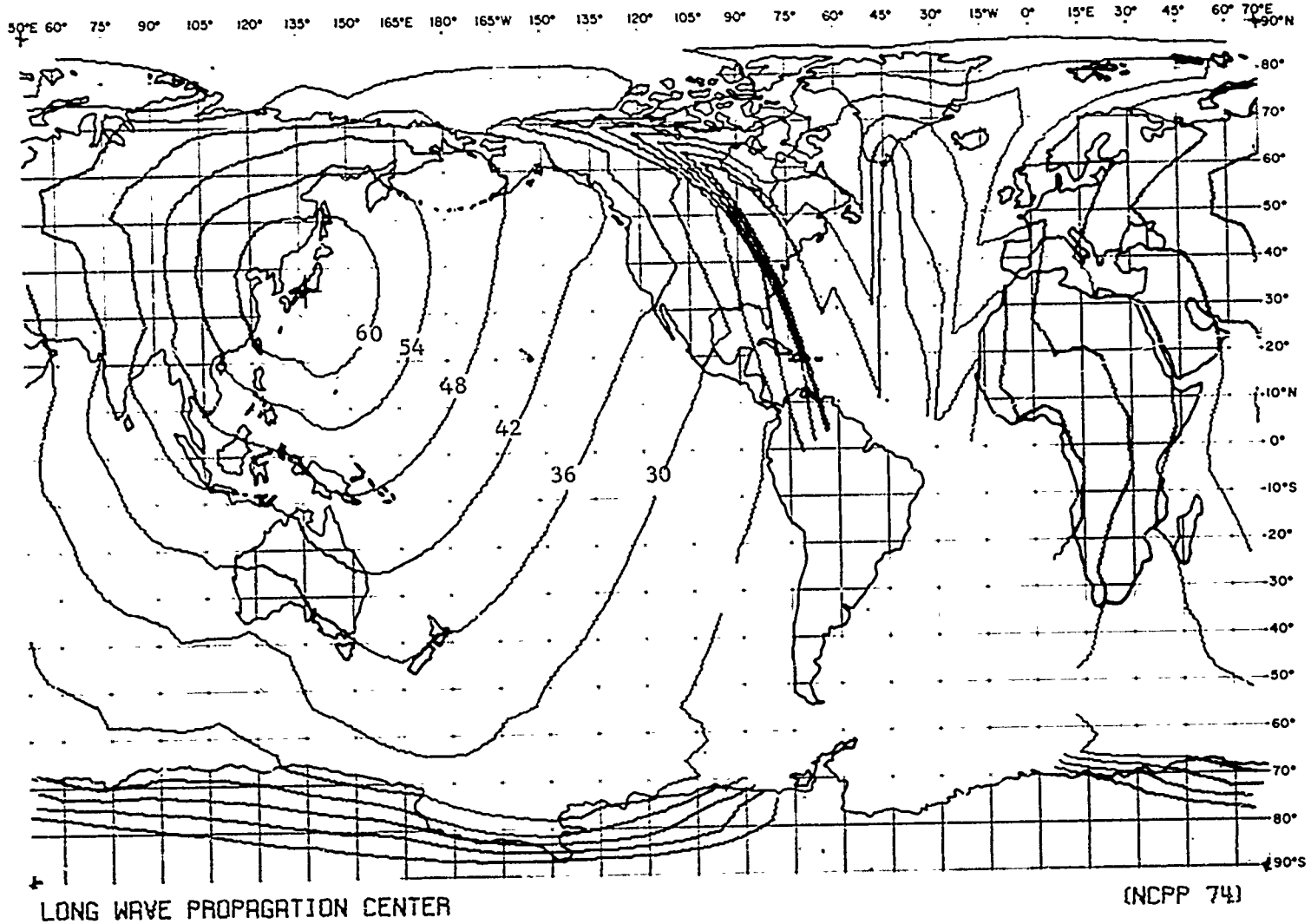


FIG. FR 9 - SIGNAL LEVEL CONTOURS IN dB>1μV/M
NDT (17.4KHZ, 40KW) , YOSAMI
FALL 90% TIME AVAILABILITY

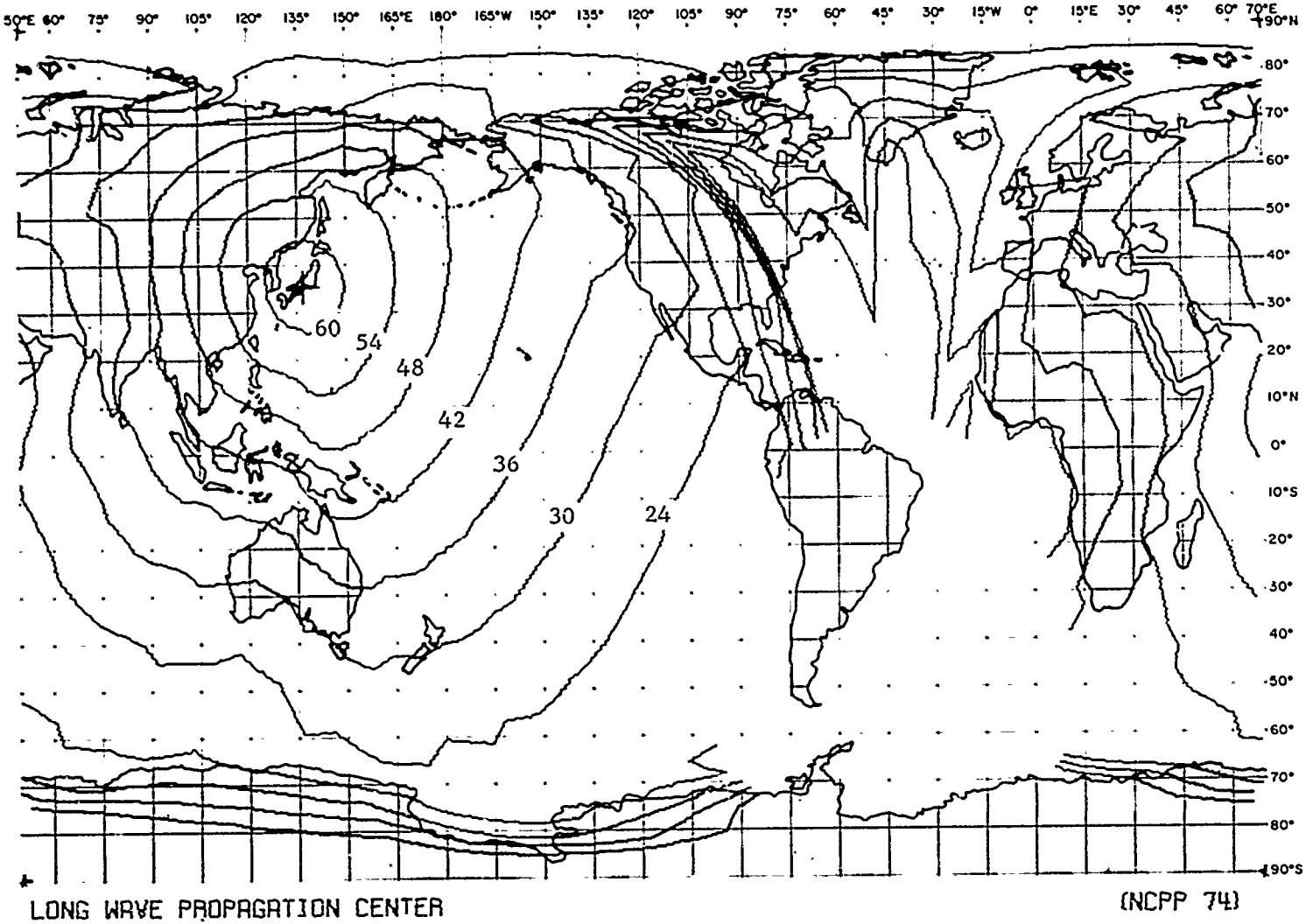


FIG. FR 10 - SIGNAL LEVEL CONTOURS IN dB>1μV/M
NDT (17.4KHZ, 40KW) , YOSAMI
FALL 99% TIME AVAILABILITY

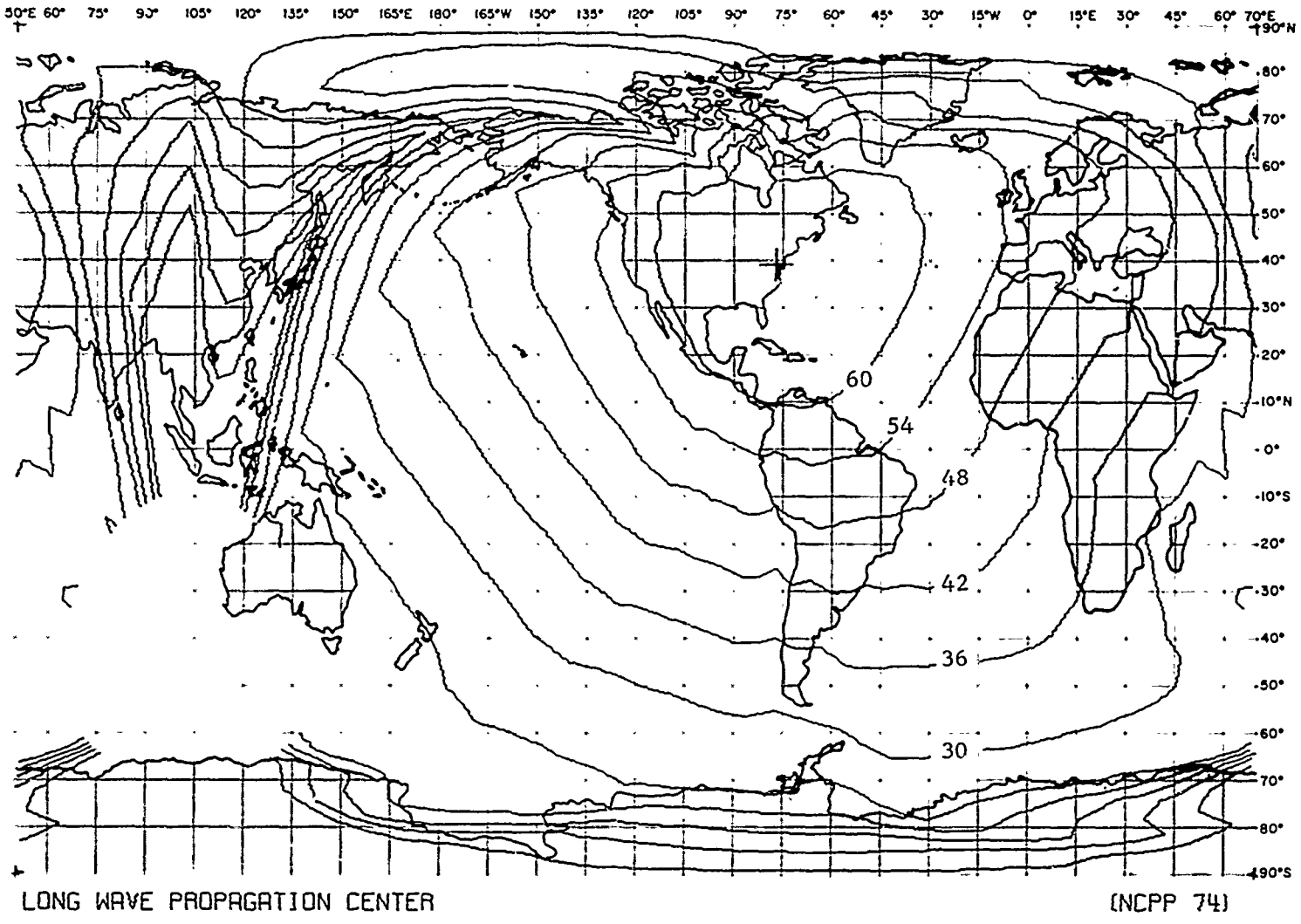


FIG. FA 11 - SIGNAL LEVEL CONTOURS IN dB>1μV/M
NSS (21.4KHZ, 400KW) , ANNAPOLIS
FALL 90% TIME AVAILABILITY

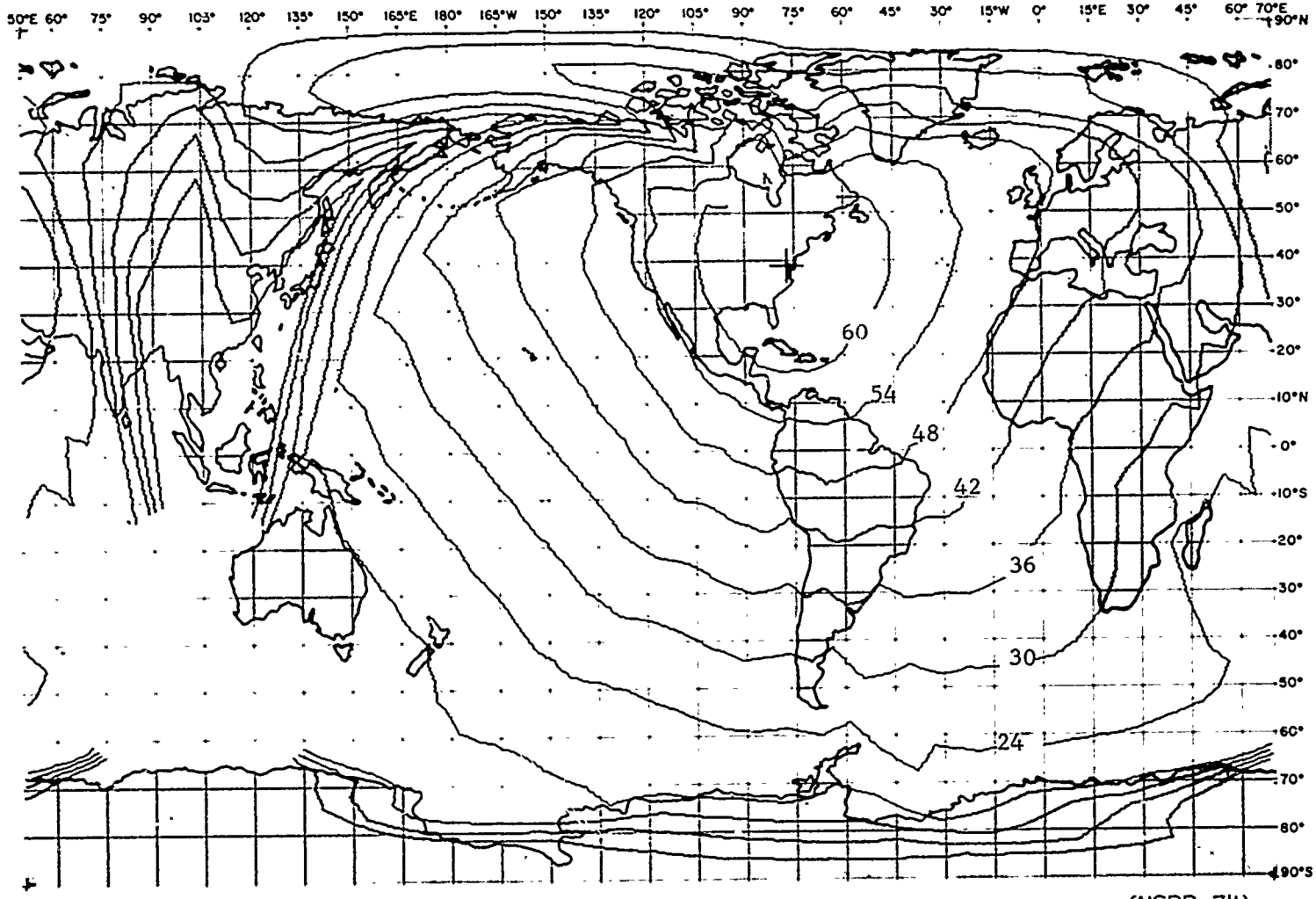


FIG. FA 12 - SIGNAL LEVEL CONTOURS IN dB>1μV/M
NSS (21.4KHZ, 400KW) , ANNAPOLIS
FALL 99% TIME AVAILABILITY

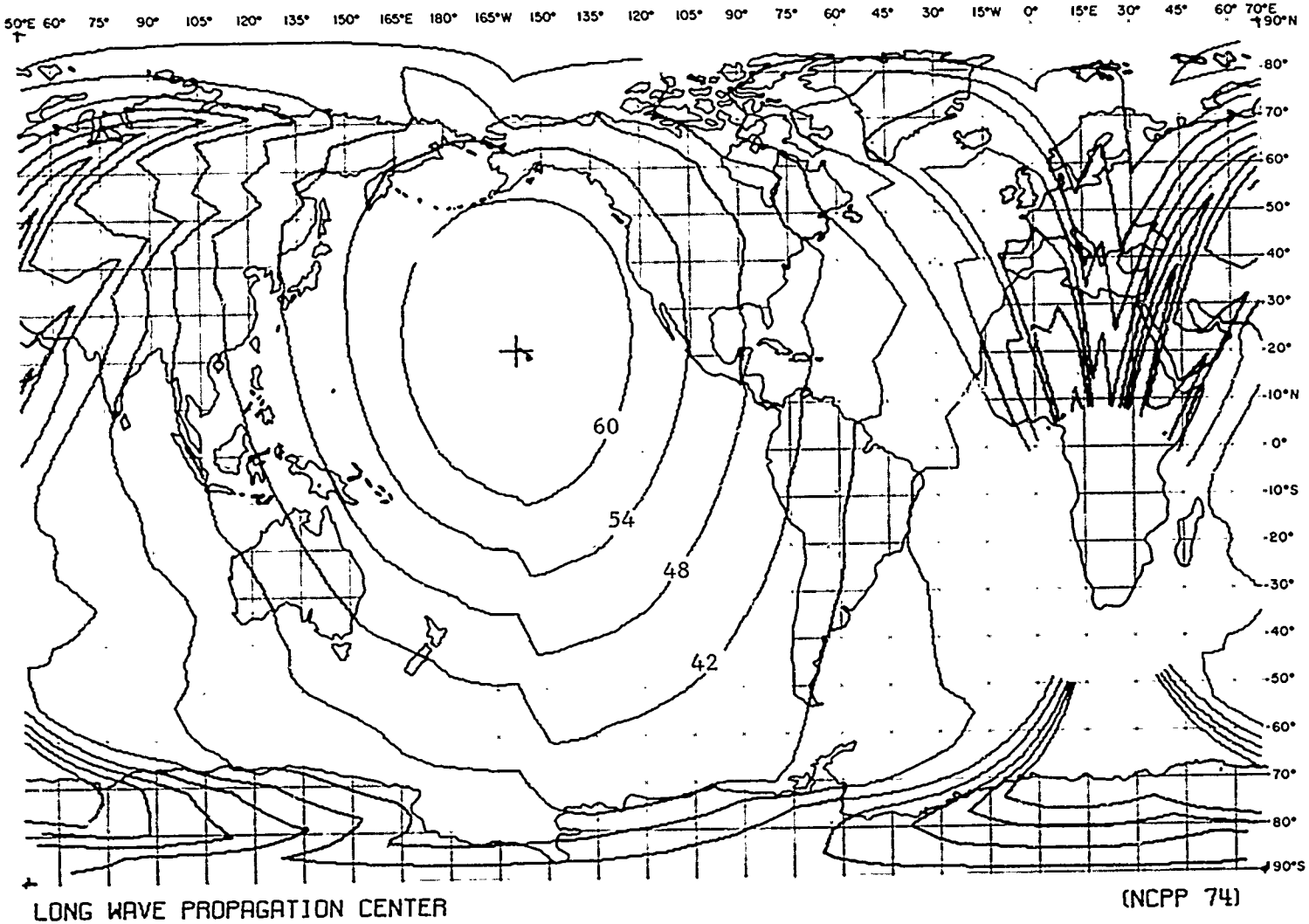


FIG. FA 13 - SIGNAL LEVEL CONTOURS IN dB>1μV/M
NPM (23.4KHZ, 630KW) , LURLURLEI
FALL 90% TIME AVAILABILITY

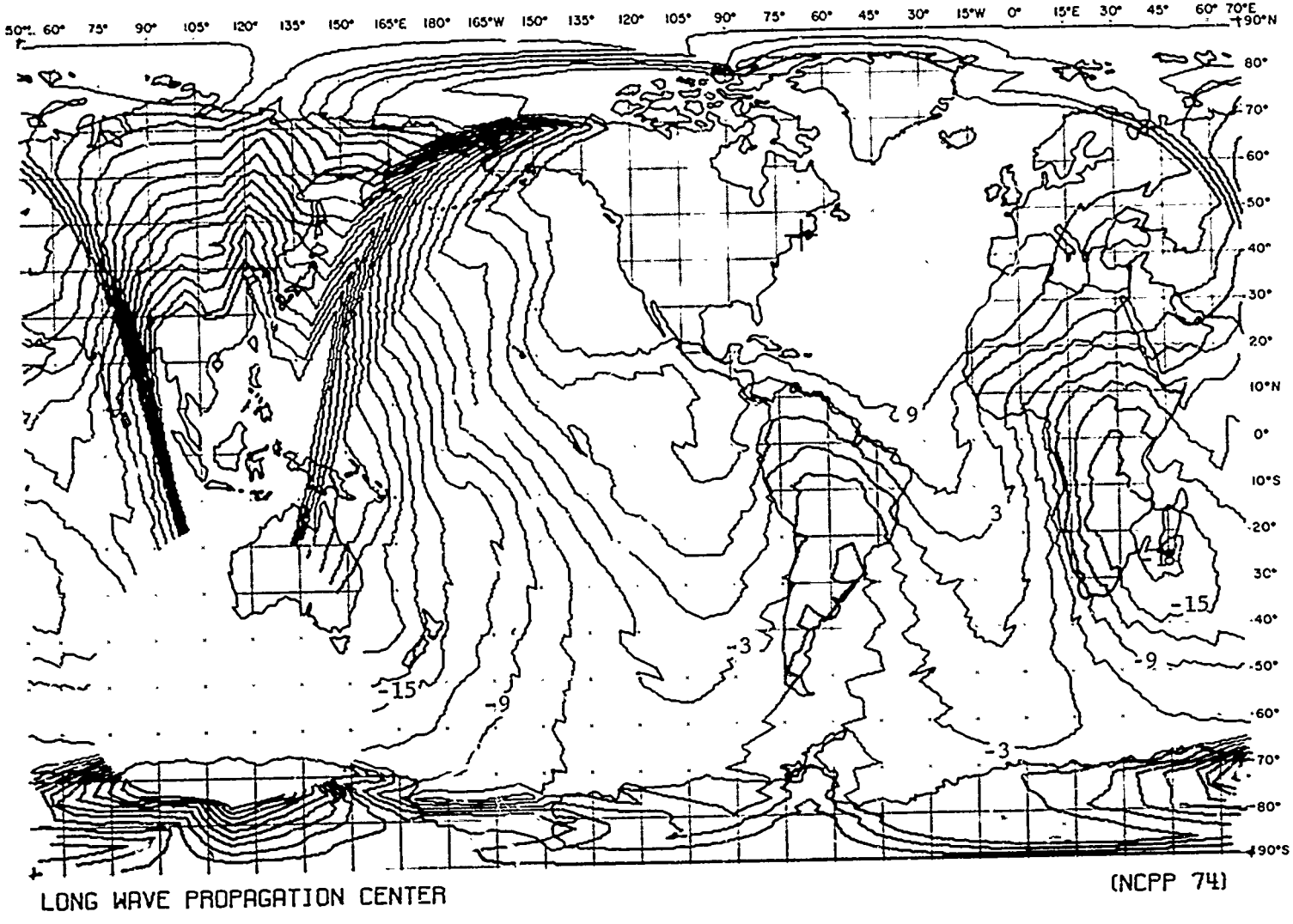


FIG. FA 15 - SIGNAL-TO-ATMOSPHERIC NOISE RATIO CONTOURS IN dB
NAA (17.8KHZ, 1000KW) , CUTLER
FALL 90% TIME AVAILABILITY 1KHZ BANDWIDTH

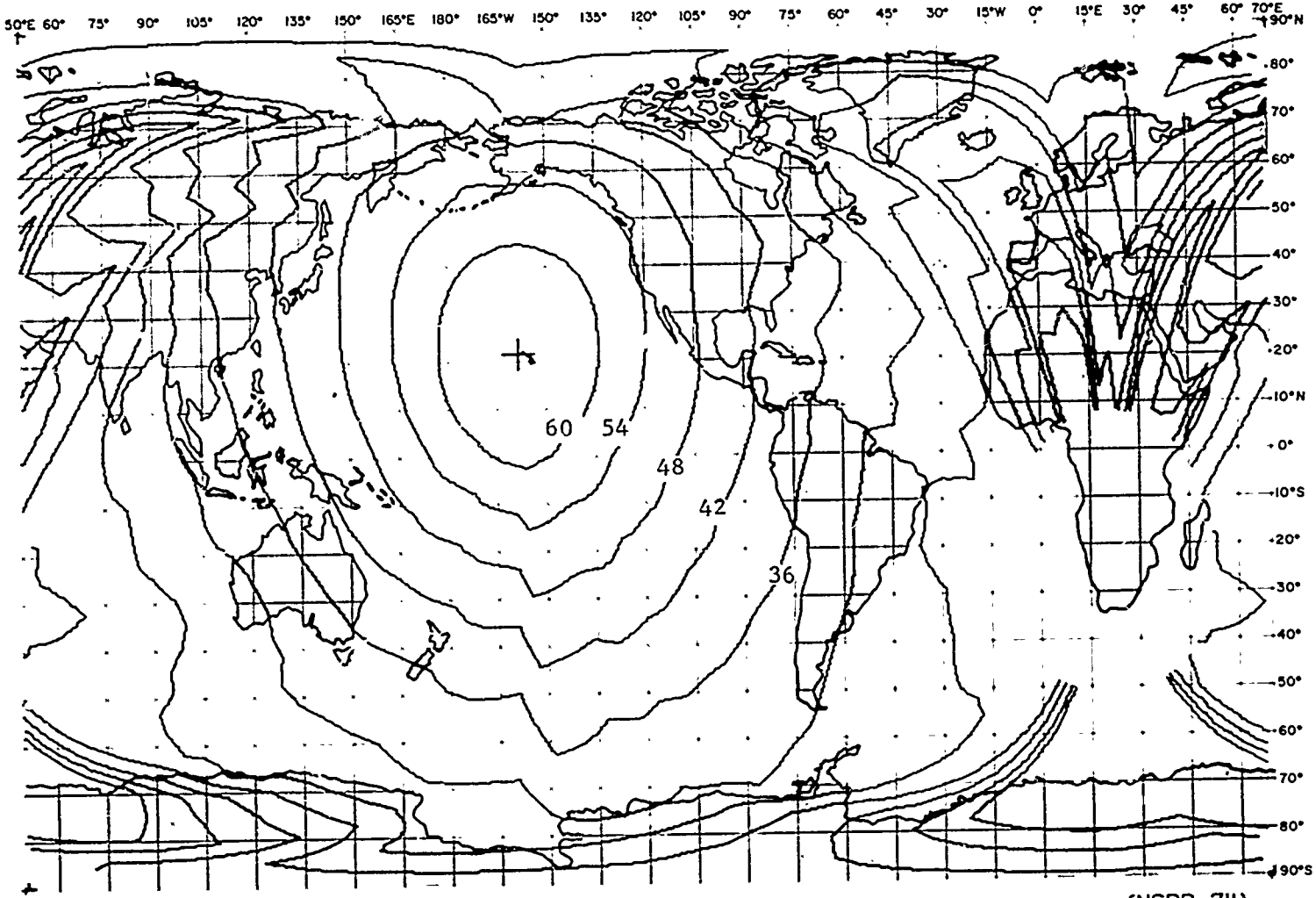


FIG. FR 14 - SIGNAL LEVEL CONTOURS IN dB>1μV/M
NPM (23.4KHZ, 630KW) , LUALUALEI
FALL 99% TIME AVAILABILITY

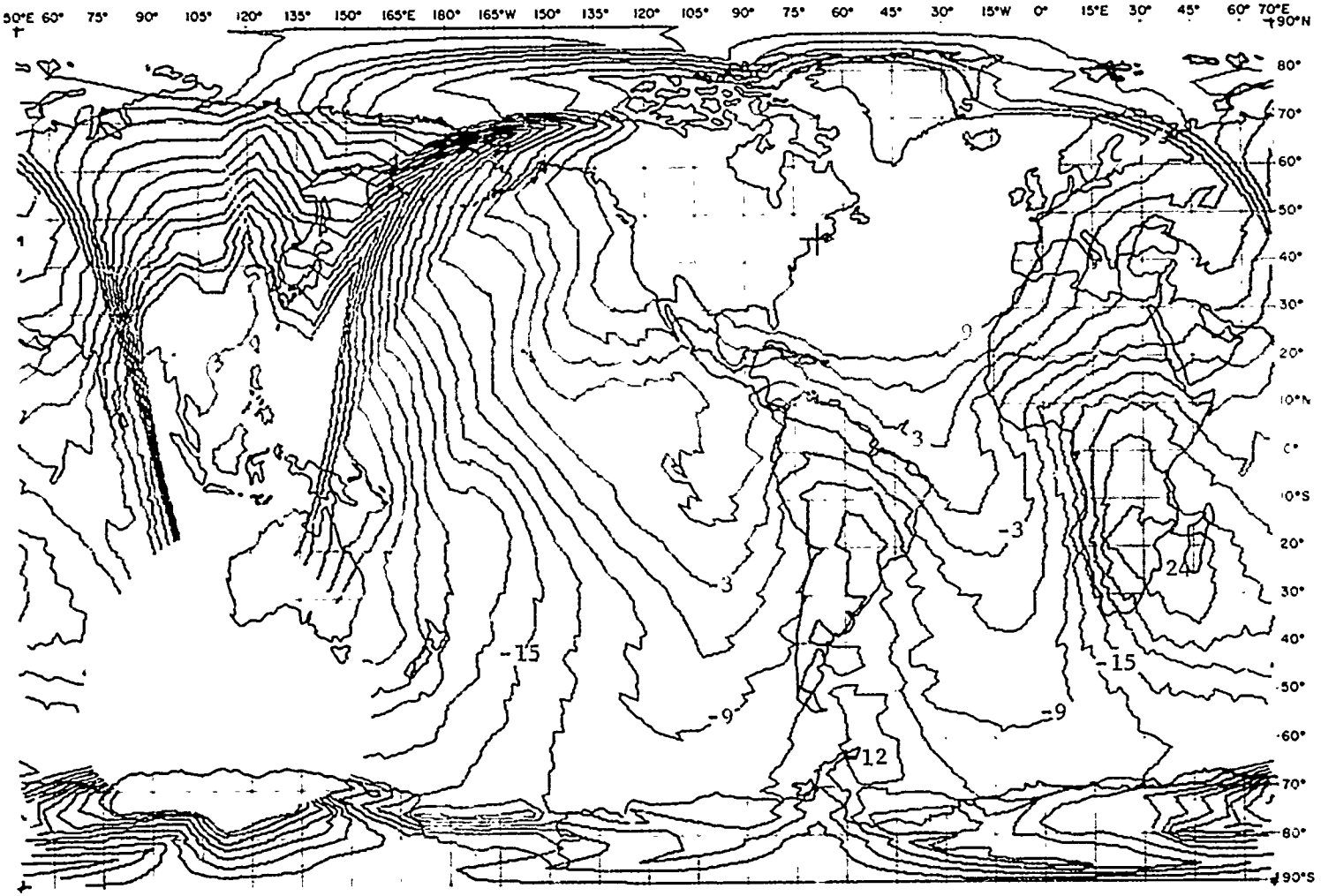


FIG. FA 16 - SIGNAL-TO-ATMOSPHERIC NOISE RATIO CONTOURS IN dB
NAA (17.8KHZ, 1000KW) , CUTLER
FALL 99% TIME AVAILABILITY 1KHZ BANDWIDTH

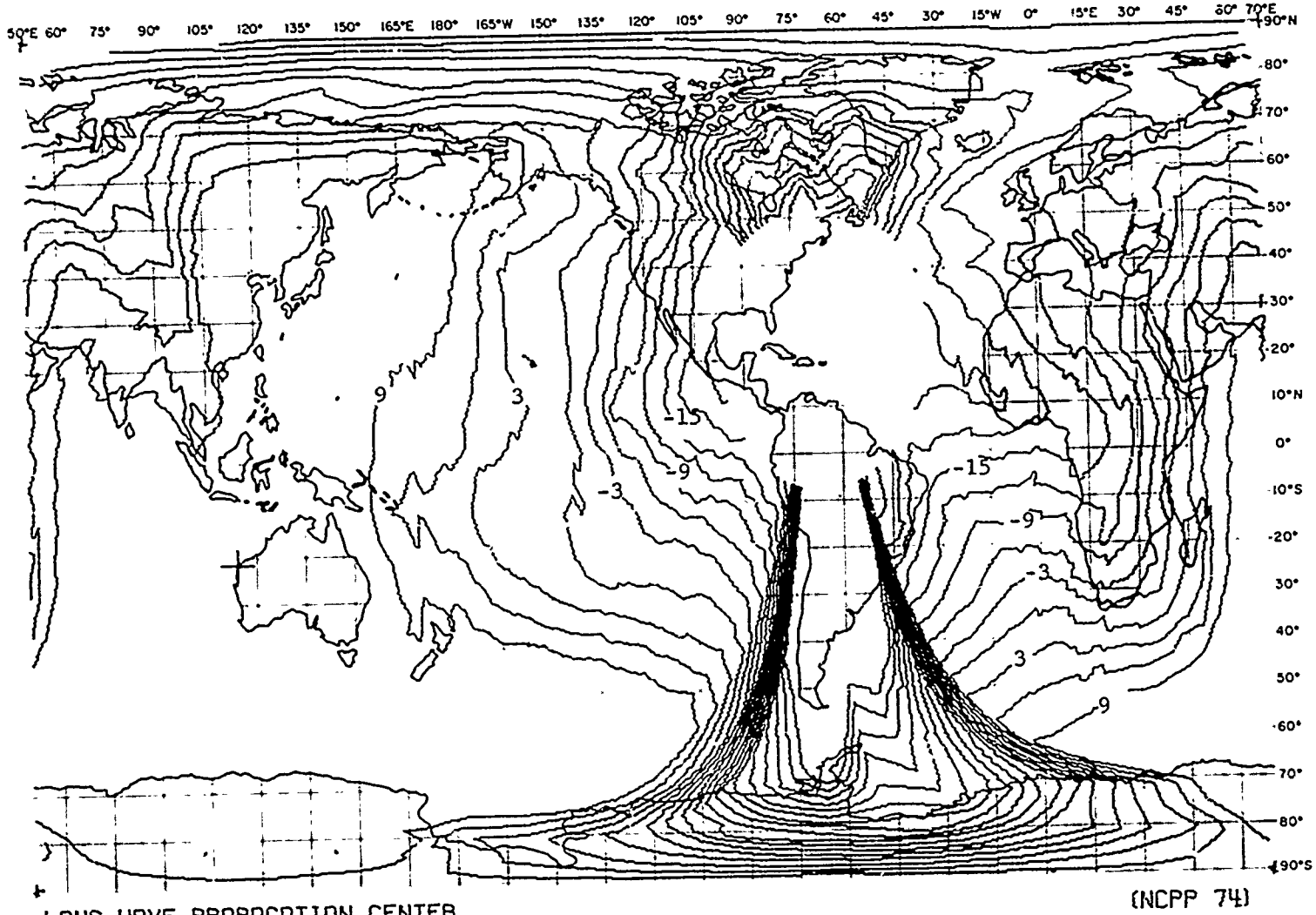


FIG. FA 17 - SIGNAL-TO-ATMOSPHERIC NOISE RATIO CONTOURS IN dB
NWC (22.3KHZ, 1000KW) , NORTHWEST CAPE
FALL 90% TIME AVAILABILITY 1KHZ BANDWIDTH

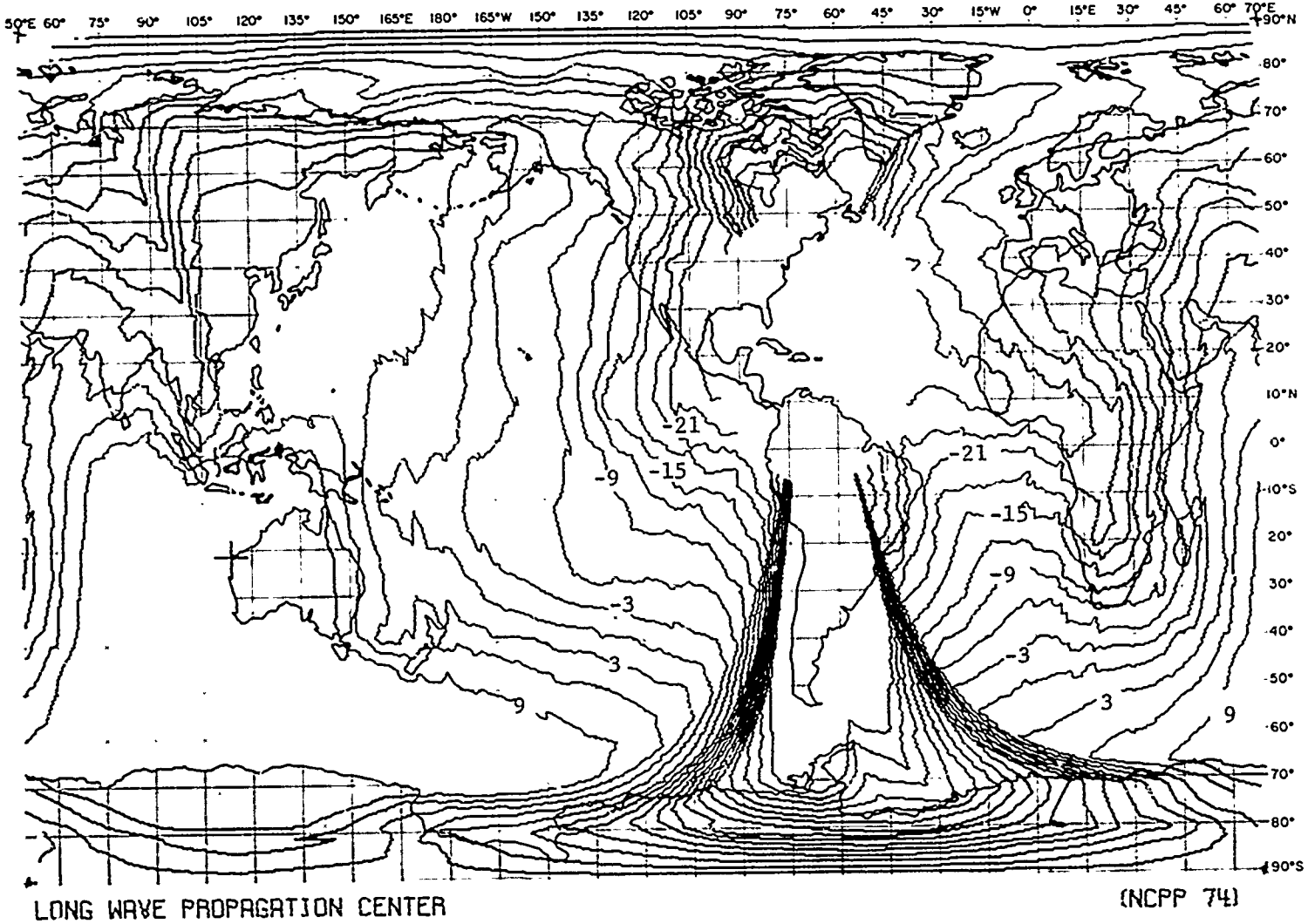


FIG. FA 18 - SIGNAL-TO-ATMOSPHERIC NOISE RATIO CONTOURS IN dB
NWC (22.3KHZ, 1000KW) , NORTHWEST CAPE
FALL 99% TIME AVAILABILITY 1KHZ BANDWIDTH

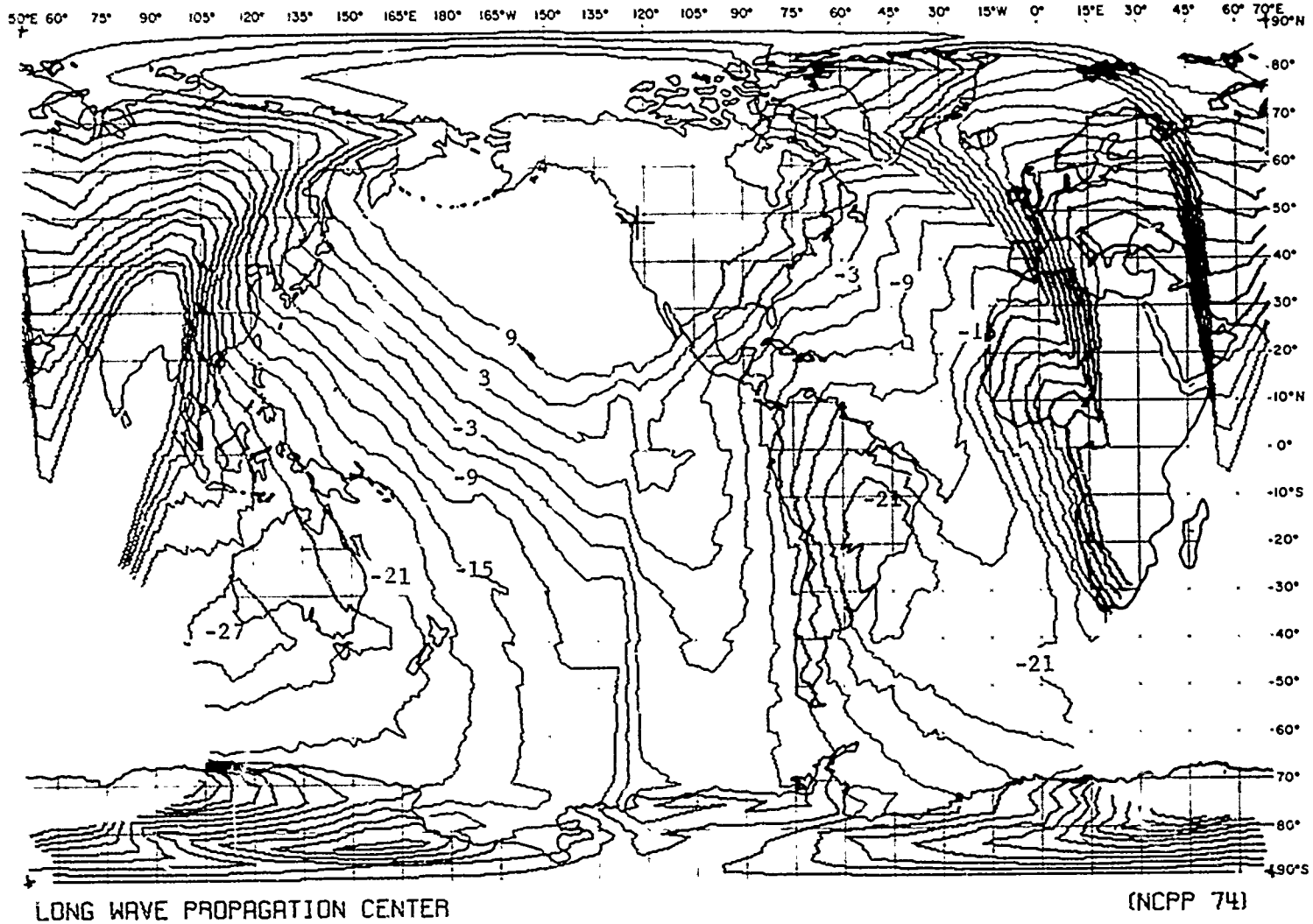


FIG. FA 19 - SIGNAL-TO-ATMOSPHERIC NOISE RATIO CONTOURS IN dB
NPG (18.6KHZ, 130KW) , JIM CREEK
FALL 90% TIME AVAILABILITY 1KHZ BANDWIDTH

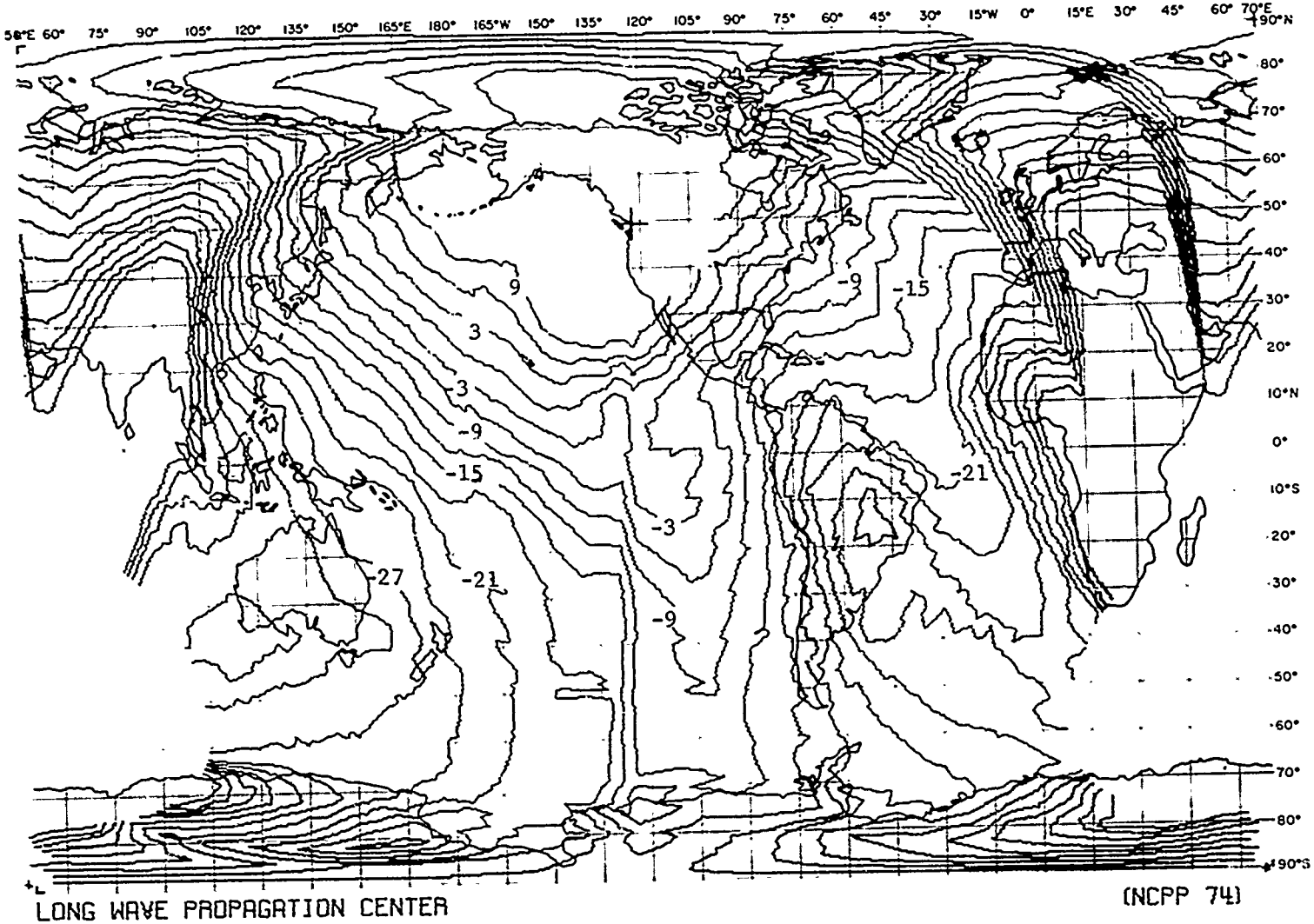


FIG. FA 20 - SIGNAL-TO-ATMOSPHERIC NOISE RATIO CONTOURS IN dB
NPG (18.6KHz, 130KW), JIM CREEK
FALL 99% TIME AVAILABILITY 1KHZ BANDWIDTH

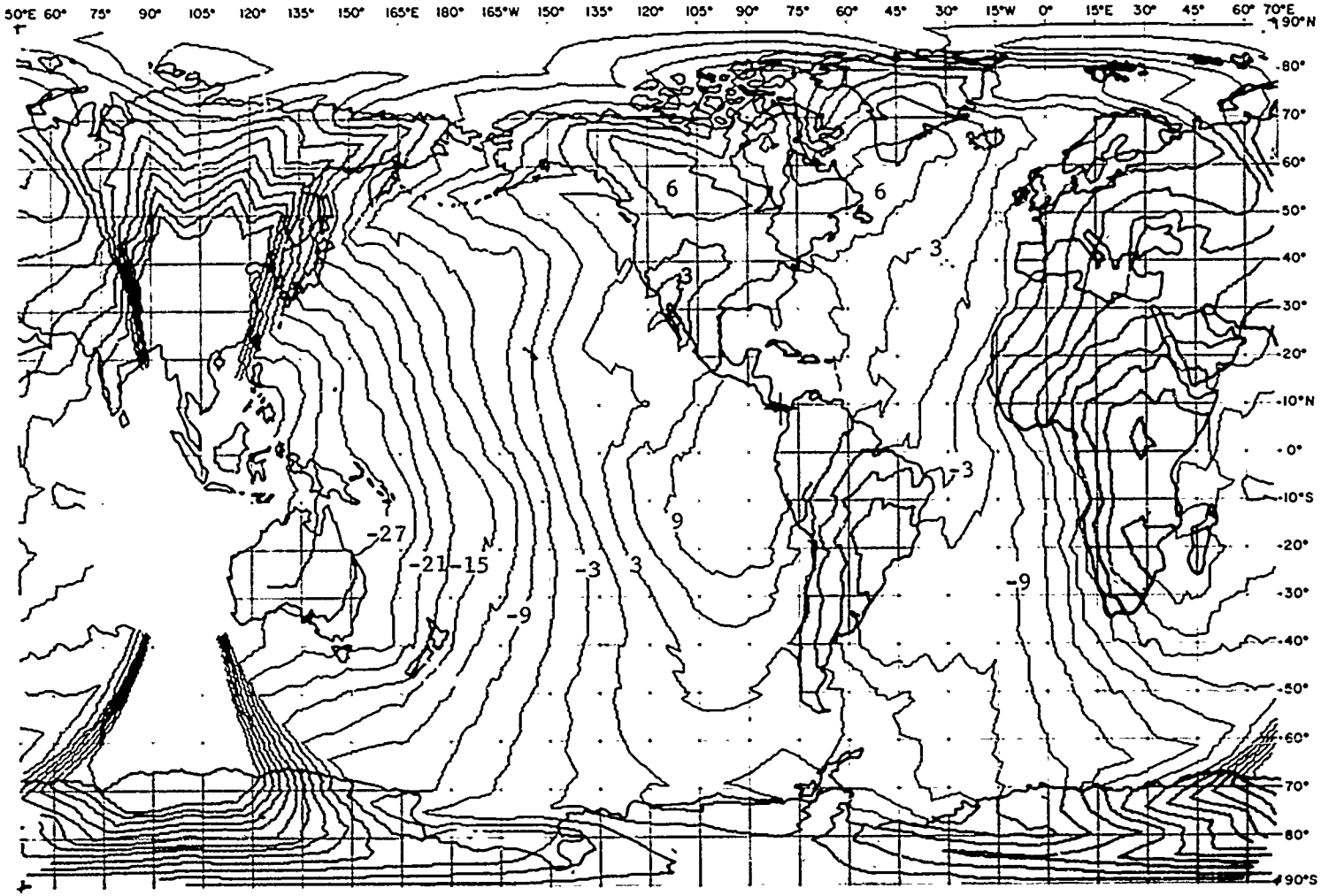


FIG. FA 21 - SIGNAL-TO-ATMOSPHERIC NOISE RATIO CONTOURS IN dB
NBA (24.0KHZ, 110KW) , BALBOA
FALL 90% TIME AVAILABILITY 1KHZ BANDWIDTH

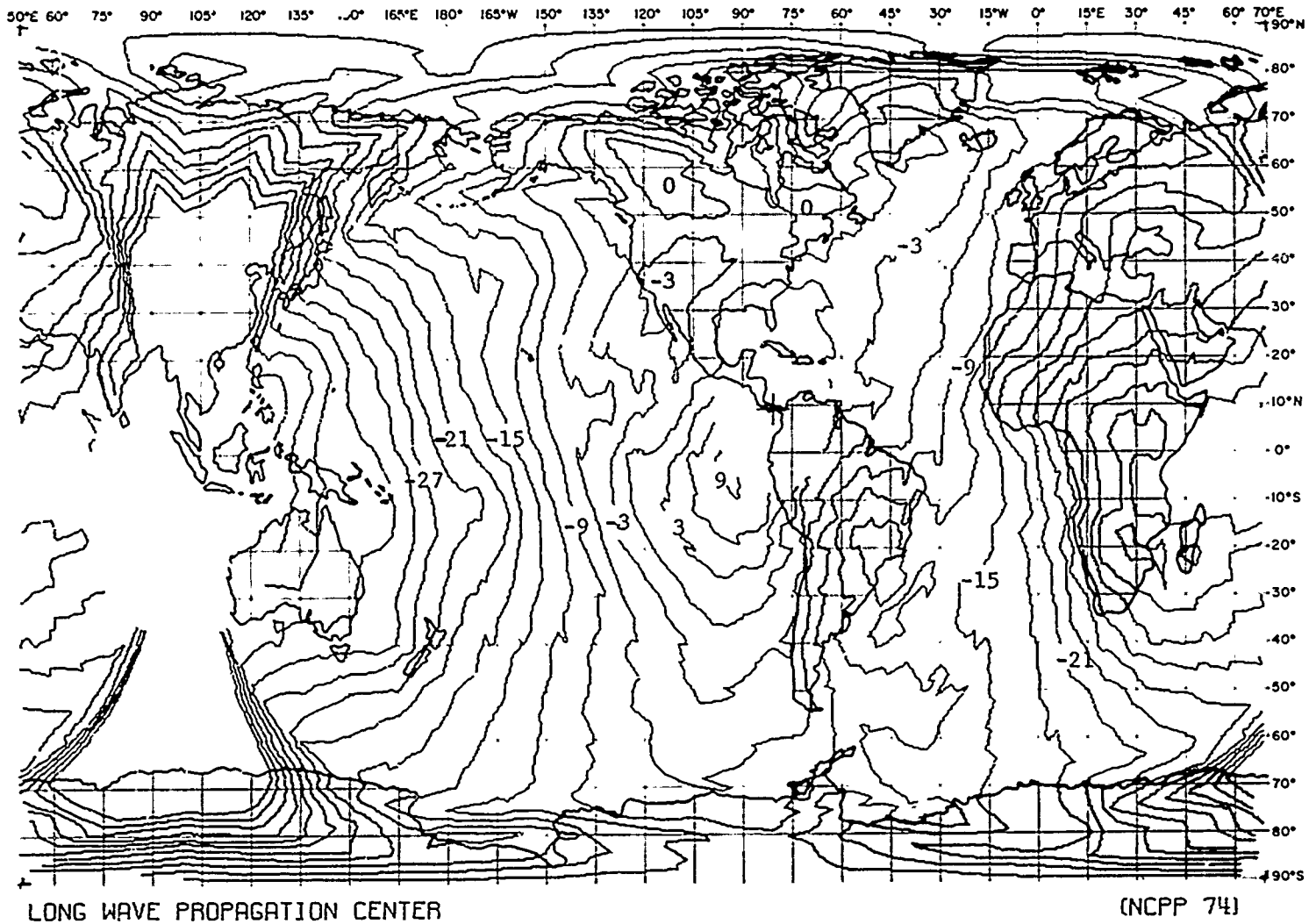


FIG. FA 22 - SIGNAL-TO-ATMOSPHERIC NOISE RATIO CONTOURS IN dB
NBA (24.0KHZ, 110KW) , BALBOA
FALL 99% TIME AVAILABILITY 1KHZ BANDWIDTH

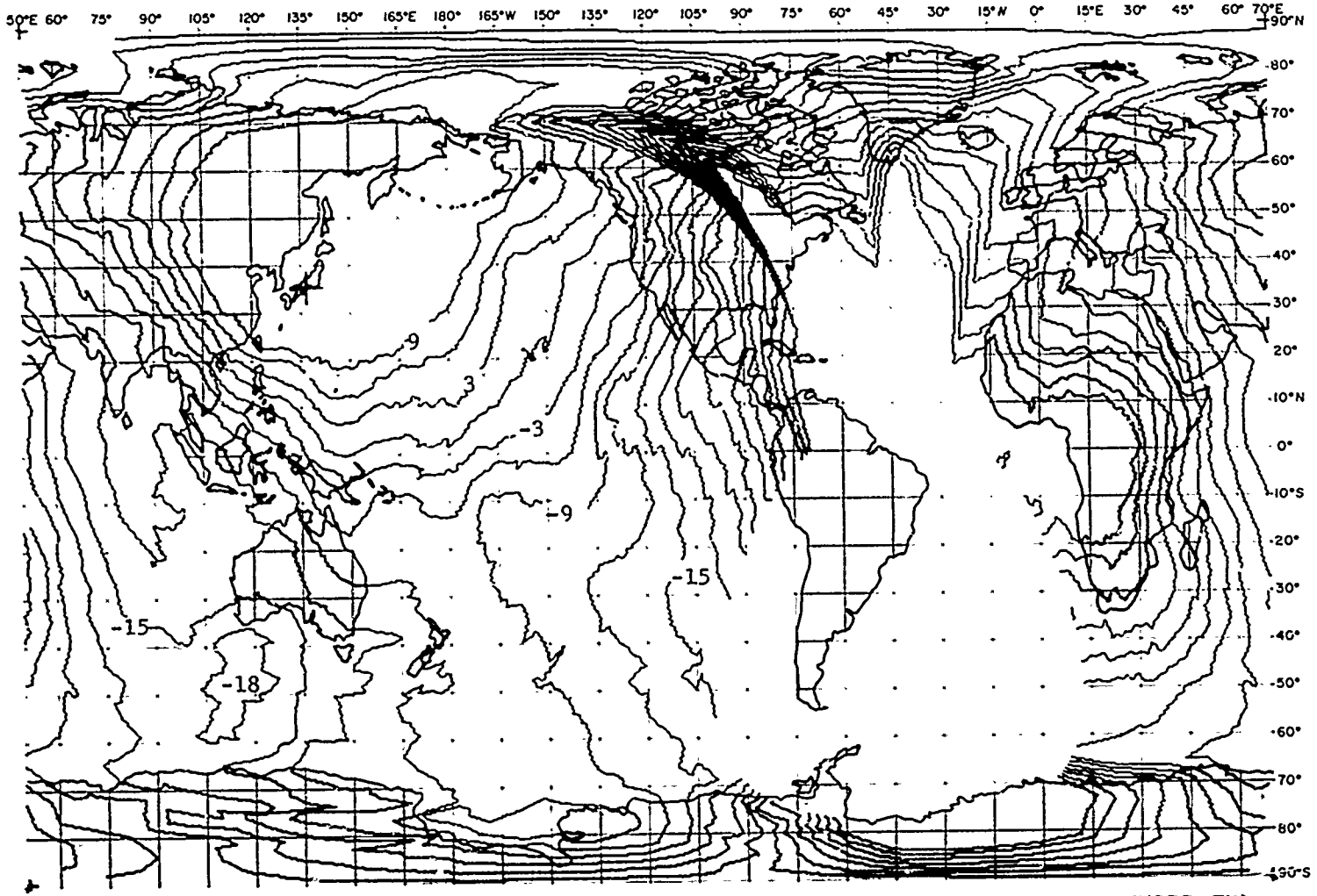


FIG. FR 23 – SIGNAL-TO-ATMOSPHERIC NOISE RATIO CONTOURS IN dB
NDT (17.4KHZ, 40KW) , YOSAMI
FALL 90% TIME AVAILABILITY 1KHZ BANDWIDTH

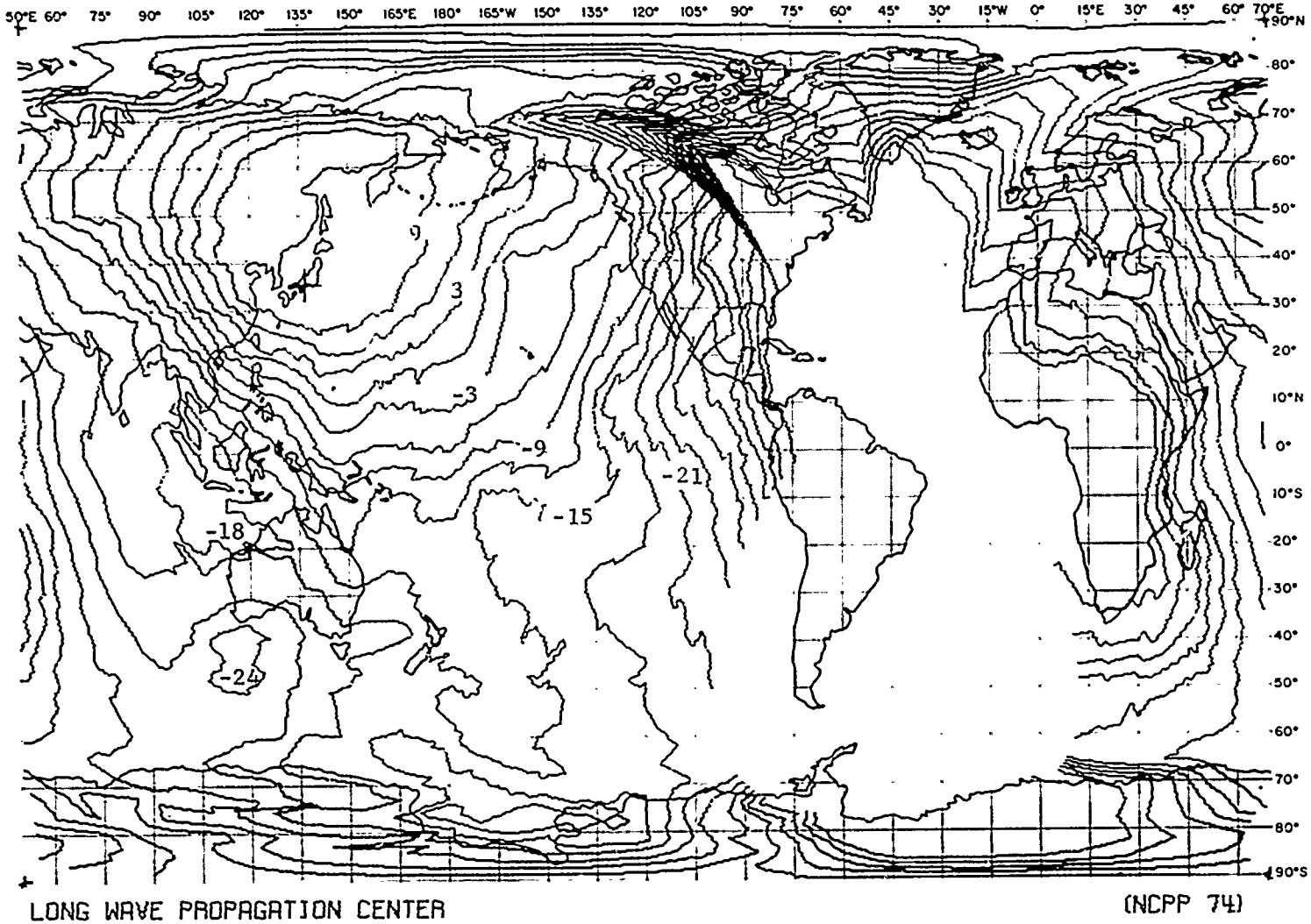


FIG. FA 24 - SIGNAL-TO-ATMOSPHERIC NOISE RATIO CONTOURS IN dB
NDT (17.4KHZ, 40KW) , YOSAMI
FALL 99% TIME AVAILABILITY 1KHZ BANDWIDTH

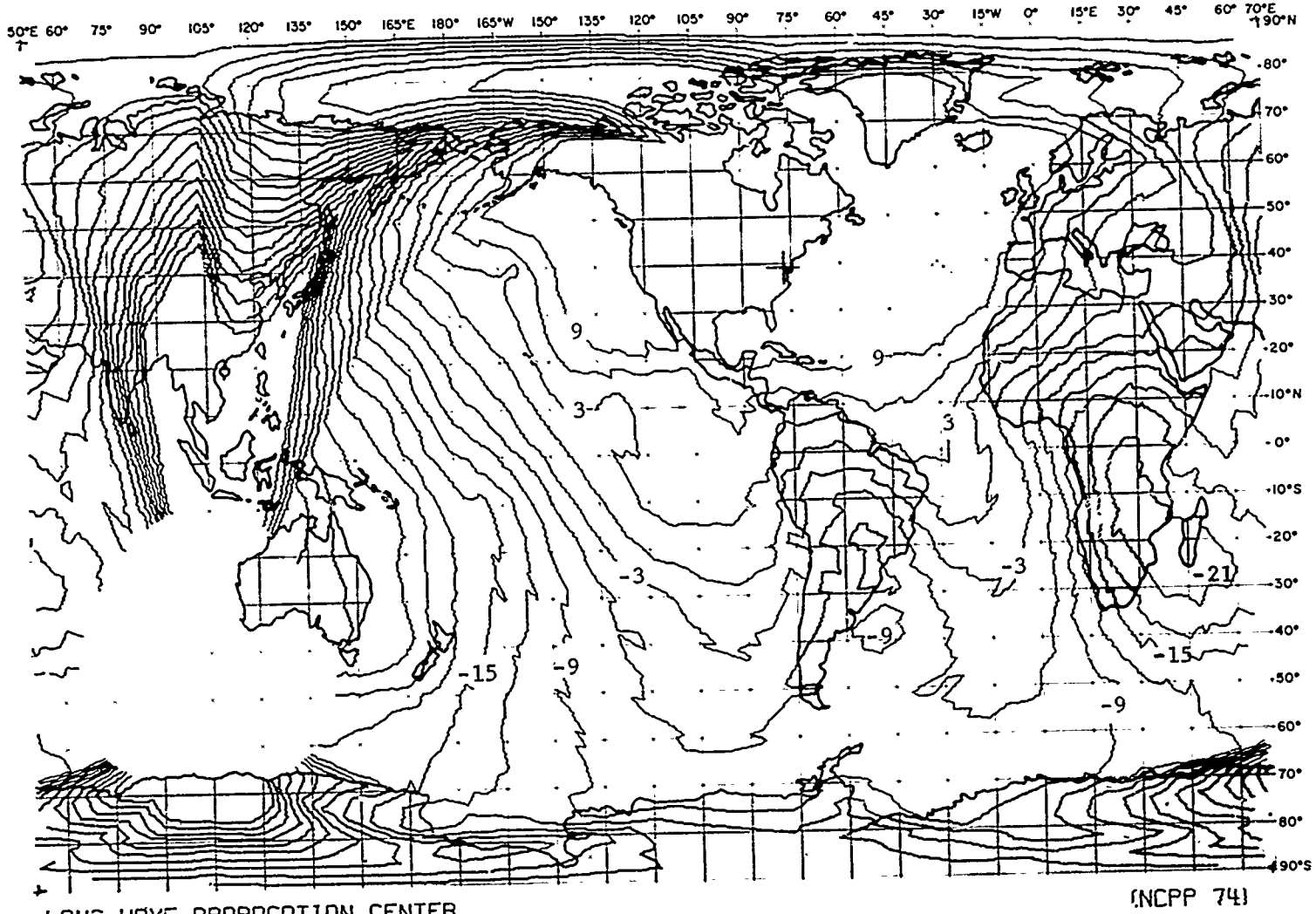


FIG. FA 25 - SIGNAL-TO-ATMOSPHERIC NOISE RATIO CONTOURS IN dB
NSS (21.4KHZ, 400KW) , ANNAPOLIS
FALL 90% TIME AVAILABILITY 1KHZ BANDWIDTH

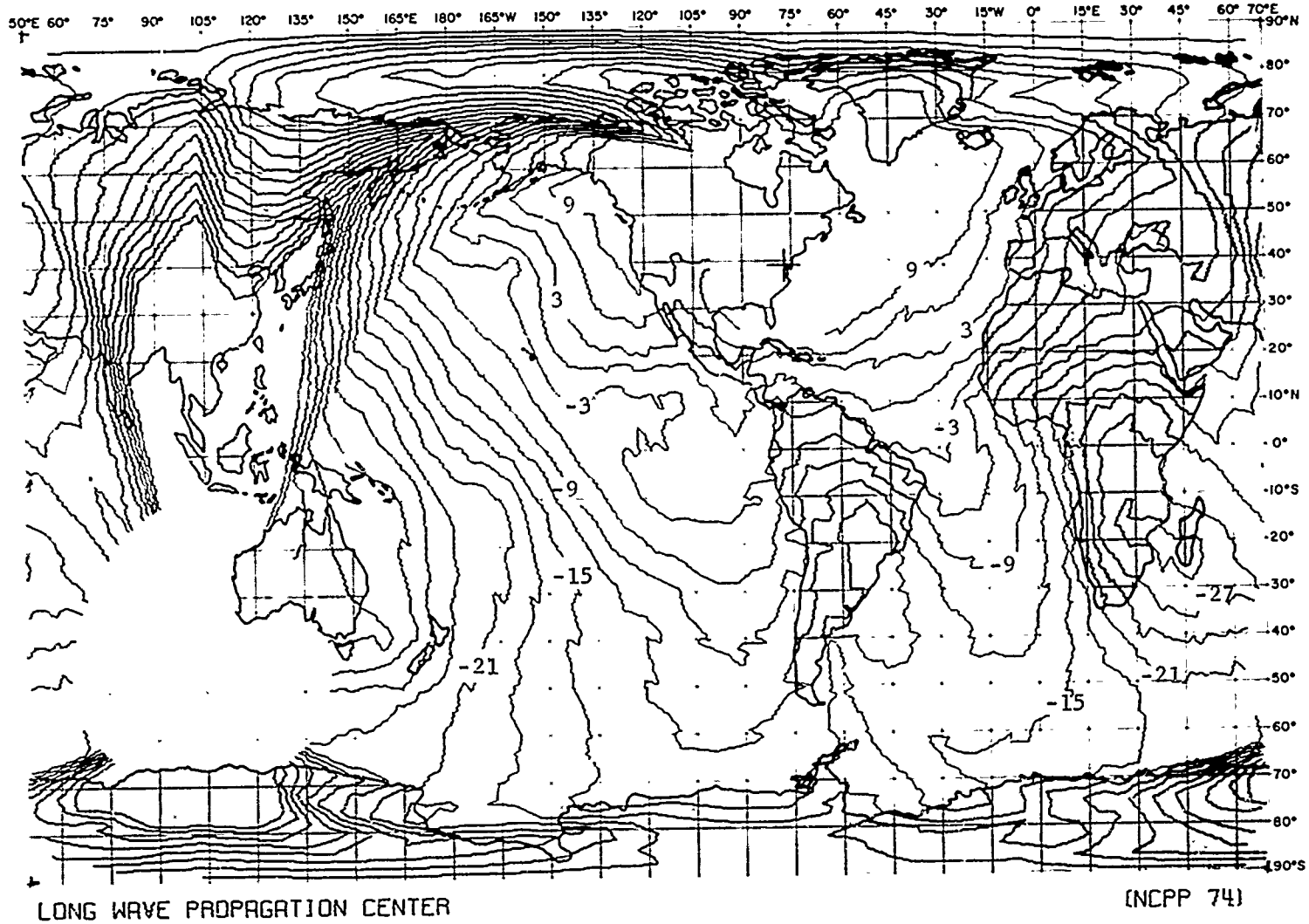


FIG. FA 26 - SIGNAL-TO-ATMOSPHERIC NOISE RATIO CONTOURS IN dB
NSS (21.4KHz, 400KW) , ANNAPOLIS
FALL 99% TIME AVAILABILITY 1KHZ BANDWIDTH

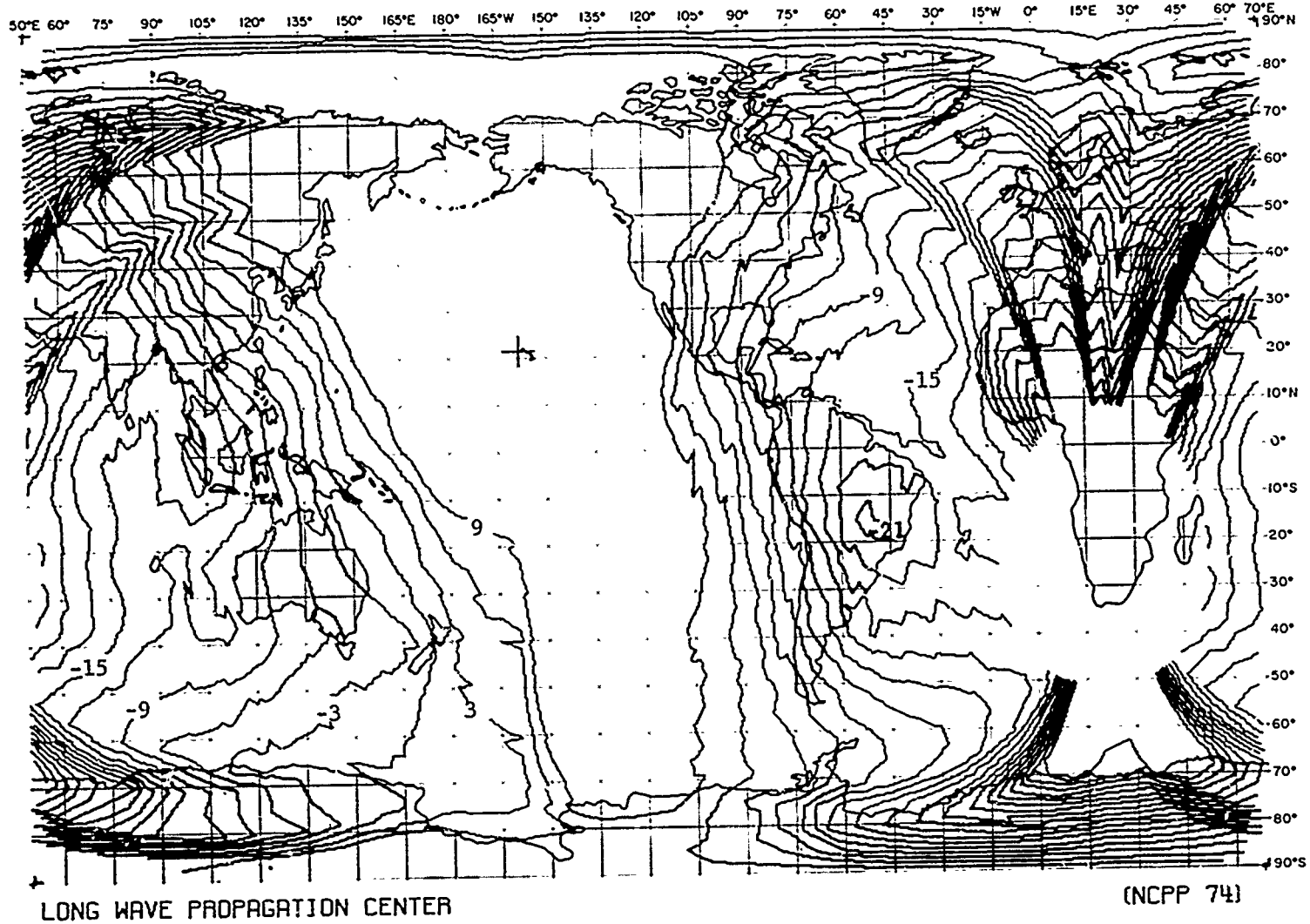


FIG. FA 27 - SIGNAL-TO-ATMOSPHERIC NOISE RATIO CONTOURS IN dB
NPM (23.4KHZ, 630KW) , LURLURLEI
FALL 90% TIME AVAILABILITY 1KHZ BANDWIDTH

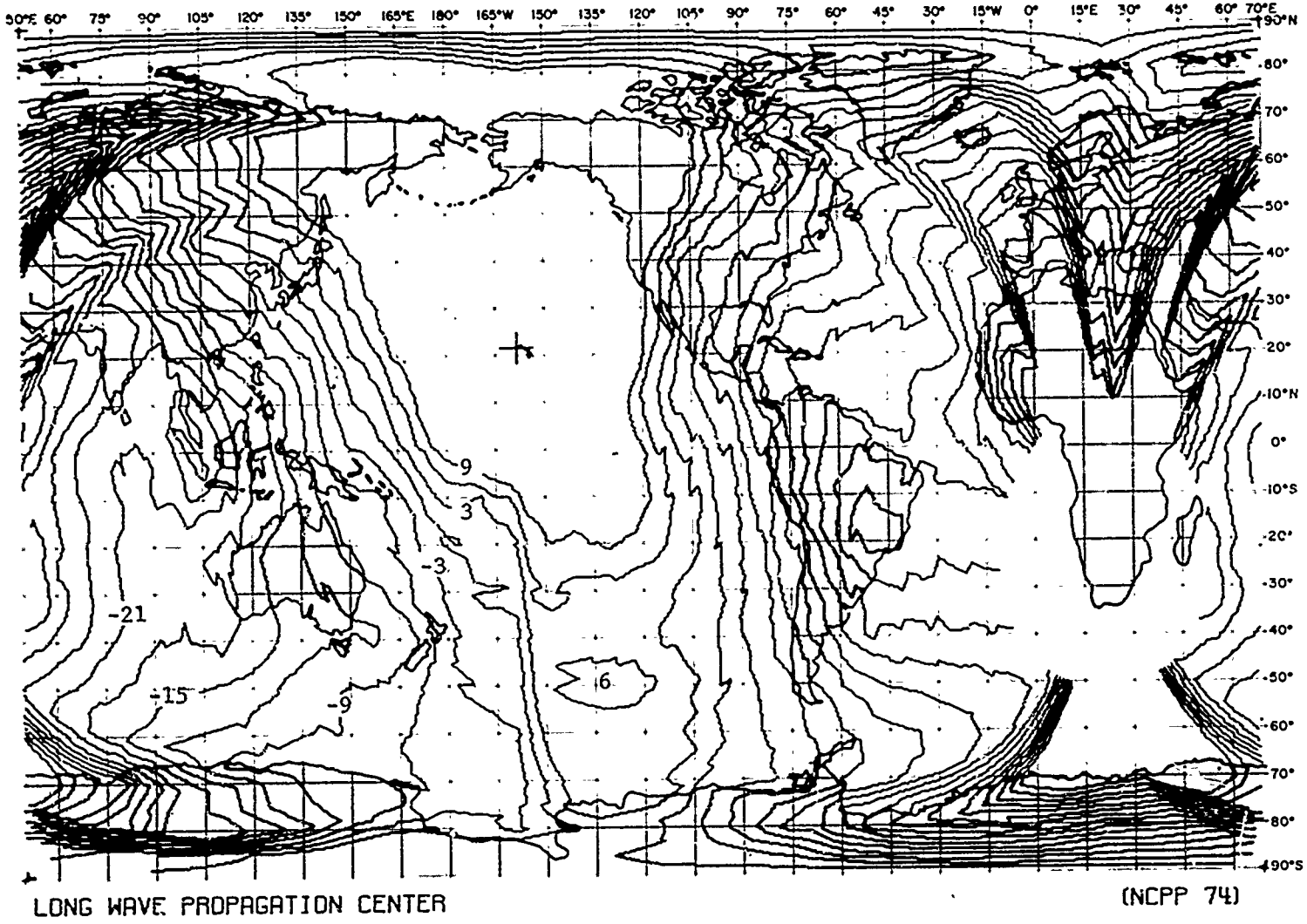


FIG. FA 28 - SIGNAL-TO-ATMOSPHERIC NOISE RATIO CONTOURS IN dB
NPM (23.4KHZ, 630KW) , LUALUALEI
FALL 99% TIME AVAILABILITY 1KHZ BANDWIDTH

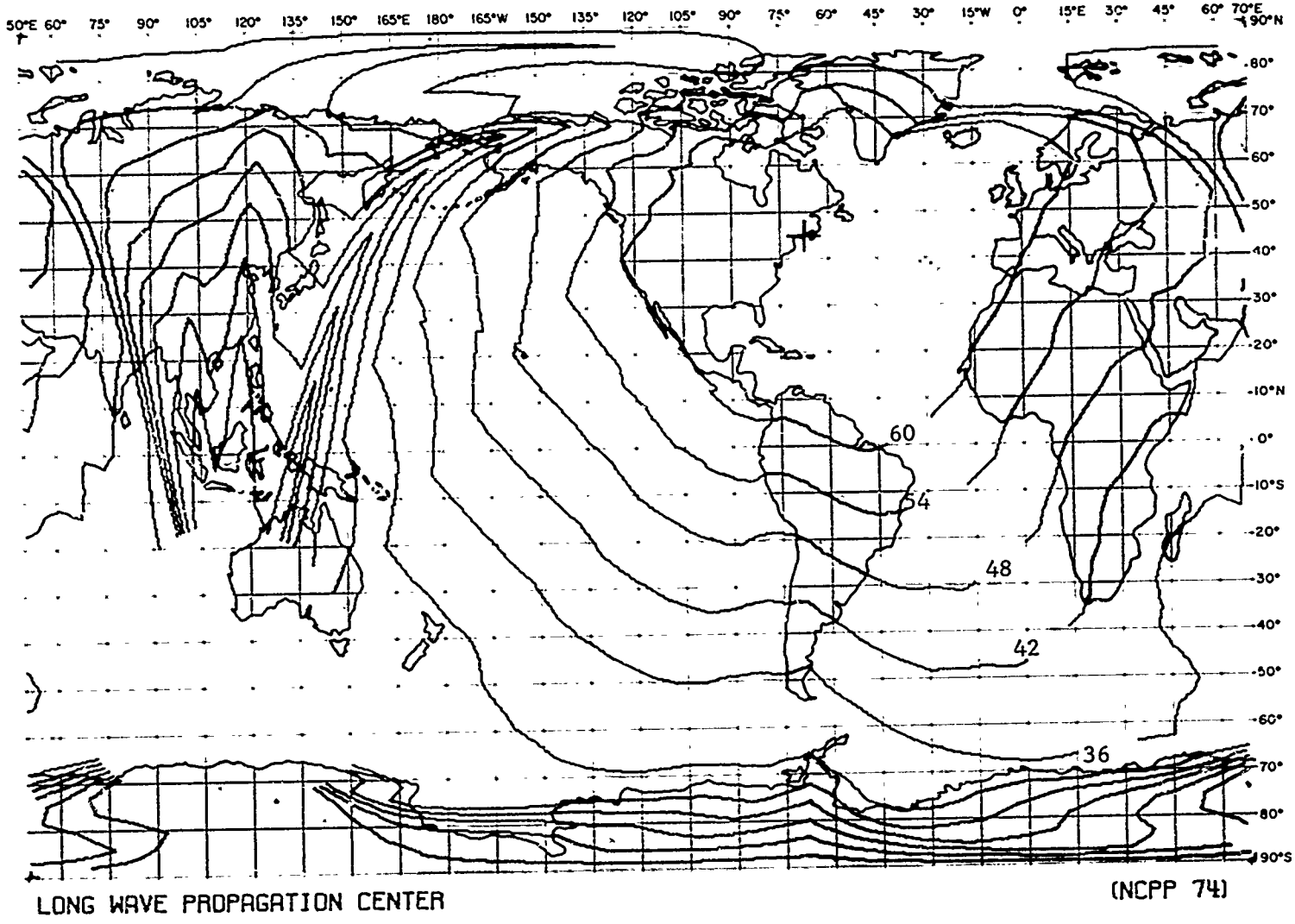


FIG. WI 1 - SIGNAL LEVEL CONTOURS IN dB>1μV/M
NAA (17.8KHZ, 1000KW) , CUTLER
WINTER 90% TIME AVAILABILITY

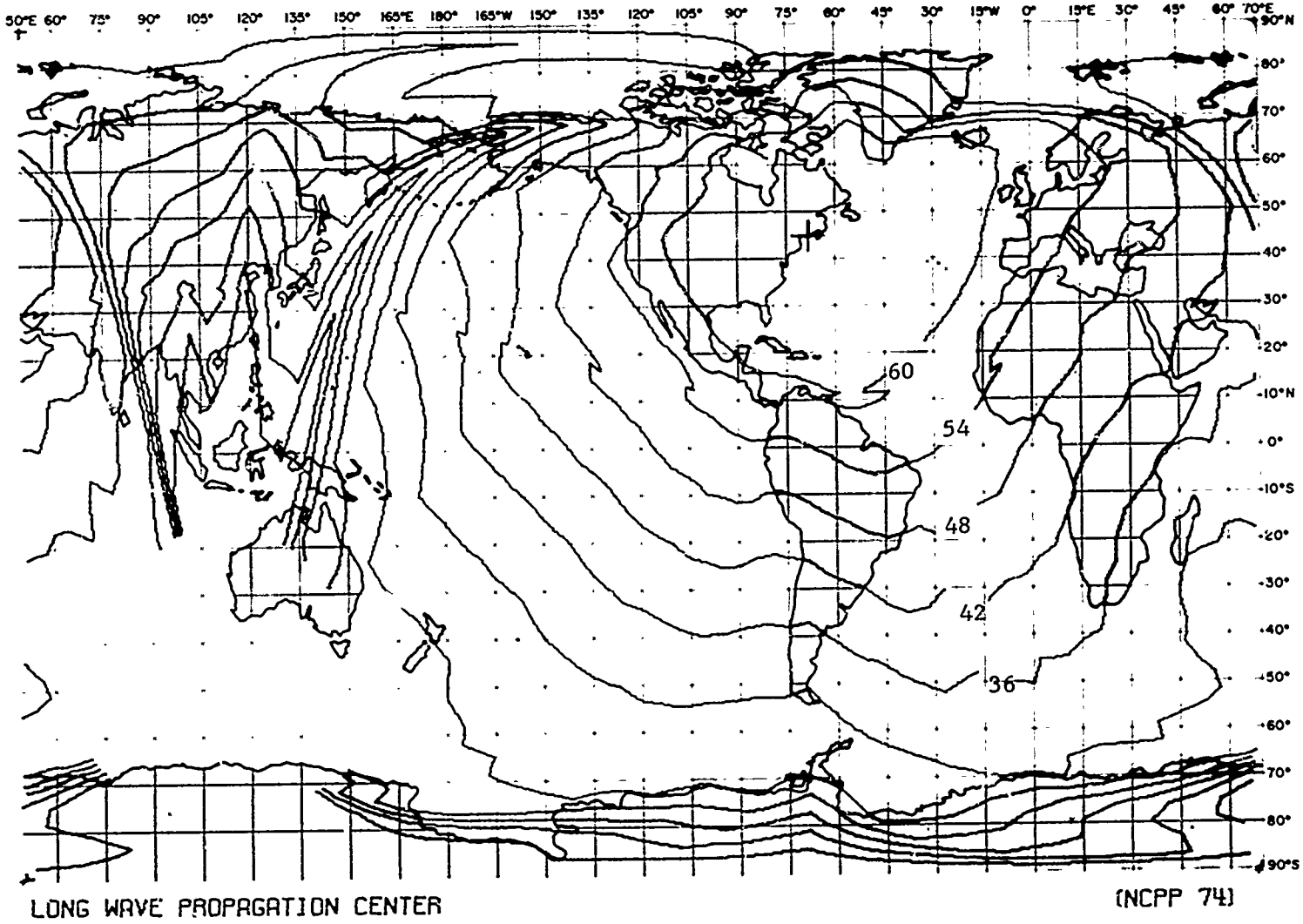


FIG. WI 2 - SIGNAL LEVEL CONTOURS IN dB>1μV/M
NAA (17.8KHZ, 1000KW) : CUTLER
WINTER 99% TIME AVAILABILITY

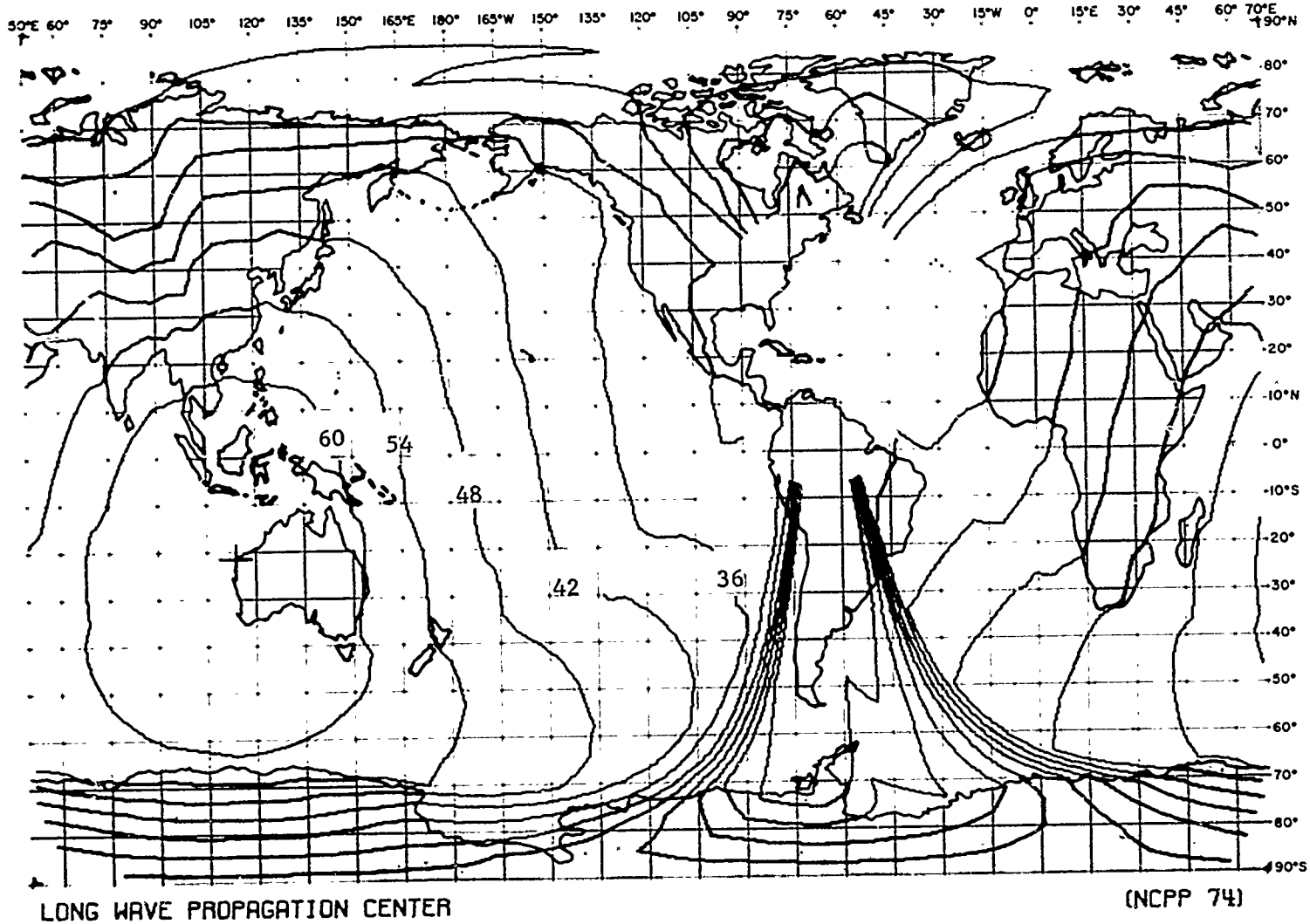


FIG. WI 3 - SIGNAL LEVEL CONTOURS IN dB>1μV/M
NWC (22.3KHZ, 1000KW) , NORTHWEST CAPE
WINTER 90% TIME AVAILABILITY

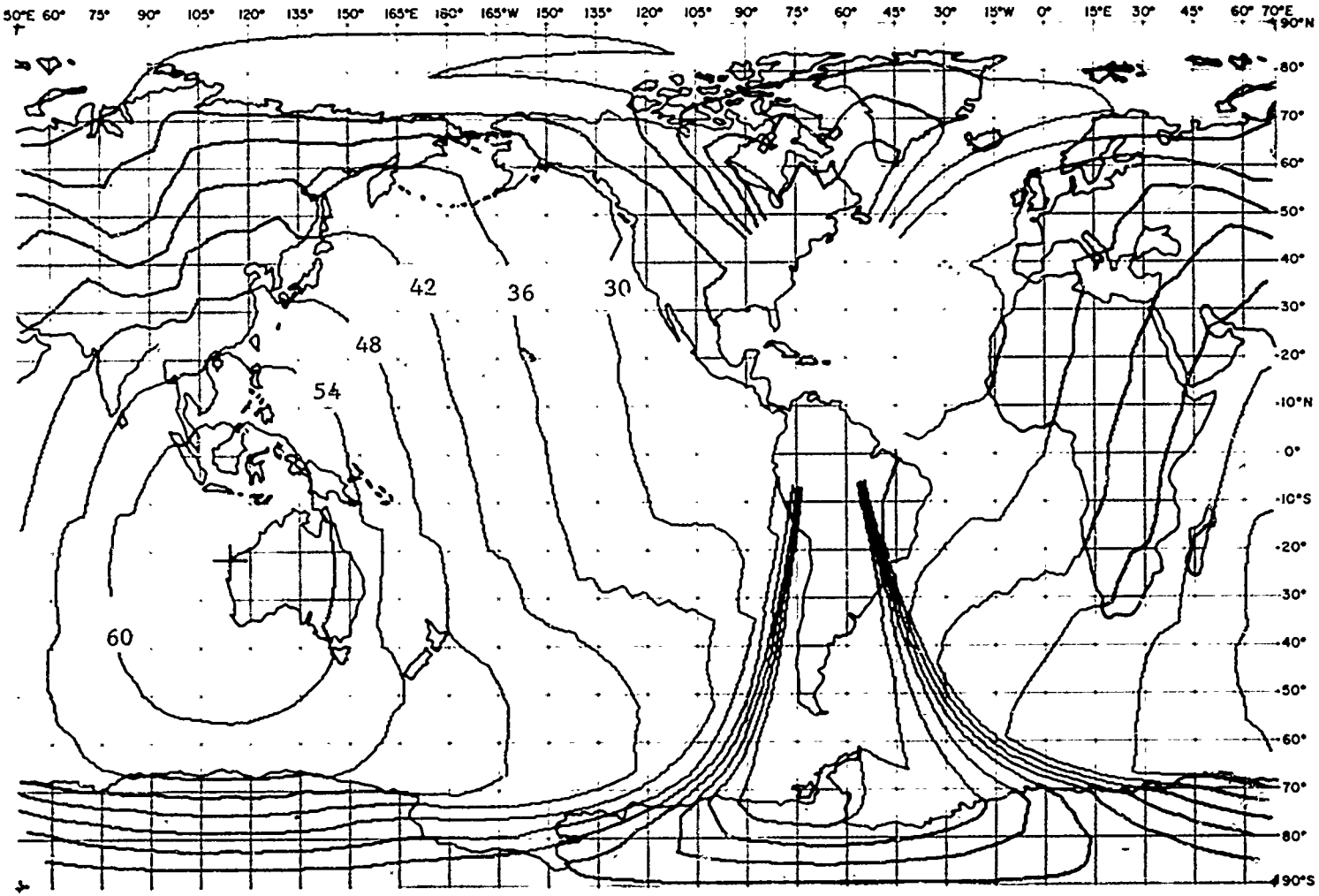


FIG. WI 4 - SIGNAL LEVEL CONTOURS IN dB>1μV/M
NWC (22.3KHZ, 1000KW) , NORTHWEST CAPE
WINTER 99% TIME AVAILABILITY

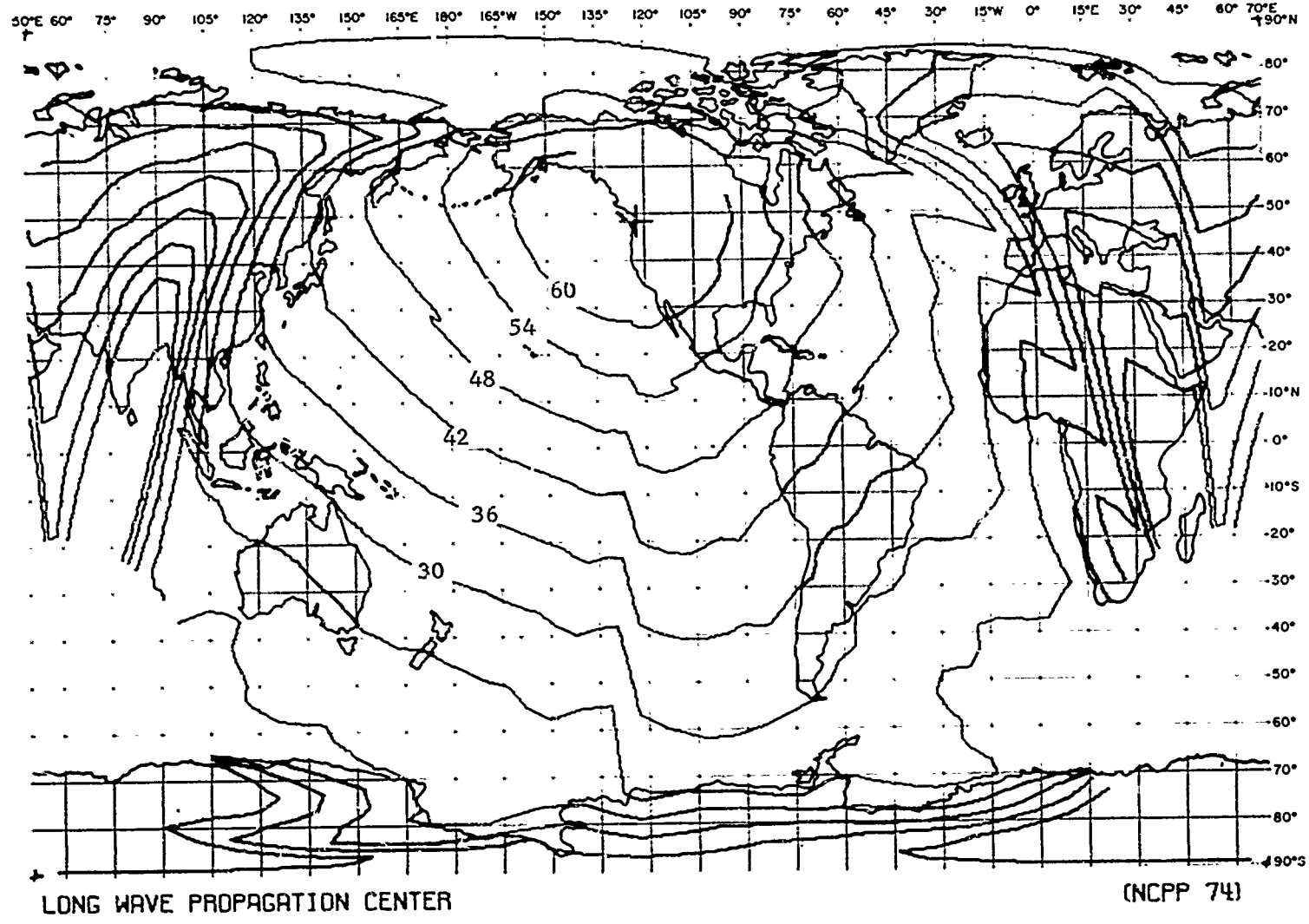


FIG. WI 5 - SIGNAL LEVEL CONTOURS IN dB>1μV/M
NPG (18.6KHZ, 130KW) , JIM CREEK
WINTER 90% TIME AVAILABILITY

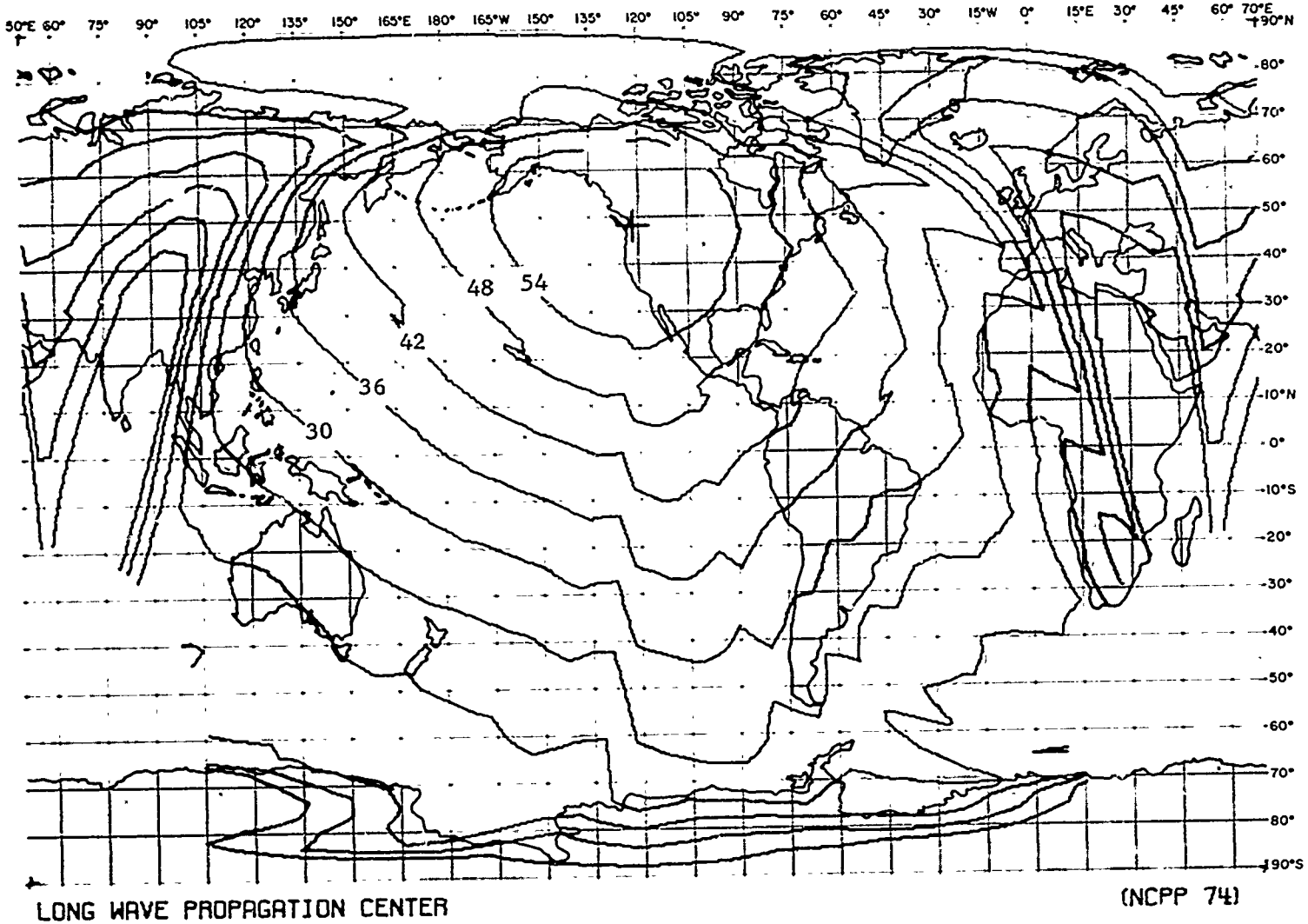


FIG. WI 6 - SIGNAL LEVEL CONTOURS IN dB>1μV/M
NPG (18.6KHZ, 130KW) , JIM CREEK
WINTER 99% TIME AVAILABILITY

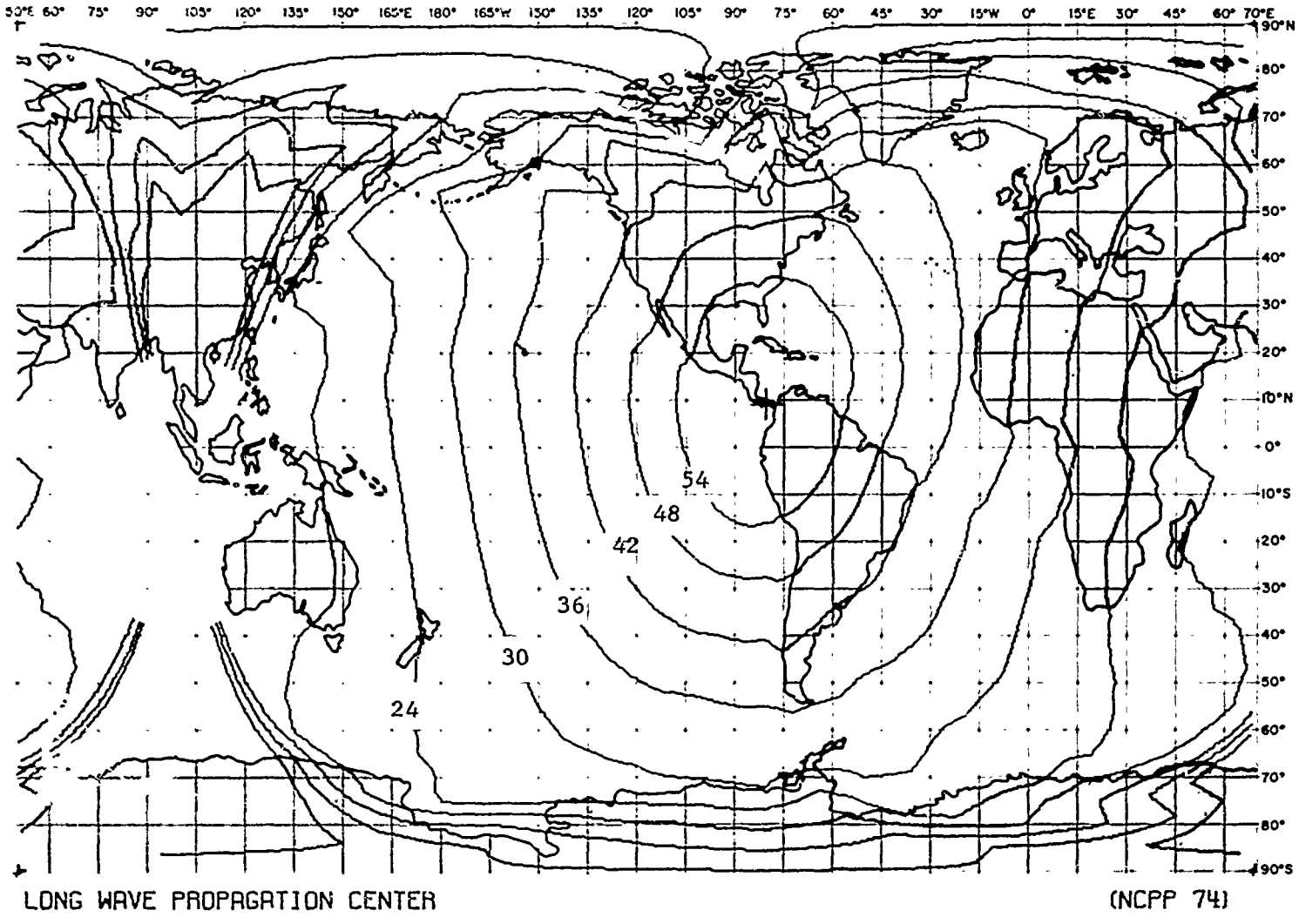


FIG. WI 7 - SIGNAL LEVEL CONTOURS IN dB>1μV/M
NBA (24.0KHZ, 110KW) , BALBOA
WINTER 90% TIME AVAILABILITY

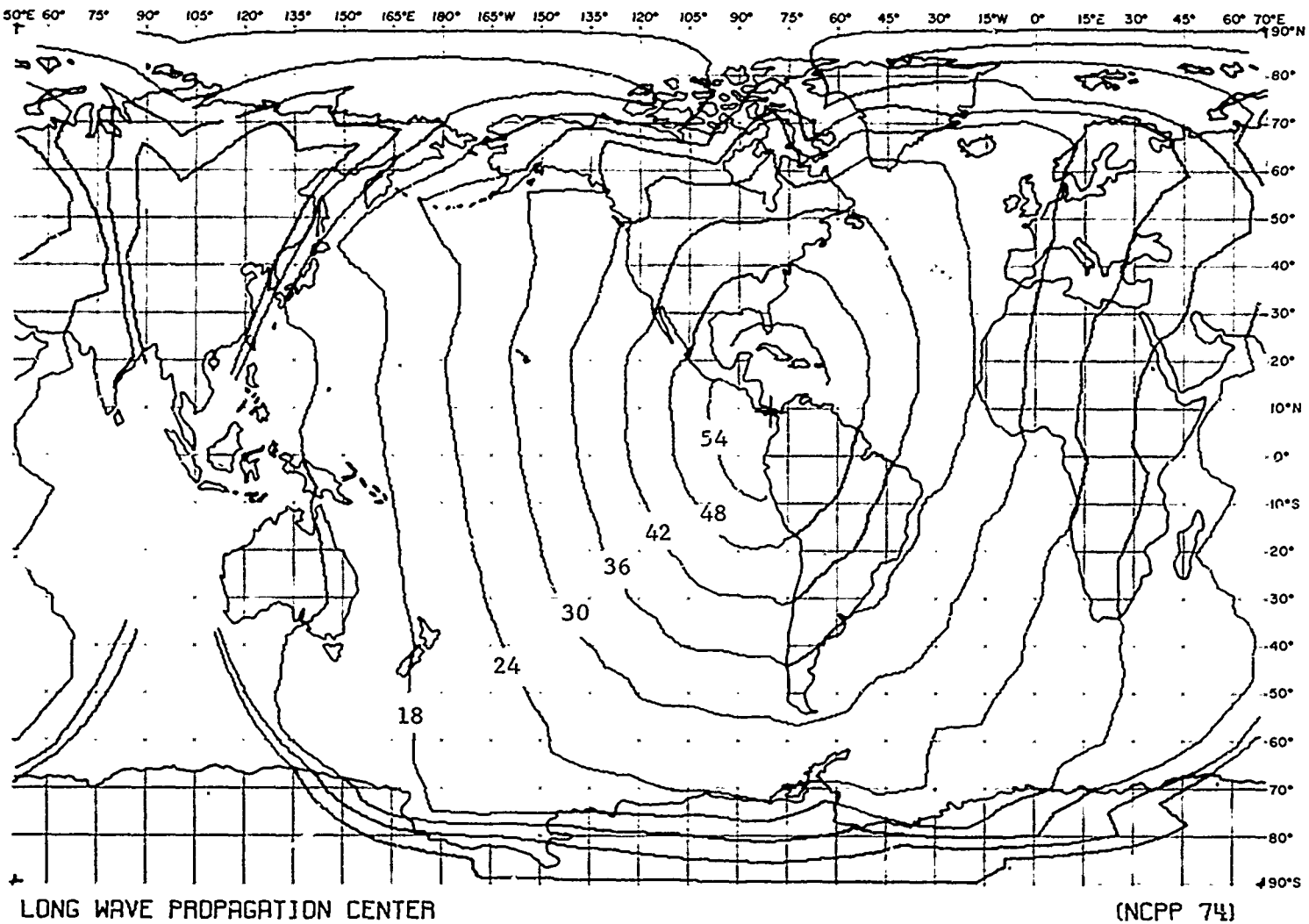


FIG. WI 8 - SIGNAL LEVEL CONTOURS IN dB>1μV/M
NBA (24.0KHZ, 110KW) , BALBOA
WINTER 99% TIME AVAILABILITY

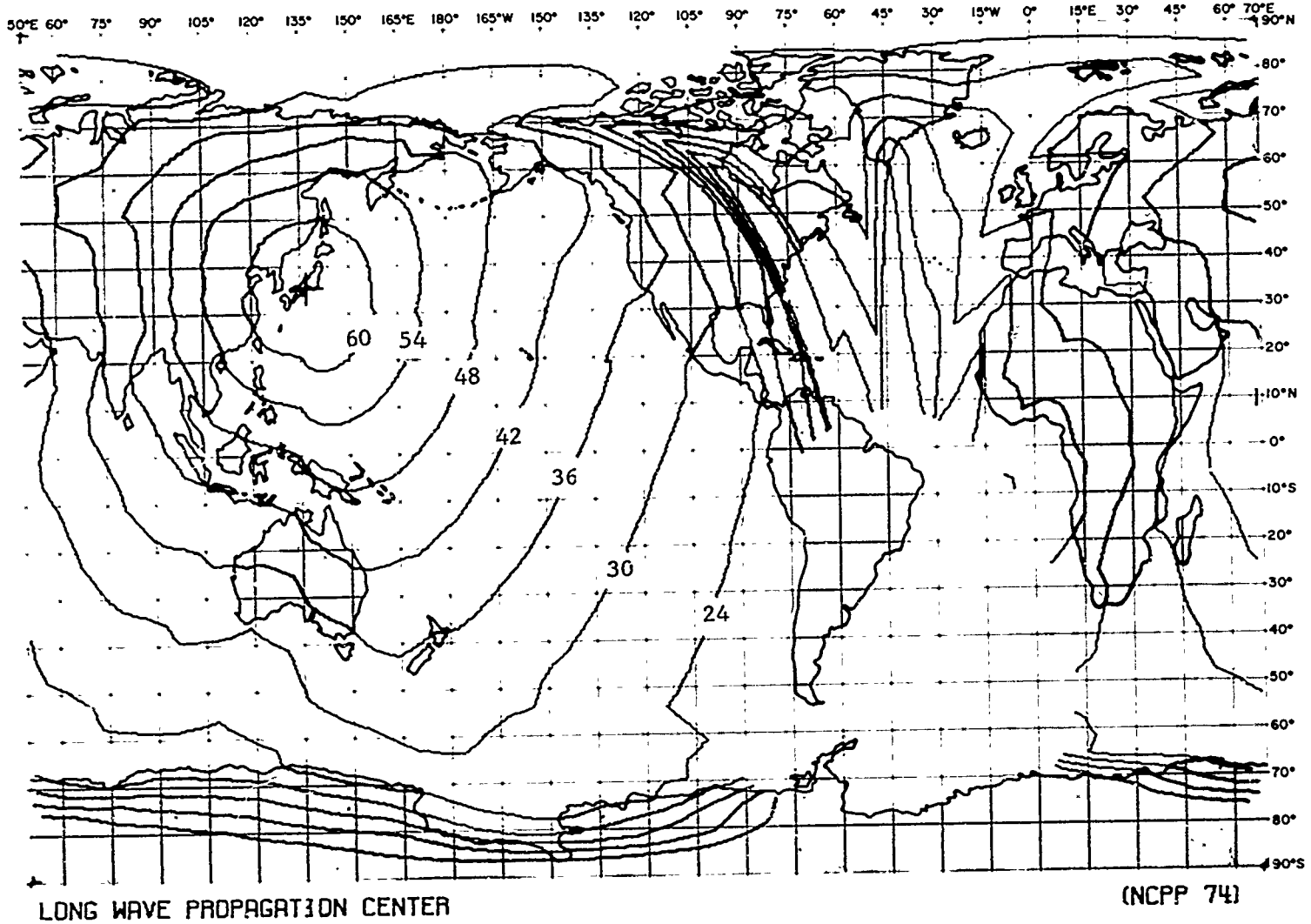


FIG. WI 9 - SIGNAL LEVEL CONTOURS IN dB>1μV/M
NDT (17.4KHZ, 40KW) , YOSAMI
WINTER 90% TIME AVAILABILITY

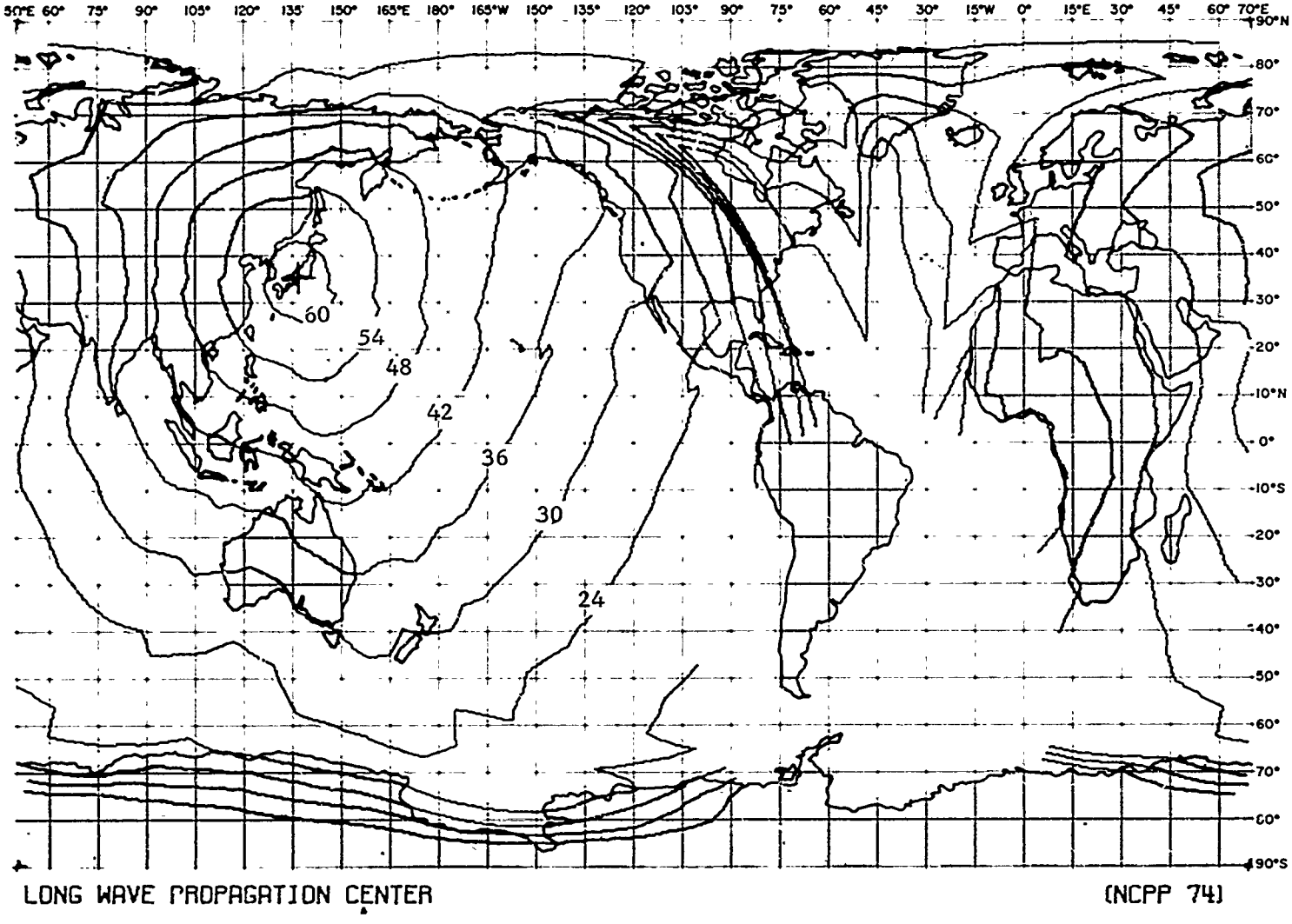


FIG. WI 10 - SIGNAL LEVEL CONTOURS IN dB>1μV/M
NDT (17.4KHZ, 40KW) , YOSAMI
WINTER 99% TIME AVAILABILITY

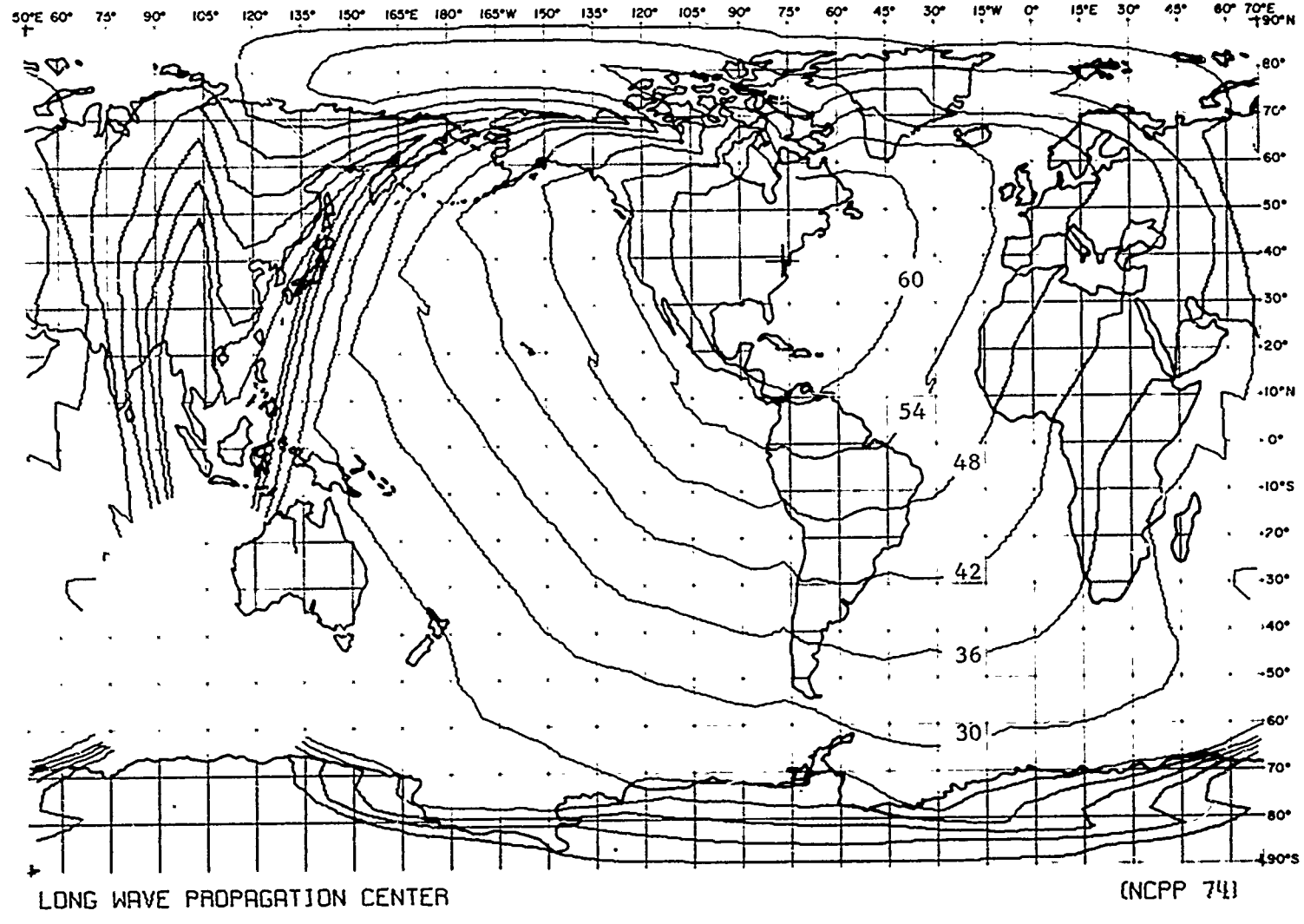


FIG. WI 11 - SIGNAL LEVEL CONTOURS IN dB>1μV/M
NSS (2).4KHZ, 400KW) , ANNAPOLIS
WINTER 90% TIME AVAILABILITY

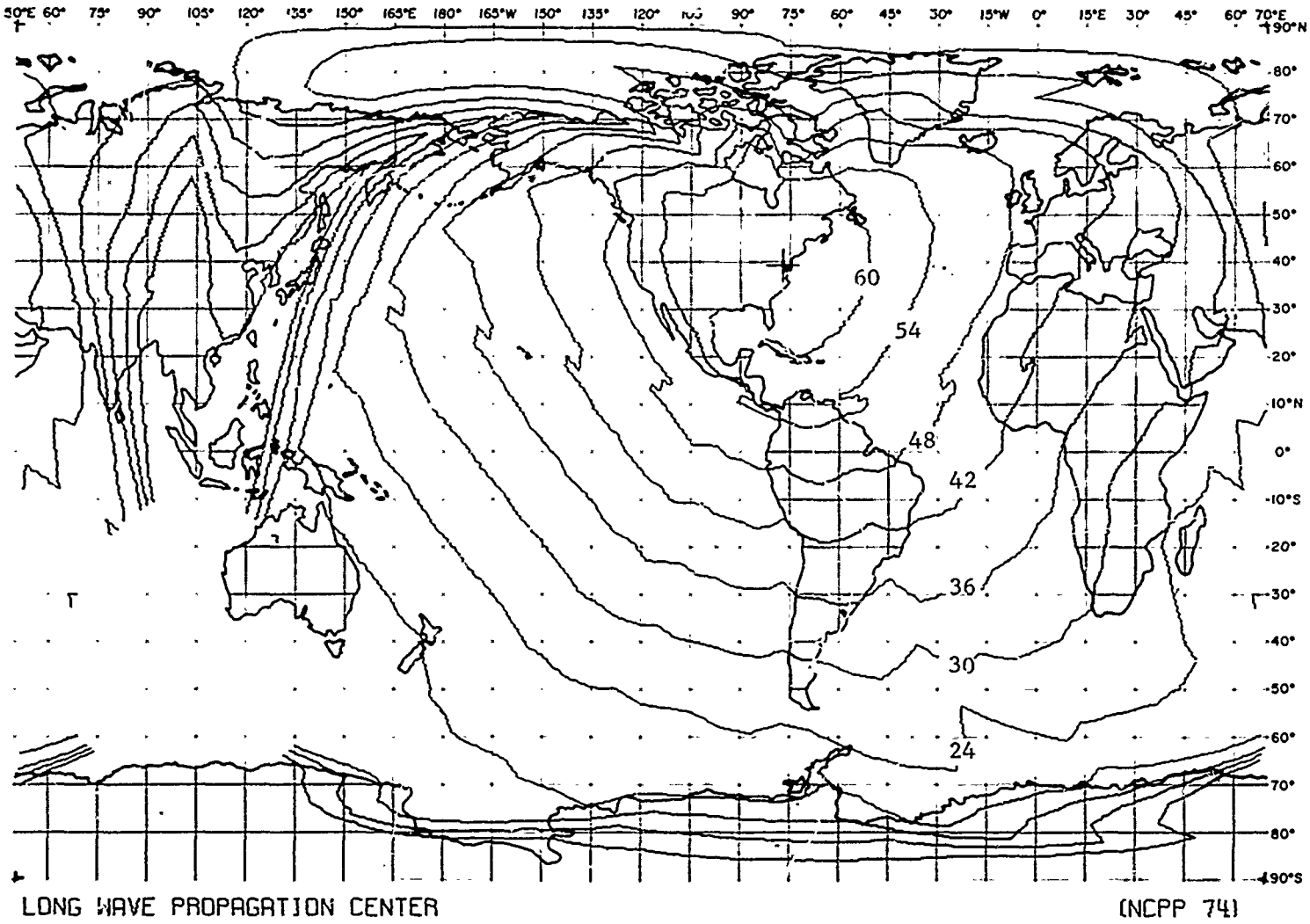


FIG. XI 12 - SIGNAL LEVEL CONTOURS IN dB>1μV/M
NSS (21.4KHZ, 400KW) , ANNAPOLIS
WINTER 99% TIME AVAILABILITY

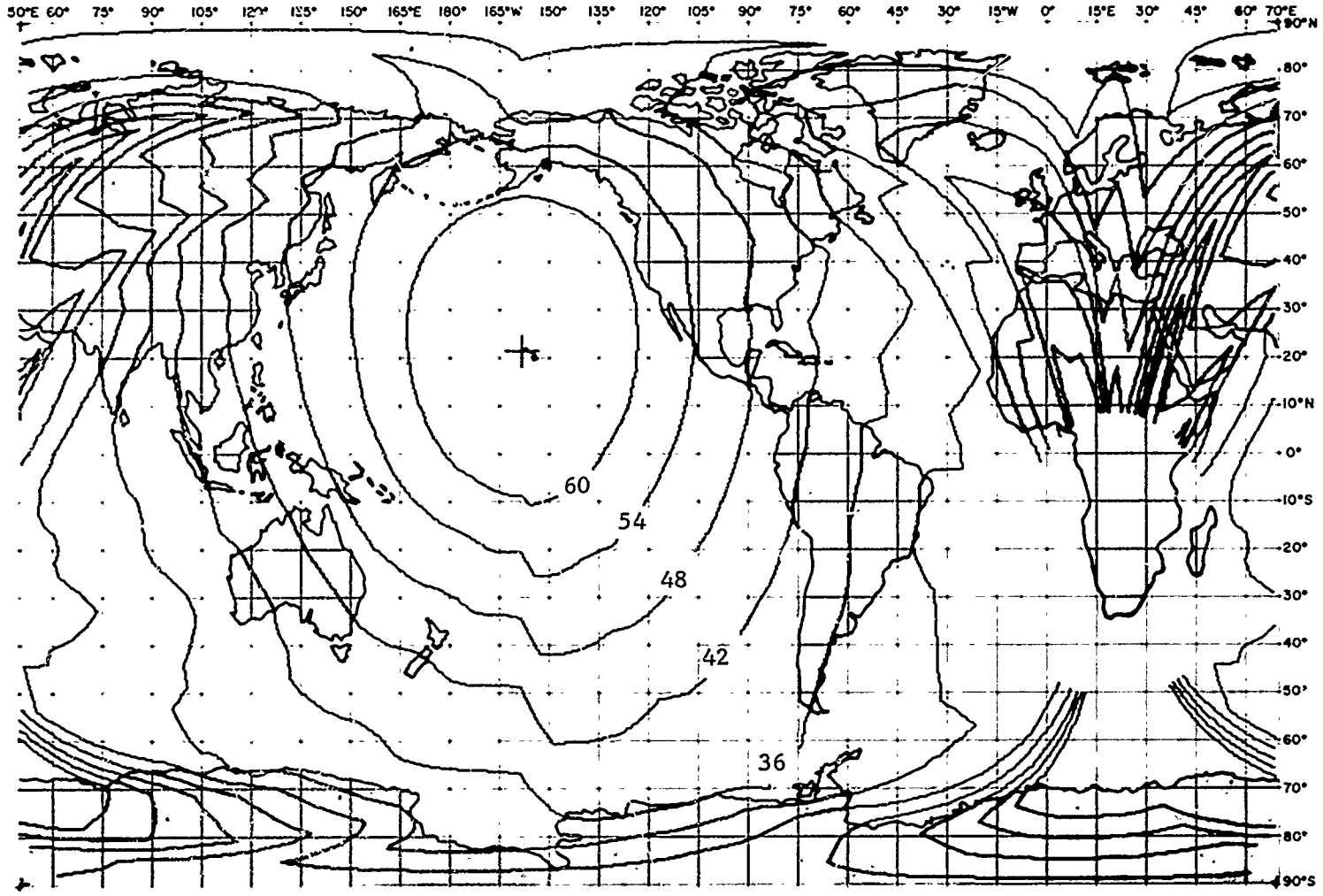


FIG. WI 13 - SIGNAL LEVEL CONTOURS IN dB>1μV/M
NPM (23.4KHZ, 630KW) , LUALUALEI
WINTER 90% TIME AVAILABILITY

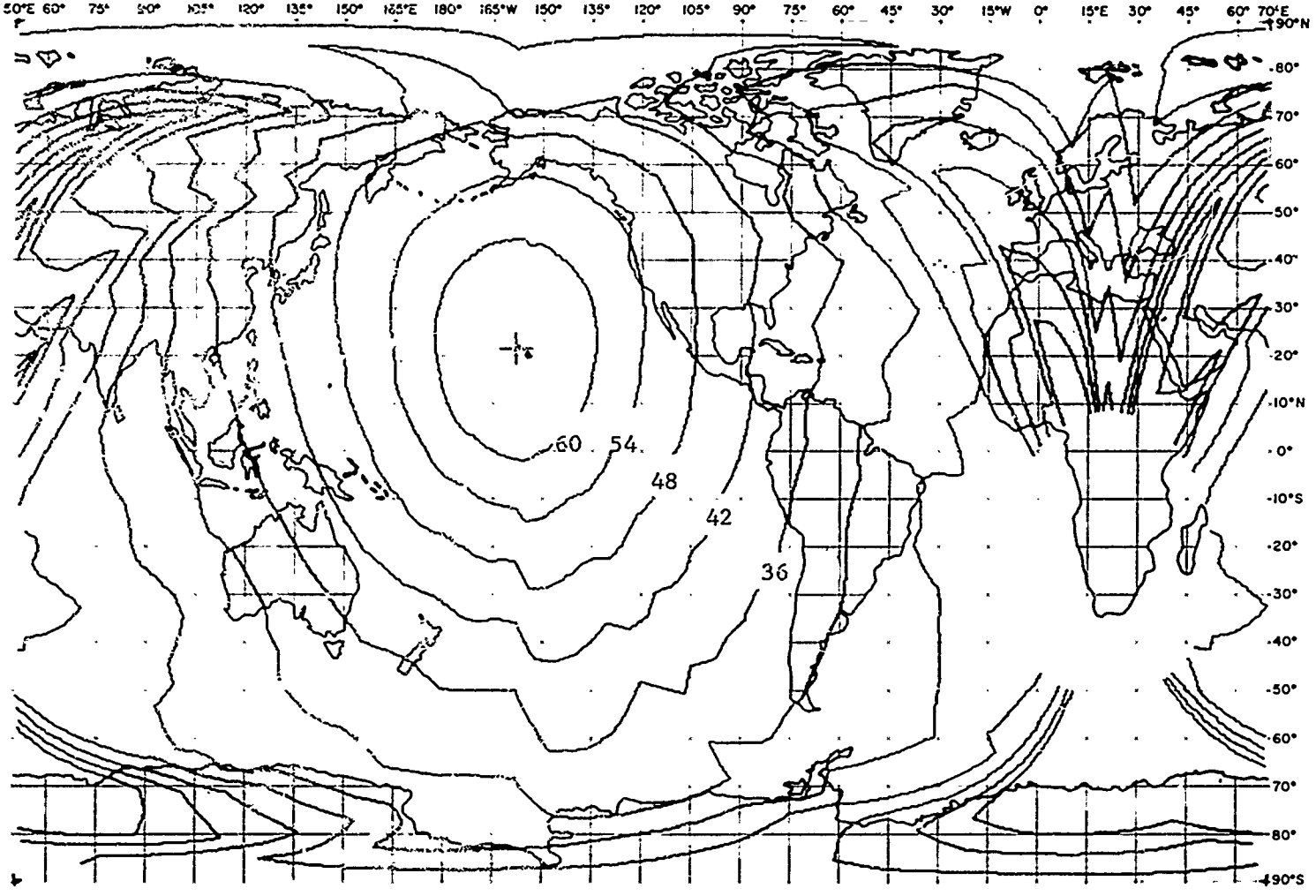


FIG. WI 14 - SIGNAL LEVEL CONTOURS IN dB>1μV/M
NPM (23.4KHz, 630KW) , LUALUALEI
WINTER 99% TIME AVAILABILITY

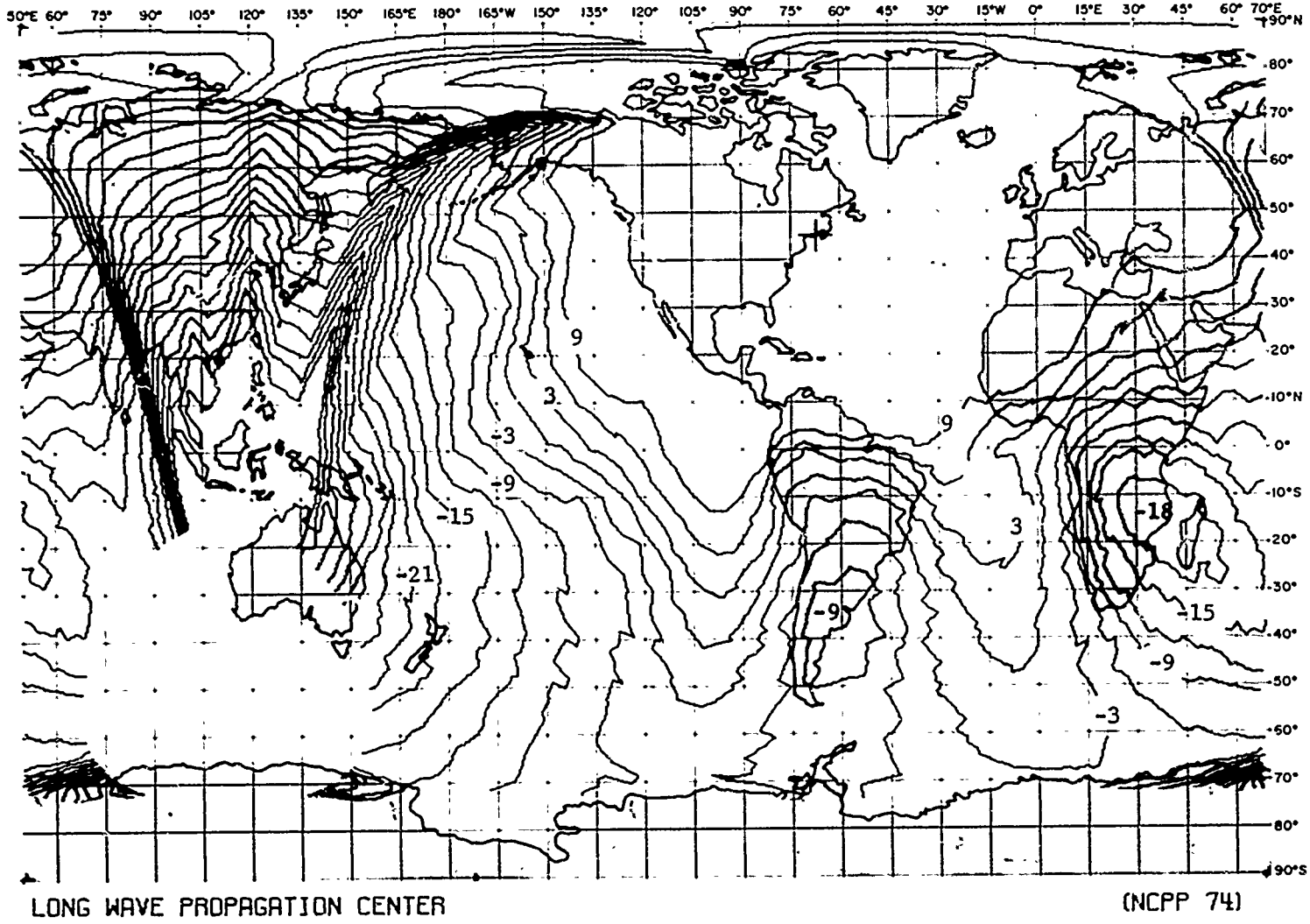


FIG. WI 15 - SIGNAL-TO-ATMOSPHERIC NOISE RATIO CONTOURS IN dB
NAA (17.8KHZ, 1000KW) , CUTLER
WINTER 90% TIME AVAILABILITY 1KHZ BANDWIDTH

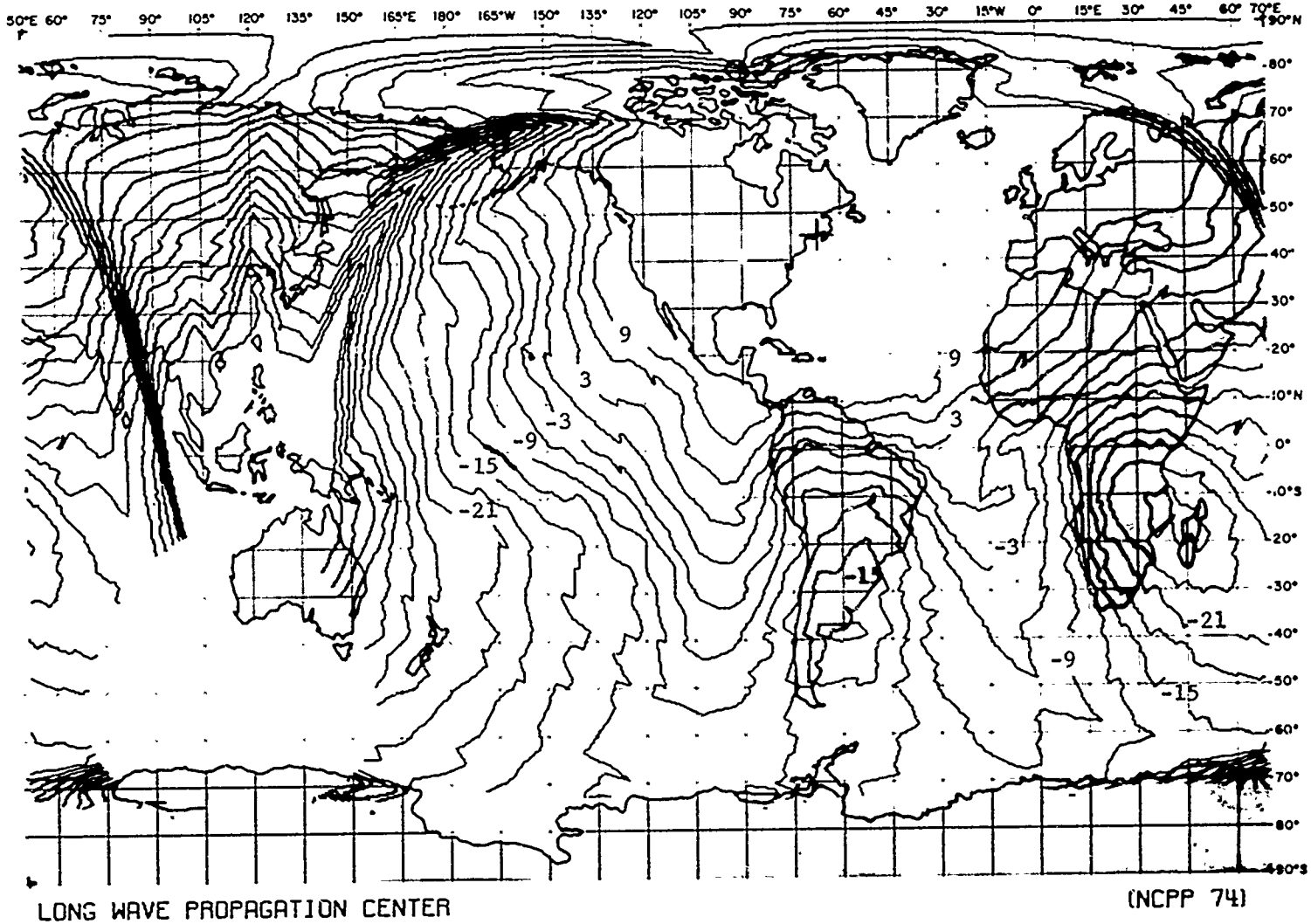


FIG. WI 16 - SIGNAL-TO-ATMOSPHERIC NOISE RATIO CONTOURS IN dB
NAA (17.8KHZ, 1000KW) , CUTLER
WINTER 99% TIME AVAILABILITY 1KHZ BANDWIDTH

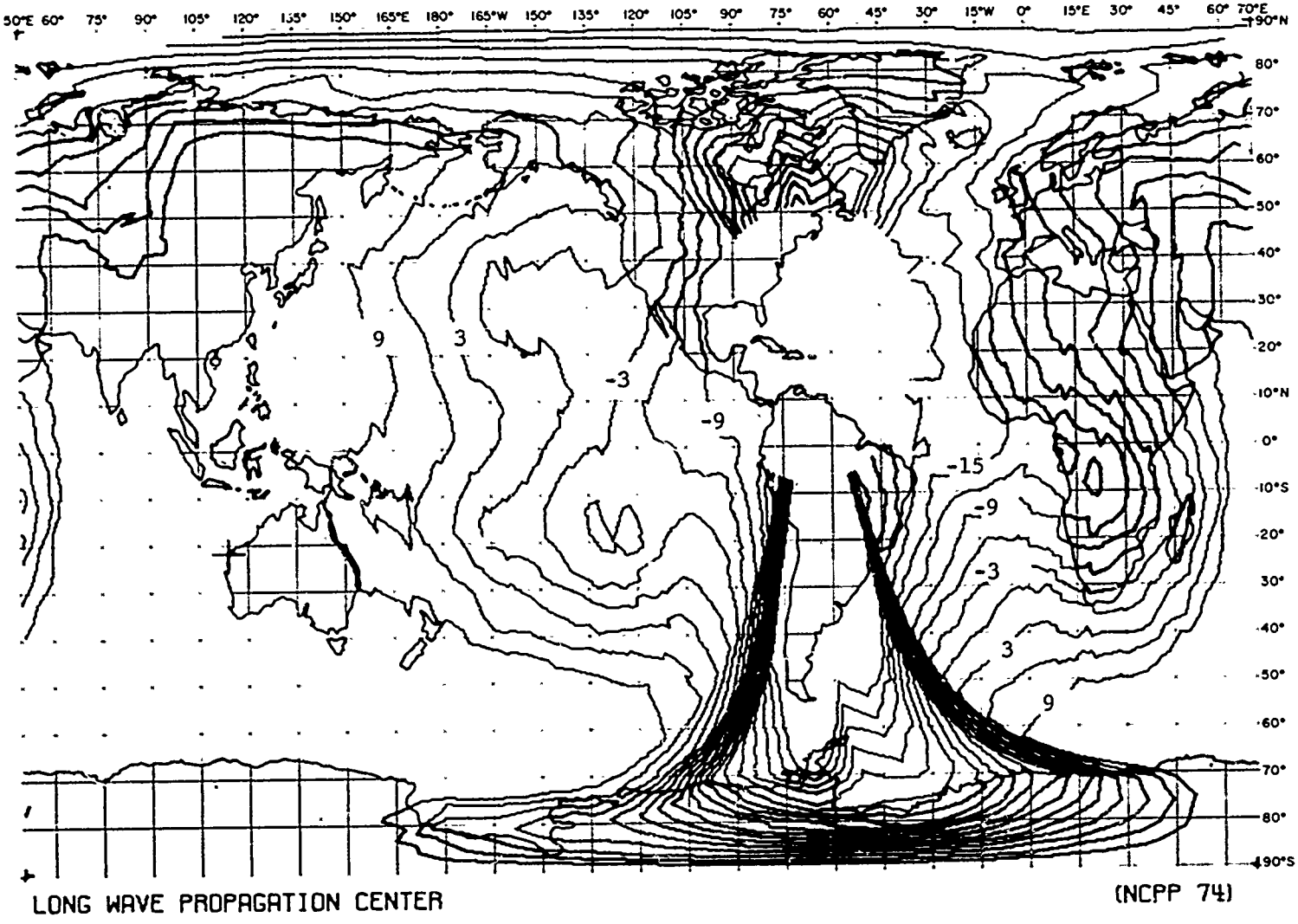


FIG. WI 17 - SIGNAL-TO-ATMOSPHERIC NOISE RATIO CONTOURS IN dB
NWC (22.3KHZ, 1000KW) , NORTHWEST CAPE
WINTER 90% TIME AVAILABILITY 1KHZ BANDWIDTH

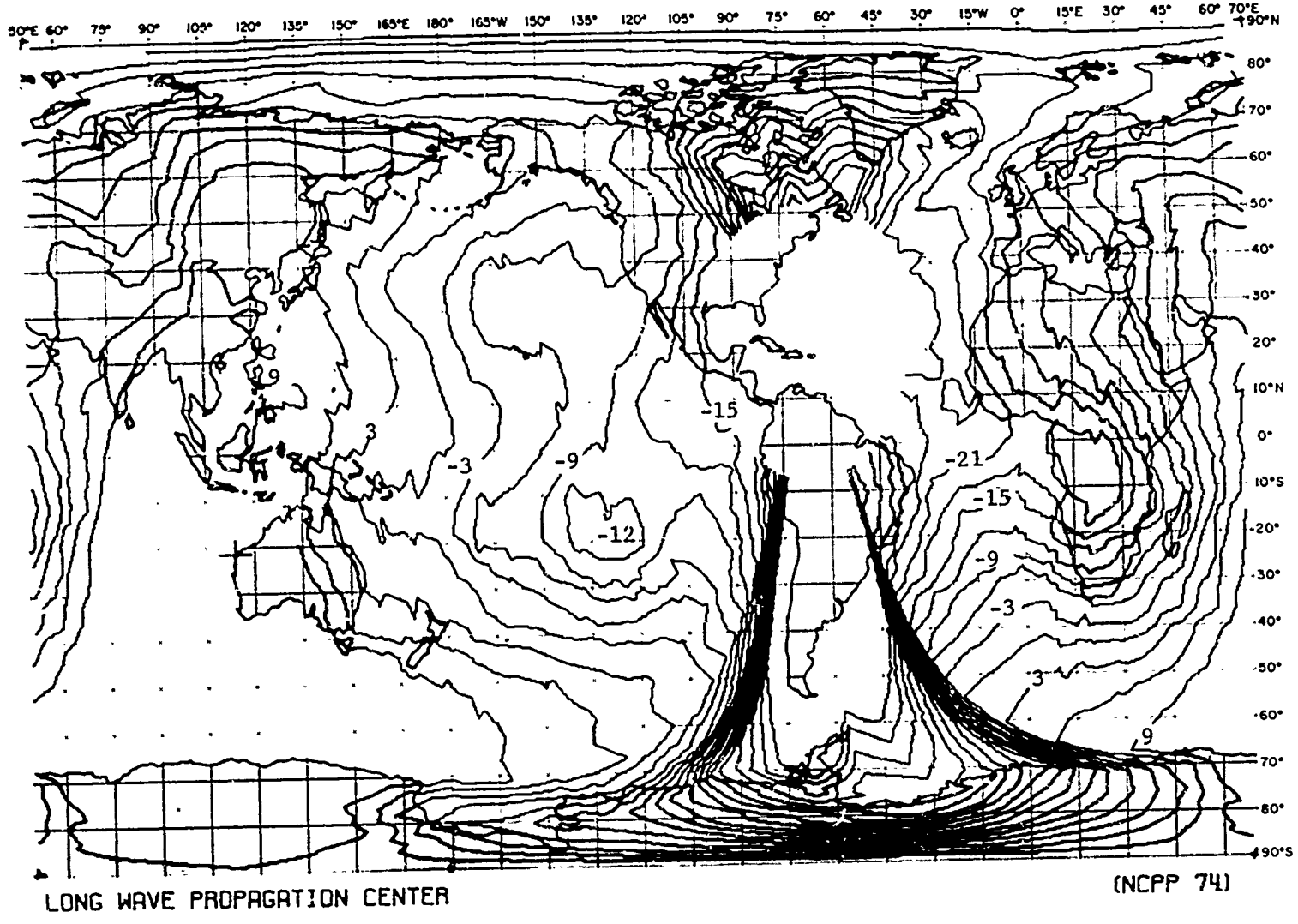


FIG. WI 18 - SIGNAL-TO-ATMOSPHERIC NOISE RATIO CONTOURS IN dB
NWC (22.3KHZ, 1000KW) , NORTHWEST CAPE
WINTER 99% TIME AVAILABILITY 1KHZ BANDWIDTH

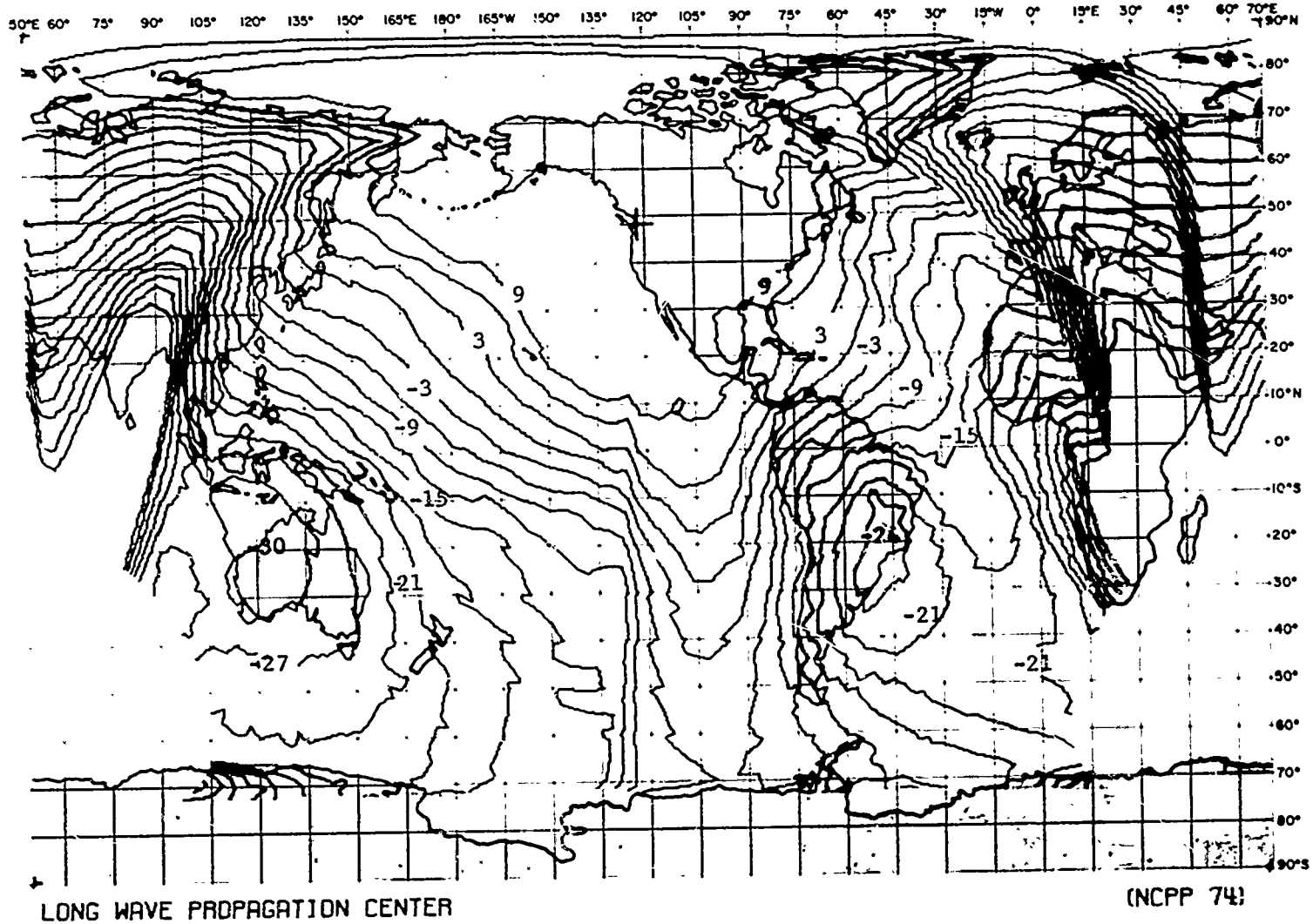


FIG. WI 19 - SIGNAL-TO-ATMOSPHERIC NOISE RATIO CONTOURS IN dB
NPG (18.6KHZ, 130KW) , JIM CREEK
WINTER 90% TIME AVAILABILITY 1KHZ BANDWIDTH

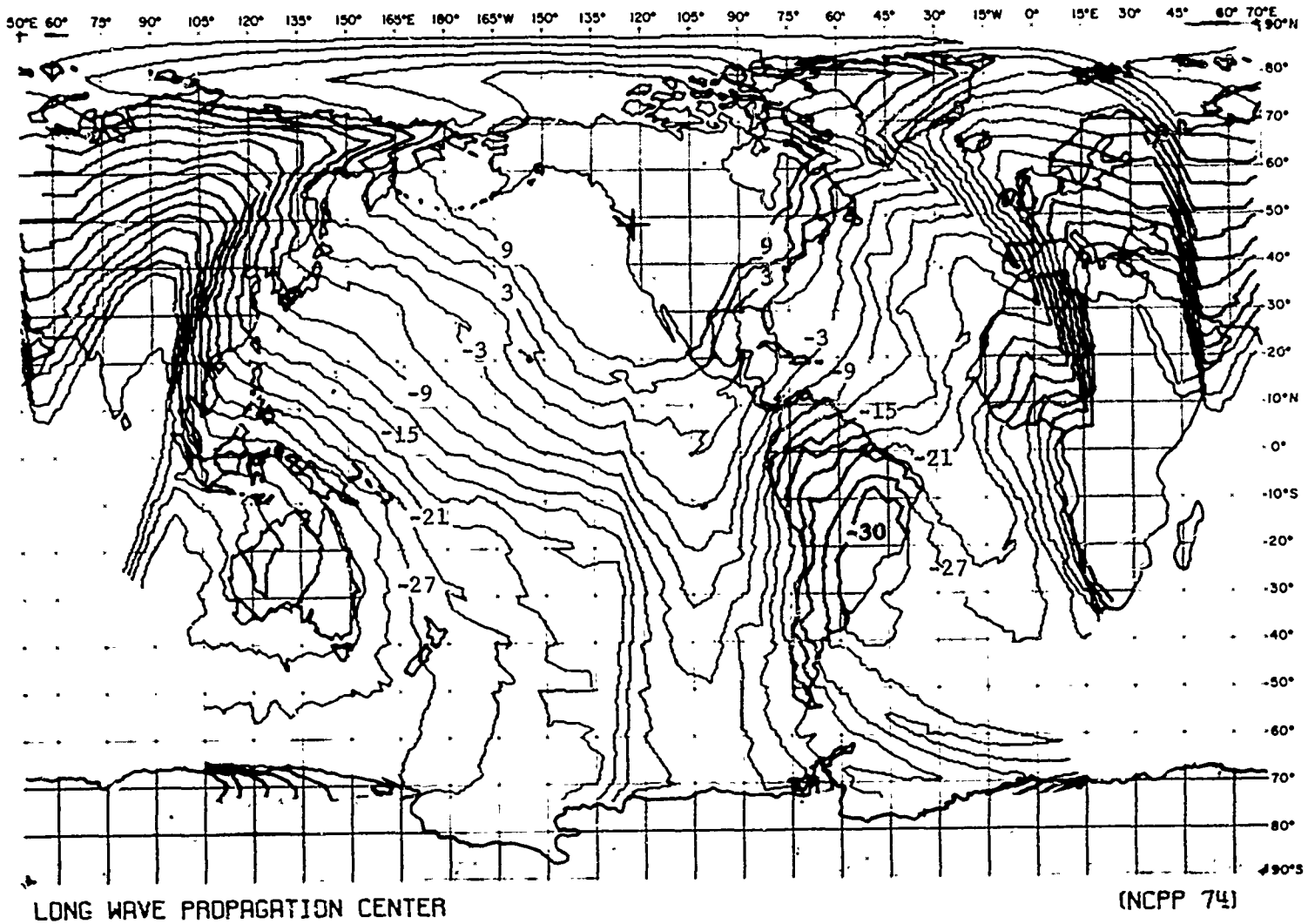


FIG. WI 20 -- SIGNAL-TO-ATMOSPHERIC NOISE RATIO CONTOURS IN dB
NPG (18.6KHZ, 130KW) , JIM CREEK
WINTER 99% TIME AVAILABILITY 1KHZ BANDWIDTH

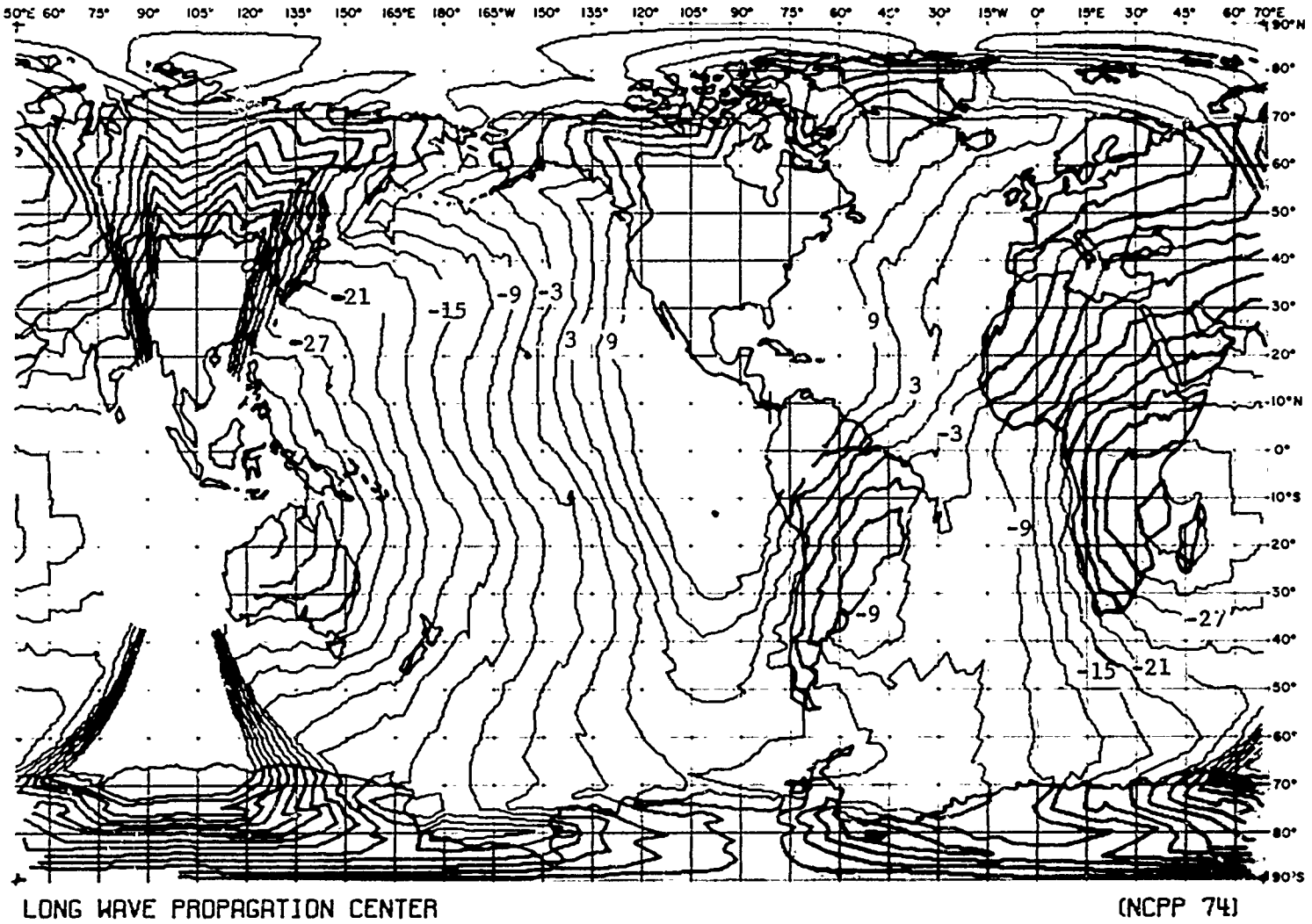


FIG. WI 21 - SIGNAL-TO-ATMOSPHERIC NOISE RATIO CONTOURS IN dB
NBA (24.0KHZ, 110KW) , BALBOA
WINTER 90% TIME AVAILABILITY 1KHZ BANDWIDTH

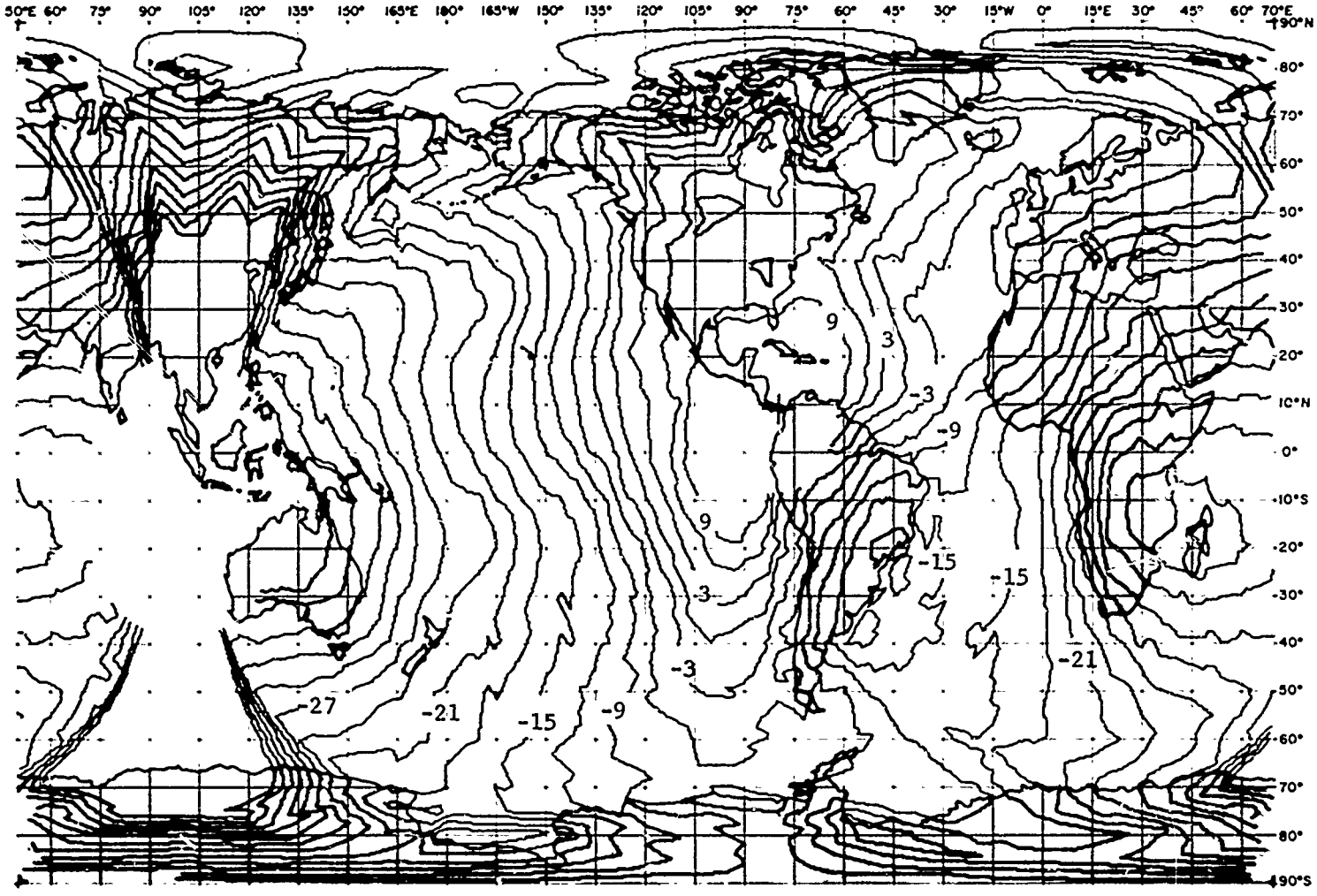


FIG. WI 22 - SIGNAL-TO-ATMOSPHERIC NOISE RATIO CONTOURS IN dB
NBA (24.0KHZ, 110KW) , BALBOA
WINTER 99% TIME AVAILABILITY 1KHZ BANDWIDTH

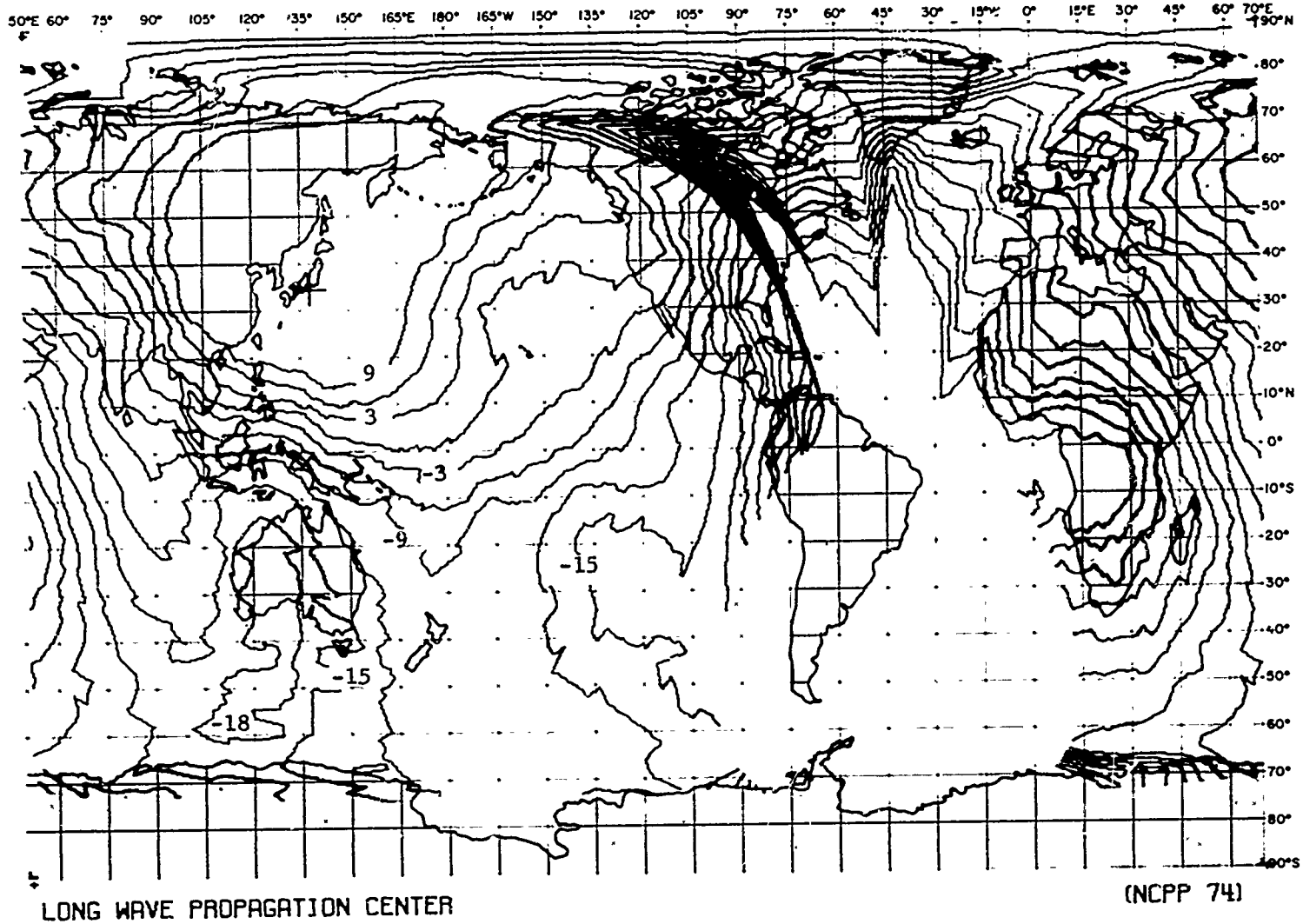


FIG. WI 23 - SIGNAL-TO-ATMOSPHERIC NOISE RATIO CONTOURS IN dB
NDT (17.4KHZ, 40KW) , YOSAMI
WINTER 90% TIME AVAILABILITY 1KHZ BANDWIDTH

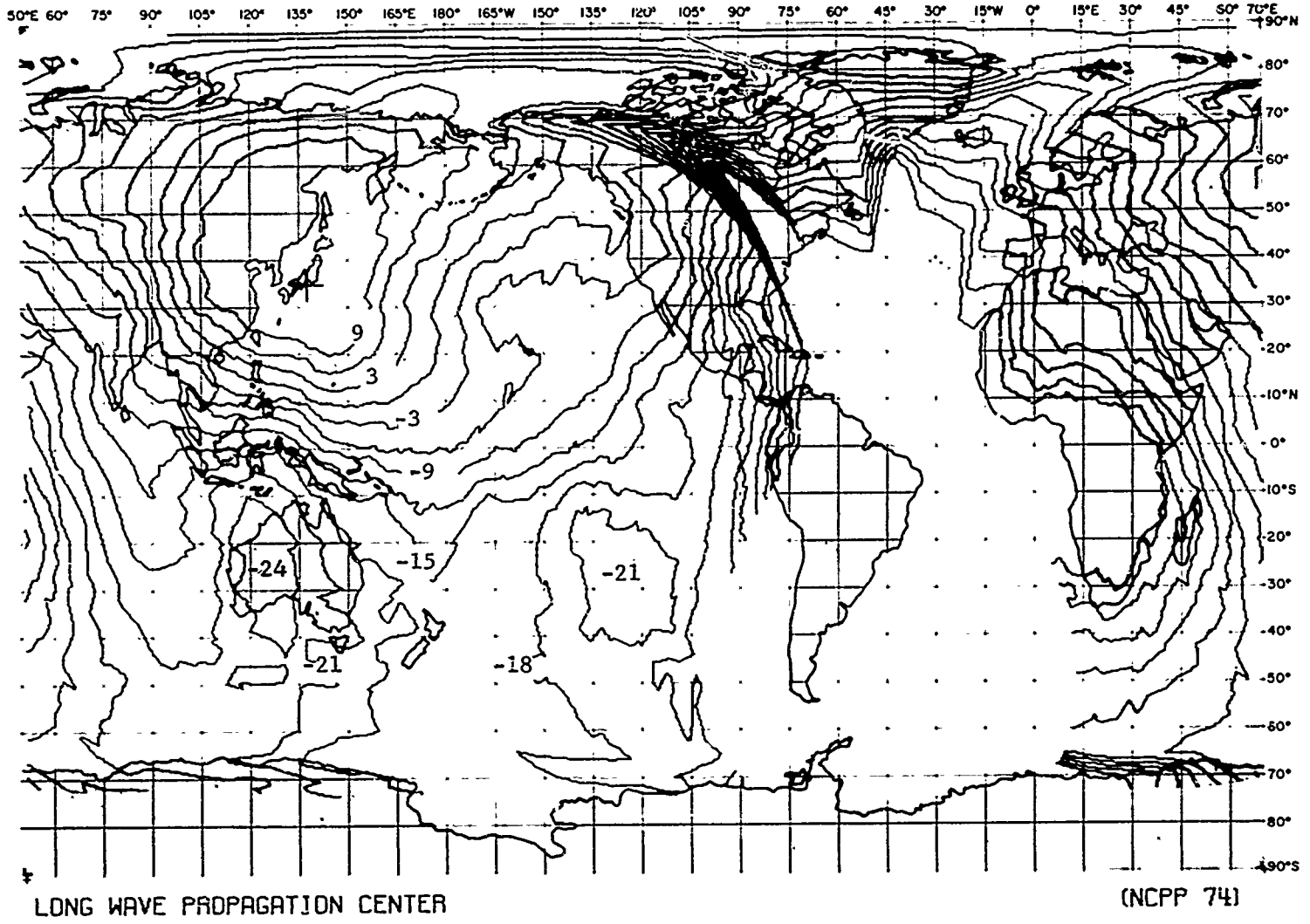


FIG. WI 24 - SIGNAL-TO-ATMOSPHERIC NOISE RATIO CONTOURS IN dB
NDT (17.4KHZ, 40KW) , YOSAMI
WINTER 99% TIME AVAILABILITY 1KHZ BANDWIDTH

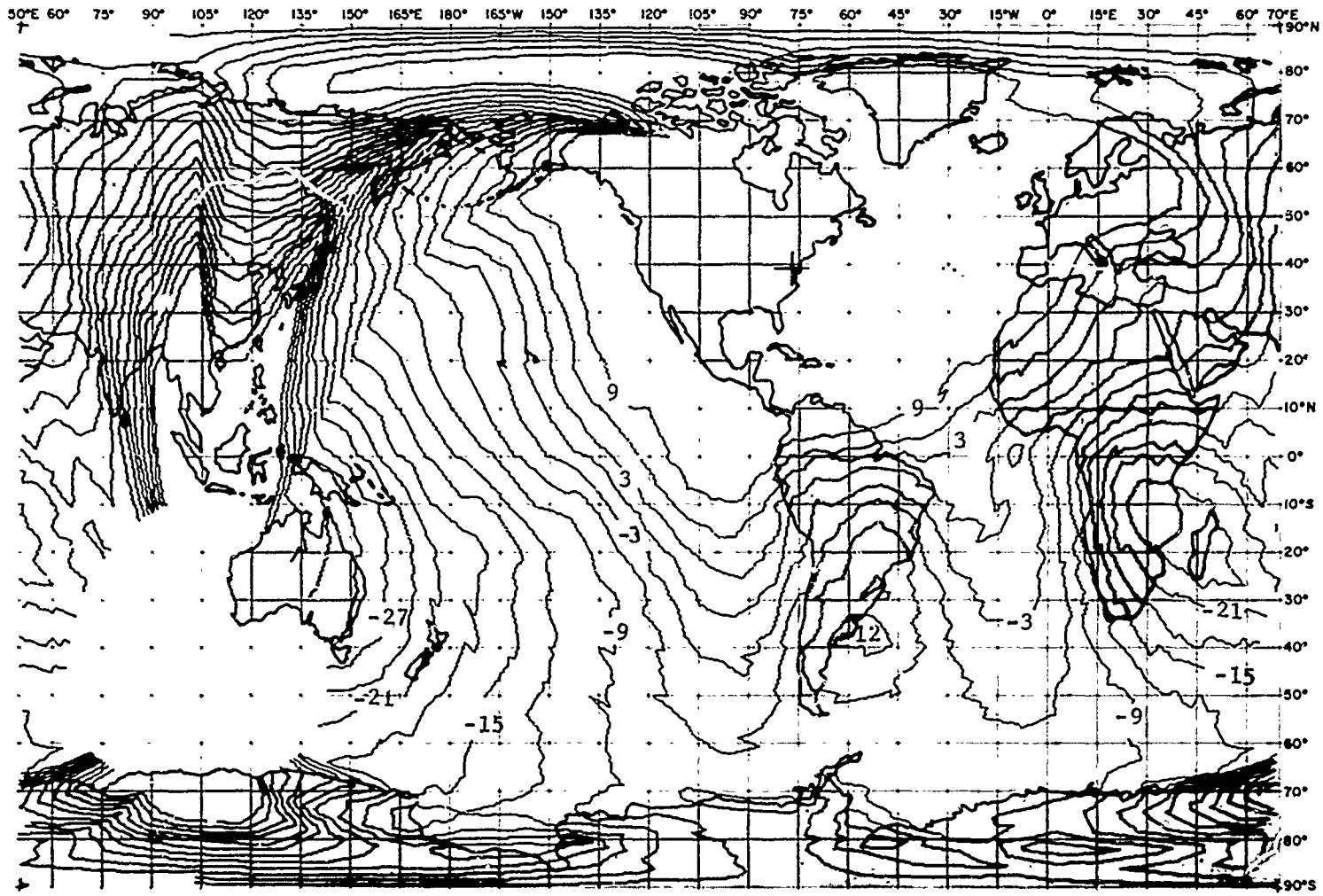


FIG. NI 25 - SIGNAL-TO-ATMOSPHERIC NOISE RATIO CONTOURS IN dB
NSS (21.4KHZ, 400KW) , ANNAPOLIS
WINTER 90% TIME AVAILABILITY 1KHZ BANDWIDTH

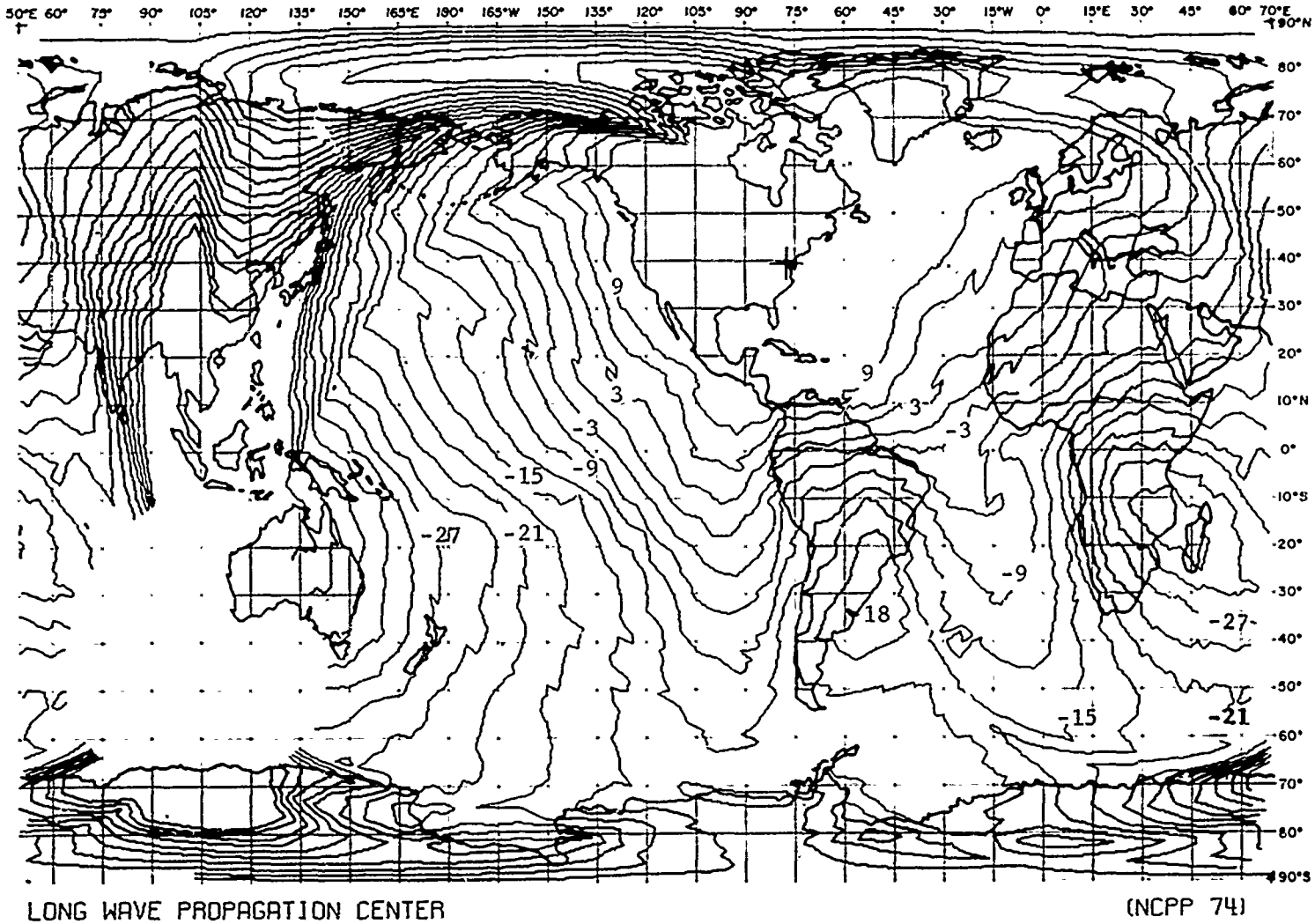


FIG. WI 26 - SIGNAL-TO-ATMOSPHERIC NOISE RATIO CONTOURS IN dB
NSS (21.4KHz, 400KW) , ANNAPOLIS
WINTER 99% TIME AVAILABILITY 1KHZ BANDWIDTH

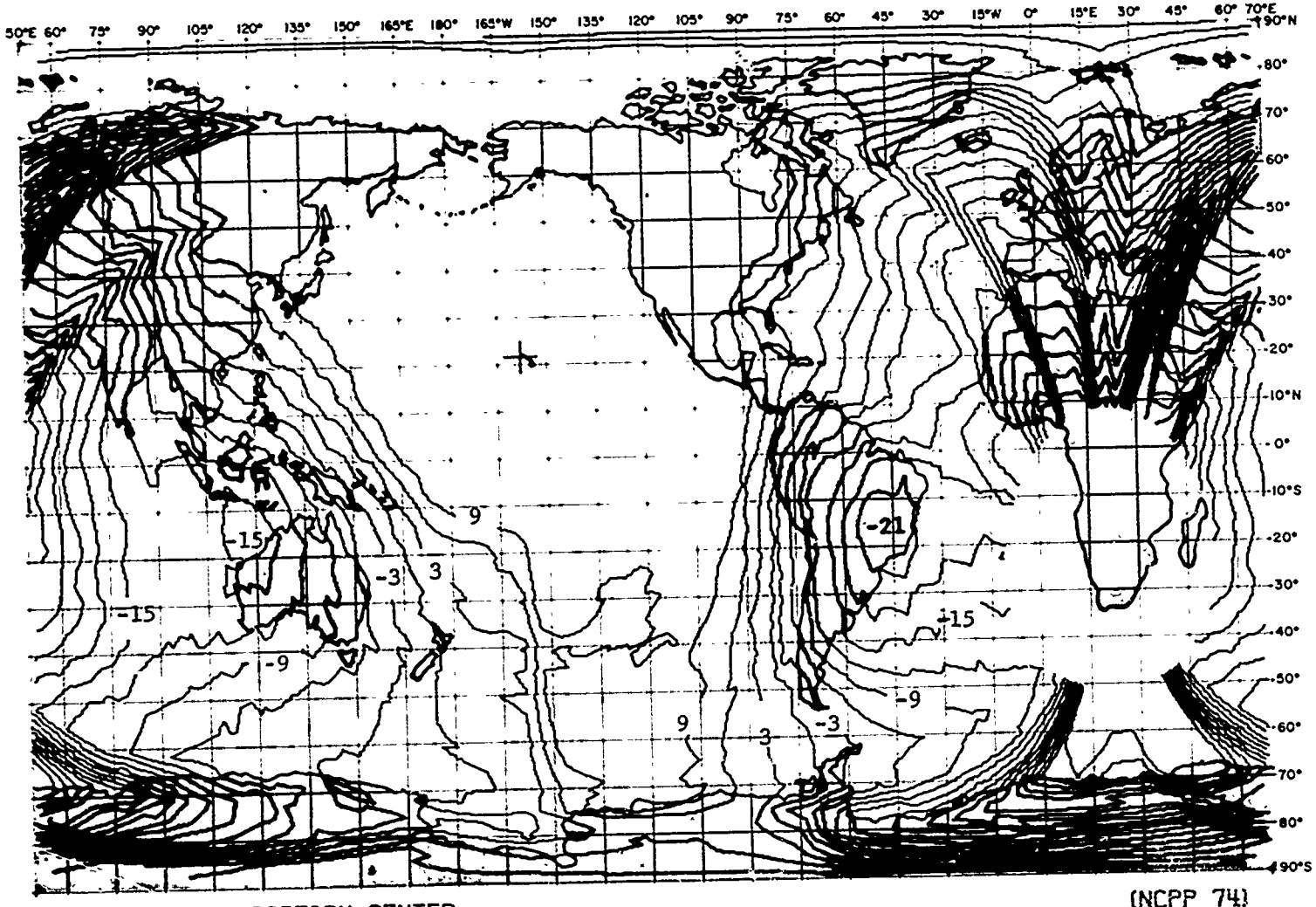


FIG. WI 27 - SIGNAL-TO-ATMOSPHERIC NOISE RATIO CONTOURS IN dB
NPM (23.4KHZ, 630KW) , LURLURLEI
WINTER 90% TIME AVAILABILITY 1KHZ BANDWIDTH

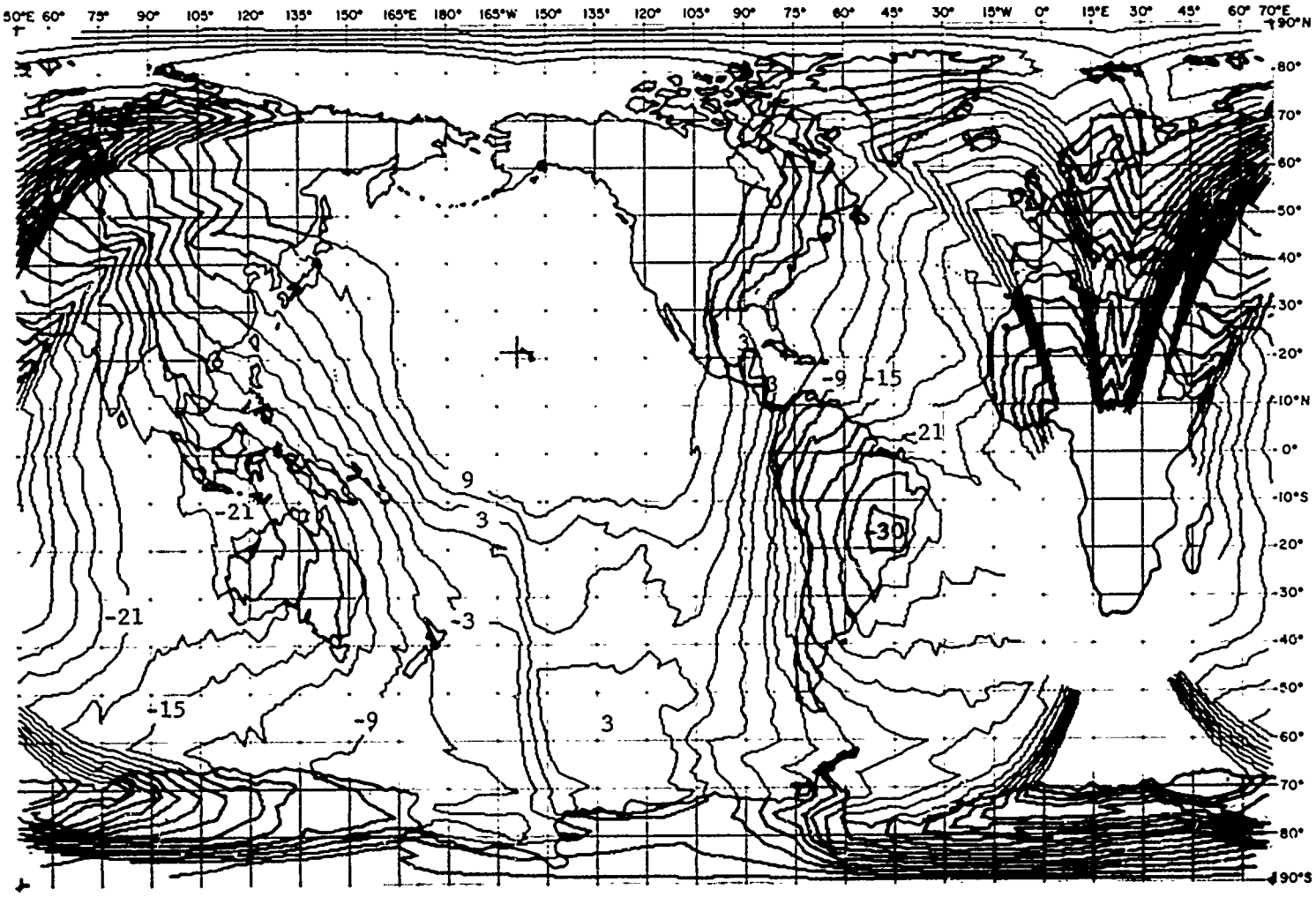


FIG. WI 28 - SIGNAL-TO-ATMOSPHERIC NOISE RATIO CONTOURS IN dB
NPM (23.4KHZ, 630KW) , LUALUALEI
WINTER 99% TIME AVAILABILITY 1KHZ BANDWIDTH

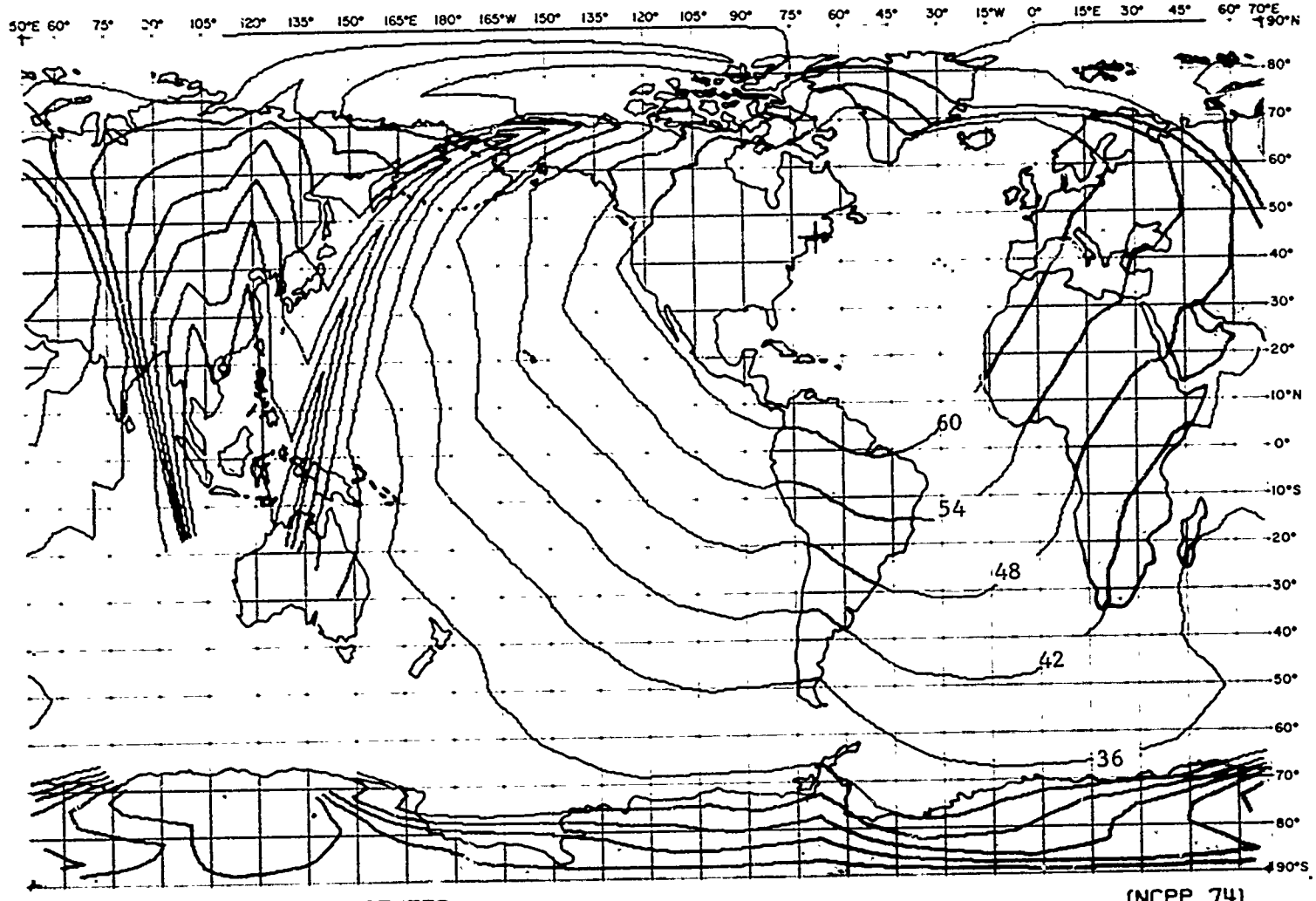


FIG. SP 1 - SIGNAL LEVEL CONTOURS IN dB>1μV/M
NAA (17.8KHZ, 1000KW) , CUTLER
SPRING 90% TIME AVAILABILITY

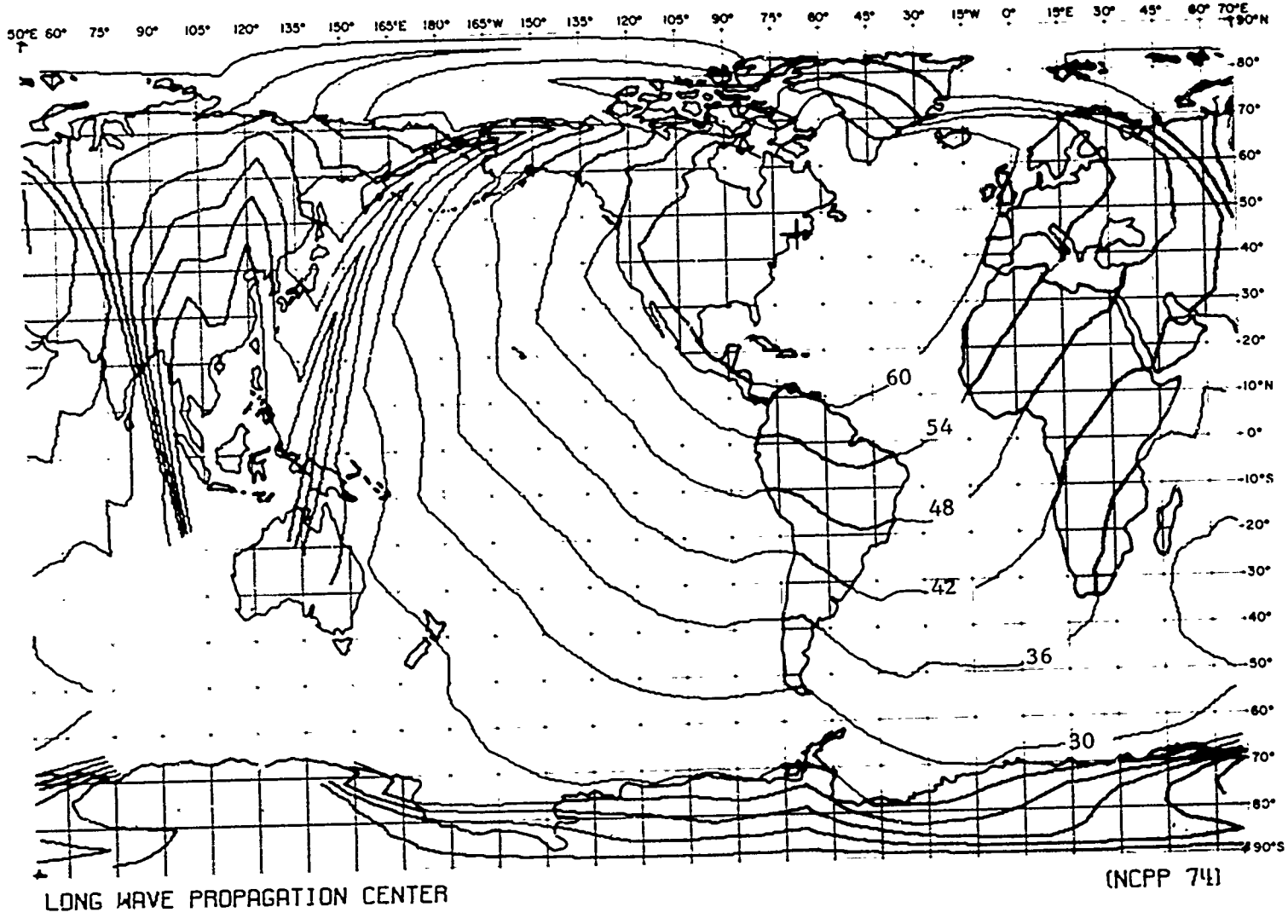


FIG. SP 2 - SIGNAL LEVEL CONTOURS IN dB>1μV/M
NAA (17.8KHZ, 1000KW) , CUTLER
SPRING 99% TIME AVAILABILITY

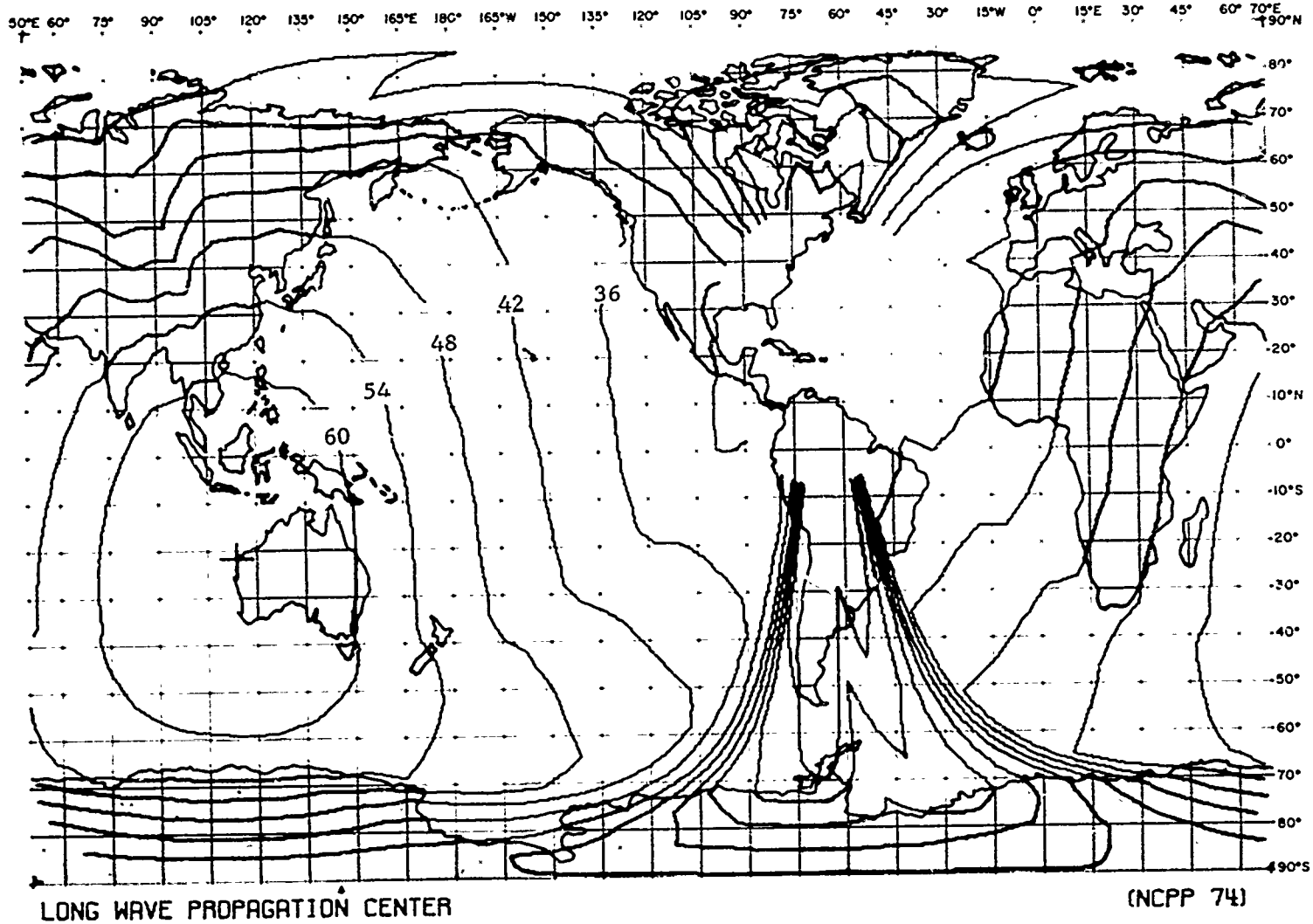


FIG. SP 3 - SIGNAL LEVEL CONTOURS IN dB>1μV/M
NWC (22.3KHZ, 1000KW) , NORTHWEST CAPE
SPRING 90% TIME AVAILABILITY

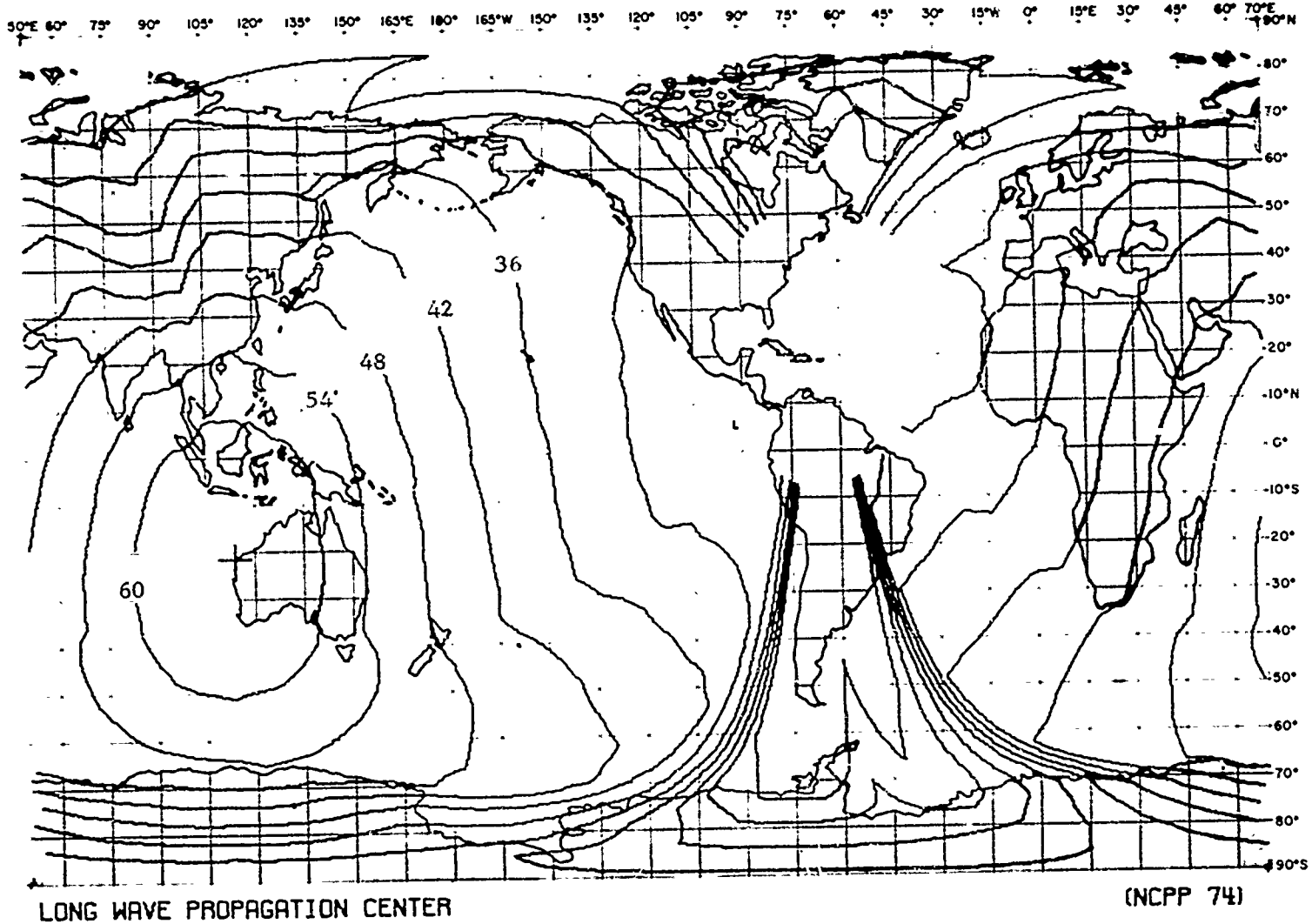


FIG. SP 4 - SIGNAL LEVEL CONTOURS IN dB>1μV/M
NWC (22.3KHZ, 1000KW) , NORTHWEST CAPE
SPRING 99% TIME AVAILABILITY

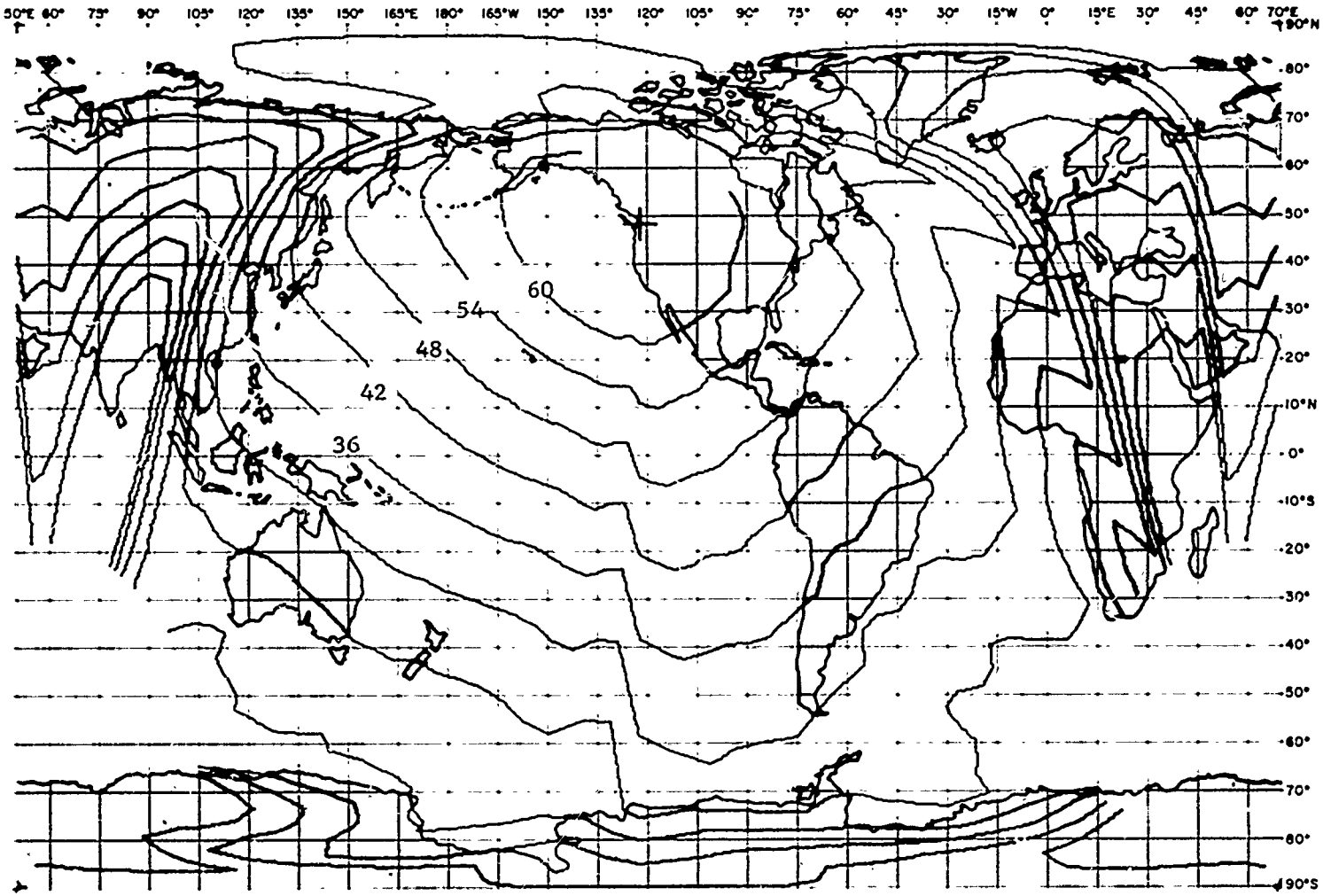


FIG. SP 5 - SIGNAL LEVEL CONTOURS IN dB>1μV/M
NPG (18.6KHZ, 130KW) , JIM CREEK
SPRING 90% TIME AVAILABILITY

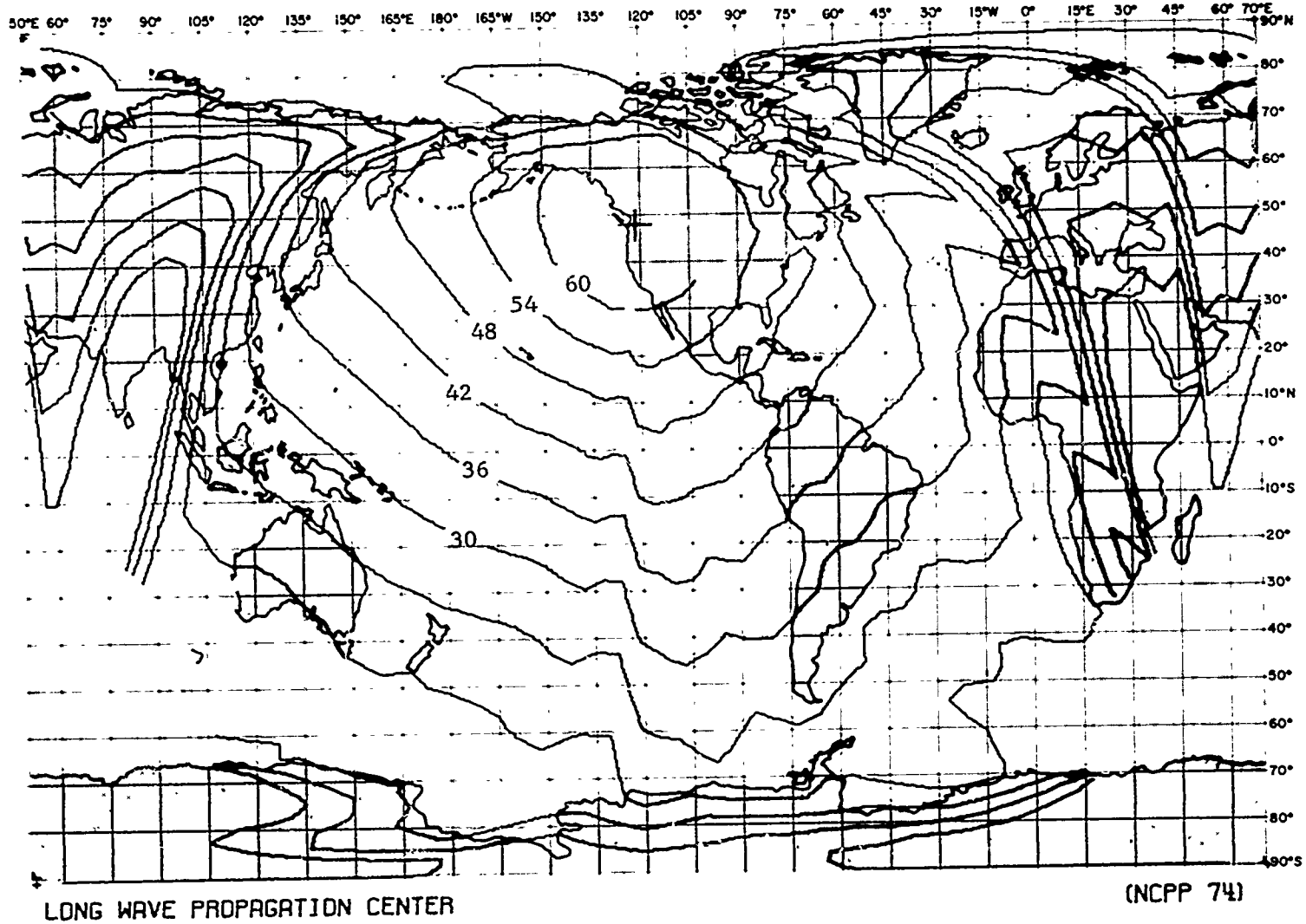


FIG. SP 6 - SIGNAL LEVEL CONTOURS IN dB>1μV/M
NPG (18.6KHZ, 130KW) , JIM CREEK
SPRING 99% TIME AVAILABILITY

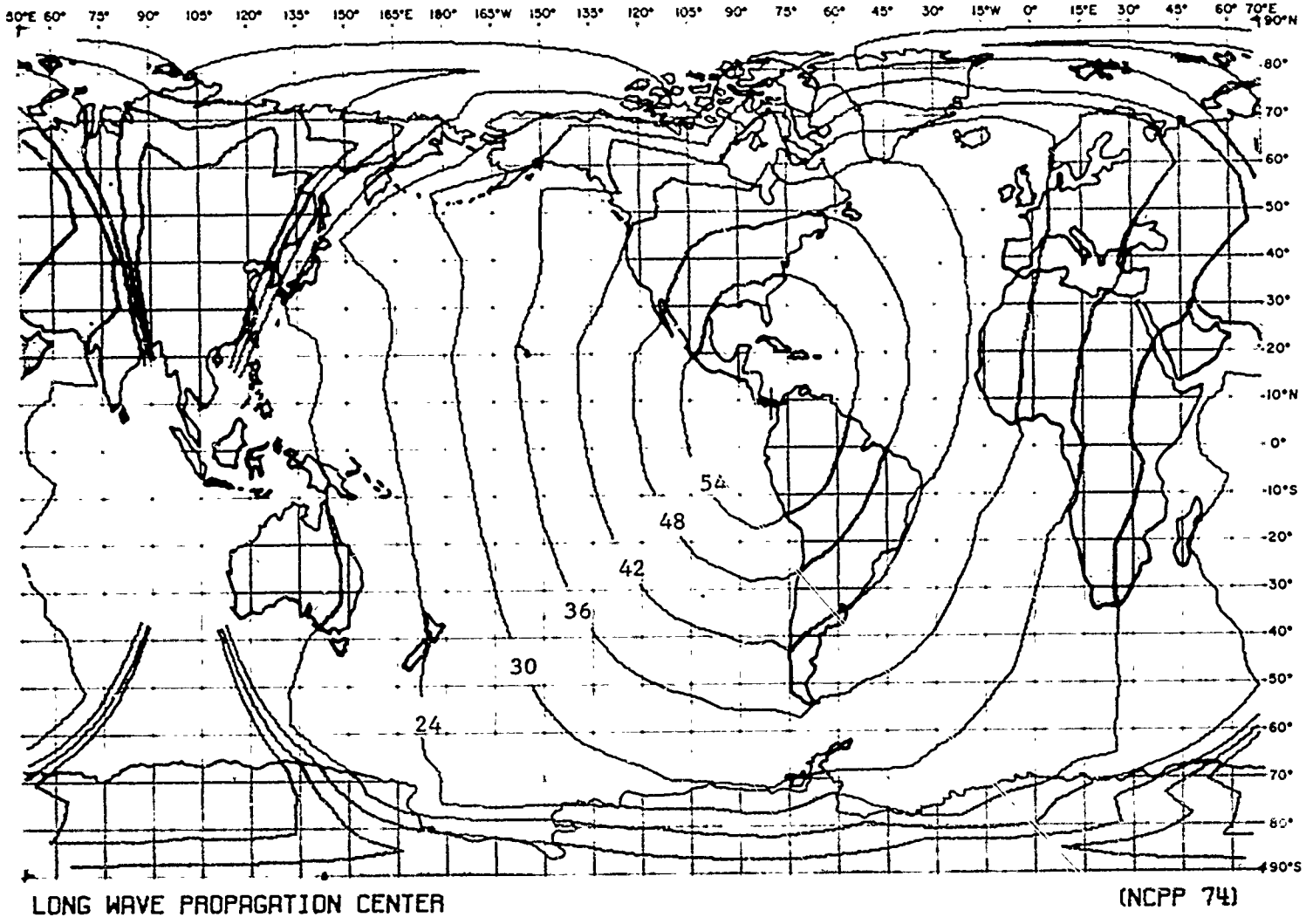


FIG. SP 7 - SIGNAL LEVEL CONTOURS IN dB>1μV/M
NBA (24.0KHZ, 110KW) , BALBOA
SPRING 90%TIME AVAILABILITY

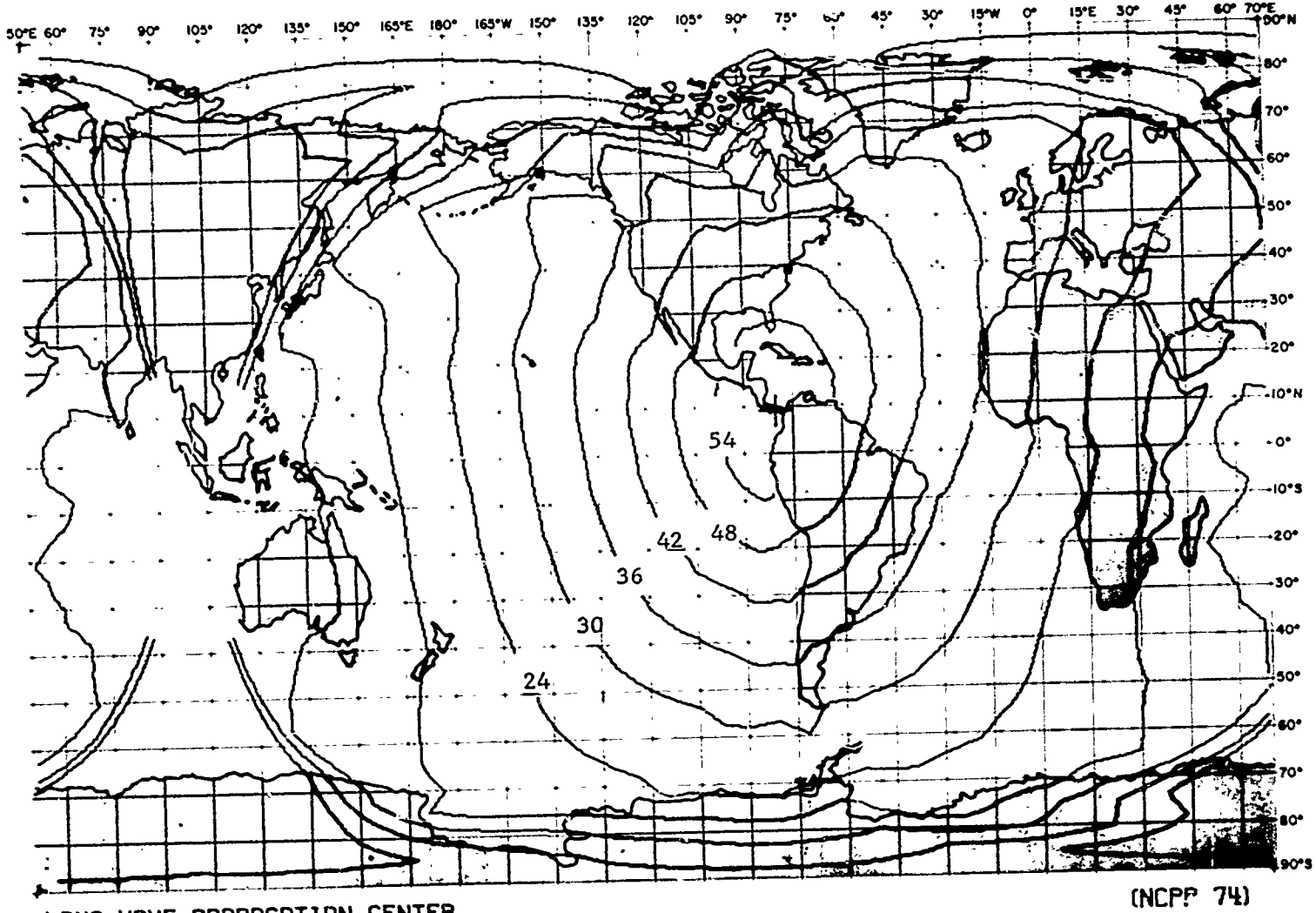


FIG. SP 8 - SIGNAL LEVEL CONTOURS IN dB>1μV/M
NBA (24.0KHZ, 110KW) , BALBOA
SPRING 99% TIME AVAILABILITY

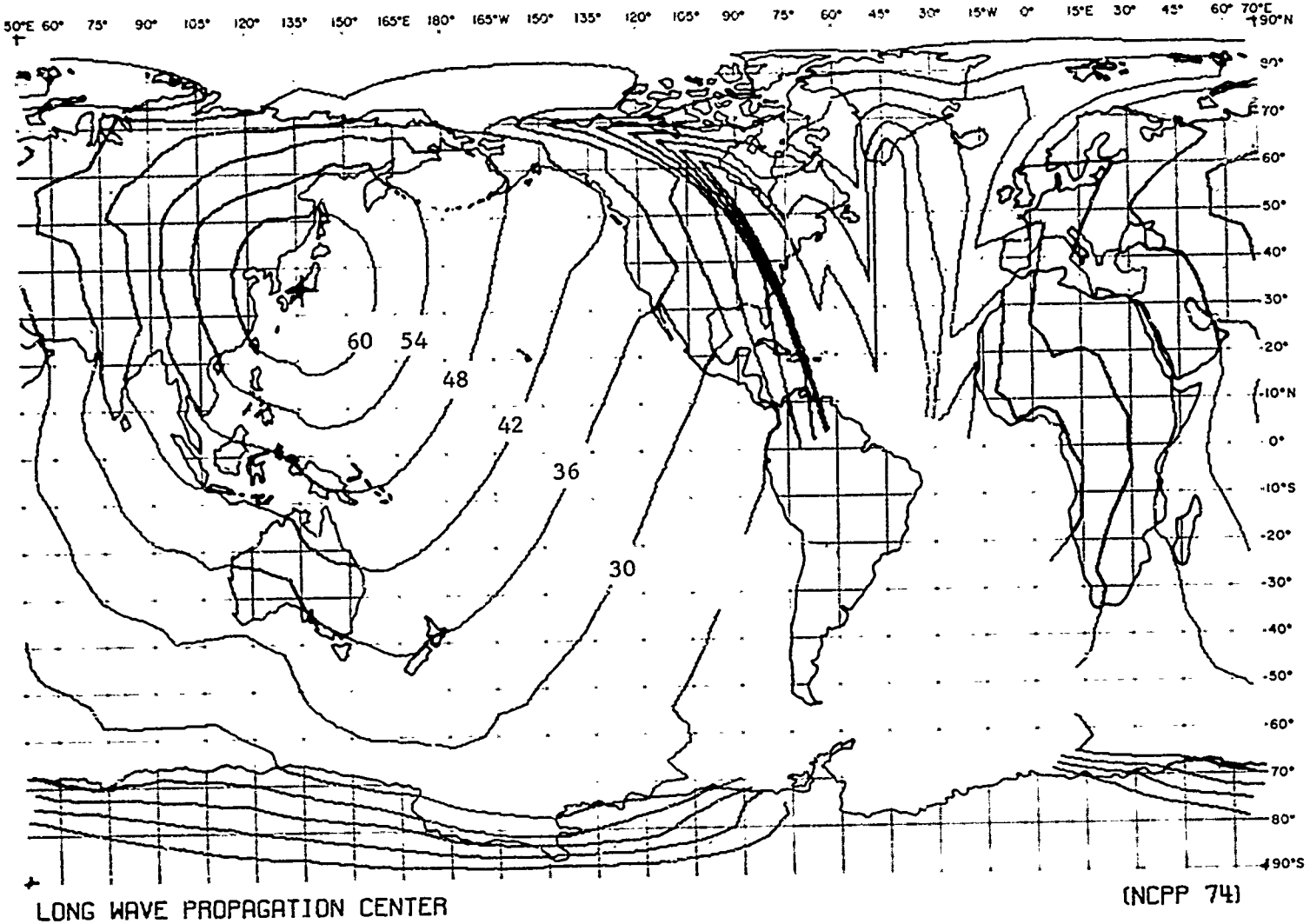


FIG. SP 9 - SIGNAL LEVEL CONTOURS IN dB>1μV/M
NDT (17.4KHZ, 40KW) , YOSAMI
SPRING 90% TIME AVAILABILITY

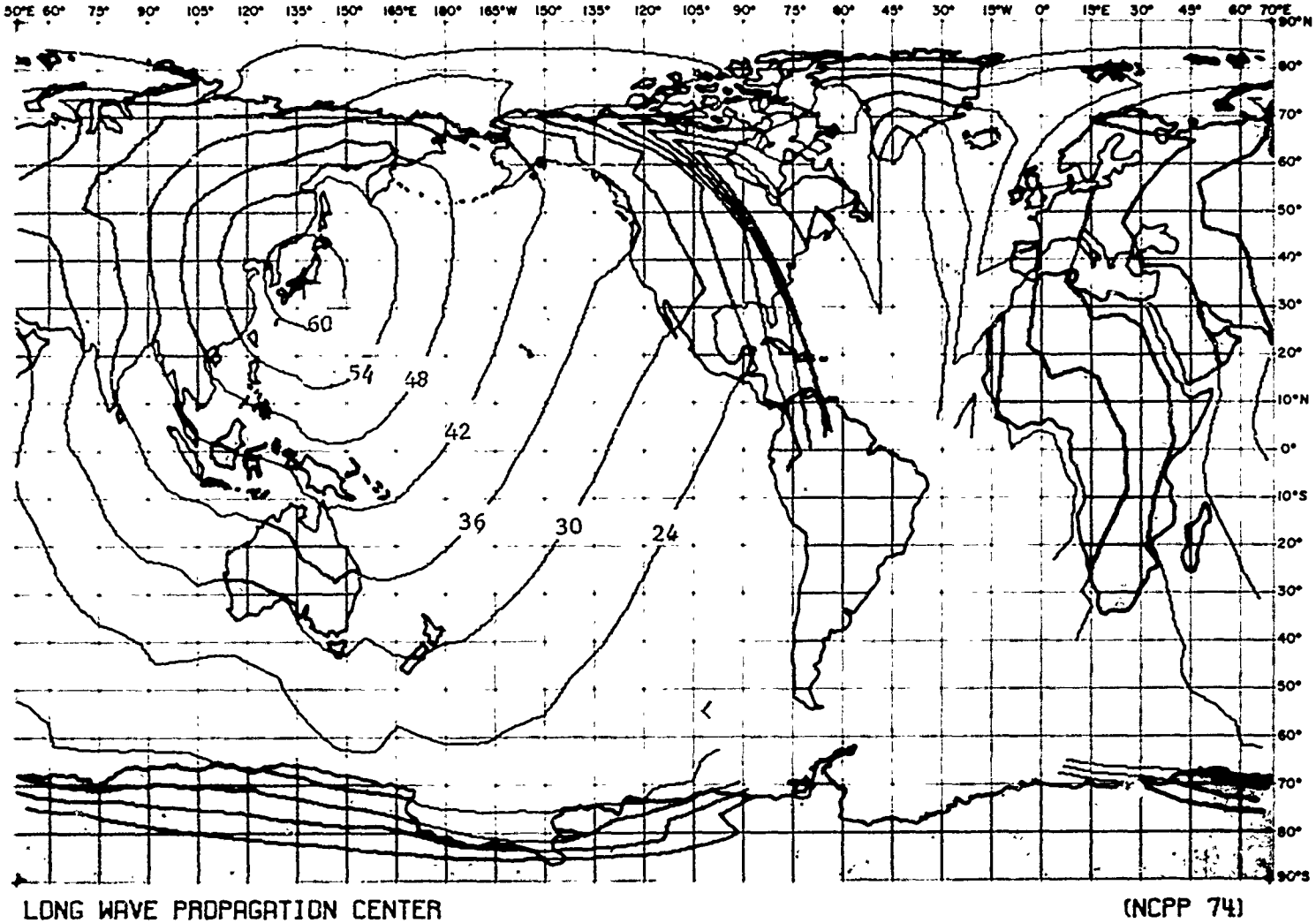


FIG. SP 10 - SIGNAL LEVEL CONTOURS IN dB>1μV/M
NDT (17.4KHZ, 40KW) , YOSAMI
SPRING 99% TIME AVAILABILITY

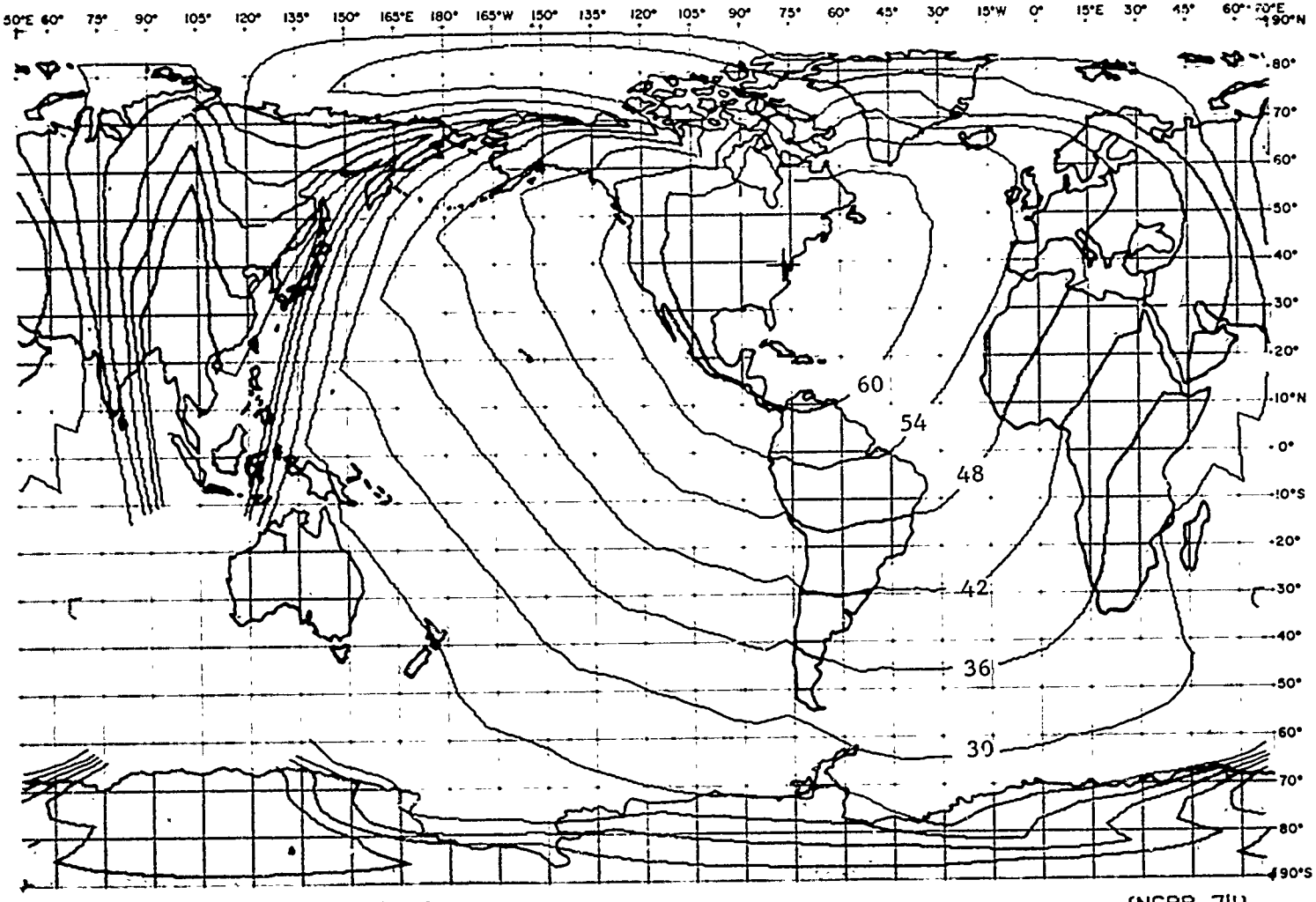


FIG. SP 11 - SIGNAL LEVEL CONTOURS IN dB>1/UV/M
NSS (21.4KHZ, 400KW) , ANNAPOLIS
SPRING 90% TIME AVAILABILITY

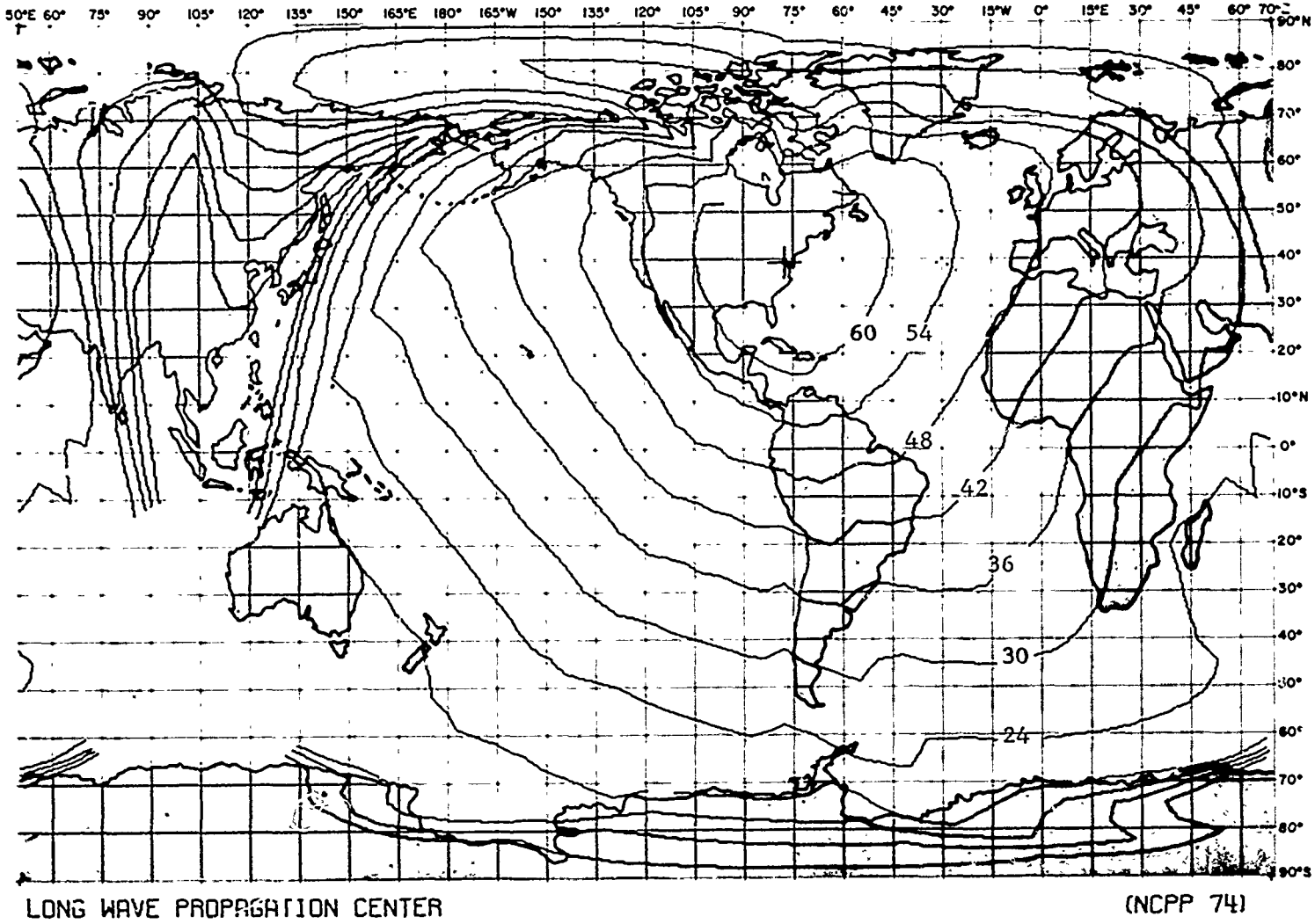


FIG. SP 12 - SIGNAL LEVEL CONTOURS IN dB>1/UV/M
NSS (21.4KHZ, 400KW) , ANNAPOLIS
SPRING 99% TIME AVAILABILITY

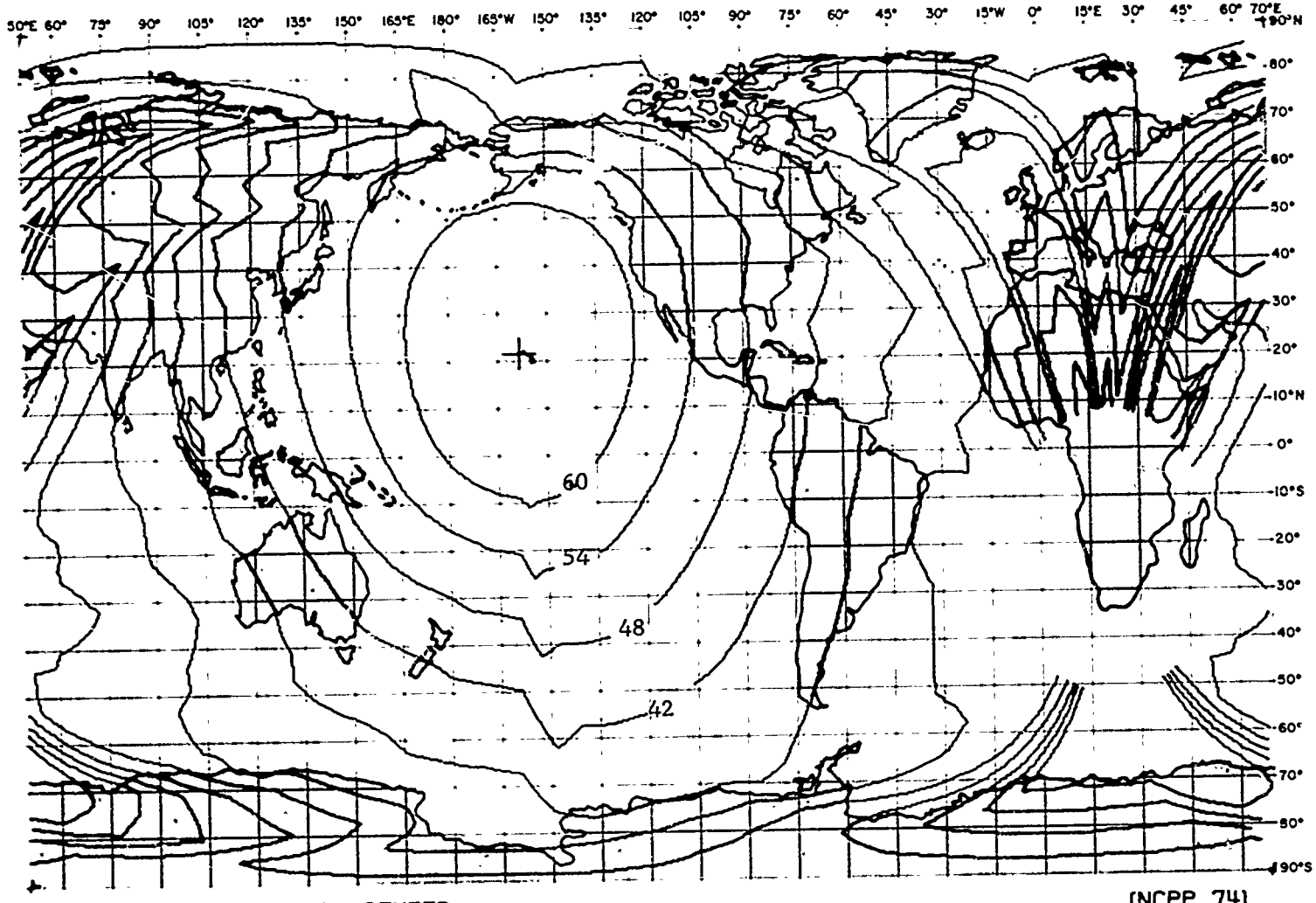


FIG. SP 13 - SIGNAL LEVEL CONTOURS IN dB>1μV/M
NPM (23.4KHZ, 630KW) , LUALUALEI
SPRING 90% TIME AVAILABILITY

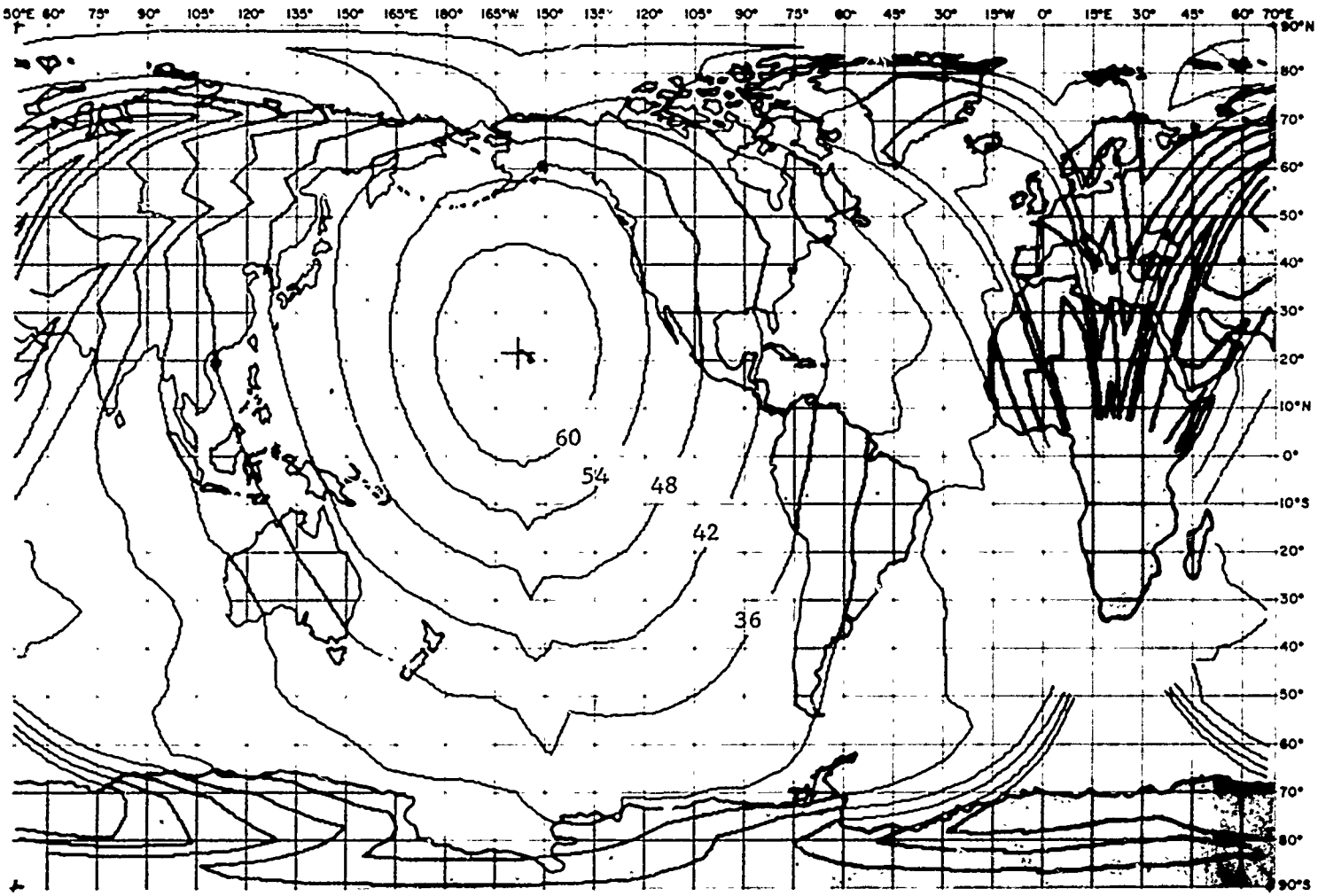


FIG. SP 14 - SIGNAL LEVEL CONTOURS IN dB>1μV/M
NPM (23.4KHZ, 630KW) , LUALUALEI
SPRING 99% TIME AVAILABILITY

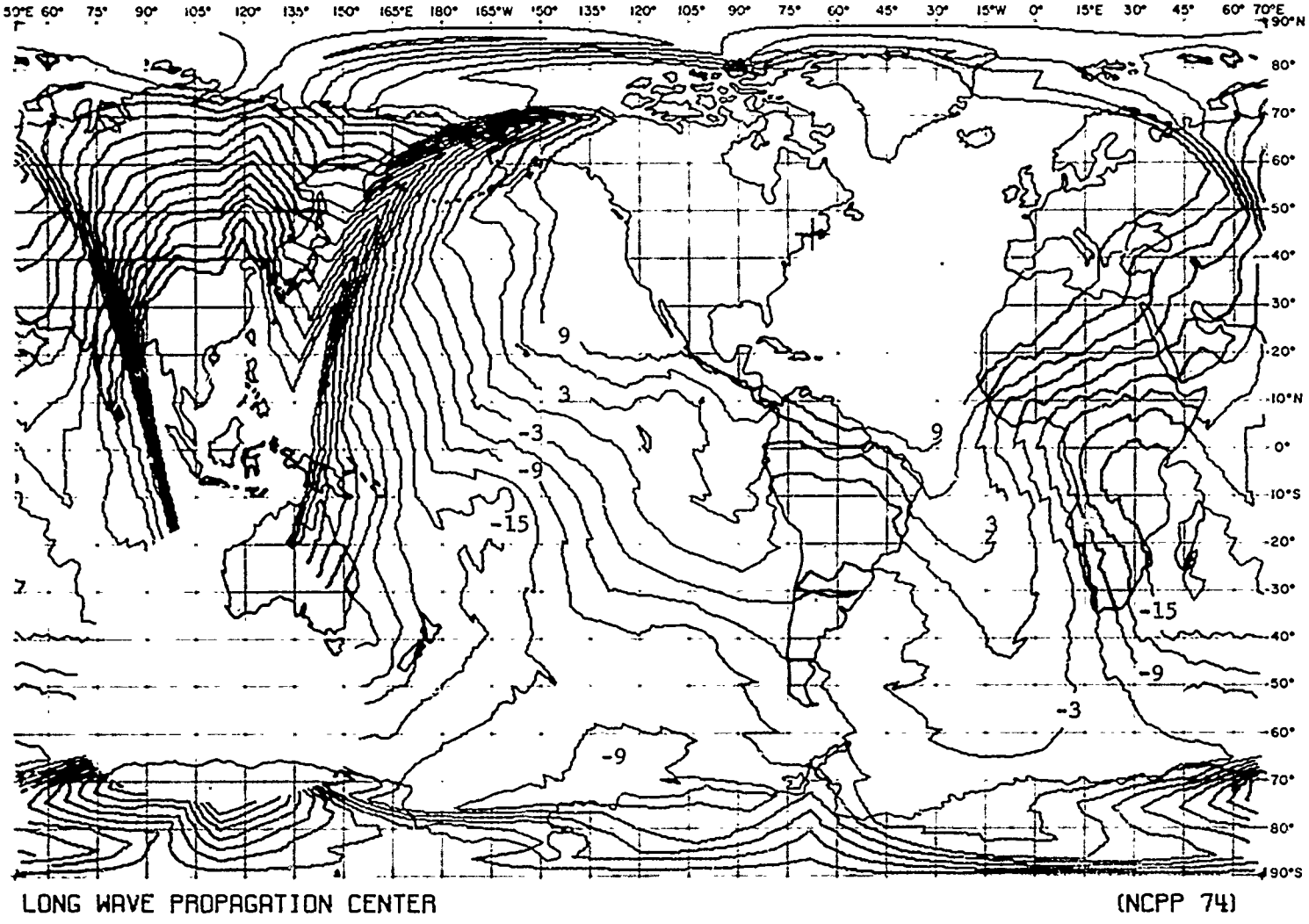


FIG. SP 15 - SIGNAL-TO-ATMOSPHERIC NOISE RATIO CONTOURS IN dB
NAA (17.8KHZ, 1000KW) , CUTLER
SPRING 90% TIME AVAILABILITY 1KHZ BANDWIDTH

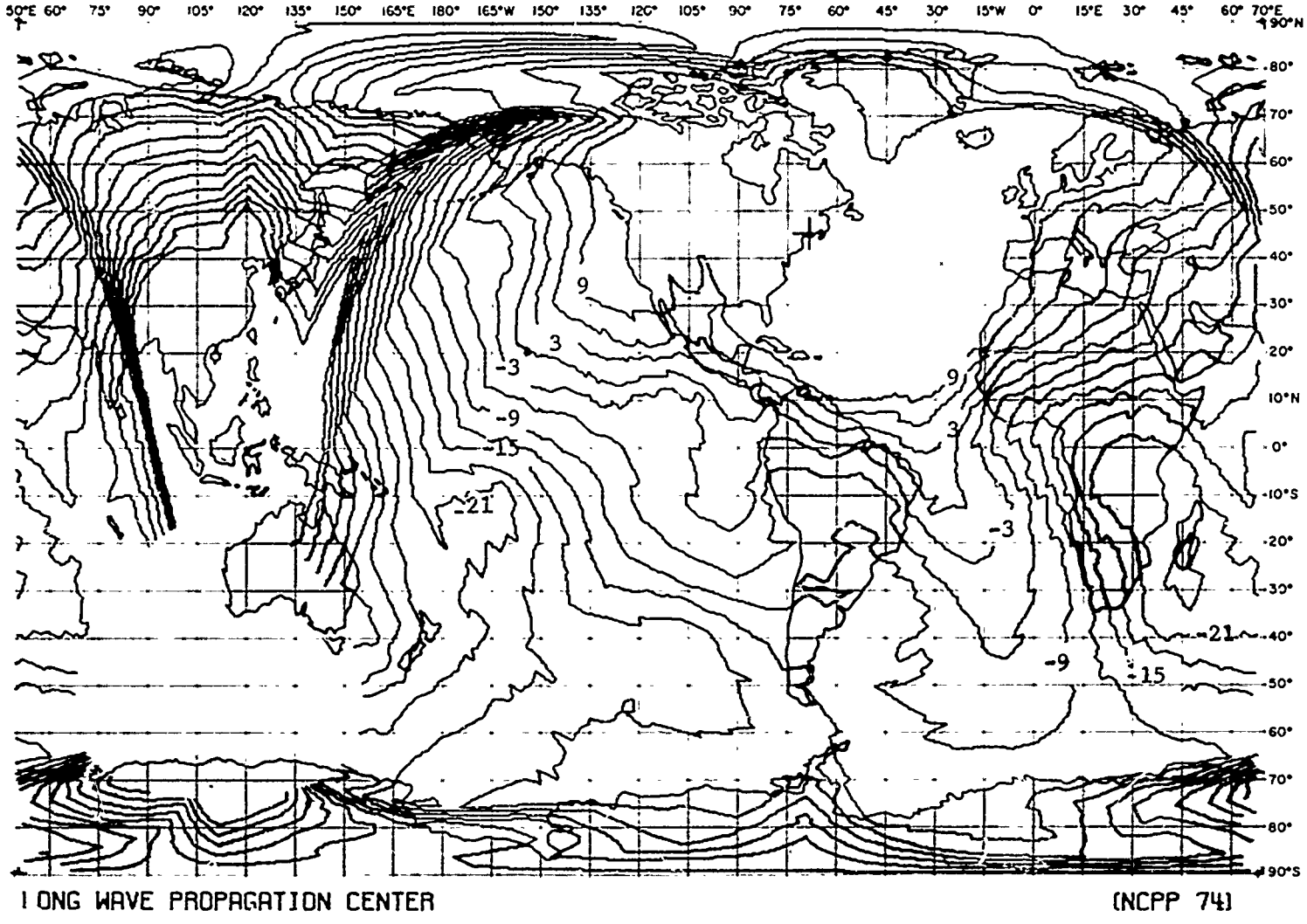


FIG. SP 16 - SIGNAL-TO-ATMOSPHERIC NOISE RATIO CONTOURS IN dB
NRA (17.8KHZ, 1000KW) , CUTLER
SPRING 99% TIME AVAILABILITY 1KHZ BANDWIDTH

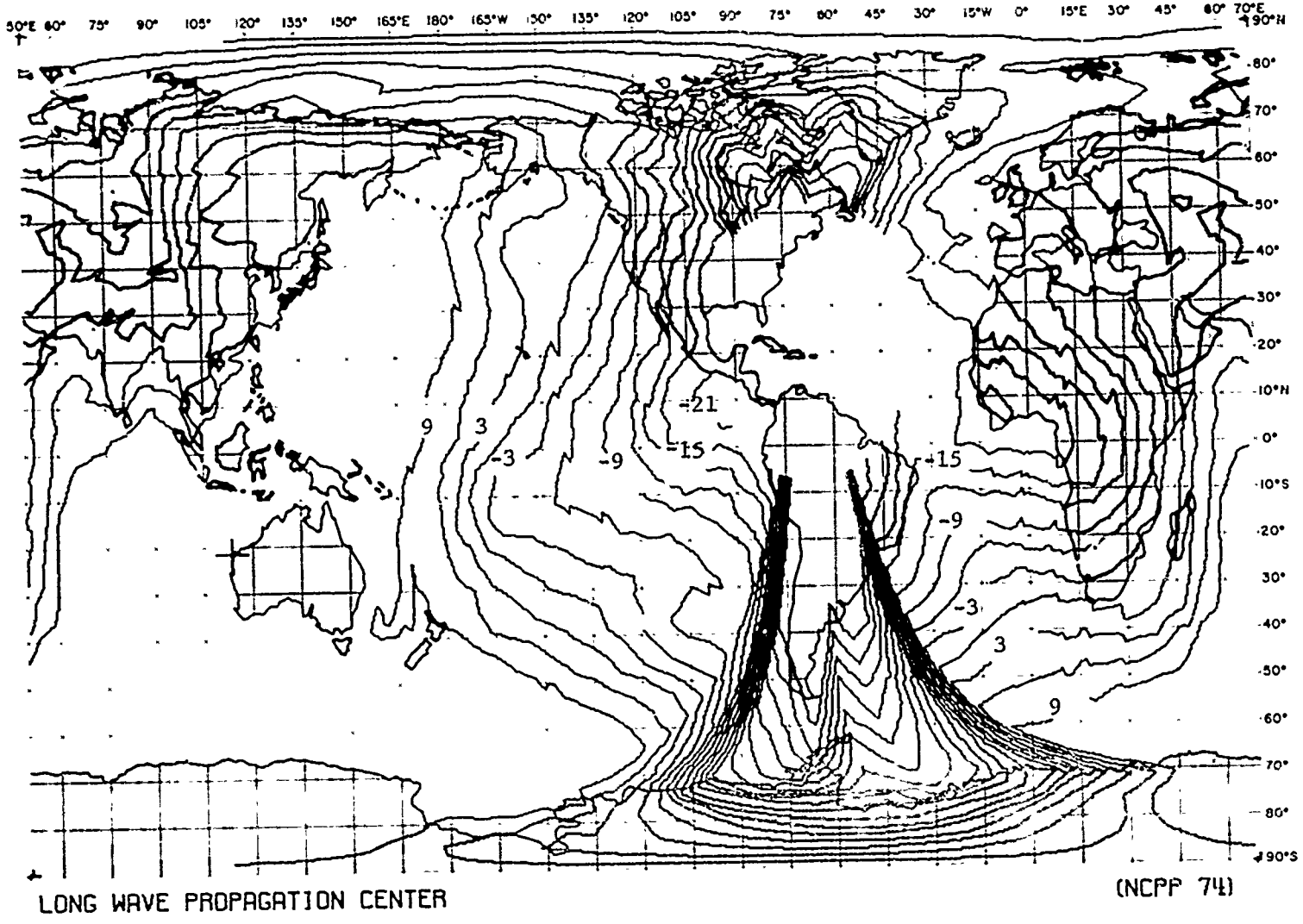


FIG. SP 17 - SIGNAL-TO-ATMOSPHERIC NOISE RATIO CONTOURS IN dB
NWC (22.3KHZ, 1000KW) , NORTHWEST CAPE
SPRING 90% TIME AVAILABILITY 1KHZ BANDWIDTH

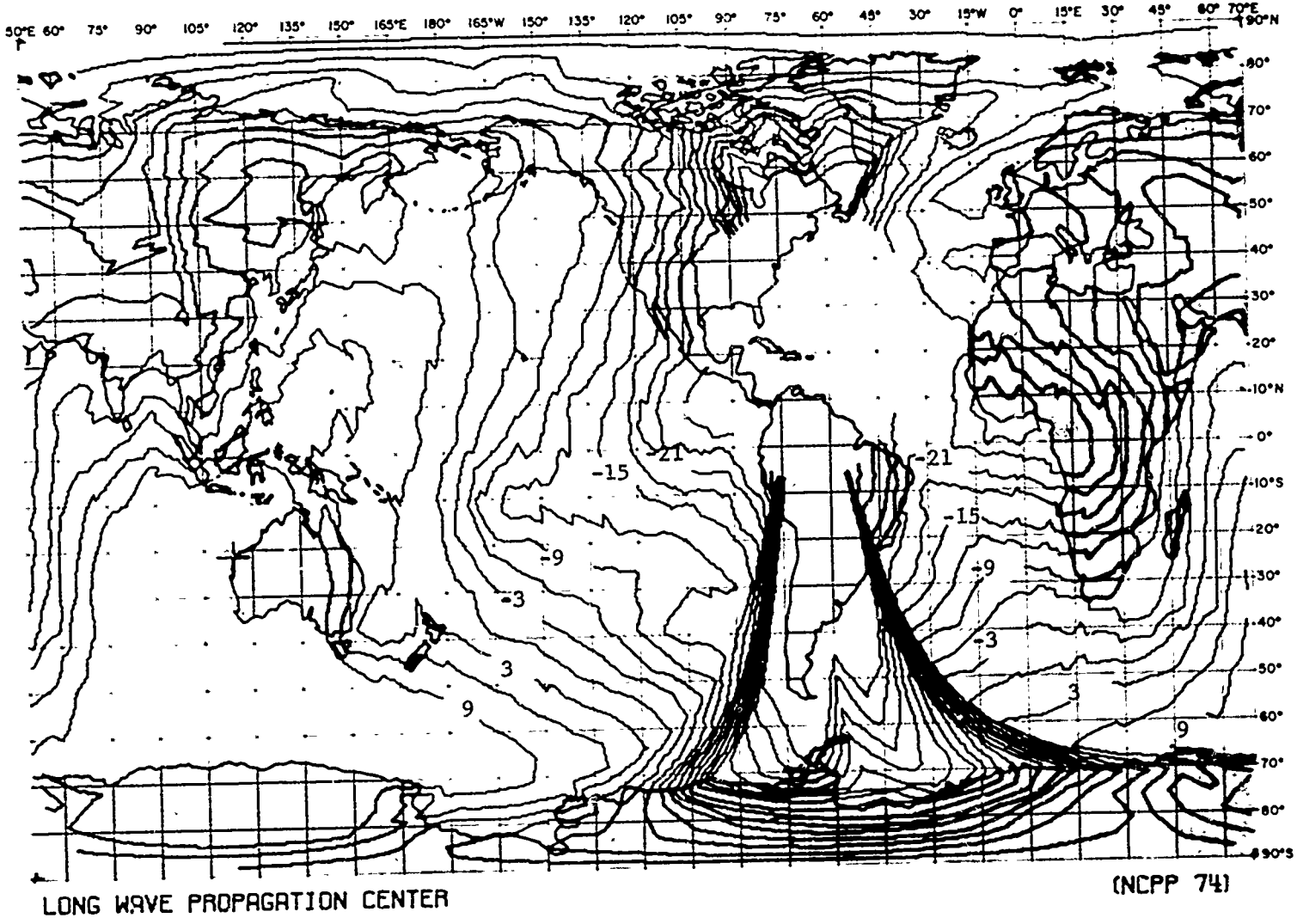


FIG. SP 18 - SIGNAL-TO-ATMOSPHERIC NOISE RATIO CONTOURS IN dB
NWC (22.3KHZ, 1000KW) , NORTHWEST CAPE
SPRING 99% TIME AVAILABILITY 1KHZ BANDWIDTH

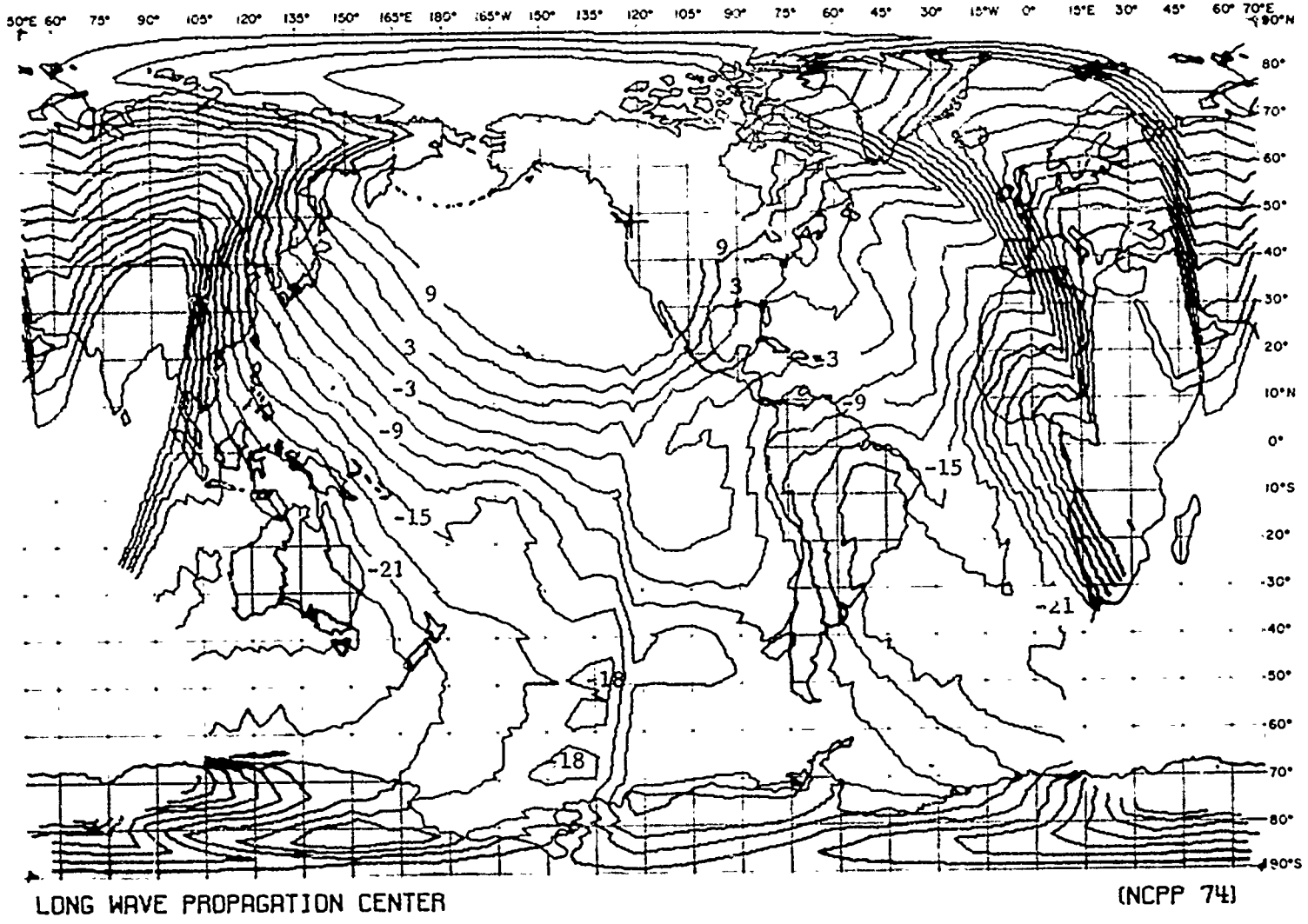


FIG. SP 19 - SIGNAL-TO-ATMOSPHERIC NOISE RATIO CONTOURS IN dB
NPG (18.6KHZ, 130KW) , JIM CREEK
SPRING 90% TIME AVAILABILITY 1KHZ BANDWIDTH

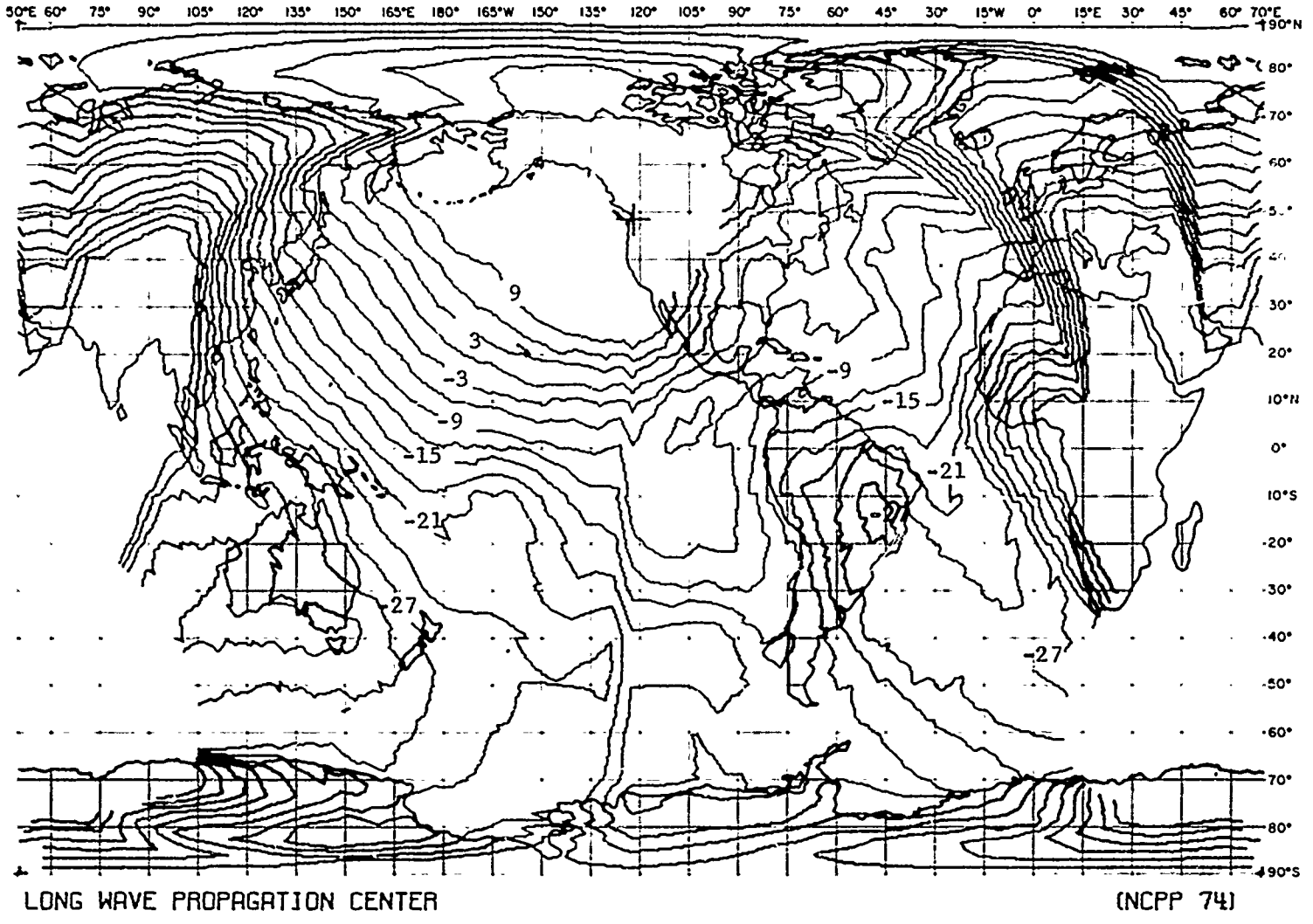


FIG. SP 20 - SIGNAL-TO-ATMOSPHERIC NOISE RATIO CONTOURS IN dB
NPG (18.6KHZ, 130KW) , JIM CREEK
SPRING 99% TIME AVAILABILITY 1KHZ BANDWIDTH

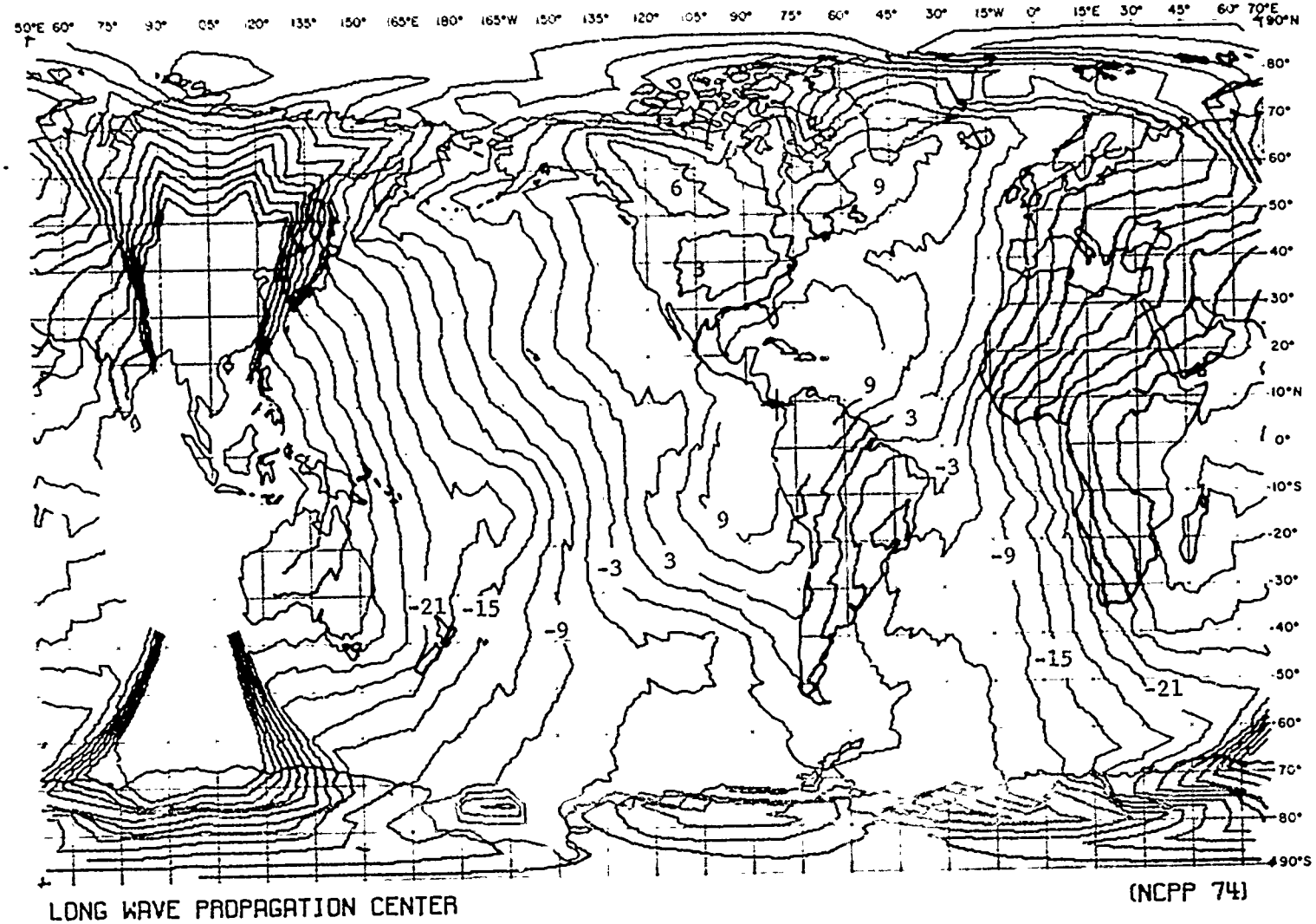


FIG. SP 21 - SIGNAL-TO-ATMOSPHERIC NOISE RATIO CONTOURS IN dB
NBR (24.0KHZ, 110KW) , BALBOA
SPRING 90% TIME AVAILABILITY 1KHZ BANDWIDTH

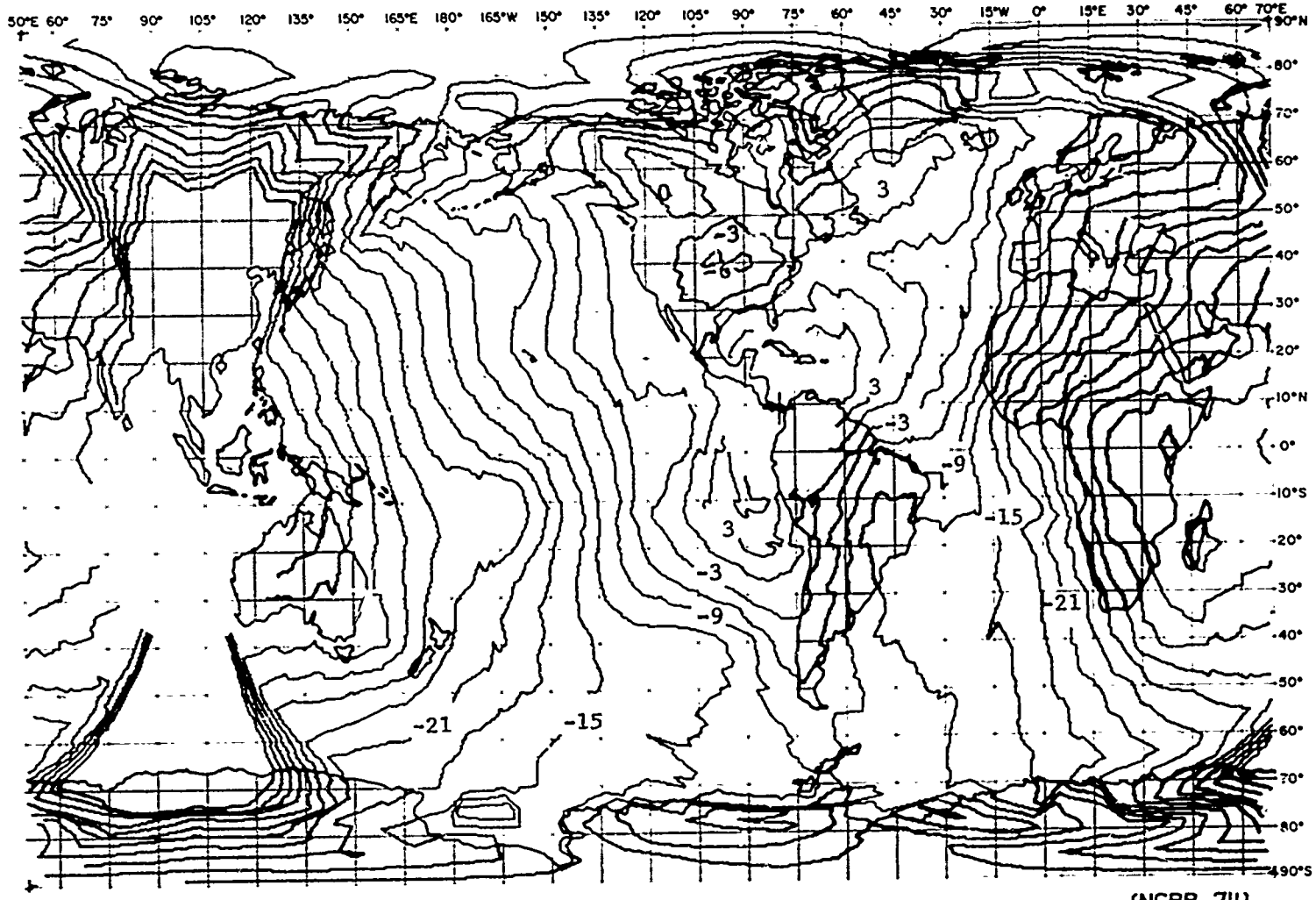


FIG. SP 22 - SIGNAL-TO-ATMOSPHERIC NOISE RATIO CONTOURS IN dB
NBA (24.0KHZ, 110KW) , BALBOA
SPRING 99% TIME AVAILABILITY 1KHZ BANDWIDTH

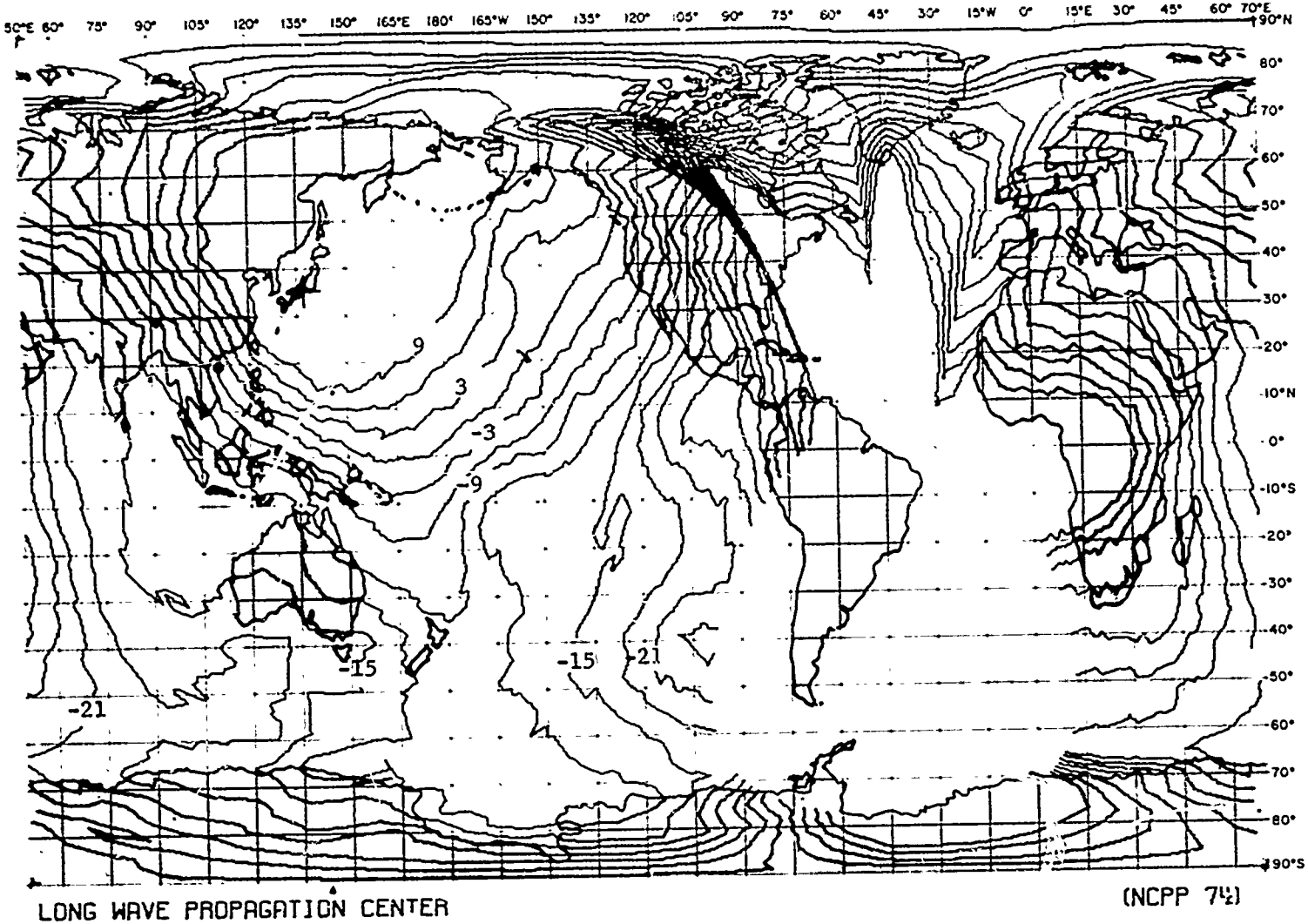


FIG. SP 23 - SIGNAL-TO-ATMOSPHERIC NOISE RATIO CONTOURS IN dB
NDT (17.4KHZ, 40KW) , YOSAMI
SPRING 90% TIME AVAILABILITY 1KHZ BANDWIDTH

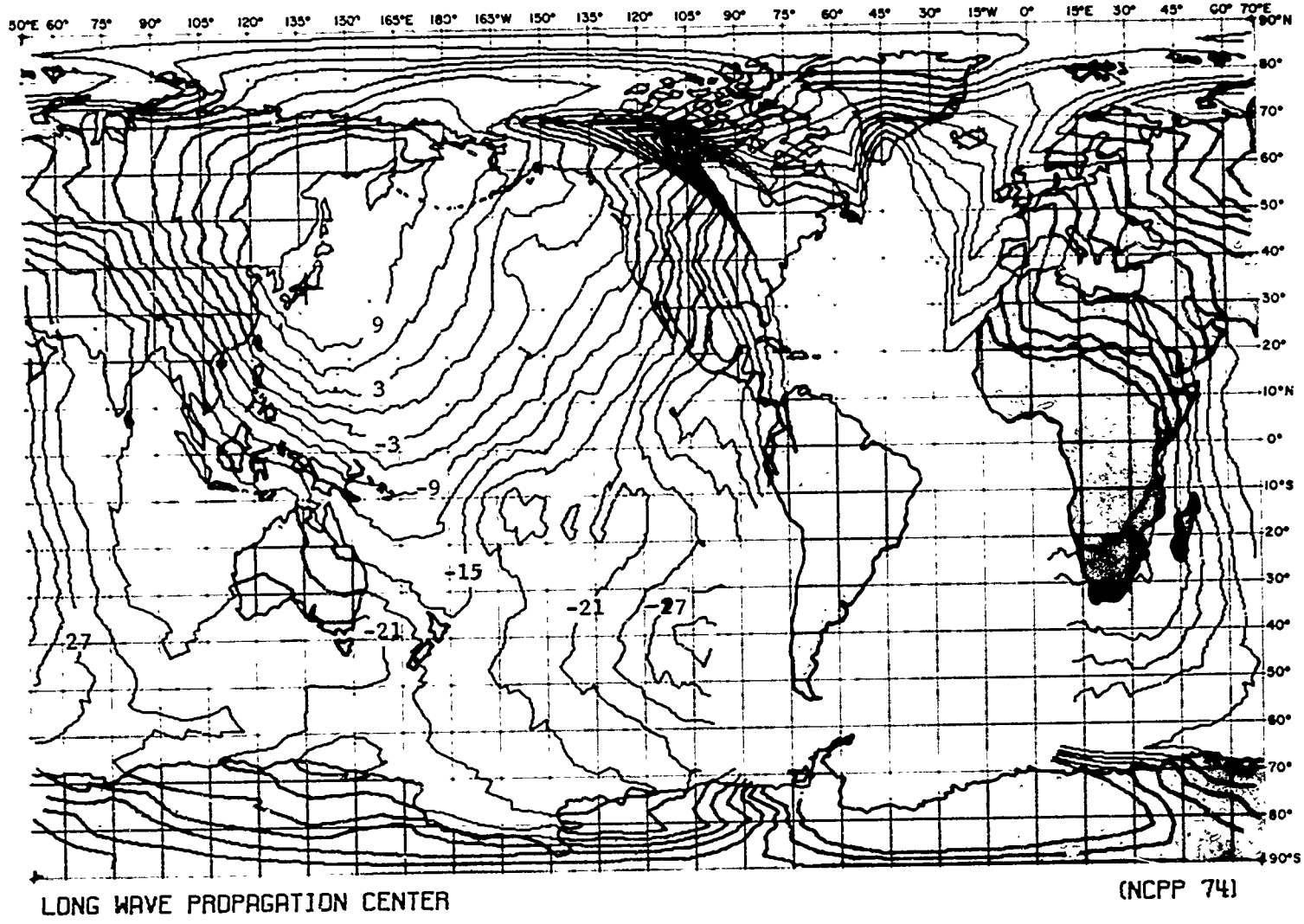


FIG. SP 24 - SIGNAL-TO-ATMOSPHERIC NOISE RATIO CONTOURS IN dB
NDT (17.4KHZ, 40KW) , YOSAMI
SPRING 99% TIME AVAILABILITY 1KHZ BANDWIDTH

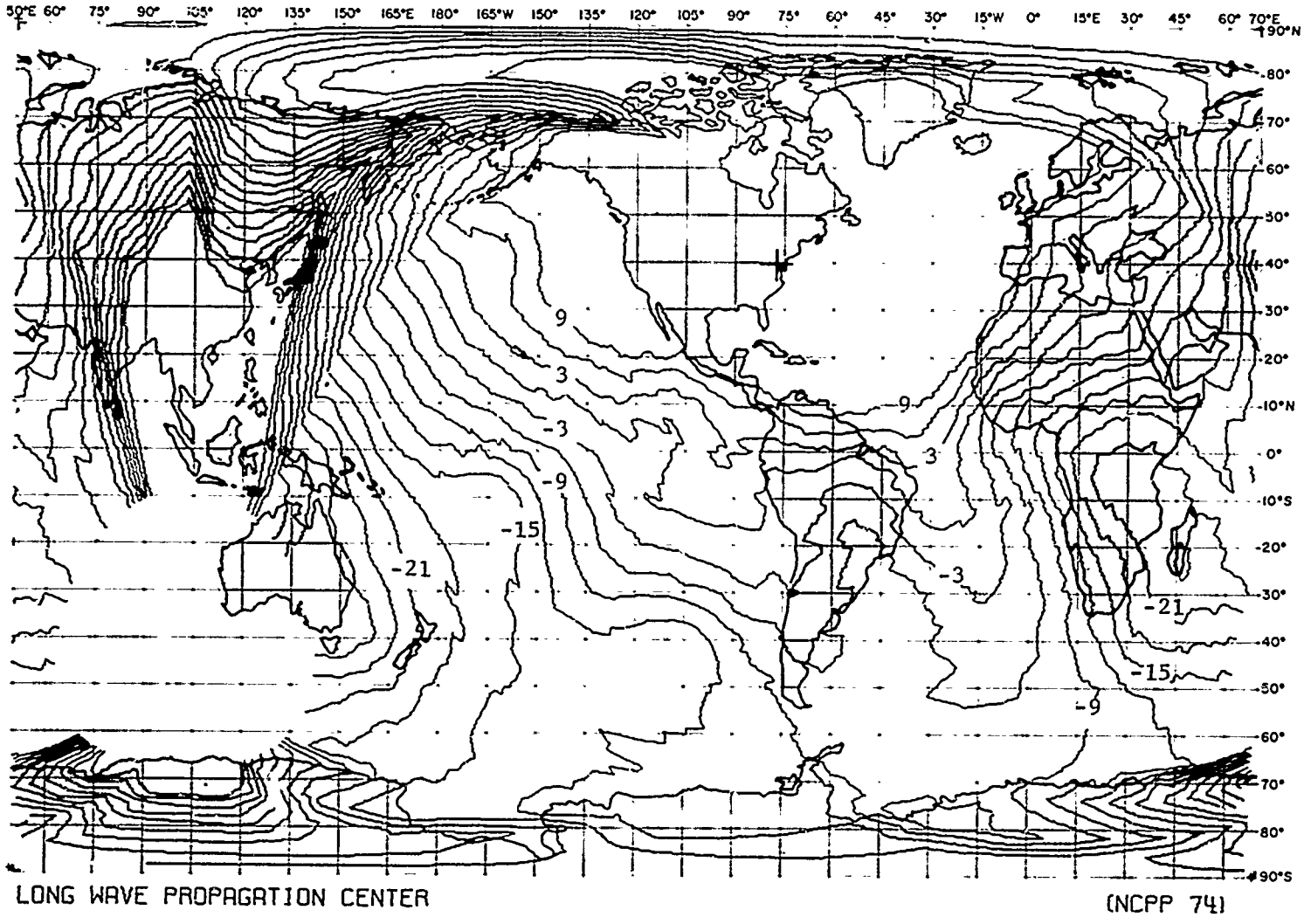


FIG. SP 25 - SIGNAL-TO-ATMOSPHERIC NOISE RATIO CONTOURS IN dB
NSS (21.4KHz, 400KW) , ANNAPOLIS
SPRING 90% TIME AVAILABILITY 1KHZ BANDWIDTH

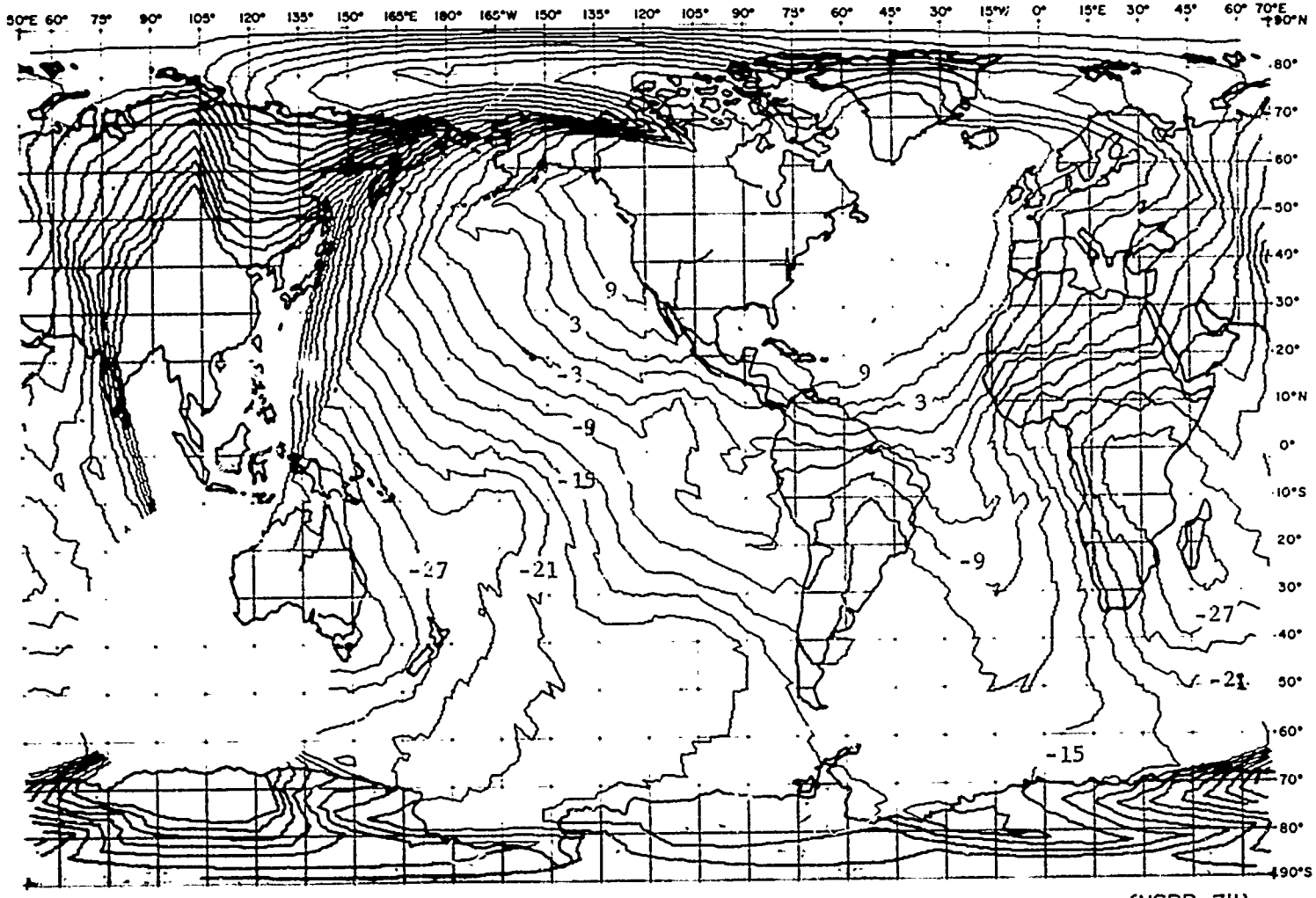


FIG. SP 26 - SIGNAL-TO-ATMOSPHERIC NOISE RATIO CONTOURS IN dB
NSS (21.4KHz, 400KW) , ANNAPOLIS
SPRING 99% TIME AVAILABILITY 1KHZ BANDWIDTH

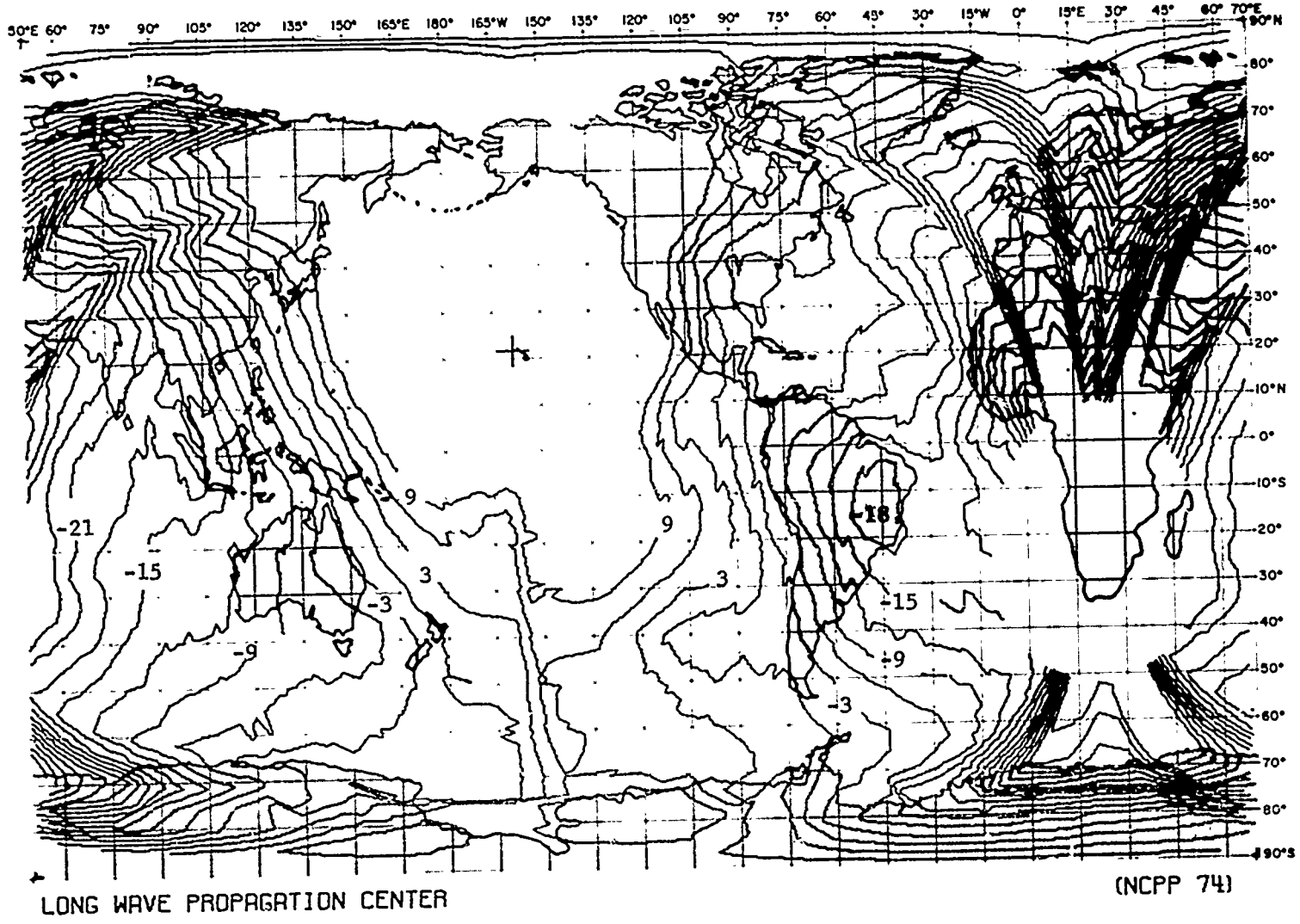


FIG. SP 27 - SIGNAL-TO-ATMOSPHERIC NOISE RATIO CONTOURS IN dB
NPM (23.4KHZ, 630KW) , LUALUALEI
SPRING 90% TIME AVAILABILITY 1KHZ BANDWIDTH

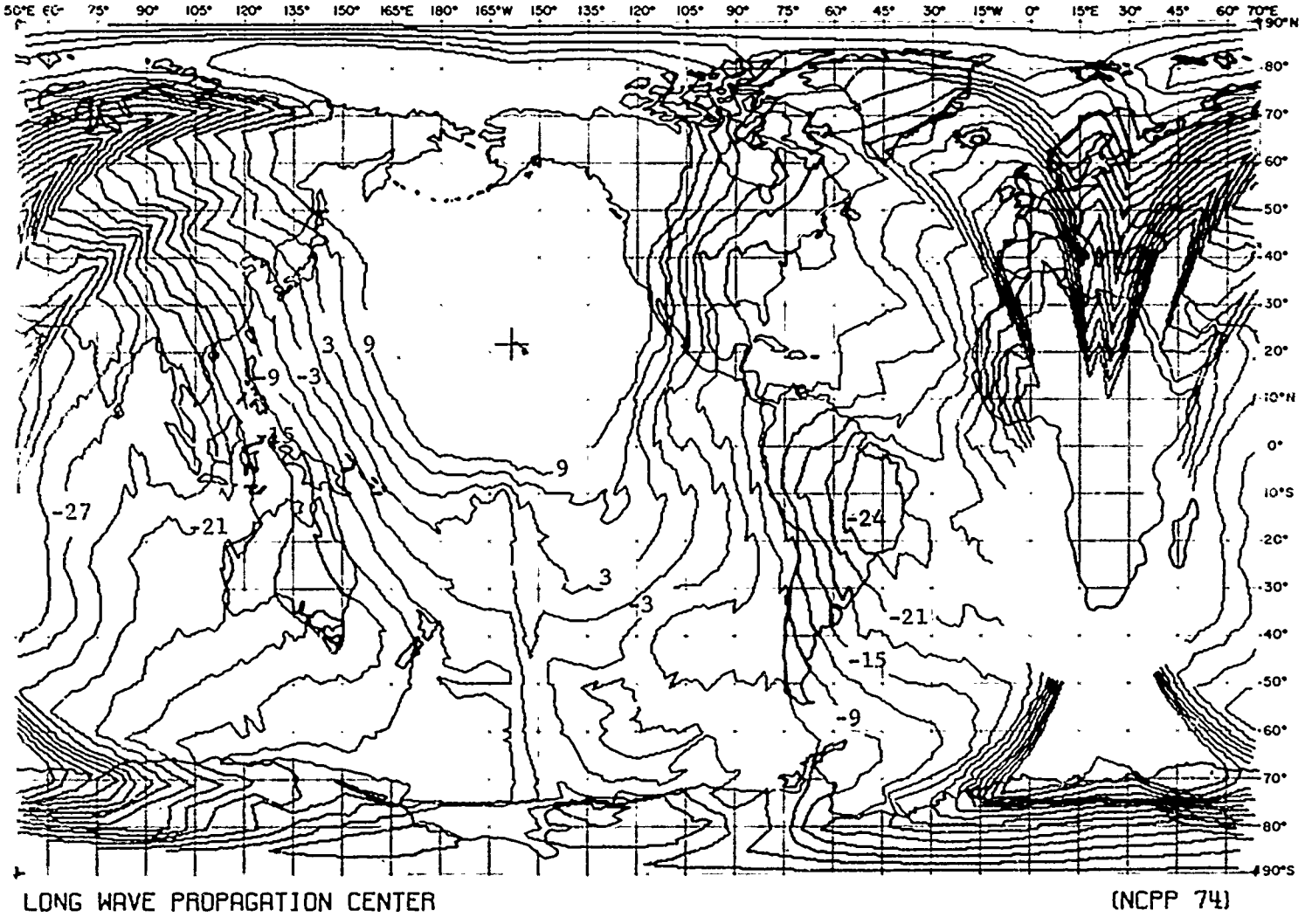


FIG. SP 28 - SIGNAL-TO-ATMOSPHERIC NOISE RATIO CONTOURS IN dB
NPM (23.4KHZ, 630KW) , LUALUALEI
SPRING 99% TIME AVAILABILITY 1KHZ BANDWIDTH